DEVELOPMENT OF A LOW PRESSURE-INDUCTIVELY COUPLED PLASMA-ION SOURCE FOR MASS SPECTROMETRY

by

Gavin Thomas O'Connor, B.Sc., MRSC, C.Chem.

A thesis submitted to the University of Plymouth

in partial fulfilment for the degree of

DOCTOR OF PHILOSOPHY

Department of Environmental Sciences

Faculty of Science

In collaboration with

British Petroleum International

Sunbury-on-Thames, Middlesex, TW16 7LN,

UK

April 1998

ABSTRACT

Development of a Low Pressure-Inductively Coupled Plasma-Ion Source for Mass Spectrometry
by
Gavin Thomas O'Connor, B.Sc., MRSC, C.Chem.

A low pressure-inductively coupled plasma (LP-ICP) ion source has been investigated for the production of atomic and molecular ions for mass spectrometry (MS). A dedicated LP-ICP-MS was constructed, by modifying a Hewlett Packard mass selective detector, to detect ions from the LP-ICP. The ion sampling interface and ion optics were designed using established theory and the use of a computer simulation program. Perfluorotributylamine was continuously introduced into the LP-ICP, via a molecular leak, and the ion sampling interface, plasma forward power, and plasma gas flow rates, were optimised.

When the LP-ICP ion source was sustained at 6W with a gas flow of 6 ml min^{-1} helium, and iodobenzene and dibromobenzene, introduced via GC, only atomic signals for iodine and bromine were observed. Detection limits were 4 and 76 pg for iodobenzene and dibromobenzene respectively.

The addition of nitrogen to a LP helium ICP increased the molecular signal for chlorobenzene, resulting in a detection limit of 2 pg. However, the addition of nitrogen did not aid the production of molecular ions of iodobenzene and dibromobenzene.

When 0.07 ml min^{-1} of isobutane was added to the LP-ICP mass spectra similar to those obtained by an electron impact source were observed. However, on the addition of more isobutane only the molecular ions (M$^+$) for chlorobenzene, iodobenzene and dibromobenzene were observed. The detection limits for the instrument operating in the molecular mode were 100, 140 and 229 pg for chlorobenzene, iodobenzene and dibromobenzene respectively.

Langmuir probe measurements were used to asses the effect of plasma forward power and gas flow rate on the local plasma potential, ion number density, electron temperature and electron number density within the LP-ICP. The local plasma potential varied from +50 V to -20 V depending on the plasma conditions used. The ion and electron number densities increased with increasing plasma power, with ion number densities of approximately 10^9 cm^{-3} and electron number densities of approximately at 10^8 cm^{-3}. The effect of extra plasma gas had a less distinct affect on the plasma excited species.

A plasma sustained at 6 W, 7 ml min^{-1} helium and 1.8 ml min^{-1} isobutane was used to provide both quantitative and qualitative information of tetraethyllead in the standard reference fuel (NBS SRM 1637 II), with the determined value of 13.06 ± 0.91 being in good agreement with the certified value of 12.9 ± 0.07 expressed as total lead.

List of Contents

Chapter 5   **Fundamental Studies**

Chapter 6   **Determination of Tetraethyllead in a Standard Reference**

Fuel by Low Pressure-Inductively Coupled Plasma-Mass

Spectrometry

Chapter 7   Conclusions and Suggestions for Future Work

LIST OF TABLES

LIST OF FIGURES

Chapter 5

Chapter 6

ACKNOWLEDGEMENTS

AUTHOR'S DECLARATION

At no time during the registration for the degree of Doctor of Philosophy has the author been registered for any other University award.

This study was financed with the aid of a studentship from the University of Plymouth, an instrument development grant from the Nuffield Foundation and the donation of instrumentation from British Petrolum International, Sunbury-on-Thames, UK.

A programme of advanvced study was undertaken, which included instruction in ICP-MS theory, design and operation, and attandance at an MSc accrediated shortcourse entitled "Frontiers in Analytical Chemistry: Trace Environmental Analysis".

Relevant scientific seminars and conferences were regularly attended at which work was often presented; external institutions were visited for consultation purposes and several papers prepared for publication.

Publications

"Feasibility Study of Low Pressure Inductively Coupled Plasma Mass Spectrometry for Qualitative and Quantitative Speciation" Gavin O'Connor, Les Ebdon, E. Hywel Evans, Hong Ding, Lisa K. Olson, and Joseph A. Caruso. Journal of Analytical Atomic Spectrometry. 1996, 11, 1151-1161.

"Low Pressure Inductively Coupled Plasma Ion Source for Molecular and Atomic Mass Spectrometry: The Effect of Reagent Gases". Gavin O'Connor, Les Ebdon and E. Hywel Evans. Journal of Analytical Atomic Spectrometry. 1997, 12, 1263-1269.

Presentations

"Low Pressure Inductively Coupled Plasma Mass Spectrometry: The Ultimate in Speciation Detection" G.O'Connor, L.Ebdon, and E.H Evans. Paper presented at Research and Development Topics in Analytical Chemistry, 2nd and 3rd July, 1997, Newcastle, UK

"Low Pressure Inductively Coupled Plasma Source Mass Spectrometry" G.O'Connor, L.Ebdon, and E.H. Evans. Poster presented at the British Mass Spectrometry Society, "22nd Annual Meeting", 8th-11th September, 1996, Swansea, UK.

"Plasma Source Mass Spectrometry- The Next Generation" G.O'Connor, L.Ebdon, and E.H Evans. Poster presented at Research and Development Topics in Analytical Chemistry, 22nd and 23rd July, 1996, Nottingham, UK.

"Fundamental Studies of a Low Pressure Inductively Coupled Plasma Source for Molecular and Atomic Mass Spectrometry" G.O'Connor, L.Ebdon and E.H Evans. Paper presented at the Eight Biennial National Atomic Spectroscopy Symposium, 17th-19th July, 1996, Norwich, UK

"Low Pressure ICP-MS - The Next Advance in Speciation" G.O'Connor, L.Ebdon, and E.H Evans. Paper presented at Atomic Spectroscopy meeting, 28th and 29th March, 1996, Dublin, Ireland.

" Low Pressure Inductively Coupled Plasma: - A Tuneable Ionisation Source for Mass Spectrometry" G.O'Connor, L.Ebdon, and E.H Evans. Paper presented at An Advance in Analytical Science- Young Scientists Competition, 20th February, 1996, Manchester, UK.

"Design and Optimisation of a Low Pressure Inductively Coupled Plasma Mass Spectrometer" G.O'Connor, L.Ebdon, and E.H Evans. Poster presented at the 1996 Winter Conference on Plasma Spectrochemistry, 8th -13th January, 1996, Fort Lauderdale, USA.

"Development of an Alternative Plasma Source for Atomic and Molecular Mass Spectrometry" G.O'Connor, L.Ebdon, and E.H Evans. Poster presented at Research and Development Topics in Analytical Chemistry, 10th and 11th July, 1995, Hull, UK.

Academic Conferences and Meetings Attended:

Analytical Division of the RSC, meeting on "Research and Development Topics in Analytical Chemistry", 2nd and 3rd July, 1997, Newcastle, UK.

British Mass Spectrometry Society, "22nd Annual Meeting", 8th-11th September, 1996, Swansea, UK.

Analytical Division of the RSC, meeting on "Research and Development Topics in Analytical Chemistry", 22nd and 23rd July, 1996, Nottingham, UK.

Royal Society of Chemistry, Analytical Division and Atomic Spectroscopy group, "Eight Biennial National Atomic Spectroscopy Symposium". 17th-19th July, 1996, Norwich, UK

North West Analytical Science Network jointly with the RSC, meeting on. "An Advance in Analytical Science" Young Analytical Scientists Competition. 20th Feburary,1996, Manchester, UK.

Molecular Spectroscopy Group, Analytical Division of RSC and The British Mass Spectrometry Society, meeting on, "Mass Spectrometry: Meeting the Analytical Challenge", 22nd November, 1995, Coventry, UK.

Analytical Division of the RSC, meeting on "Research and Development Topics in Analytical Chemistry", 10th and 11th July, 1995, Hull, UK.

Atomic Spectroscopy Group jointly with the Western Analytical Division of the RSC, meeting on, "Application of Atomic Spectroscopy in Trace Elemental Speciation", 30th March, 1995, Bristol, UK.

Atomic Spectroscopy Group jointly with the Analytical Division of the RSC, 1995 European Winter Conference on Plasma Spectrochemistry, 8th - 13th January, 1995, Cambridge, UK.

Lectures and associated studies

RSC Lecture, 24th February 1995, University of Plymouth, Dr G. Greenway, "Flow Injection Analysis for Ultra Trace Metal Determination and Speciation".

ERASMUS Eurocourse, "Frontiers in Analytical Chemistry: Trace Environmental Analysis" 10th - 14th September, 1995, Plymouth, UK.

RSC Lecture, 18th October 1995, University of Plymouth, Prof. T Fell, "New Dimensions on Hyphenated systems for separation Science".

RSC Lecture, 15th November 1995, University of Plymouth, Prof. W. Davison, "Freshwater Chemistry".

RSC Lecture, 6th December 1995, University of Plymouth, Dr. S. Jarvis, "Gaseous Emissions from Grasslands and their Potential Impact".

RSC Lecture, 18th January 1996, University of Plymouth, Prof. L Ebdon, "Advances in Speciation".

RSC Lecture, 1st March 1996, University of Plymouth, Dr. T Jickells, "Atmospheric Inputs to the Ocean".

RSC Lecture, 25th March 1996, University of Plymouth, Prof. N.U. Novotny, "Bioanalytical Separations in Capillaries: Current Status and Future Prospects".

RSC Lecture, 23rd October 1996, University of Plymouth, Dr. D Cooper, "Molecular Similarity in Drug Design".

RSC Lecture, 8th November 1996, University of Plymouth, Dr S Branch, "Food Authenticity".

RSC Lecture, 20th November 1996, University of Plymouth, Dr G Davidson, "Supercritical Fluid Chromatography from Polymers to Cannibas".

RSC Lecture, 4th December 1996, University of Plymouth, Dr G Wolff, "How Biology Influences Chemistry and Vice Versa. The Case of the Deep Sea".

RSC Lecture, 11th February 1997, University of Plymouth, Prof. J. M. Mermet,

"Analytical Atomic Emission Spectroscopy: Towards the 21st Century".

RSC Lecture, 19th March 1997, University of Plymouth, Prof. K. Jones,

"Environmental Cycling and Foodchain Transfer of Peristent Organic

Contaminants".

RSC Lecture, 12th March 1997, University of Plymouth, Dr S. Wallace,

"Contaminated Land".

Departmental Research Colloquia, weekly meetings, September 1994 to August

1997.

Signed:...........................

Date:.....22 - 7 - 98.................

Chapter 1

INTRODUCTION

CHAPTER 1 - INTRODUCTION

1.1 INTRODUCTION

Throughout the last two decades concern about the effect of man on the environment has gradually increased. This increase has been due, in part, to increased knowledge of toxic compounds as pollutants in the environment. Some of these pollutants occur naturally *e.g.* as a result of weathering or biological activity, however, many toxins are released by industrial processes. Relatively little is known about the fate of some toxins in the environment because few methods of quantification and identification actually exist, especially at trace and ultra trace levels. In addition, the toxicity of some metals is dependent on chemical form or speciation. This is exemplified by the butyl tin series of compounds, where the tributyl tin form is extremely toxic to marine life while the dibutyl tin form is less so. The requirement to obtain information about the speciation of metals in the environment has led to the development of numerous chromatographic techniques coupled with element selective detectors. Mass spectrometry, one of the most applicable and widely used analytical tools, provides qualitative and quantitative information about the atomic and molecular composition of inorganic and organic materials and is therefore well suited to the identification of this type of toxic compound.

1.2 MASS SPECTROMETRY

The first mass spectrometer dates back to the work of J.J. Thompson in 1912, but the instrument that serves as a model for more recent mass spectrometers was built in 1932[1]. The ionisation source of the mass spectrometer produces charged particles that consist of atomic and molecular ions characteristic of the analyte molecule. The source can be chosen to yield varying degrees of fragmentation, i.e. ranging from complete atomisation and ionisation to the formation of molecular ions. The mass spectrometer then sorts these ions according to their mass to charge ratio (m/z). The mass spectrum is a record of the relative

number of ions of different m/z which is characteristic of the analyte compound and its isomers[2].

Functionally, all mass spectrometers perform three basic tasks:

i) create gaseous ion fragments from a sample;

ii) separate these ions according to their mass to charge ratio;

iii) measure the relative abundance of ions at each mass.

To date there is no universal mass spectrometer, because different configurations of sources, analysers and detection systems lend themselves to different types of analysis[1]. This fact is troublesome for institutions that wish to perform a diverse range of analyse at trace levels, since this may require different types of mass spectrometer, hence leading to increased capital cost. A block diagram of the components of a mass spectrometer is shown in Figure 1.1. The essential parts of a mass spectrometer are:

i) sample inlet system;

ii) ion source;

iii) ion acceleration and mass analyser;

iv) ion collection system;

v) data handling system;

vi) vacuum system.

These individual components are discussed in later subsections.

Successful operation of a mass spectrometer requires a collision free path for ions. To achieve this the pressure in the analyser section of the spectrometer should ideally be below 10^{-6} Torr[3]. Ions are produced by the ionisation source, which may be subject to the same vacuum conditions as the analyser or may be at atmospheric conditions. These ions are then transported to the analyser, the method of transportation being dependent on the source

2

Sample

Inlet system → Ionisation source → Mass analyser → Ion collection system

Vacuum System

Data handling system
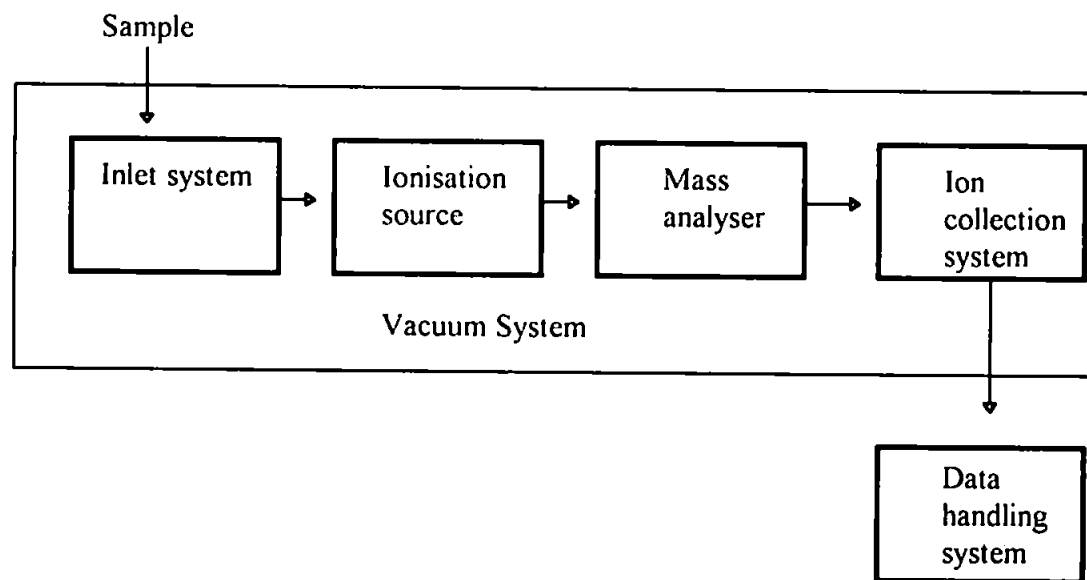
Figure 1.1 Block diagram of the components of a mass spectrometer.

used. Once in the analyser the ions are sorted into discrete mass/charge ratios depending on the energy, momentum and velocity of the ions. A measurement of any two of these allows the mass /charge ratio to be determined.[4]

1.2.1 Mass Analysers

The function of the mass analyser is to separate the ions. The ions are transported from the ionisation source to the analyser by a series of electrostatic lenses which accelerate and focus the ion beam. The way in which the ions enter the analyser is critical for optimal sensitivity and resolution.

1.2.1.1 Magnetic Sector Mass Analysers

In a magnetic sector analyser, ions are subjected to a magnetic field which causes the ions to be deflected along curved paths. The ions are introduced into the analyser via a series of electrostatic slits which accelerate and focus the ions into a dense ion beam. The velocity of the ions is controlled by the potential (V) applied to the slits. As the ions enter the magnetic sector analyser they are subjected to a magnetic field parallel to the slits but perpendicular to the ion beam. This causes the ions to deviate from their initial path and curve in a circular fashion. A stable, controllable magnetic field (H) separates the components of the beam according to momentum. This causes the ion beam to separate spatially and each ion has a unique radius of curvature or trajectory (R) according to its m/z. Only ions of a single m/z value will posses the correct trajectory that focuses the ion on the exit slit to the detector. By changing the magnetic field strength, ions with differing m/z values are brought to focus at the detector slit.

The ion velocity(v) in the magnetic field is given by the equation[1];

$$\frac{1}{2}mv^2 = zV \text{ or } v = \sqrt{\frac{2zV}{m}} \qquad (1)$$

as the ions enter the magnetic field, they are subjected to a magnetic force at right angles to both the magnetic lines of force and their line of flight. This leads to a centrifugal force resulting in curvature of the ion beam.

$$\frac{mv^2}{R} = Hzv \qquad (2)$$

The radius of curvature of the flight path is proportional to its momentum and inversely proportional to the magnetic field strength.

$$R = \frac{mv}{zH} \qquad (3)$$

Eliminating the velocity term (v) between equations 1 and 3 gives

$$R = \frac{1}{H}\sqrt{2V\left(\frac{m}{z}\right)} \qquad (4)$$

Ions of different mass are accelerated through an electrostatic field, that is uniform in nature, and then subjected to a uniform magnetic field, have different radii of curvature. This leads to ions of a specific m/z value being focused on to the detector slit while all other ions hit the side of the analyser. Thus, the magnetic field classifies and separates ions into a spectrum of beams with each part of the spectrum having a different m/z ratio, where

$$\frac{m}{z} = \frac{H^2R^2}{2V} \qquad (5)$$

To obtain a complete mass spectrum from a magnetic sector analyser, either the accelerating voltage (V) or the magnetic field strength (H) is varied. Each m/z ion from light to heavy is focused sequentially on the detector, hence producing a mass spectrum.

1.2.1.2 Double Focusing Sector Mass Analyser

Single focusing magnetic sectors, as described above, have the disadvantage that ion energies vary depending on their point of formation in the ion source. The difference in ion energy is accentuated by the accelerating voltage, which leads to peak broadening and low resolution in the single focusing mass analyser.

Double focusing magnetic/electrostatic sector instruments use magnetic and electrical fields to disperse ions according to their momentum and translational energy[1]. An ion entering the electrostatic field travels in a circular path of radius (R) such that the electrostatic force acting on it balances the centrifugal force. The equation of motion or transmission is;

$$\frac{mv^2}{R} = Ez \qquad (6)$$

where (E) is the electrostatic field strength. Hence the radius of curvature of the ion path in the electrostatic sector is dependent on its energy rather than its mass[3]. A narrow slit placed in the image plane of the electrostatic sector can be used to transmit a narrow band of ion energies. If this type of analyser was placed in front of a magnetic sector analyser an increase in resolution would result however a decrease in detection would be inevitable because of the decrease in ions exiting the electrostatic sector in comparison with ions exiting the ion source. This loss in sensitivity can be compensated for by the choice of a suitable combination of electrostatic and magnetic sectors, such that the velocity dispersion is equal and opposite in the two analysers.

1.2.1.3 Time of Flight Mass Analyser

Time of flight (TOF) mass analysers have a quite different mode of operation compared with other analysers. In conventional analysers the ion signal is a continuous beam, while in TOF mass spectrometry the ion beam is pulsed so that the ions are either formed or

introduced into the analyser in "packets". These ion packets are introduced into the field free region of a flight tube 30-100 cm long. The principle behind TOF analysis is that if all ions are accelerated to the same kinetic energy, each ion will acquire a characteristic velocity dependent on its m/z ratio[1]. The ion beam reaches its drift energy (2700eV) in less then 2cm. The ions are then accelerated down the TOF tube with the velocity they have acquired. Each ion has a kinetic energy (zV) as expressed by equation 1. All ions have essentially the same energy at this point, therefore their velocities are inversely proportional to the square roots of their masses. As a result, ions of different mass travel down the flight tube at different speeds thereby separating spatially along the flight tube with lighter, faster ions reaching the detector before the heavier ions. Hence the m/z ratio of an ion, and its transit time (T, in microseconds) through a flight distance (L, in cm) under an acceleration voltage (V) are given by

$$T = L\sqrt{\left[\left(\frac{m}{z}\right)\left(\frac{1}{2V}\right)\right]} \text{ or } \frac{m}{z} = \frac{2VT^2}{L^2} \qquad (7)$$

TOF mass analysers are calibrated using two ions of known mass, so exact values of L and V need not be known. The mass calibration is based on the conditions of the analyser during the entire period of measurement.

1.2.1.4 Quadrupole Mass Analysers

The quadrupole mass filter is comprised of four parallel electrically conducting rods arranged in a square geometry. Opposite rods are connected and parallel rods are supplied with a dc voltage, one pair being held at +U volts and the other set at -U volts. The first set of rods are supplied with a radio frequency (rf) voltage (+V cos wt) and the second set of rods are supplied with an rf voltage out of phase by 180° (-V cos wt). This results in the formation of an oscillating hyperbolic field in the area between the rods. As ions pass down the quadrupole analyser (z axis) they experience transverse motion in the x and y planes and

so start to oscillate. The dc field tends to focus positive ions in the positive plane and defocus them in the negative plane. The rf field accelerates the ions, so that when the ions are in the negative half of the rf cycle they are accelerated towards the rods and when they are in the positive half of the rf cycle they are repelled and are accelerated away from the rods[5]. The ions oscillate with increasing amplitude until they either reach the detector or collide with the rods and become neutral. Hence, the quadrupole mass analyser has the ability to transmit certain ions and reject others depending on the stability of their paths[5]. When ions are inside the inside the quadrupole they are forced to follow certain trajectories which are dependent on a number of factors. These include the geometry of the field, the amplitude (V_o), angular frequency (Ω) of the alternating potential, the magnitude (U) of the dc bias applied to the rods, the mass to charge ratio (m/z) of the ions, the initial conditions (position and velocity) and the phase angle with which the ions enter the field. Stable ions are transmitted the length of the quadrupole while unstable ions hit the rods.

The mass spectrum is scanned by varying U and V_o whilst maintaining a constant ratio U/V_o. The recorded mass is proportional to V_o so that a linear increase of V_o provides an easily calibrated linear mass scale[3].

The advantages of the quadrupole mass analyser are: its relatively small size; it is not restricted to the detection of mono energetic ions and ions are accepted within a 60° cone around the axis so that a focusing slit is not necessary. This should result in higher detection limits compared with sector instruments[1].

1.2.1.5 Ion Traps

The most common ion trap (IT) MS consists of a doughnut shaped ring electrode supplied with an rf voltage and capped with two end cap electrodes[3]. The electrodes are contained in

a chamber at a pressure of 10^{-3} Torr with a helium bath gas. Ions entering the trap through a hole in the end cap beguin to oscillate. The stability of the oscillating ions is determined by the rf frequency, voltage supplied to the ring electrode and the m/z of the ion. Increasing the rf amplitude causes ions of increasing m/z to destabilise and leave the trap, where they may be detected. A mass spectrum is obtained by scanning the rf supply and detecting ions as they are ejected from the trap. This method of operation is known as the mass selective instability mode.

A second method of ion ejection is known as axial modulation. In this method a second rf voltage, lower in frequency than that of the ring electrode, is supplied to the end caps. Scanning the rf amplitude on the ring electrode, causes mass selective instability, and ions are sequentially brought into resonance with the rf of the end caps. This causes an increase in translational energy of the ion ejecting the ion from the trap. This is considered advantageous as m/z ions are ejected at much lower rf voltages than those required for mass selective instability. This has the desired effect of increasing the mass range of the analyser. Selective ejection and trapping can also be performed, enabling the concentration of a single ion in the trap. This process has further developed and ion traps are now used successfully for MS-MS and MS^n experiments[3].

1.2.2 Detectors for Mass Spectrometry

On exiting from the mass analyser the ions will sequentially strike the detector. Several types of detector are available, although the electron multiplier is the most common.

1.2.2.1 Faraday Cup Collector

This consists of a grounded collector cup which is capable of detecting and measuring small currents. Currents as low as 10^{-15} A have been measured successfully in this way[1].

9

1.2.2.2 Electron Multiplier

For currents of less then 10^{-15}A an electron multiplier is necessary for detection. When the ion beam exits the analyser the ions are drawn towards a coversion plate by a strong voltage applied to it. On striking the conversion plate, the ions stimulate the ejection of electrons which are accelerated by the voltage applied to the plate. The electrons are multiplied in one of two ways.

An array of discrete dynode multipliers, usually containing 15 to 18 dynodes, are coated with a metal oxide that has high secondary electron emission properties. The dynodes are placed in one of two configurations, either venetian blind or box and grid fashion. Secondary electrons emitted by the metal oxide are forced to follow a circular path, by a magnetic field, so they strike successive dynodes thereby multiplying the signal.

Continuous dynode multipliers consist of a leaded glass tube which contains a series of metal oxides. The tube is curved and electrons are drawn down the tube by the potential gradient established by the resistivity of the glass. The tube is curved to stop electron feedback. For either of the above multipliers an increase in signal of 10^5-10^7 is expected. The major restricting factor is the background noise of the system.

1.2.2.3 Channel Plate Electron Multiplier Array

This type of multiplier consists of an array of small channels cut in a semiconducting material. Each channel has an entrance diameter of about 10-25μm. The channels are coated internally with a metal oxide so each channel acts as a micro multiplier. To increase detection limits further, a series of these plates can be placed in tandem, so the multiplied electrons from the first plate are further multiplied by the second.

<u>1.2.2.4 Photographic Plate.</u>

Double focusing analysers can use their focusing power to separate the ions spatially and so a photographic plate can be used to detect the ions. Photographic detection is time integrated and can therefore provide very high sensitivity.

1.2.3 Ionisation Sources for Mass Spectrometry

The function of the ionisation source is to provide an ion or ions representative of the analyte molecule. The most common process of ionisation is the removal of an electron which produces a positively charged molecular radical ion

$$M \rightarrow M^{\cdot+} + e^-$$

Some ionisation sources also break down the analyte molecule into fragment ions, or in some cases totally dissociate the analyte molecule into its constituent atoms and ions. The ability to produce atomic or molecular ions, and the physical form in which the sample is presented to the ionisation source, are the main differences between most ionisation sources.

<u>1.2.3.1 Electron Impact Source</u>

The electron impact (EI) source is by far the most common ionisation source[1]. This is mostly because of the popularity of gas chromatography mass spectrometry (GC-MS) for which it is ideal. The EI source is situated in a heated (150-200°C) vacuum chamber (10^{-8} Torr) preceding the analyser section. Ions produced by the source are accelerated towards the analyser by a series of focusing ion lenses[7]. The analyte is introduced into the chamber, usually in a gaseous form. An electron gun, usually a glowing filament, emits electrons which are drawn across the analyte stream by a positive electrode. The electrons are forced into a tight beam by a set of magnets which keep the electrons within the source chamber. Ions are formed by interaction of the electron beam with the analyte molecules. This results

in a Frank Condon transition producing molecular ions in a highly excited state[6]. Electron impact is not an efficient form of ionisation, as under the low pressure conditions, only one in a million analyte molecules is ionised[7]. EI sources are usually operated at 70eV, but the low mass and high kinetic energy of the electrons causes little increase in the translational energy of the analyte molecule. Instead the molecular ion exists in a highly excited rotational and vibrational state which causes it to fragment[8]. These fragments are often referred to as daughter ions and are typical of different classes of compounds. Hence, the resulting mass spectrum from an EI source consists of a clutter of fragment ions. This is considered an advantage as these fragments often lead to the unambiguous identification of the analyte molecule. However, certain molecules undergo extensive fragmentation and yield no molecular ions, this is disadvantageous when molecular weight information is required.

It is also possible to form negative ions using EI sources, however, the probability of electron capture (yielding a negative ion) is one hundred time less then that of electron removal (yielding a positive ion). In negative ion formation the translational energy of the electron must be considered as this will be transferred to the molecular ion (M^-). This translational energy is usually converted into vibrational energy[6]. As already stated this excess energy causes excessive fragmentation leading to the formation of small negative molecular fragments which provide little structural information.

1.2.3.2 Chemical Ionisation

Chemical ionisation (CI) results from ion-molecule chemical interactions involving the analyte and a reagent gas. Gas in a partially evacuated chamber, normally 1 Torr, is ionised by electron impact forming a dense cloud of reagent ions. The analyte is then introduced into this reagent ion cloud in a gaseous form. The ratio of reagent ions to analyte is in the

region of 1000:1, so the probability of analyte molecule-reagent ion interaction is substantial[3]. Reactions between ions and molecules normally take one of the following forms;

proton transfer $\quad M + XH^+ \rightarrow MH^+ + X$

charge exchange $\quad M + X^+ \rightarrow M^+ + X$

electrophilic addition $M + X^+ \rightarrow MX^+$

anionic abstraction $\quad MH + X^+ \rightarrow M^+ + HX$

Proton transfer is by far the most common CI process. The occurrence of such a reaction is related to the proton affinities of the analytes and reagent ion. If the proton affinity of the analyte is greater than that of the reagent ion, then proton transfer will occur. Typical reagent gases used for proton transfer CI are hydrogen, methane, isobutane and ammonia, with the proton affinity increasing $H < CH_4 < C_4H_{10} < NH_3$[7].

If the reagent gas does not possess an available hydrogen, charge exchange (electron transfer) is an alternative ionisation process. Electron transfer can yield molecular ions with excessive internal energy causing them to fragment, giving rise to spectra similar to those produced using an electron impact source. The internal energy of the analyte ion can be calculated using the following equation

$$E_{(int)} = RE(X^+) - IP(M)$$

where $RE(X^+)$ is the recombination energy of the reagent ion and $IP(M)$ is the ionisation energy of the analyte. Molecular ions will be formed if a reagent gas with a $RE(X^+)$ slightly greater then $IP(M)$ is used, while extensive fragmentation is expected if $E_{(int)}$ is greater than 5eV[7].

If the proton affinity (PA) of the analyte is similar to that of the reagent ion an addition complex ion may result. This process is known as electrophilic addition and is characterised by the addition of NH_4^+ to the analyte, when using ammonia as the reagent ion[3].

$$PA(M) > PA(NH_4^+) \qquad M + NH_4^+ \rightarrow [M\text{--------}H\text{--------}NH_3]^+ \rightarrow [M+H]^+ + NH_3$$

$$PA(M) \approx PA(NH_4^+) \qquad M + NH_4^+ \rightarrow [M\text{--------}H\text{--------}NH_3]^+ \rightarrow [M + NH_4]^+$$
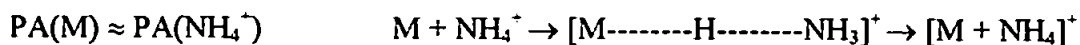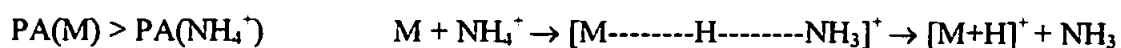
This type of ionisation process yields quasimolecular ions with the m/z being the sum of the molecular ion plus the mass of the added electrophile.

Proton transfer reagents can also partake in anion abstraction reactions with samples of low proton affinity. A common example of such an ionisation process is the hydride abstraction experienced by long chain alkanes, which yields M-1 molecular ions.

A major advantage of CI is that ion-molecular reactions, such as proton transfer, are much lower in energy then EI ionisation. This yields a large number of molecular ions, thereby increasing the chance of molecular weight identification. Also, selective ionisation of a molecule can be effected by careful selection of reagent gas. This can prove useful for separating analyte ions from matrix ions. One disadvantage of CI is that many processes result in a high proportion of neutral species. However the presence of such species can be detected by reagent ion monitoring[9].

1.2.3.3 Field Ionisation

Field ionisation (FI) occurs when a gaseous molecule passes between two electrodes. A strong electric field is produced between the two electrodes (10^7-10^8 V/cm) by applying 10-20 kV to a specially constructed anode. The anode consists of a fine wire with a sharp tip, or a wire which has been specially coated with carbon or silica dendrites, also known as whiskers, which act as a cluster of tips[10]. Ionisation occurs by removal of an electron from

the analyte molecule, yielding a molecular ion. This occurs by a quantum mechanical tunnelling mechanism in which electrons are removed from the analyte by the anode tips. In this process little energy is transferred to the analyte so the molecular ion dominates the spectrum.

1.2.3.4 Field Desorption

Field desorption (FD) is similar in experimental set up to FI. However, in FD the anode is coated with the analyte, negating the need for analyte in the gaseous state. In FD the anode may also be heated to aid desorption before ionisation occurs. This heating may cause thermal decomposition of some analytes. Ionisation in FD can be dependent on the analyte. The four most common ionisation mechanisms are, field ionisation, cation attachment, thermal ionisation, and proton abstraction. Field ionisation, described above, occurs for non polar or slightly polar organics.

Cation attachment occurs when cations, usually H^+ or Na^+, attach themselves to receptor sites on the analyte molecule. The combination of anode heating and high electric field strength leads to the desorption of cation attachment ions. This mechanism is more common for polar organics[10].

Thermal ionisation is common for organic and inorganic salts. The anode acts as a probe to hold and heat the sample. The high electric field strength reduces the desorption temperature of the salts, which facilitates focusing and increases the ion signal[10]. Proton abstraction is a mechanism for negative ion FD. Polar organics will often exhibit M-1 ions . However, the three mechanisms described above all have analogues in negative ion FDMS.

1.2.3.5 Plasma Desorption

Plasma desorption (PD) occurs when the analyte is subjected to a high energy beam of fission fragments from the decay of californium-252. This process is highly energetic, and results in a wide range of fission products which are heavy atom-ion pairs. The analyte is coated on a thin aluminium foil. The fission products pass through the foil and cause the analyte coated to it to desorb and ionise. One fission fragment can cause the production of many positive and negative ions. The analyte ions formed can often be controlled by mixing the analyte with asubstrate, such as nitro-cellulose. This has led to increased fluxes of molecular ions[3].

1.2.3.6 Laser Desorption

In laser desorption (LD) ionisation the sample is subjected to a pulsed laser beam, which both vaporises and ionises the sample. The sample is placed on a piece of metal foil. The laser is focused into a beam which hits the back of the metal foil. Ions emerge from the front side of the metal foil through a minute hole caused by the laser pulse. The laser pulse produces a micro plasma that consists of neutral fragments together with elemental, molecular and fragment ions. The laser pulse lasts several micro seconds so time of flight mass analysis must be used with this ionisation source[6].

The reliance of ionisation on the sample matrix has played a major role in the development of LDMS instrumentation. One method of overcoming matrix effects is to separate the ionisation and desorption processes, which involves the use of two lasers. One laser is used to desorb the analyte and a second laser ionises the desorbed analyte cloud. This has paved the way for resonance enhanced multiphoton ionisation (REMPI) where the ionising laser can be tuned to a specific wavelength[12]. One photon promotes the molecule to an excited

electronic state, whilst a second photon ionises it. For this to occur the first photon must be of a specific wavelength characteristic of the energy required to excite the molecule.

Single laser methods are generally considered as softer ionisation techniques than dual laser methods. Another method of overcoming desorption problems is to mix the sample with a known matrix, chosen to absorb energy of the same wavelength as the laser pulse. This increases molecular ion formation as excess energy from the laser pulse is absorbed by the matrix. This technique is commonly known as matrix assisted laser desorption ionisation (MALDI)[12].

1.2.3.7 Secondary Ion sources

The use of secondary ion mass spectrometry (SIMS) can be traced back to the pioneering mass spectrometry studies of 1912[13]. Analyte ions are produced by subjecting the analyte surface to a stream of high kinetic energy (5-20keV) primary ions[8]. The primary ions are produced by an ion gun, by passing a high velocity gas stream across an electron emitting filament which induces ionisation of the gas by electron impact. These high energy ions are focused onto the solid sample surface where they collide with the sample surface and become impacted. This causes a shuffling effect in the matrix atoms and induces the emission of secondary particles, which may be neutral in charge or ionised. This high energy source has been used successfully for trace element analysis, providing atomic mass spectra of the analyte surface[13].

Molecular information has been obtained using a SI source. This was achieved by greatly reducing the energy of the primary ion beam. This technique has become known as static SIMS and has the advantage of being able to produce ions from non volatile samples[14].

1.2.3.8 Fast Atom Bombardment

Fast atom bombardment (FAB) is a process directly related to SIMS and is often called liquid SIMS. However, the process is slightly different as the primary ions used to induce secondary emission are neutralised, by electron capture or charge exchange, before striking the analyte.

The analyte is dissolved in a special solvent, such as glycerol or 2,4, dipentylphenol, which does not evaporate, even in vacuum conditions. The analyte ionisation process is quite similar to CI but, as a complete layer of sample can be sputtered in seconds, constant sample replacement is needed[15].

1.2.3.9 Spray Ionisation Methods

Desorption of analyte from a liquid is achieved by first forming a fine mist of charged droplets. The desorption process occurs into a bath gas of approximately ambient pressure and not into a vacuum as in other desorption techniques. There are three different ways of droplet formation, thermospray (TS), aerospray(AS) and electrospray (ES), but the ionisation processes have the same basic mechanism[16].

Electrospray is operated at atmospheric pressure. The sample solution flows through a stainless steel capillary maintained at 3-5kV. The resulting field generated at the capillary tip charges the surface of the emerging liquid. This disperses the liquid into fine charged droplets because of the coulombic repulsions in the resulting charged liquid. The droplets travel towards the grounded orifice and into the mass analyser. A bath gas causes the droplets to desolvate thereby decreasing the diameter of the droplet. As a result the charge density on the droplet surface increases as the droplet reaches its Raleigh limit. At this point the coulombic forces are greater then the surface tension of the droplet, which causes the

droplet to explode, leading to smaller droplets. This sequence of events continues to occur until the charge density on the surface of the droplet causes an ion to desorb. The desorbed ion will be a quasimolecular ion comprised of the analyte and an ion present in the original liquid.

Ionisation has also been achieved using aerospray sample introduction[16]. Droplets are produced by pneumatic nebulisation of a sample solution, which contains a high concentration of ions in solution. The ions are thought to be charged by statistical fluctuations in the distribution of cations and anions amongst the droplets. Once in droplet form ionisation occurs as in electrospray.

Thermospray droplets are formed by passing the analyte dissolved in a volatile solvent through a heated steel capillary. The capillary walls must be hot enough to vaporise greater than 90% of the solvent. The solvent vapour expands quickly and the resulting shear and acceleration forces cause the remainder of the liquid to nebulise. The liquid exits the end of the capillary as a supersonic jet of small droplets, which then start to desolvate and ionise.

A combination of AS and ES has been seen to improve analyte ion formation. Such a combination is often termed as ionspray (IS). A major advantage of the spray techniques is the amount of multiply charged species present in the spectra. This is considered an advantage as the mass to charge ratio for very large molecules can be recorded on a mass analyser of intermediate mass range.

1.2.3.10 Spark Source Mass Spectrometry

Spark source (SS) ion formation is based on the emission of ions from a conducting sample, induced by an electric discharge. The ion source consists of two electrodes in an evacuated

chamber. A radio frequency (1MHz) high voltage supply is pulsed across the electrodes, one of which contains sample material. The pulsing of the power supply induces a spark across the electrodes causing ions to be emitted from the solid sample. The ions produced are normally elemental in nature so SS is almost exclusively used as an atomic source for MS[13].

1.2.3.11 Plasma Ionisation Sources

Gray *et al*[17,18,19] first demonstrated that plasma source mass spectrometry was possible using a directly coupled plasma, and Houk *et al*[20] produced the first analytical mass spectra from an inductively coupled plasma (ICP) in 1978. Since then inductively coupled plasma mass spectrometry (ICP-MS) has become an invaluable tool for trace level determinations at ng ml^{-1} and pg ml^{-1} levels. The way in which plasma source MS has matured since its origins is highlighted by a series of review articles[21-32] and book chapters[31-37]. The atmospheric argon ICP is the most widely used ion source for plasma mass spectrometry because the combination offers good stability, excellent detection limits and wide linear range. More recently, alternative plasma sources other than atmospheric argon ICPs have been coupled to the mass spectrometer with notable advantages. Plasma sources for mass spectrometry can be split into three major groups, namely inductively coupled plasmas (ICPs)[21-23,33-36], microwave induced plasmas (MIPs)[31,35], and glow discharges (GDs)[32,37].

Inductively Coupled Plasma Ionisation source

The ICP was first developed by Read[38-40] in 1960, and was first used by Greenfield[41] for spectrochemical analysis. An atmospheric ICP is formed when an inert gas, usually argon, is forced down a quartz torch which consists of three tubes of varying diameter. The inner tube carries the sample aerosol in a flow of argon, and the intermediate and outer tubes carry gas flows which form the plasma and cool the torch respectively. On entering the

torch the argon is seeded with electrons by initial excitation with a tesla coil. The electrons are then accelerated in the magnetic field, induced by the application of rf energy to a copper coil surrounding the torch, collide with neutral argon atoms, and ionise them. The ions and electrons collide continuously, and as long as the RF field is maintained the plasma is sustained.

The resulting plasma is a dense annular shaped ball of highly excited electrons, ions, metastable and neutral species. The ionisation of the analyte in ICP-MS is a complex process which has invoked major discussion in the past[34,35] and will continue to do so in the future. The operating temperature of an ICP is of the order of several thousand Kelvin. This leads to desolvation and thermal atomisation of analytes introduced into the central region of the plasma. Once atomised, ionisation may occur by a number of processes[35].

Thermal ionisation: induced by collisions in the plasma between ions, atoms and free electrons.

$$A + e^- \rightarrow A^+ + 2e^-$$

$$A + M \rightarrow A^+ + M + e^-$$
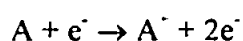
Penning ionisation: caused by charge exchange between plasma gas metastable species and analyte atoms.

$$X^* + A \rightarrow X + A^+ + e^-$$
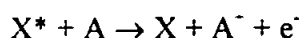
Charge Transfer: caused by transfer of energy from an ion to an analyte ion.

$$X^+ + A \rightarrow X + A^+$$
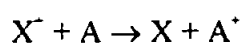
From the above processes it is easy to see how the extent to which an analyte is ionised can be influenced. Simply by changing the plasma gas, the three ionisation process can be influenced greatly. The physical properties for the most commonly used plasma gases are

shown in Table 1.1. By using a plasma gas with a higher ionisation energy than argon an increase in charge transfer ionisation would be expected. Penning ionisation with helium is more efficient and energetic due to the increased energy possessed by the metastables compared with those of argon. Also, the coupling of RF power is greater into the outer region of the plasma fireball, termed the skin effect, and heat is transferred to the centre of the plasma by conduction. Hence, the use of a gas with a high thermal conductivity will increase the temperature of the centre of the plasma, thereby increasing ionisation. This description suggests that helium ICPs are far superior to those of argon. However, power-coupling and instability problems, partially caused by the dissipation of energy from the helium plasma, due to the increased thermal conductivity, and the high cost of helium compared with that of argon, make such an option less attractive[35].

Atmospheric pressure ICPs have been shown to deviate from local thermal equilibrium (LTE)[42], i.e. collisions between atoms, ions and electrons do not result in an equilibrium being maintained between the various states, so that when the plasma temperature is measured in different ways the temperature varies[43]. This plasma phenomenon has led to the experimental measurement of the gas kinetic temperature (T_g),[34] ionisation temperature (T_{ion}),[44,45] rotational temperature (T_{rot}),[46] excitation temperature (T_{exc}),[47] and electron number density (n_e),[47,48] which help reflect the overall characteristics of the plasma as an ionisation source. Further investigations into the degree of analyte ionisation in an ICP have been performed by Caughlin and Blades[49].

The atmospheric pressure argon ICP is not an efficient ionisation source for elements with high ionisation energies, above approx. 10 eV. Spectroscopic interferences can also lead to problems in argon ICP-MS work[50], e.g. hydrochloric acid can cause problems if used in sample digestion especially for $^{51}V^+$ and $^{75}As^+$ due to interferences by $^{35}Cl^{16}O^+$ and $^{40}Ar^{35}Cl^+$.

22

Table 1.1   Physical properties of commonly used plasma gases.

Plasma gas	Ionisation energy (eV)	Thermal conductivity ($J\ K^{-1}\ m^{-1}\ s^{-1}$)	Metastable energy (eV)
Helium	24.59	0.141[a]	$^1S_0=20.16$ $^3S_0=19.82$
Neon	21.56	0.0461[b]	$^3P_0=16.76$ $3P_2=16.62$
Argon	15.76	0.0162[b]	$3P_0=11.75$ $3P_2=11.55$
Krypton	13.99	0.0086[b]	$3P_0=10.56$ $3P_2=9.92$
Hydrogen	13.60	0.166[a]	
Nitrogen	14.53	0.0237[b]	
Oxygen	13.62	0.0242[b]	

[a] At 273 K; [b] at 293 K

23

The use of alternative gas plasmas consisting of oxygen[51-55], nitrogen[56-57], air[58] and helium[59-68] as well as mixed gas plasmas[69,70] have been investigated to reduce these and other matrix effects.

Microwave Induced Plasmas

Helium microwave induced plasmas (MIPs) have been used increasingly in recent years[31,71-79] and these have the added advantage of being able to ionise elements with high IEs, such as the halogens. The plasma is normally contained inside a cylindrical shaped quartz torch, which is surrounded by the microwave cavity. The plasma is much smaller in physical size than an ICP and can be sustained in gas flows between 0.06-6 l min^{-1}. The ionisation processes in MIPs are directly related to those in ICPs so need no repetition here. One other method of altering the plasma gas kinetics is to change the plasma pressure. Reduced pressure helium MIPs have also been described for the analysis of a variety of compounds considered difficult to analyse by conventional ICP-MS[80-82]. Helium MIPs have been used to produce molecular fragments of organic compounds introduced to the plasma via a gas chromatography column[83-85]. Microwave plasmas have the disadvantage that they are difficult to operate in excess of 200 watts due to problems associated with tuning. Also, their small physical size make them intolerant of large amounts of solvent, hence gas sample introduction has been the method of choice, either via GC or hydride generation[86]. However, solution nebulisation has been achieved using a Meinhard nebuliser[87].

Glow Discharge Sources

Glow discharge (GD) sources are predominantly used for the analysis of conducting solids. However, new source geometries and power supplies are the subject of continuing research, to enable a wider range of analytes to be analysed by glow discharge[32].

The simplest GD source is the direct current (DC) GD. This consists of a sealed vacuum chamber containing two electrodes. An inert plasma gas (usually argon) fills the chamber to a pressure of between 0.1 and 10 Torr. The discharge is sustained by maintaining a high potential difference between the two electrodes which are in contact with the plasma gas. This potential difference (200- 2000V) causes the gas to break down into positive ions and free electrons. Electrons start to move towards the positively charged anode, while ions are accelerated towards the cathode surface. On striking the cathode the ions transfer their energy to the cathode surface which induces sputtering. The products of sputtering are ejected atoms and small atom clusters of cathode material, as well as ions and secondary electrons[88]. The secondary electrons aid in sustaining the plasma, and the free atoms are ionised in the plasma. Samples can be coated on to the cathode[89] or can actually act as the cathode if they are conducting or are mixed with a conducting matrix.

As in other plasma sources there are many possible modes of ionisation in GD sources. The ionisation processes may be separated into primary collisions, such as electron ionisation,

$$A + e^- \rightarrow A^+ + 2e^-$$
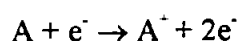
and secondary collisions,

$$\text{Penning ionisation} \qquad A^* + X \rightarrow A + X^+ + e^-$$
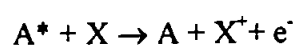
associative ionisation $\quad$ $A^* + X \rightarrow AX^+ + e^-$

symmetric charge exchange $\quad$ $A^+ + A \rightarrow A + A^+$

asymmetric charge exchange $\quad$ $A^+ + B \rightarrow A + B^-$

However, Penning ionisation is thought to be the dominant process in most GD sources[37].

A considerable disadvantage of DC-GD is the need for a conducting sample or sample mixing. This has been overcome by the use of rf-GD sources[90] and these have been used successfully for the analysis of non-conducting matrices such as polymers[91]. GD sources have also been used successfully to provide elemental spectra of analytes introduced into the negative glow region of the GD, via GC sample introduction[92].

Although used almost exclusively for the production of elemental ions, GD sources have been used for CI[93]. The reagent gas was added to the GD chamber and analytes were introduced via a membrane probe. The reagent ions were produced from water vapour introduced with the analyte, which was the main reason for the use of GD rather than EI excitation of the reagent gas, as water drastically decreases the life of an EI filament. The predominant ions produced in such a source from organic analyte compounds, were the M+H and M+H$_2$O cluster quasimolecular ions[93]. An in-depth study on the operating parameters of a GD source for the production of molecular ions has been performed by Carazzato and Bertrand[94]. It was shown that different molecular species resulted in optimum signals at different source conditions, however, spectra similar to EI source MS were obtained. More importantly, the source was seen to produce representative ions when the sample was introduced in the gaseous or desolvated liquid form. Detection limits for molecular species were in the 100 pg range, however, continuous sample introduction was

performed. An atmospheric sampling GD source has also been developed and used for the detection of explosives at trace levels[95]. This source was used for the production of negative molecular ions which were introduced into an ion trap analyser. Detection of molecular species were in the femtogram range.

Liquid sample introduction into a hollow cathode GD has been achieved by first desolvating the sample using a particle beam interface[96]. Detection in this instance was by atomic emission, however, the authors mentioned the possibility of using MS detection in the near future[96]. Liquid sample introduction into an atmospheric pressure helium GD has been achieved[97]. A series of organic solutions was injected, 100 µl min^{-1}, through a heated pneumatic nebuliser, which vaporised the sample. The predominant ions formed in this instance were M+H quasimolecular ions.

Low Pressure Inductively Coupled Plasmas

Atmospheric plasmas give rise to numerous polyatomic interfering species, the entrainment of air into the plasma gas being a major cause of these polyatomic species. Reduced pressure ICPs have been studied using atomic emission spectroscopy[98-103] and Smith and Denton[104] have performed a study of the effects of pressure on the operation of an ICP. They observed that plasmas of most gases would form easily under reduced pressure even without initial excitation from a tesla coil.

Recently, a low pressure (LP) ICP-MS has been developed by Evans and Caruso using argon and helium[105]. The concept behind the use of such a source was to exclude air and

hence reduce molecular interferences in the plasma. A list of the most common molecular interferences, associated with air entrainment, along with the element they interfere with, is shown in Table 1.2. The helium LP-ICP-MS has been used successfully for the analysis of halogenated compounds, using gaseous sample introduction via a GC. The LP helium plasma used in this work was operated at 100W, was sustained with between 430-460 ml min^{-1} plasma gas and totally atomised the samples to yield elemental spectra[106].

Yan et al.[107] have investigated the use of a water cooled, shielded torch to sustain a 0.021 l min^{-1} argon LP-ICP at 200W. The LP-ICP was shown to improve non-metallic element signals in comparison with a conventional atmospheric ICP. This instrument was used later for the analysis of halogens using electrothermal vaporisation sample introduction[108]. Castillano et al.[109] have achieved solution sample introduction into a 2 l min^{-1}, 200W helium LP-ICP. Sample introduction was via both ultrasonic and glass frit nebulisers and elemental mass spectra were obtained.

Evans et al.[110] have obtained atomic and molecular spectra using the same LP-ICP-MS instrumentation. This was achieved by simply altering the plasma gas, torch pressure and forward power[111].

1.2.3.12 Tuneable Ionisation Sources

Several research groups have investigated novel, tuneable sources for MS. Many sources can provide a small degree of flexibility, e.g. changing the electron voltage in EI may yield a larger number of molecular ions, but no commercial source can provide a tuneable degree of

Table 1.2 Common molecular interferences associated with air entrainment in atmospheric argon ICP-MS.

m/z	Molecular species	Element	Isotopic abundance
15	$^{14}N^1H$		
17	$^{16}O^1H$		
28	$^{14}N^{14}N$	Si	92.2
29	$^{14}N^{15}N$	Si	4.7
30	$^{16}O^{14}N$	Si	3.1
31	$^{16}O^{15}N$	P	100
32	$^{16}O^{16}O$	S	95
34	$^{18}O^{16}O$	S	4.2
41	$^{40}Ar^1H$	K	6.7
56	$^{40}Ar^{16}O$	Fe	91.52

fragmentation, ranging from, elemental spectra to molecular spectra. Many instrument manufacturers have addressed this problem by supplying multiple source instruments, the most common being the EI-CI combination.

A metastable beam source has been investigated by Faubert *et al.*[112] for the selective fragmentation and ionisation of a series of organic compounds. Analytes were introduced into an extracted metastable beam where Penning ionisation occurred. It was shown that by changing the noble gas used to form the metastable species, the fragmentation of the analytes altered. Little fragmentation was observed using krypton, yielding spectra not dissimilar to those obtained by CI, whereas helium caused extensive fragmentation, similar to EI source MS. The degree of fragmentation followed the trend of energies for metastable species He>Ne>Ar>Kr. The proposed use for such a source was to provide physical data for organic molecules. Also proposed was its use as a source for liquid chromatography (LC) MS. By selecting a noble gas, which did not ionise the mobile phase, selective ionisation could be achieved. The source was tuneable across the EI-CI modes of fragmentation.

Kohler and Schlunegger[113,114] used a low pressure Penning ionisation source to achieve a tuneable degree of fragmentation for a wide range of aliphatic, aromatic and halogenated compounds. The pure compounds were introduced continuously into the source at a sample pressure between 5×10^{-6} and 1×10^{-3} mbar. Once in the source the analyte formed a plasma and by altering the current across the Penning electrodes, it was possible to alter the spectra of the analytes. At low discharge currents ($10\mu A$), spectra similar to EI-MS were

obtained. At higher currents (120μA), extensive fragmentation was observed and the spectra consisted of elemental species and small molecular fragments. The source was also investigated for the production of negative ions, with extensive fragmentation occurring even at low operating currents.

A summary of the ionisation sources, their method of ionisation and expected base peaks is shown in Table 1.3

1.2.4. Sample Introduction Methods

Sample introduction into a mass spectrometer is dependent on the type of sample, source, and analyser being used, and is usually a two stage process, often complicated by the vacuum conditions in the mass analyser. Where the source is subjected to the same pressure conditions as the analyser the problem is less acute because ions produced by the source need only be accelerated towards the analyser using a series of electrostatic lenses, e.g. the electron impact source. Hence, the greatest problem is getting the sample from atmospheric conditions into the source, while still maintaining a vacuum. If a gaseous sample is to be analysed the sample can be introduced into the source via a molecular leak, which is a hole of small diameter ($1-5 \times 10^{-2}$ mm). Liquid samples cause obvious problems for sampling, because introduction of a liquid into a vacuum chamber would cause a rapid fluctuation in pressure. These problems have been addressed in recent years by thermospray and electrospray methods of ionisation, which form a spray of very small analyte droplets that are desolvated prior to entering the vacuum conditions of the analyser. If the sample is thermally inert and has a high vapour pressure it is possible to introduce a liquid sample as a

Table 1.3   Summary of ionisation sources for mass spectrometry.

Ionisation source	Common sample introduction method	Ionisation reaction	Base peak in spectrum
Electron impact	gas	electron removal	fragment ion
Chemical ionisation	gas	ion molecule reaction	molecular
Field ionisation	gas	electron removal	molecular
Field desorption	solid/adsorbed liquid	desorption	molecular
Plasma desorption	solid	desorption	molecular
Laser desorption	solid	desorption	molecular
Secondary ion	solid	desorption	atomic
Static secondary ion	solid	desorption	molecular
Fast atom bombardment	liquid	desorption	molecular
Electrospray	liquid	desorption	molecular
Thermospray	liquid	desorption	molecular
Inductively coupled plasma	liquid/gas	Penning/thermal/ charge transfer	atomic
Microwave induced plasma	gas	Penning/thermal/ charge transfer	atomic
Glow discharge	gas/solid	Penning ionisation	atomic/molecular
Low pressure ICP	gas	Penning/thermal/ charge transfer	atomic/fragment ion
Rare gas metastable beam source	gas	Penning	molecular/ fragment ion
Penning source	gas/desolvated liquid	Penning	tuneable molecular/fragment ion

gas by using gas chromatography (GC). This also has the added advantage of separating sample components before ionisation. Therefore, GC-MS has become the most common form of mass spectrometric analysis.

The introduction of solid samples into the mass analyser has been achieved by using samples which have a very low vapour pressure. The sample is placed on a silica or platinum probe and is volatilized by heating the probe until a spectrum is obtained[1]. Solid samples have also been introduced using laser desorption mass spectrometry.

The most robust ionisation source for mass spectrometry is the inductively coupled plasma. The normal mode of sample introduction into the ICP is a pneumatic nebuliser, in which a liquid sample is nebulised and a fine spray of analyte is swept into the central channel of the plasma using argon as carrier gas. Gaseous sample introduction from a GC[115-120] and solid sample introduction has also been performed using, for example, slurry nebulisation[121-122] and laser ablation[123].

The ICP will atomise and ionise most samples with relative ease, however, most ICPs operate at atmospheric pressure so for ICP-MS, ions must be sampled from the plasma by an interface designed using molecular beam theory[35]. Ions are extracted from the plasma through a sampling orifice (1-1.5 mm), into an area of low pressure. The movement of gaseous ions from a high pressure region into a low pressure one, through a small orifice, forms a supersonic, conical shaped shock structure with its apex at the sampling orifice[124]. As the jet expands adiabatically it cools rapidly[125], so by sampling inside this supersonic jet a representative sample of the ions from the plasma is obtained. Campargue[125] has discussed

the formation of the free jet structure and has studied the effects of skimming distances and skimmer shape. Olivares and Houk[126] have studied the gas throughput for sampling orifices of a conventional ICP-MS interface, and have shown how to calculate the ideal skimming distance behind the sampler which gives maximum beam intensity down stream of the skimmer. The ion extraction processes for ICP-MS have been the subject of a recent review[127] and a more detailed description of the sampling process is outlined in chapter 3 .

1.2.5 Ion Focusing

Once the ions have been extracted into the vacuum chamber they must be focused and directed toward the mass analyser with a certain velocity. The velocity of the ions and the spread in their kinetic energies will affect resolution of the mass spectrum, so lens systems are different for each type of analyser. The ion optics used are also dependent on the type of ionisation. For example in an EI source the ions are repelled by a positive voltage at the entrance to the source and are focused by a series of negative lenses at the exit of the source, whereas for ICP-MS, the ion optics are down stream of the source, a small negative voltage extracts the ions from the skimming orifice and the beam is then focused using a series of charged lenses. However, due to photons present in the plasma a photon stop is necessary, so the ion beam must be focused around the photon stop. The optimisation of the ion lenses for ICP-MS has been the subject of studies by many groups[128-132]. The design of ion optical systems is said to be more of an art form than a science[2], however, the fate of ions subject to an electrostatic field under vacuum conditions, can be calculated by a series of equations[2]. This method, although time consuming, can be used to calculate the focal length of an electrostatic lens. Ion optics, however, usually consist of a series of lenses and so an advanced computer model is needed to truly simulate the ion trajectories.

Ion beam interactions have been one cause of interferences in mass spectrometers. Tanner *et al.*[131,132] have described the effects of space charge (ion-ion repulsion) on the lens voltage settings for ICP-MS. Vijgen *et al.*[133] have described improvements in beam properties to eliminate beam interactions, and Tanner *et al.*[134,135] described an improved interface for ICP-MS which consisted of three apertures, rather then the conventional two, to reduce space charge in the beam. Burgoyne *et al.*[136] studied the effect of lens potentials on space charge and showed that at low acceleration potential (800V) considerable mass bias was experienced, which was attributed to space charge effects, whereas, at high acceleration potentials (4000V) the mass bias was absent. This suggests that the higher accelerating potentials normally associated with sector instruments, could help reduce space charge in ICP-MS instruments.

1.3 GAS CHROMATOGRAPHY

Mass spectrometry is a powerful analytical tool in its own right, however, its potential increases by coupling it with a separation technique. The separation step is required because ion sources ionise non-selectively, resulting in complex spectra for sample mixtures.

Chromatography is a well established separation technique in analytical science and enables the separation of similar compounds in complex samples[1-8]. Many forms of chromatography exist, although the underlying principles for each are similar. Chromatographic separation requires two phases. The mobile phase, in which the sample mixture must be soluble, may be a liquid, gas or a super-critical fluid. The mobile phase passes over an immiscibble stationary phase which may be contained in a column or coated onto an inert surface. The

two phases are chosen with regard to the analytes of interest. A discrete sample is injected onto the stationary phase, or into the mobile phase, and the analytes in the sample mixture distribute themselves between the two phases. The analytes will have different affinities for the two phases which will cause them to separate as they are forced over the stationary phase. i.e. analytes with a high affinity for the mobile phase will pass quickly along the stationary phase, whereas, analytes with less affinity for the mobile phase may partition themselves between the two phases. If a continuous supply of mobile phase is supplied to the start of the stationary phase it will force the partitioning analytes to move slowly along the stationary phase, separating as they go. The time taken for an analyte to pass the whole way along the stationary phase is know as its retention time.

In gas chromatography the mobile phase consists of an inert carrier gas, such as nitrogen, argon or helium. In its most common form, an open tubular fused silica capillary column is coated internally with a thin film of the stationary phase. The 0.25 to 0.5 mm diameter, 10-50 m long column is coiled and placed in a temperature controlled oven and the carrier gas is connected to the column via the sample injection port. A constant head pressure (30-400 KPa) of carrier gas maintains a flow of 1-25 ml min^{-1} through the column. The sample (0.1-5 µl), which must be volatile and thermally stable, is placed onto the top of the column by injecting it through a septa or valve. The injection port is commonly held at typically 50°C above the boiling point of the least volatile sample component and the column must remain at an elevated temperature in order to stop the analytes condensing within it. The elution time of an analyte can be controlled by programming the oven temperature which reduces analysis times for many analytes considerably.

1.4 AIMS AND OBJECTIVES

The work described in this thesis was directed towards the use of LP-ICP-MS as a tuneable ion source, capable of the production of atomic and molecular ions, for MS. Such a source would be of great advantage to atomic speciation analysts, as it would provide trace level detection while operating in the atomic mode, as well as species identification which is not dependent on analyte chromatographic retention time, when operating in the molecular mode.

Initially, commercially available ICP-MS instrumentation was used to investigate an argon LP-ICP-MS for the production of atomic signals, while a helium LP-ICP was used for the production of molecular ions. Whilst it was possible to form and monitor atomic and molecular ions using commercially available instrumentation, certain insurmountable problems necessitated the construction of a dedicated instrument. Therefore the design, construction and testing of a dedicated LP-ICP-MS was the major objective of the work described. The new instrument was designed using established theory, computer simulations and the experience gained while using the commercial instrumentation. Once constructed, many of the design aspects of the new instrument were optimised. An investigation into whether the established theories could also be applied to the LP-ICP-MS, was also performed.

In an attempt to improve the linear calibration range of the LP-ICP, a number of different gases were added to the LP plasma. The effect of this added plasma gas on molecular and atomic ions was also investigated. In an effort to obtain more information on the ionisation process in the LP-ICP a number of physical measurements were performed. These included ion kinetic energy, ion density, electron number density and electron temperature

measurements. Finally the newly constructed instrument was applied to the analysis of a known environmental contaminant.

Chapter 2

USE OF A COMMERCIAL ICP-MS TO OBTAIN ATOMIC AND MOLECULAR MASS SPECTRA

CHAPTER 2 - USE OF A COMMERCIAL ICP-MS TO OBTAIN ATOMIC AND MOLECULAR MASS SPECTRA

2.1 INTRODUCTION

There are a large number of ion sources used for mass spectrometry (MS), which can generally be divided into three major categories, e.g.:

(i) those which totally atomise the sample components and provide predominantly atomic ions, such as inductively coupled plasmas (ICPs) [33-35], microwave induced plasmas (MIPs) [33] and glow discharges (GDs) [88]; (ii) those which provide structural information by causing analyte molecules to partially break down into smaller but representative fragment ions, such as electron impact (EI) sources; and (iii) those which yield molecular weight information by providing a high proportion of molecular ions, be they singly or multiply charged, such as electrospray ionisation (ESI), fast atom bombardment (FAB) and chemical ionisation (CI) sources. The use of a tandem or trap MS analyser in conjunction with the latter of these sources has yielded molecular weight determinations and structural information afforded by analyte fragmentation, and the production of daughter and grand daughter ions, in the analyser section of the mass spectrometer. While such a combination has bridged the gap between the latter two groups of ion sources, attempts to affect complete fragmentation and obtain atomic information have proved difficult. A contributing factor to this is the formation of metal ion clusters which complicate the spectra[137].

Plasma source mass spectrometry, which is dominated by the atmospheric pressure ICP, has been the choice of many groups for trace element speciation. The use of such a technique has many advantages. Firstly, the high ionisation energy source coupled with mass spectrometry has yielded detection limits, for many elements, in the sub picogram range[24]. Another advantage of using such a high energy source is its ability to quantify an unknown species. This is achieved by calibrating the instrument with a known compound, which has

at least one element in common with the unknown species. This is possible because the compounds are atomised completely to their constituent elements in the plasma source. A major disadvantage of such techniques is that qualitative identification of analyte species has relied on chromatographic retention times, requiring a pure standard of the analyte in question, or the use of an alternative technique. This effectively limits the technique to the analysis of known compounds.

Low pressure plasma ionisation sources have been developed to overcome a number of the shortfalls in atmospheric plasmas (section 1.2.3.11). The reduced pressure enables plasmas to be sustained in a variety of gases and at reduced power. Low pressure MIPs have been operated between 60 to 400W at pressures ranging between 0.6 to 7 mbar using helium, nitrogen and hydrogen, to provide trace level determination of a number of organometallic, organohalide, organphosphorus and sulphur containing compounds[81-82]. In these studies the MIP was operated as a source of elemental ions.

Heppner[73] utilised a reduced pressure MIP operating between 30 and 150W sustained in hydrogen and helium for the production of low weight molecular species. These molecular species, formed in the MIP, were analysed by EI source MS to provide elemental information of the analyte compounds. Since then, a number of workers have studied reduced pressure MIPs to obtain molecular information. Poussel[85] investigated the effect of power, pressure and plasma gas on the formation of molecular species in the MIP source. Olson *et al.*[83] also used a low pressure helium MIP to yield molecular information, however in this case the sample was introduced into the low pressure region in the interface of the mass spectrometer.

Evans et al.[105] investigated the possibility of forming argon and helium low pressure ICPs using commercially available atmospheric pressure ICP-MS instrumentation. Using this instrumentation it was possible to sustain a 0.5 l min^{-1}, 350W argon ICP at 0.2 mbar. While a 63 ml min^{-1}, 0.02 mbar helium plasma was sustained at 100W. However, it should be noted that both plasmas operated with reflected power readings in excess of 30W, suggesting that the ICP generator and matching network were not ideally suited to the task. Nevertheless a similar instrument was used later for the analysis of halogenated compounds, with detection limits in the low picogram range being obtained, using gaseous sample introduction via a gas chromatograph[106].

Since these initial investigations, low pressure ICP-MS has been applied to the analysis of non-metallic elements, using continuous sample introduction[107] and electrothermal vaporisation[108]. More recently solution nebulisation has been achieved in a 2 l min^{-1} helium low pressure ICP. In this instance samples were introduced via glass frit and ultrasonic nebulisers[109].

Evans et al.[110] investigated the use of a low pressure ICP-MS as a dual source for mass spectrometry, providing both trace level elemental analysis and qualitative information of a series of organohalide and organometallic compounds. This required only moderate alteration to a commercially available ICP-MS instrument. Atomic ions were observed, in the absence of molecular fragments, using a 1 l min^{-1} argon low pressure ICP operated at 200W. Molecular fragments were observed on removing the argon supply and sustaining a 3.5 ml min^{-1} helium low pressure ICP at forward powers of between 15 and 50 W.

Olson et al.[92] have studied the use of a low pressure glow discharge source as a detector for gas chromatography. Atomic ions were monitored for a series of organometallic compounds

with detection limits comparable to other low pressure atomic sources. On the introduction of large amounts of analyte, molecular fragments were observed. Whilst these fragments were of low abundance they nevertheless provided structural information of the analyte. This suggests that such a source did not possess the required energy to atomise the analytes totally.

Shen and Satzger[87] have produced molecular fragment ions using an atmospheric pressure helium MIP. The use of such a plasma yielded spectra similar to those produced by an EI source. The analyte was introduced into the tail flame of the plasma because only atomic ions were observed when the analyte was introduced into the base of the plasma.

To date, low pressure plasma sources have been operated in two modes, providing both atomic and molecular information. However, while trace level determinations have been possible when the sources were operated in the atomic mode, molecular ions have only been observed on the introduction of large amounts of analyte, and in some cases the continuous introduction of the pure compounds was necessary. This is unrepresentative of real world analyses. If such sources are to be used in a dual mode, it is necessary to produce molecular information without the need to introduce large amounts of analyte.

Hooker and DeZwaan [84] have taken a more conventional approach to the problem. The effluent stream from a GC was split, with equal amounts of analyte going to an EI source mass selective detector, and a MIP-atomic emission detector. This technique provided both atomic and molecular information but was costly due to the requirement of two detectors.

2.2 EXPERIMENTAL

2.2.1 Instrumentation

All experiments were performed using a modified, commercially available, inductively coupled plasma mass spectrometer (VG PlasmaQuad 2, VG Elemental, Winsford, UK). The instrument was modified in several respects. The standard sampler cone was replaced with a low pressure aluminium sampler, which had a 2mm orifice and an ultra torr fitting for a 12.7 mm pipe (Machine shop, University of Plymouth). This sampler made it possible to form a vacuum seal between the low pressure torch and the expansion chamber of the instrument (Figure 2.1).

The low pressure torch consisted of a 12cm long quartz tube with an i.d. of 12.7 mm. For the argon-helium plasma the torch had an additional 6.35 mm side arm tube to allow the addition of argon plasma gas. The pumping in the expansion chamber was increased by adding an additional pumping port at ~130° to the original port. This port was connected to the same rotary pump (Edwards E1M-18, Edwards High Vacuum, Crawley, Sussex, UK) as the original port.

A gas chromatograph (Carlo Erba HRGC 5300, Fisons Instruments, Crawley, Sussex, UK) with a cold on-column injector was interfaced to the low pressure torch via a heated transfer line (manufactured in-house), maintained at 200°C. The GC column used was a DB-5, 0.32mm, 35m with a 0.1μm film thickness (J & W, Fisons, Loughborough, UK). This was passed through the heated transfer line and then through 10cm of 1.58 mm titanium tubing, with a vacuum tight seal being accomplished using a Swagelok union and graphite ferrules. This was then connected to the back of the low pressure torch using a standard ultra-torr fitting. The column extended up the middle of the torch until it was
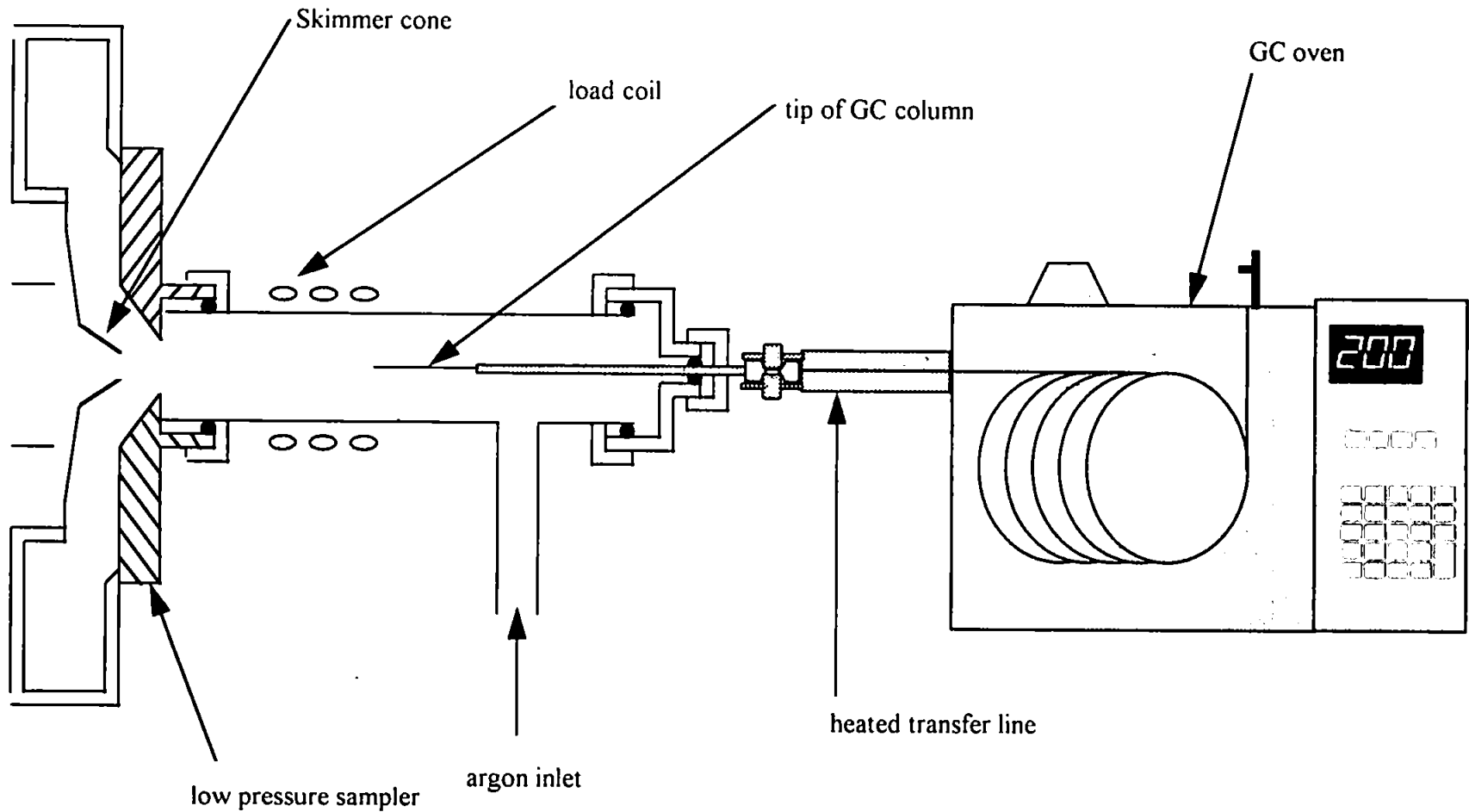
Figure 2.1   Diagram of the low pressure ICP-MS interface

Skimmer cone

load coil

tip of GC column

GC oven

low pressure sampler

argon inlet

heated transfer line

44

positioned 10mm behind the rearmost turn on the ICP load coil. The GC temperature program was 50-200°C with a ramp rate of 20°Cmin⁻¹. A constant-pressure, constant-flow (Carlo Erba, Fisons Instruments, Crawley, Sussex, UK) gas control unit was used to keep the column carrier gas head pressure at 54 kPa leading to a resulting column flow of ~3.0 ml min⁻¹. Figure 2.1 shows the low pressure instrument set-up.

2.2.2   Operating Conditions

To obtain atomic spectra a low pressure argon-helium plasma was used as the ion source. The plasma operating conditions are shown in Table 2.1. A sample mixture of monobutyltintrichloride, dibutyltindichloride and tetrabutyltin was injected, 250 ng on column, separated by the GC, and the tin detected using the LP-ICP-MS, monitoring the tin isotope at 120 m/z. Dibromobenzene was also injected, 250ng on column and the low pressure system was used to monitor bromine at 79 m/z. The data acquisition parameters are shown in Table 2.2. This mode of operation will henceforth be called the "atomic mode"

For the production of molecular mass spectra using LP-ICP-MS, a helium-only plasma was required. The carrier gas from the GC was sufficient to sustain a low pressure helium-only plasma. The plasma operating conditions are presented in Table 2.3.

Iodobenzene, chlorobenzene and 1,2 dibromobenzene (all 250ng on column) and ferrocene, decane, undecane and naphthalene (500 ng on-column) were all injected and fragment molecular ions were detected using the LP-ICP-MS. The data acquisition parameters for molecular mass spectra are shown in Table 2.4. This mode of operation will henceforth be call the "molecular mode".

45

Table 2.1 Operating conditions for low pressure argon-helium ICP-MS.

RF Forward Power (W)	150
Reflected Power (W)	25
Argon Plasma Gas Flow (l min^{-1})	1.0
Helium GC Column Flow (ml min^{-1})	~3.0
Pressure in Expansion Chamber (mbar)	2.2

Table 2.2 Data acquisition parameters used to obtain atomic spectra.

Sample	Tin compounds	Dibromobenzene
Mode	Single ion monitoring	Single ion monitoring
Mass monitored	120	79
Dwell time (ms)	130	130
Channels	3701	3701
Scan Time (s)	606	606

Table 2.3 Operating conditions for low pressure helium ICP-MS.

RF forward power (W)	~25
Reflected power (W)	<10
Argon plasma gas flow (l min^{-1})	0.0
Helium GC column flow (ml min^{-1})	~3.0
Pressure in expansion chamber (mbar)	0.038

Table 2.4 Data acquisition parameters used to obtain molecular spectra.

Mode	Peak Jumping
No. of masses monitored	150
Mass range (m/z)	60-250
Dwell time (ms)	1.28
No. of sweeps per time slice	2

2.2.3 Effects of Skimmer Distance

The normal skimming distance for an atmospheric pressure ICP-MS instrument is 8.6mm (this is the distance between the sampler orifice and the skimmer orifice). This distance is set in order to place the tip of the skimmer cone upstream of the Mach disc, formed behind the sampler orifice. Due to the difference in torch pressure and the size of the sampler orifice compared with a conventional torch, theory predicted[35] that the Mach disc would form at a different position, hence the optimal skimming distance would change. The skimming distance was altered by placing a series of copper spacers behind the skimmer mounting plate. The skimming distance was varied between 5.6mm and 11.6mm in 1mm increments and ion counts for $^{40}Ar^-$, $^{40}Ar^4He^+$ and the molecular ion peaks for chlorobenzene, iodobenzene and dibromobenzene were monitored.

2.2.4 Reagents and Standards

All standards were diluted to the desired concentration in hexane (HPLC grade, Rathburn Chemicals, Scotland, UK). Monobutyltintrichloride, dibutyltindichloride, tetrabutyltin, iodobenzene, chlorobenzene, 1,2 dibromobenzene, ferrocene, decane, undecane and naphthalene were obtained from Aldrich Chemicals (Gillingham, UK).

2.3 RESULTS AND DISCUSSION

The 150 W argon-helium torch was used successfully to obtain element selective chromatograms for three organo-tin compounds (Figure 2.2) and dibromobenzene (Figure 2.3). It should also be noted that these two spectra exhibited very little background noise with a background of only a few counts. This decrease in noise may be the result of fewer molecular ions being produced by the plasma gas compared with atmospheric argon plasmas, but could also be caused by the decrease in photon noise.

48
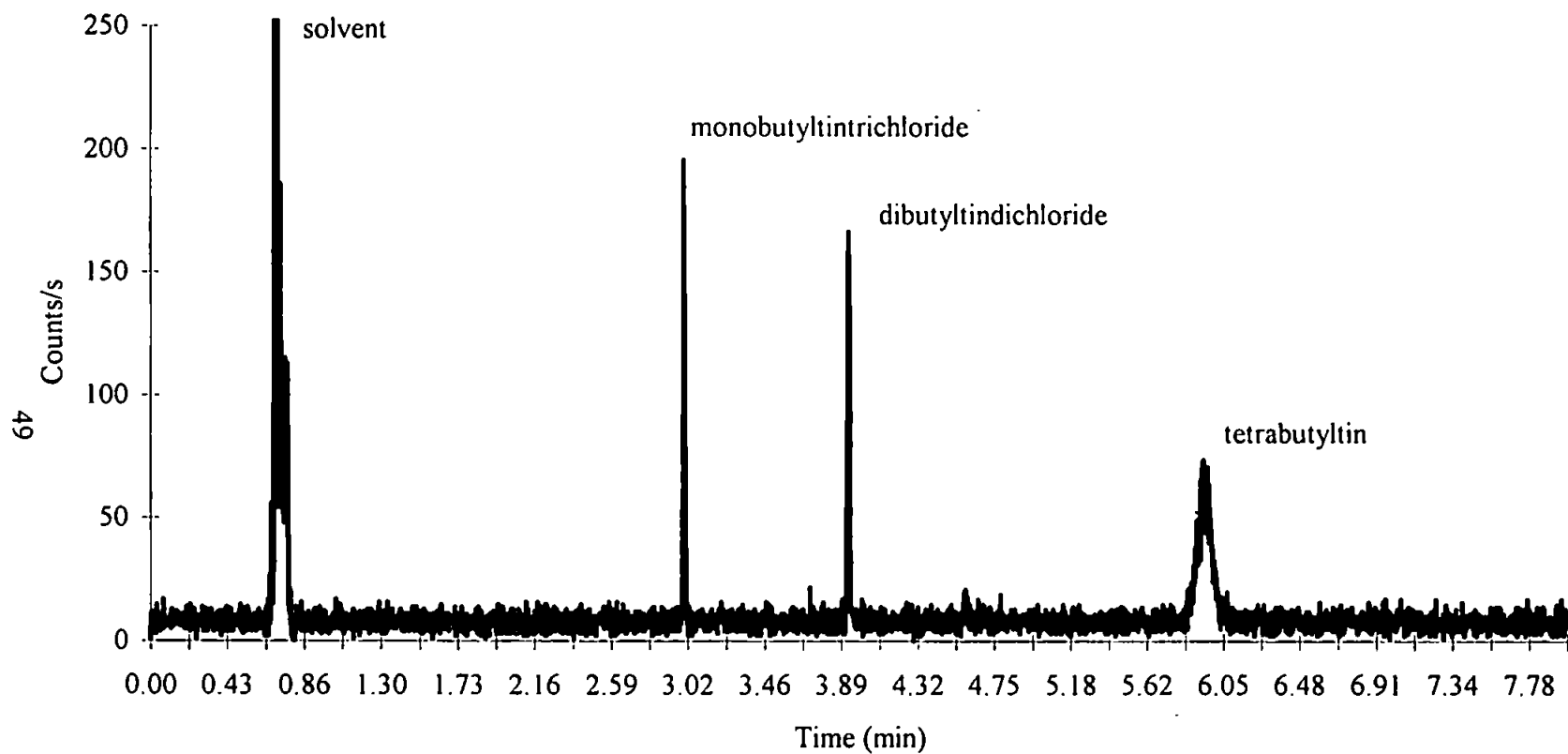
Figure 2.2   Element selective chromatogram at m/z 120 of butyltin species (250 ng on-column) using low pressure ICP-MS in the atomic mode.
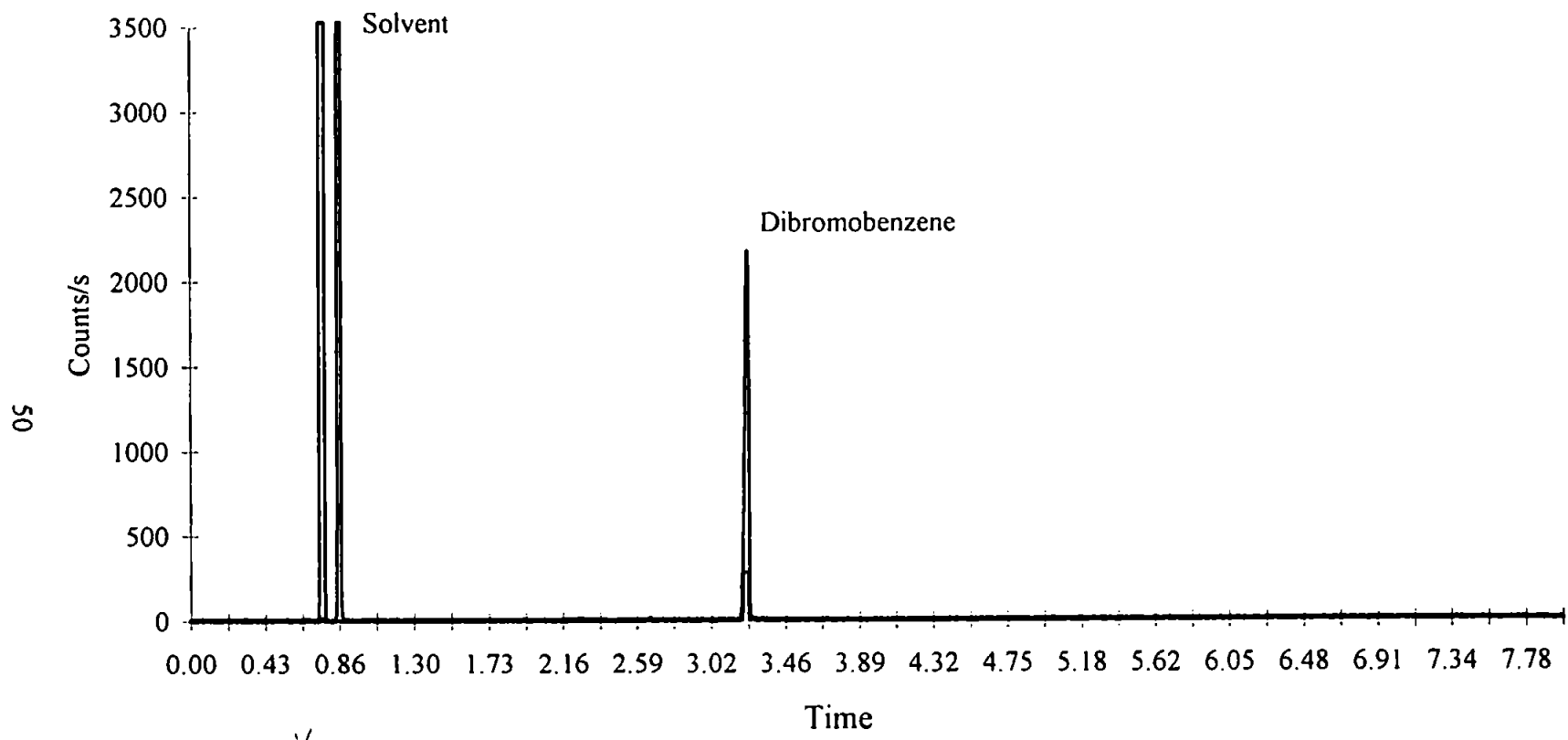
Figure 2.3   Element selective chromatogram at m/z 79 of dibromobenzene (250 ng on-column) using low pressure ICP-MS in the atomic mode.

The analyte signals obtained in the element selective mode were low considering the concentration of analyte injected into the gas chromatograph. This was thought to be caused by the non-optimal position of the skimmer cone in the low pressure system compared with operation at atmospheric pressure. Also, the ion optics did not seem to be as effective when tuning the ion beam from the low pressure plasma. The extraction lens was set at its minimum value (-100 V) even though the ion signal was still increasing as the voltage was decreased. The LP-ICP-MS system operating in the atomic mode has been investigated by previous workers[103]. Because of this, it was decided to concentrate on the use of the low pressure plasma ionisation source for the production of molecular fragment information, as this was considered the more challenging of the two applications.

Conversion of the low pressure system from an atomic ionisation source, to a molecular ionisation source was quick and simple. By removing the argon makeup gas, and thus reducing the pressure in the torch it was possible to sustain a low pressure helium-only plasma using ~25 W forward power. Multi-mass time resolved monitoring was performed using this plasma, and the total ion chromatograms for a series of different compounds are shown in Figures 2.4, 2.5 and 2.6. The mass spectra under each analyte peak resembled mass spectra produced by an electron impact ionisation source (Figure 2.7-2.13). The mass spectra obtained for the halobenzene compounds (Figures 2.7-2.9) closely resembled the EI source spectra. The chlorobenzene spectrum (Figure 2.7) shows a large abundance for the molecular ion compared with the EI spectrum, however, the iodobenzene (Figure 2.9) and dibromobenzene (Figure 2.8) spectra show a diminished molecular ion peak but relatively high signals for iodine and bromine. This suggests that the low pressure plasma source is more energetic than the 70 eV EI source. This would be considered a disadvantage as many organic compounds readily acquire high internal energies from a 70 eV EI source which

51
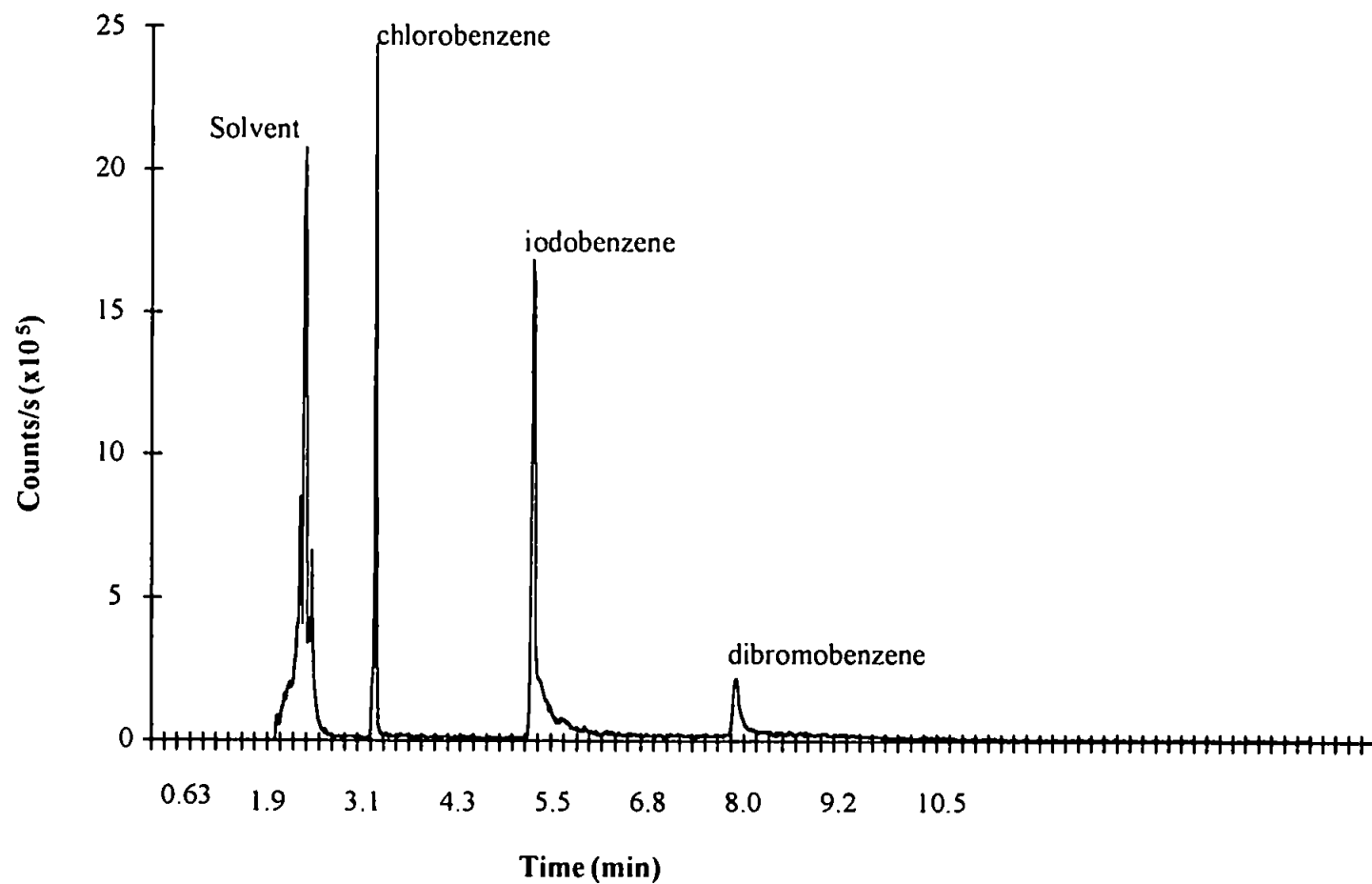
Figure 2.4   Total ion chromatogram for chlorobenzene, iodobenzene and dibromobenzene (250 ng on-column) using low pressure ICP-MS in the molecular mode
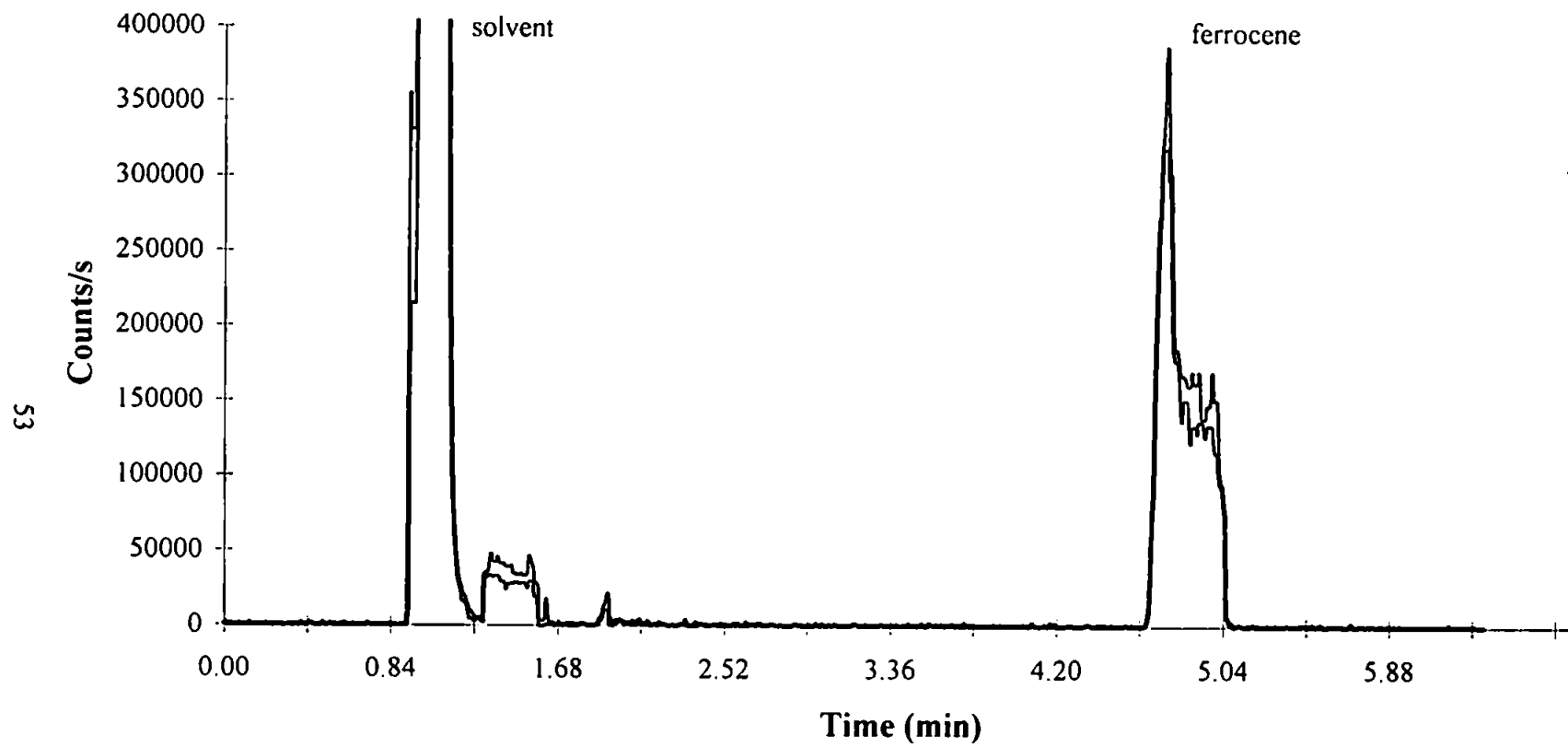
Figure 2.5: Total ion chromatogram of ferrocene (500 ng on-column) using low pressure ICP-MS in the molecular mode.
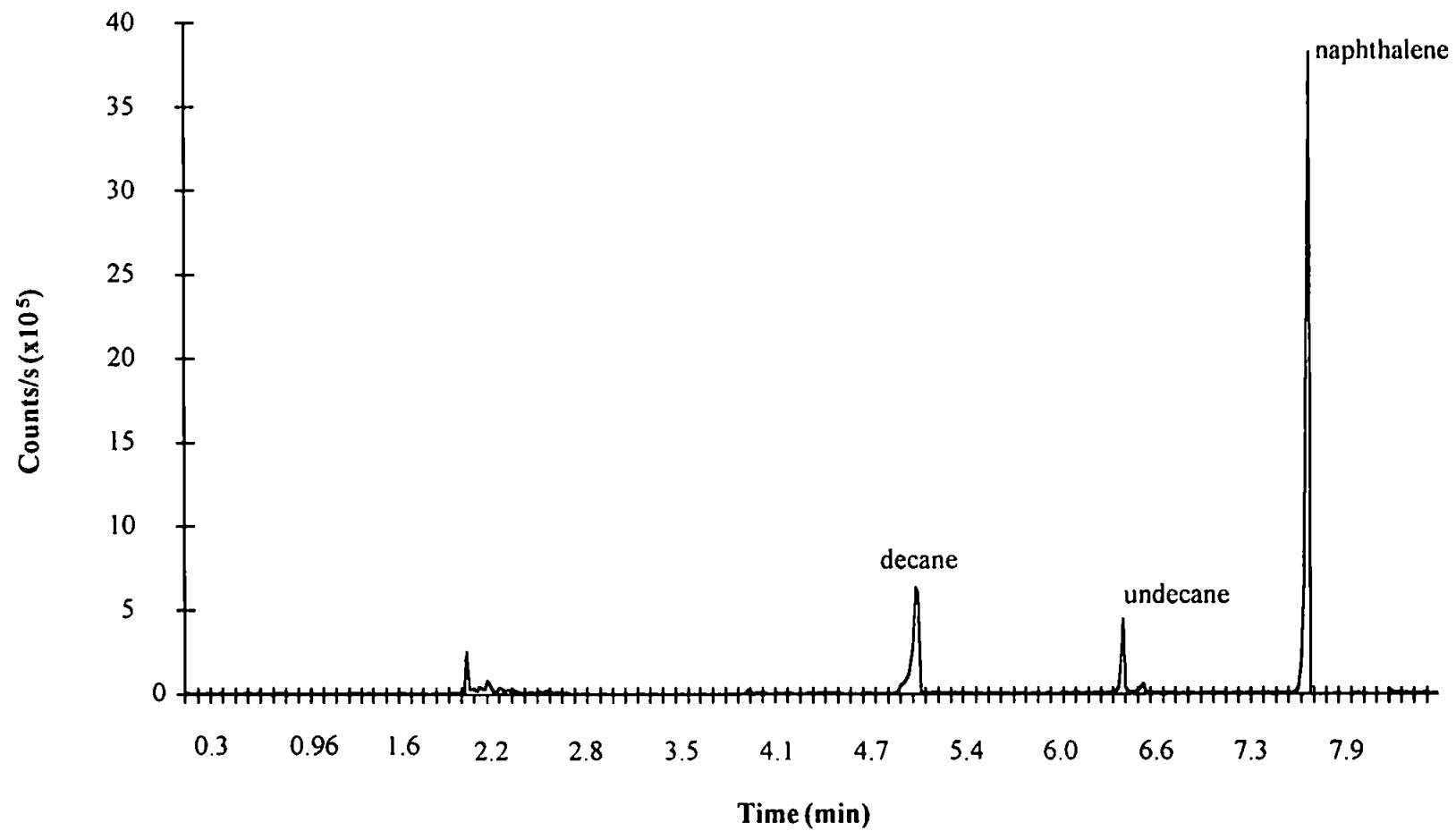
Figure 2.6 Total ion chromatogram for decane, undecane and naphthalene (500 ng on-column) using low pressure ICP-MS in the molecular mode
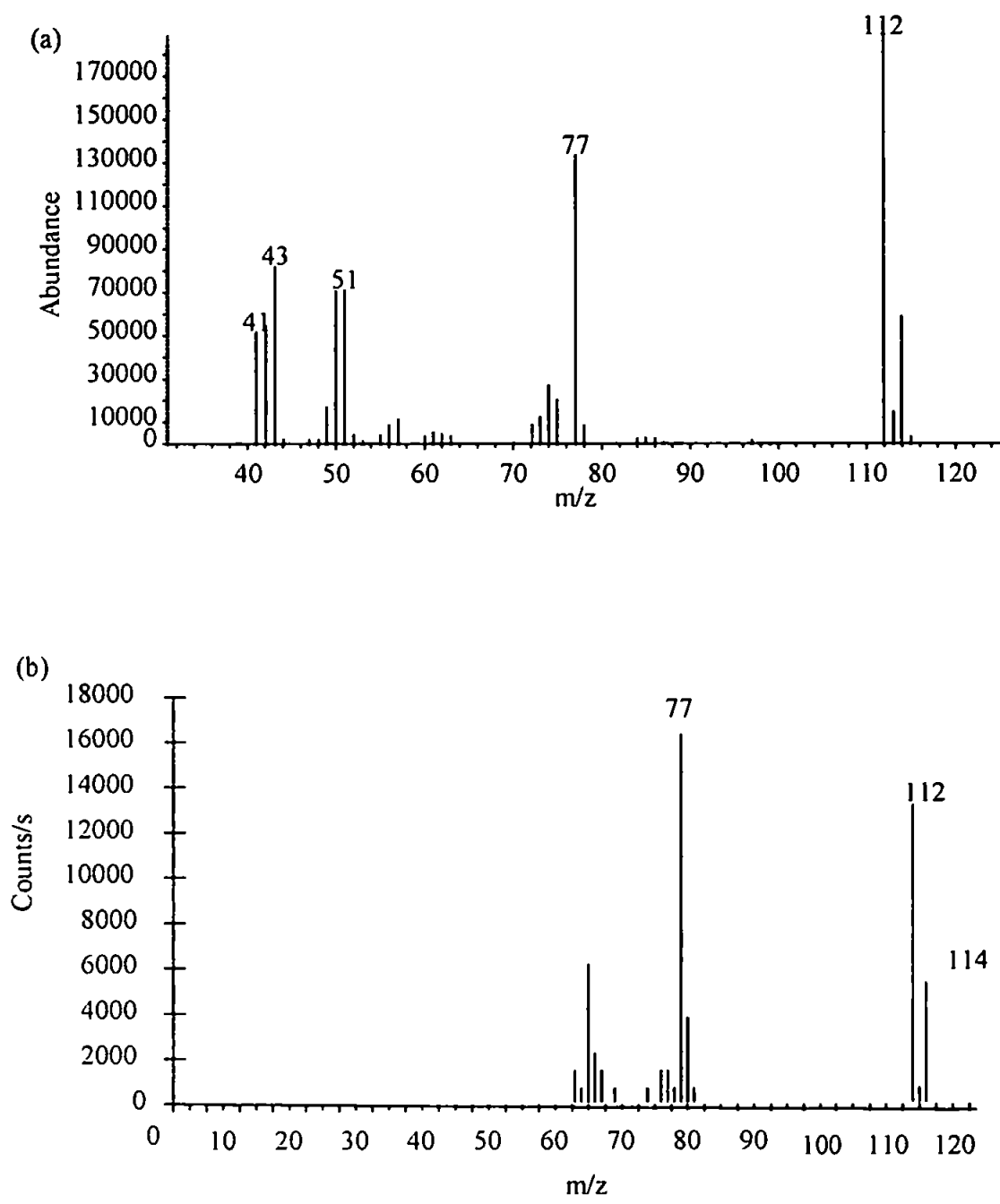
Figure 2.7   Fragmentation mass spectrum for chlorobenzene obtained using:
(a) electron impact at 70eV ; (b) low pressure inductively coupled plasma
operating in the molecular mode

(a)

(b)
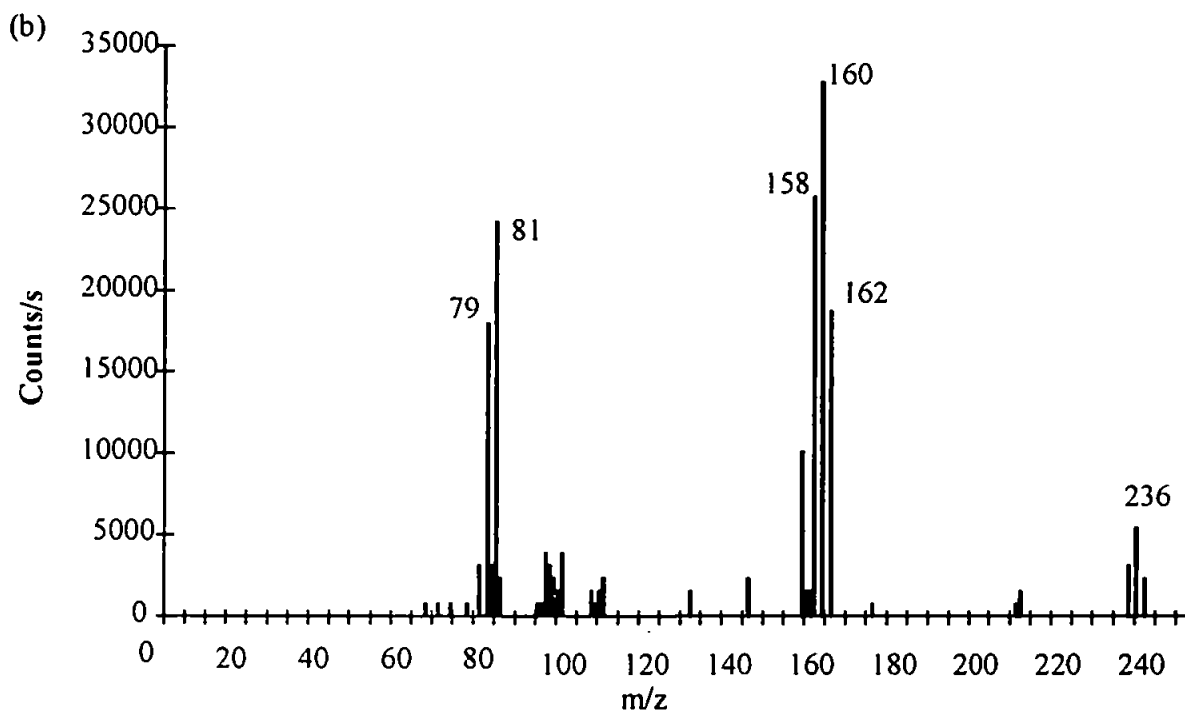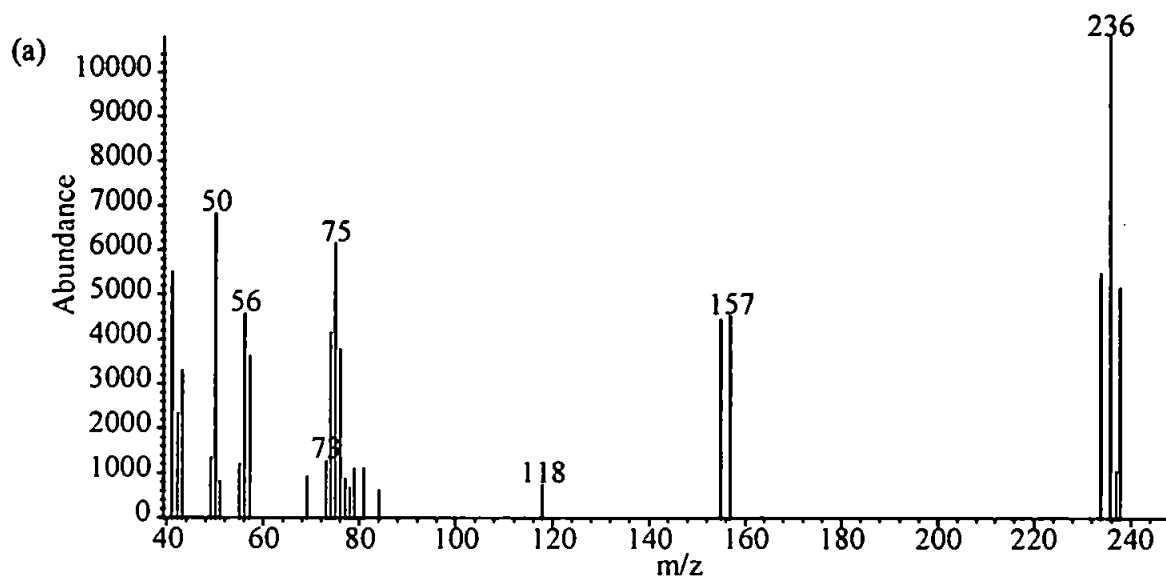
Fragment	Mass
$C_6H_5^-$	77
$Br^{79}Br^{79+}$	158
$Br^{79}Br^{81-}$	160
$Br^{81}Br^{81+}$	162
$Br^{79}Br^{81}C_6H_4^+$	236

Figure 2.8   Fragmentation mass spectrum for dibromobenzene obtained using:
(a) electron impact at 70eV ; (b) low pressure inductively coupled plasma
operating in the molecular mode
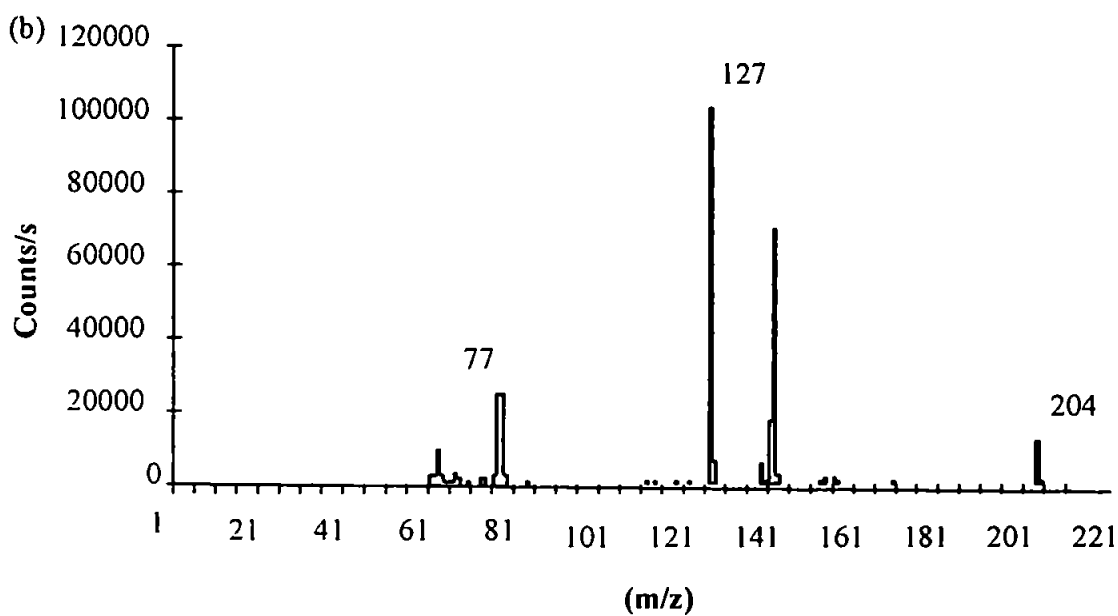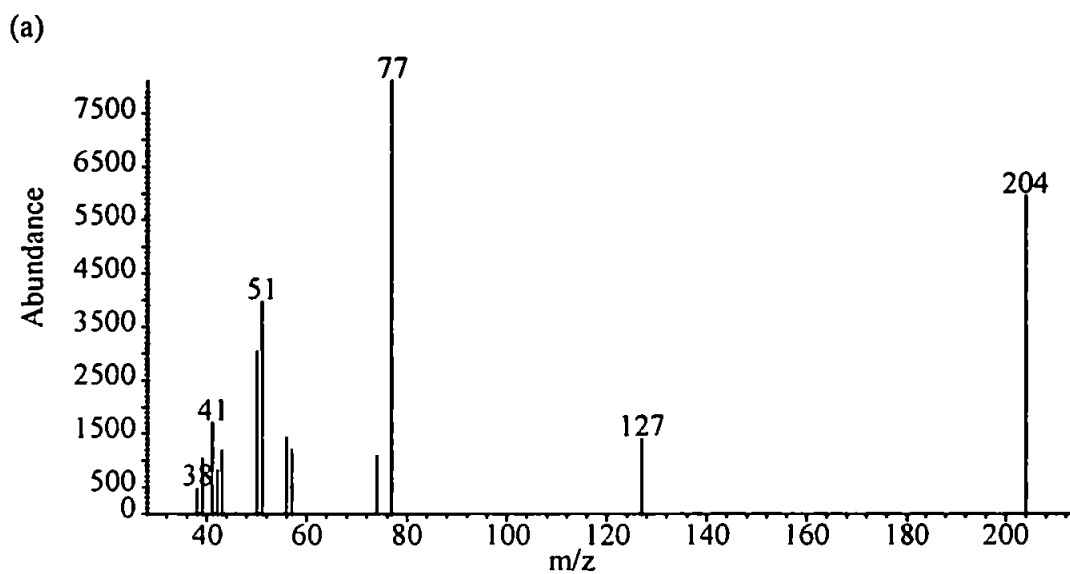
Figure 2.9 Fragmentation mass spectrum for iodobenzene obtained using:
(a) electron impact at 70eV ; (b) low pressure inductively coupled plasma
operating in the molecular mode
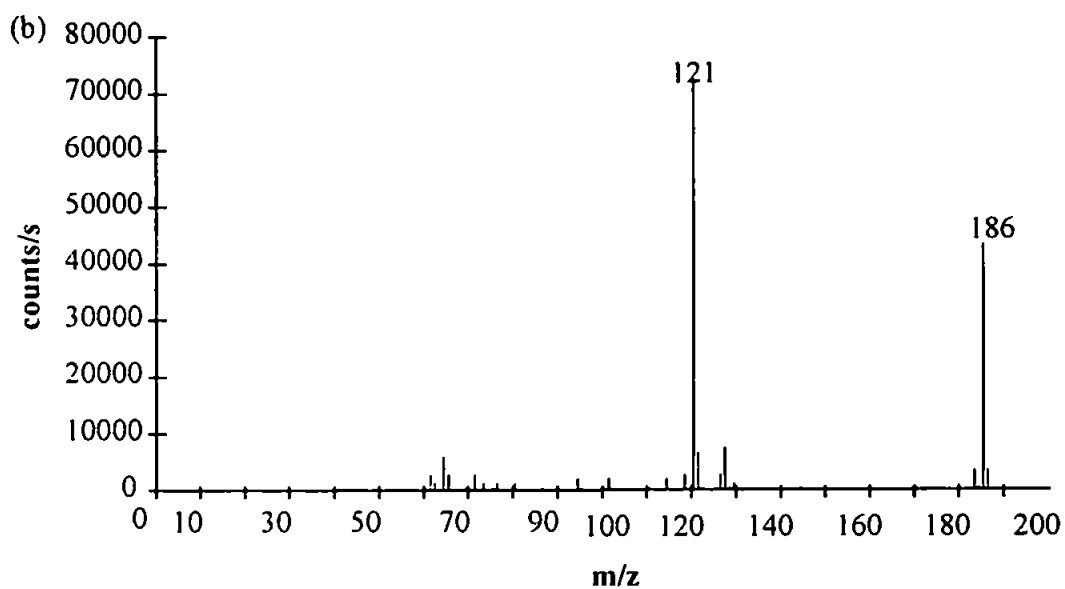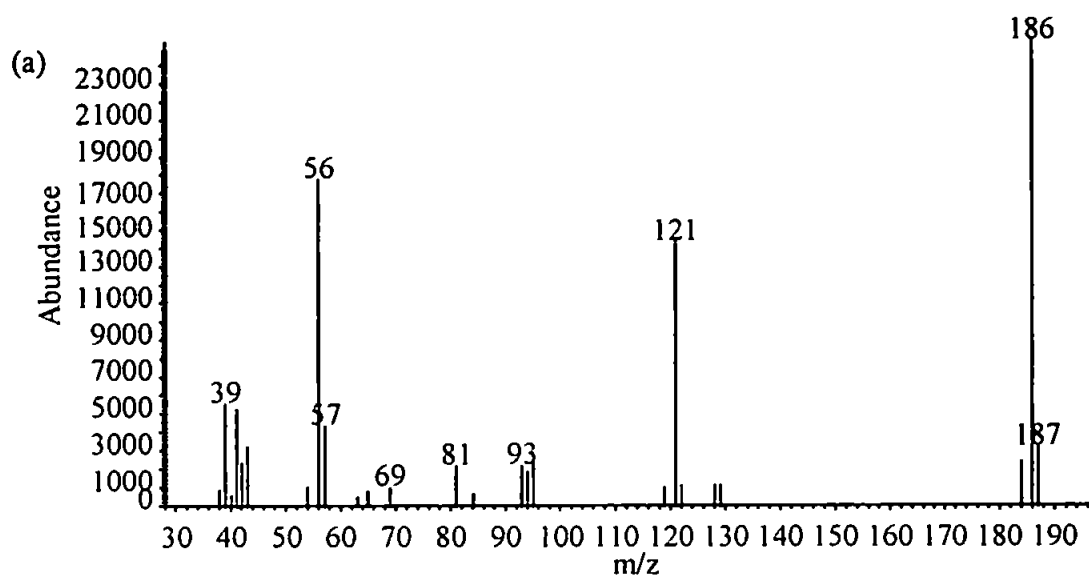
Fragment	Mass
$FeC_5H_5^+$	121
$Fe(C_5H_5)_2^+$	186

Figure 2.10 Fragmentation mass spectrum for ferrocene obtained using:
(a) electron impact at 70eV ; (b) low pressure inductively coupled plasma
operating in the molecular mode

(a)

(b)
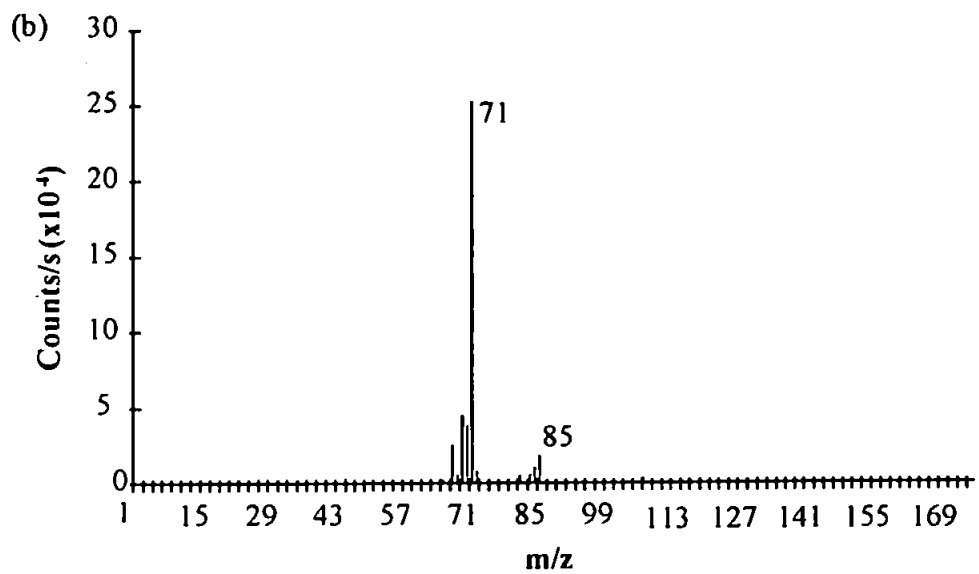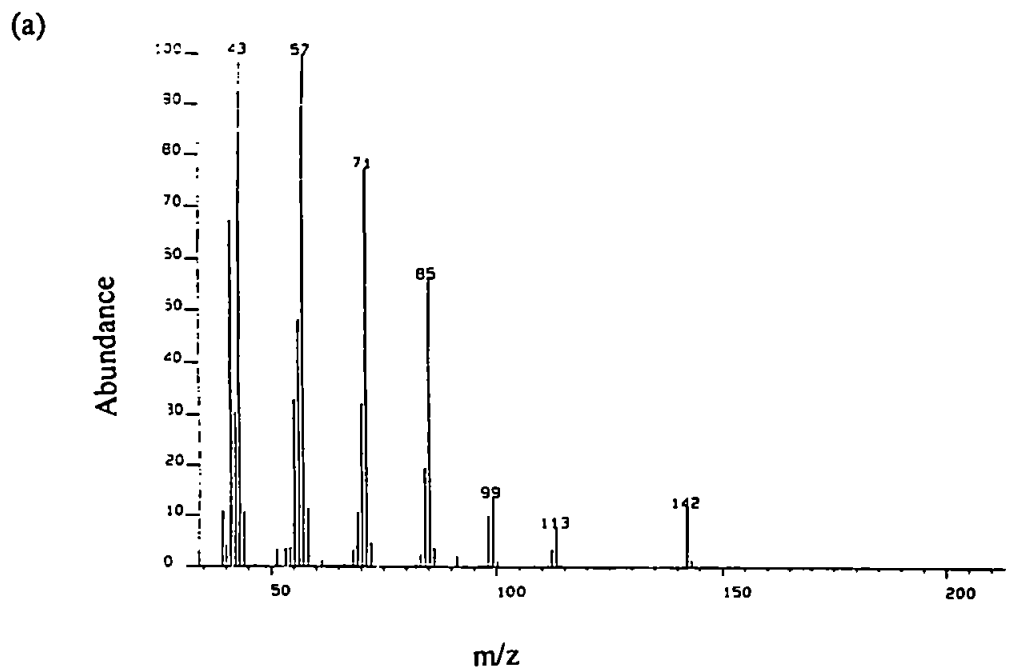
Fragment	Mass
$C_5H_{11}^+$	71
$C_6H_{13}^+$	85
$C_8H_{17}^+$	113
$C_{10}H_{22}^+$	142

Figure 2.11 Fragmentation mass spectrum for decane obtained using:
(a) electron impact at 40eV ; (b) low pressure inductively coupled plasma
operating in the molecular mode

Fragment	Mass
$C_5H_{11}^+$	71
$C_6H_{13}^+$	85
$C_8H_{17}^+$	113
$C_{11}H_{24}^+$	156
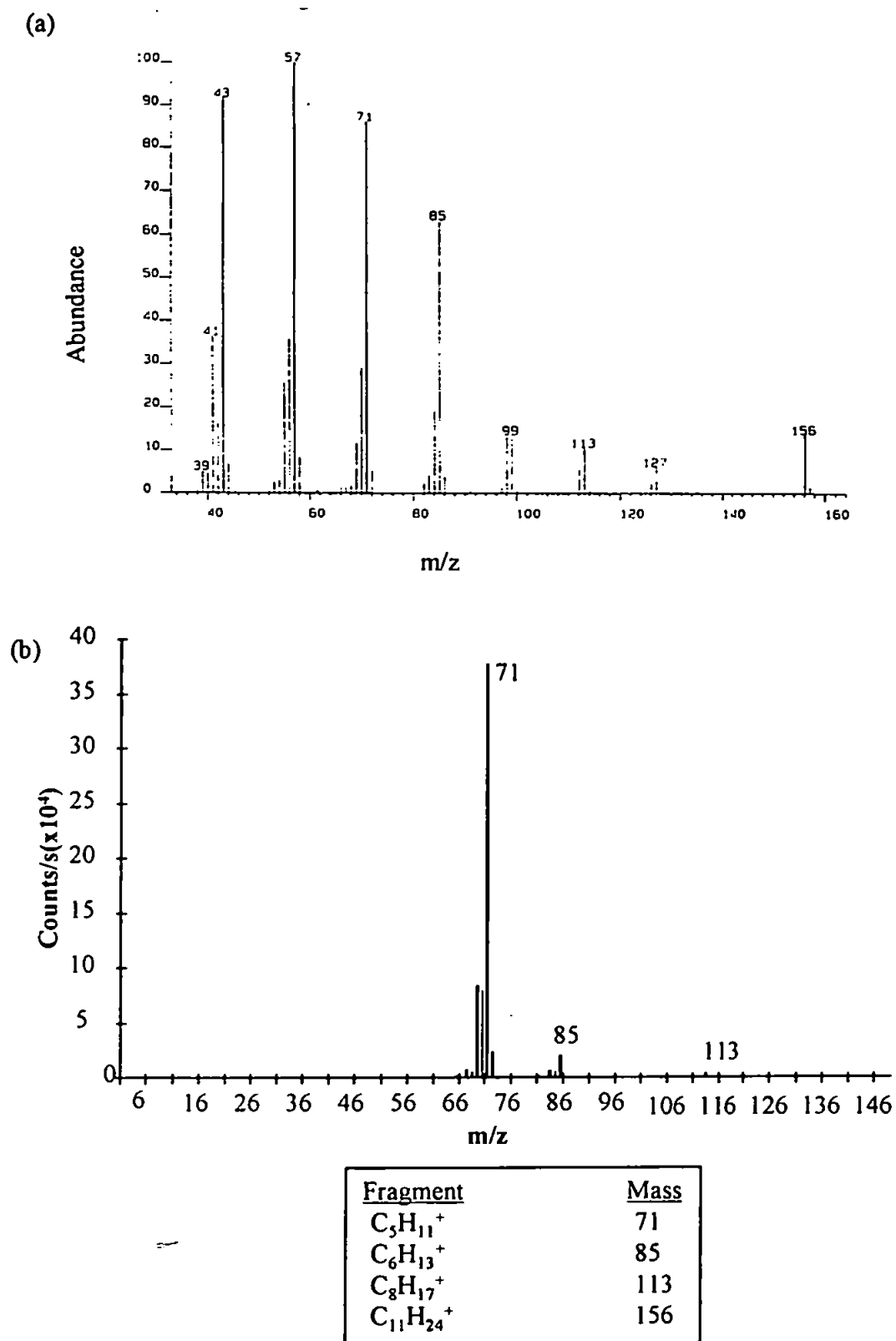
Figure 2.12 Fragmentation mass spectrum for undecane obtained using: (a) electron impact at 40eV ; (b) low pressure inductively coupled plasma operating in the molecular mode
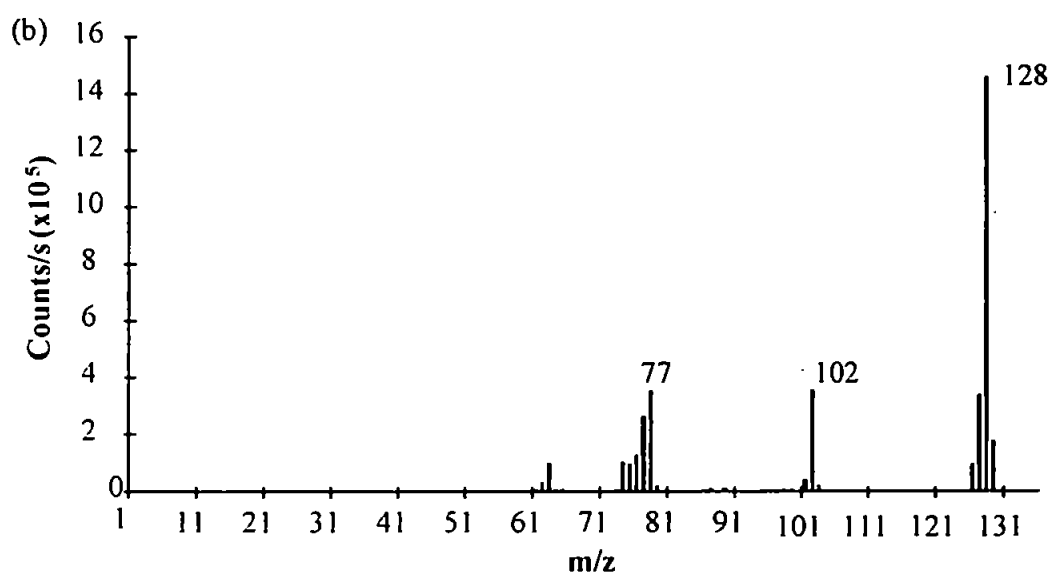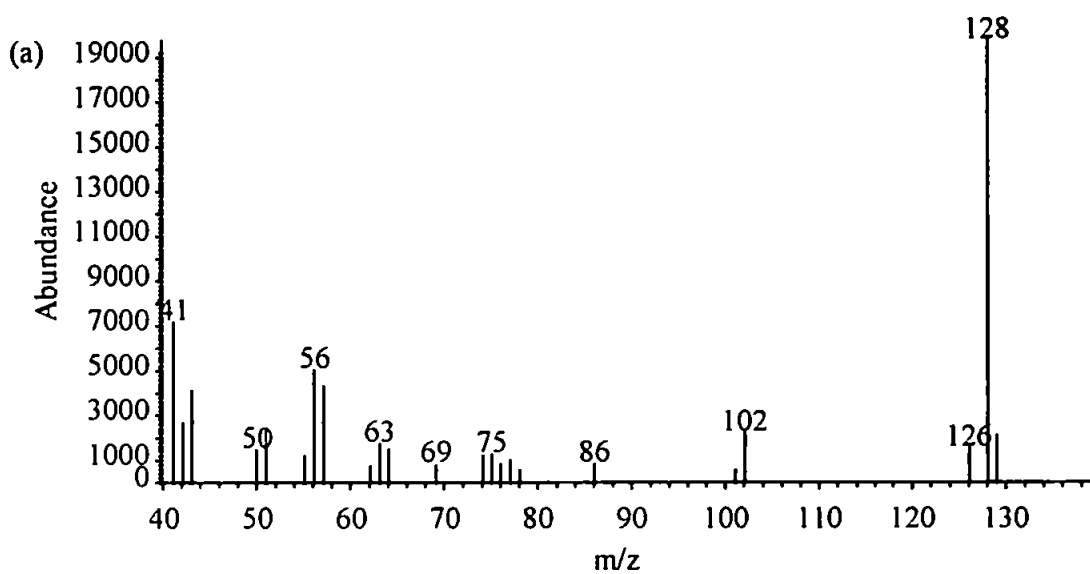
Fragment	Mass
$C_6H_5^+$	77
$C_8H_6^+$	102
$C_{10}H_8^+$	128

Figure 2.13 Fragmentation mass spectrum for naphthalene obtained using:
(a) electron impact at 70eV ; (b) low pressure inductively coupled plasma
operating in the molecular mode

61

leads to excessive fragmentation of the analyte molecule rendering molecular weight determination difficult. The mass spectrum for dibromobenzene (Figure 2.8), obtained by the LP-ICP, differs from the EI source in the 158-162 m/z range. The appearance of Br_2 (158, 160, 162 m/z) signals suggest that molecular recombinations occurred in either the plasma or the ion sampling interface. Also an unidentifiable fragment in the LP-ICP spectrum of iodobenzene (Figure 2.9) at 142 m/z suggests the formation of molecular clusters. This type of cluster formation is indicative of non-optimum skimming of the plasma as clusters may form in the barrel shock, Mach disc and subsequent shock regions. Skimming should ideally be performed upstream of these structures.

A 250 ng on-column injection of ferrocene yielded no molecular spectra so a greater amount of analyte was injected. The resulting mass spectrum (Figure 2.10) was again similar to that obtained by EI source. This suggests that a form of "self ionisation" was occurring, whereby a high concentration of analyte altered the ionisation conditions in the plasma. This will cause problems when trying to use the low pressure plasma in the molecular mode to provide quantitative information. Such a problem is highlighted in Figure 2.10 where over 23000 counts were obtained for the molecular ion peak of ferrocene but half that concentration failed to produce a molecular ion. The fragmentation of two alkanes at high concentration can be observed in Figures 2.11 and 2.12. Compared with the naphthalene spectrum (Figure 2.12), which was taken from the same chromatographic run, fragmentation is excessive. However, it should be noted that the EI source used to produce the comparative spectra was operated at 40 eV, as higher voltages caused the destruction of the molecular ions.

The helium-only plasma was very susceptible to decoupling of the RF power from the plasma gas. The RF generator was designed to operate at 1500W, so the stability of the generator output at ~25W was poor. Also, with such a small torch, the load coil was too large for optimal coupling and the matching network had to be tuned constantly to prevent the helium plasma from extinguishing. Additionally, during a chromatographic run the pressure in the expansion chamber dropped, indicating that the pressure in the torch had also dropped. At the same time the plasma discharge, which was normally confined within the region of the load coil, extended down the whole length of the torch and when this occurred all fragment ions were lost.

An investigation into the effect of skimming distance was performed in order to optimise skimming, and hence improve analyte signal. As the skimmer distance was decreased the signal did increase for the dibromobenzene (236 m/z) and the iodobenzene (204m/z), but not greatly (Figure 2.14). The signal for chlorobenzene seemed to give a maximum at *ca.* 10.65 mm. This increase could have been caused by variation in plasma power coupling since this was difficult to control precisely. The signal for 40 and 44 m/z did increase greatly as the skimming distance decreased. However, these species did not originate from the analyte, and a more likely cause of this increase was a small vacuum leak leading to the presence of carbon dioxide (44 m/z) in the plasma. It should also be noted that the stability of these signals was poor with relative standard deviations of approximately 20%. Again the most likely cause of this was instability in the plasma.
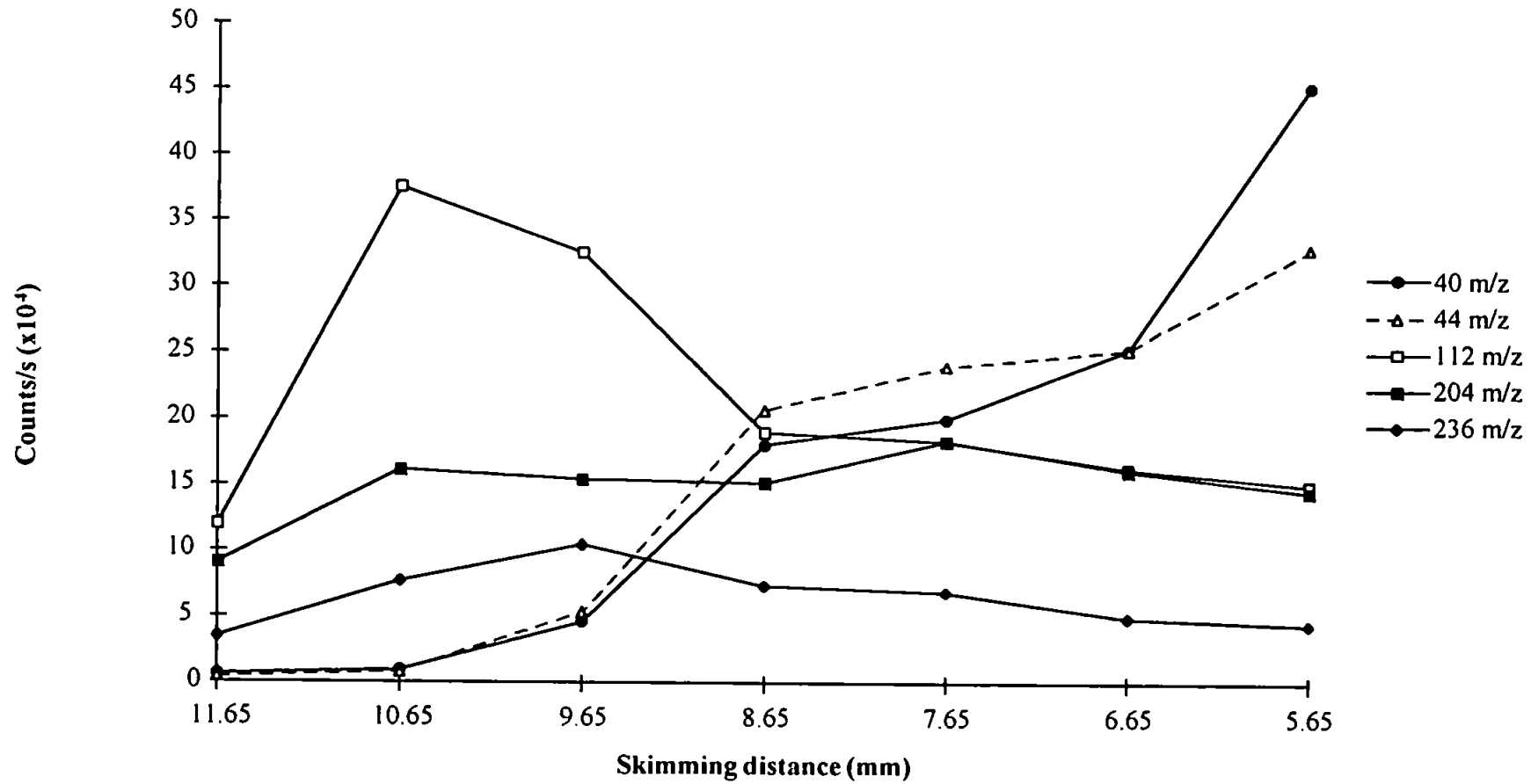
Figure 2.14 Effect of skimming distance on molecular ion signals formed in the low pressure plasma operated in the molecular mode.

2.4 CONCLUSIONS

The low pressure plasma source has been used successfully for the production of atomic and molecular mass spectra with simple modification to commercial instrumentation. Molecular spectra for a small but varied range of analytes yielded spectra similar to those obtained by conventional EI source mass spectrometry. While this was possible the initial studies have highlighted shortcomings in using such instrumentation.

These shortcomings can be summarised as follows:

(i)   The radio frequency generator, matching network and load coil configuration were inadequate to sustain such a low pressure helium plasma. This was not unexpected as they were designed to sustain a 12 to 18 l min^{-1} atmospheric argon plasma at between 1000 and 2000 W.

(ii) The ion sampling interface was designed for sampling ions from an atmospheric pressure plasma. This sampling process is sensitive to pressure and temperature changes so is not ideal for use with the low pressure plasma.

(iii) The quadrupole analyser of the mass spectrometer had a mass range from 5 to 255 m/z. This was adequate for atomic analysis, however, many organometallic species have molecular masses which greatly exceed this upper limit. Hence using such an instrument in its molecular mode would be restricted to the analysis of low molecular weight compounds.

DESIGN AND CONSTRUCTION OF A LOW PRESSURE-INDUCTIVELY COUPLED PLASMA-MASS SPECTROMETER

CHAPTER 3 - DESIGN AND CONSTRUCTION OF A LOW PRESSURE-INDUCTIVELY COUPLED PLASMA-MASS SPECTROMETER.

3.1 INTRODUCTION

It has been shown that a commercial instrument can easily be altered to sustain and monitor ions from a LP-ICP. Initial studies have shown that the LP-ICP is capable of producing elemental ions of compounds introduced into it, and molecular fragment ions which give structural information of the compound. This instrument yielded detection limits in the picogram range, when operating in the atomic mode, for a series of organometallic and organohalide compounds. However, linear calibration and low level detection was not possible when operating in the molecular mode.

Initial studies have shown that the LP-ICP can be used as a tuneable ion source for MS, but many changes to the commercial instrumentation would be necessary to make it a viable analytical tool. First, plasma formation and stability must be improved if the LP plasma is to be operated in both modes. Therefore, a rf generator and matching network capable of supplying a stable low power, and of coupling this power into a variety of gases, is required.

The ion extraction process, which transports the ions from the plasma to the analyser of the mass spectrometer, is a pressure dependent process. Therefore the ion sampling interface will require redesign to maximise the ion flux from the LP-ICP to the analyser.

The mass analyser of commercial ICP-MS instruments have an upper mass range of 255 m/z. This is sufficient for elemental analysis, however, even relatively low mass organometallic compounds can easily exceed this limit for molecular ions. Therefore, a mass analyser with an upper mass limit capable of transmitting large organometallic molecular

ions to the detector, and capable of unit mass resolution across its m/z transmission range is required.

The data acquisition software must be capable of rapid multi-ion scanning, enabling the detection of molecular and fragment ions, as well as selected ion monitoring (SIM) enabling trace analysis. Both of these functions should be possible in a time resolved manner, providing atomic and molecular information of transient signals, such as those exhibited by chromatographic sample introduction methods. Hence, it was decided to construct a dedicated LP-ICP-MS instrument to fulfil all the above requirements.

3.2 DESIGN AND CONSTRUCTION OF INSTRUMENT

3.2.1 Low Pressure Plasma Formation

Commercial ICP-MS instruments were originally designed to form argon plasmas at gas flow rates of between 15 and 17 l min^{-1} and forward powers of between 1300 and 1500 W. Most commercial instrument manufacturers use a 1.5 kW radio frequency (rf) generator with a matching network designed to couple rf power into an atmospheric argon plasma. With such a generator it is impossible to form a stable low pressure plasma, and the matching network is inappropriate for plasmas of gases other then argon at reduced pressures. Hence a 1.5 kW, 27.12 MHz rf generator was modified to give a stable output between 1 and 300 W, and a new rf matching network was purchased (RF Applications Ltd., Eastbourne, East Sussex, UK) to enable coupling of rf power from the modified generator into the low pressure plasma source.

The new rf matching network was much simpler in design than a conventional torch box of a commercial instrument. Due to the reduced power, the load coil did not require water cooling. This enabled different load coil geometries to be investigated for stable low pressure plasma formation. The load coil of the commercial ICP-MS and in chapter 2 was a

water cooled 3.175mm o.d. copper tube which was coiled 2.5 times. The diameter of the coil is 25 mm, which allows a conventional torch of 22 mm diameter to fit snugly inside. The low pressure ICP torch consisted of a 140 mm long quartz tube of 12.7 mm o.d., with a 6.35 mm o.d. side-arm through which the plasma gas could be introduced. Therefore the conventional load coil design was not considered to be optimal.

The low pressure sampling cone was machined from aluminium (Technical Services Mechanical, University of Plymouth), had a 2 mm orifice and an Ultra-Torr fitting for 12.7 mm pipe, to form a vacuum seal between the low-pressure torch and sampler. The low pressure torch was interfaced at its rear end with a gas chromatograph (PU 4550, Pye Unicam, Cambridge, UK) fitted with an on-column injector, by way of a heated transfer line held at a temperature of 250°C. The GC capillary extended through the transfer line and into the torch, the vacuum seal being made using a combination of Ultra-Torr and Swagelok fittings with graphite ferrules.

3.2.2 Ion Sampling Interface

Ion sampling interfaces, for plasma source mass spectrometry, have been designed using theory derived from molecular beam studies[138]. These studies give a detailed description of gas flow and kinetics, when sampled through small diameter orifices.

The sampling of the plasma gas, and hence the ions it contains, is performed through a series of chambers which are held at consecutively lower pressure. The gas is sampled and transported from an area of high pressure to an area of lower pressure through a series of small orifices. An in-depth study of the effect of orifice size and shape has been performed by Campargue[125].

In order to sample gas from an area of high pressure into an area of lower background pressure the gas must pass through a sampler orifice. On passing through this orifice the gas expands almost adiabatically, which causes a decrease in gas density and kinetic temperature, the enthalpy of the source gas is converted into directional flow and the gas temperature drops[139]. The gas flow speed increases and exceeds the local speed of sound and a supersonic, free jet is formed. The free jet structure is approximately conical in shape with its apex originating at the sampler orifice. The base of the cone is called the Mach disc and this is the region where the sampled gas collides with the background gas causing the gas flow to become subsonic and the gas kinetic temperature to rise again. The area between the sampler orifice and the Mach disc is known as the zone of silence. It is thought that in the zone of silence, the sampled gas is representative of the plasma gas, so it is in this region that the second orifice, called the skimmer, is placed. Once skimmed, the ions are extracted and focused using a series of electrostatic lenses. A diagram of the ion sampling process is shown in Figure 3.1.

The flow of plasma gas through the sampler orifice is given by[140];

$$U_o = \frac{\pi . f(\gamma) N_A D_o^2 P_o}{4(MRT_o)^{\frac{1}{2}}} \qquad 3.1$$

Where U_o is the flow of gas through the sampler in molecules sec^{-1}; γ is the ratio of the heat capacities at constant pressure and constant volume; N_A is Avogadro's constant; D_o is the sampler orifice diameter (m); P_o is the torch pressure (Pa); M is the relative molecular mass of the plasma gas (Kg mol^{-1}); R is the gas constant; and T_o is the source temperature.

$$X_m = 0.67 \, D_0 \, (P_0/P_1)^{1/2}$$
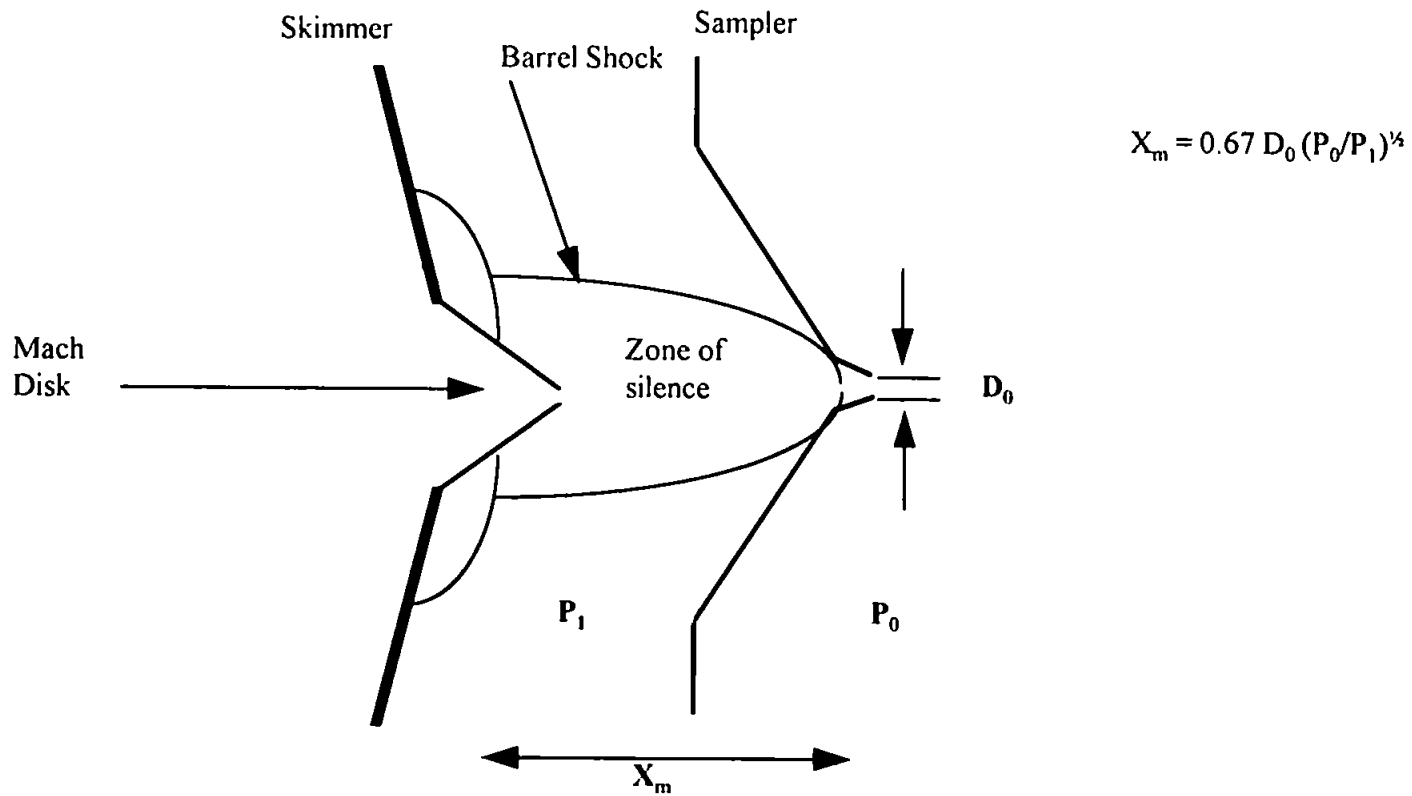
Figure 3.1   Diagram showing the expansion process in ion sampling for ICP-MS.

The function f(γ) is given by,

$$f(\gamma) = \gamma^{\frac{1}{2}} \left[\frac{2}{(\gamma+1)} \right]^{\frac{\gamma-1}{2(\gamma-1)}}$$ 3.2

The position of the first Mach disc down stream from the sampler orifice is given by[125];

$$X_m = 0.67 D_o \left(\frac{P_o}{P_1} \right)^{\frac{1}{2}}$$ 3.3

where P_1 is the pressure in the expansion stage (Pa). In order for a representative sample to be obtained from the plasma, the skimmer orifice must be placed upstream of the first Mach disc. Campargue[125] gives the skimming distance which yields maximum beam intensity (X_s) as,

$$X_s = 0.125 D_o \left[\left(\frac{1}{Kn} \right) \left(\frac{P_o}{P_1} \right) \right]^{\frac{1}{3}}$$ 3.4

where Kn is the Knudsen number at the sampling orifice, P_o is the torch pressure (Pa) and P_1 is the pressure in the expansion stage. The Knudsen number is given by;

$$Kn = \frac{\lambda}{D}$$ 3.5

where D is the diameter of the orifice through which the gas passes and λ is the mean free path given by[126];

$$\lambda = \frac{\left(\frac{16}{5} \right) \eta}{NM \left(\frac{2\pi KT}{M} \right)^{\frac{1}{2}}}$$ 3.6

where η is the viscosity coefficient of the plasma gas, N is the number density, M is the mean molecular mass of the plasma gas (g), K is the Boltzmann constant and T is the local temperature (K)[126]. Campargue[125] has calculated this value to be approximately $0.75X_m$.

The flow of gas through the skimming orifice is related to the gas flow through the sampler by[140];

$$U_s = U_o f(\gamma) \left(\frac{D_s}{X_s} \right)^2 \qquad 3.7$$

where D_s is the skimmer orifice diameter and X_s is the sampler to skimmer orifice distance (m).

Hoglund and Rosengren[140] state that the flow conditions, as described in equations 3.1-3.7, prevail when the pressure ratio across the sampler orifice is greater than 2, or analytically for an ideal gas when;

$$\frac{P_o}{P_1} \geq \left[\frac{\gamma + 1}{2} \right]^{\frac{\gamma}{\gamma - 1}} \qquad 3.8$$

Typical gas flow rates through the sampler and skimmer orifices, for atmospheric and low pressure plasmas were calculated and are shown in Table 3.1.

When designing a new ion extraction interface, these flow conditions have to be considered carefully, because the vacuum pumps used to maintain operating pressures in the interface and analyser sections of the instrument will require sufficient pumping to remove the gas flowing through the sampler. The vacuum expansion chamber was manufactured in-house (Technical Services Mechanical, University of Plymouth) and had two pumping ports which were connected to two separate rotary pumps (Leybold D16B). This enabled a pressure of 2×10^{-2} Torr to be maintained inside the sealed interface.

The most important criterion for the construction of a new ion sampling interface is the distance between the sampler and the skimmer orifices. This distance must be no greater

Plasma Gas	T_o (K)	P_o (Pa)	P_1 (Pa)	D_o (mm)	D_s (mm)	X_m (mm)	X_s (mm)	U_o (atoms sec^{-1})	U_s (atoms sec^{-1})
Argon	5000	101000	200	1	0.7	15	7	8.5×10^{20}	6.17×10^{18}
Helium	2200	101000	200	0.46	0.7	6.9	4	8.6×10^{20}	1.9×10^{19}
Argon	1000	1300	200	2	0.7	3.3	3	9.7×10^{19}	3.8×10^{18}
Helium	330	27	4	2	0.7	3.5	3	1.1×10^{19}	4.3×10^{17}

Table 3.1   Comparison of gas flows through the sampling orifices of atmospheric and low pressure ICPs, under typical operating conditions.

T_o is the source temperature, P_o is the source pressure, P_1 is the expansion stage pressure, D_o is the sampler orifice diameter, D_s is

the skimmer orifice diameter, X_m is the position of the Mach disc, X_s is the skimmer to sampler distance, U_o is the gas flow through

the sampler, and U_s is the gas flow through the skimmer.

then 0.75 X_m, X_m being the distance downstream from the sampler orifice of the first Mach disc, given by equation 3.3. The interface must be able to maintain vacuum conditions suitable for Mach disc formation and hence ion sampling, so must be vacuum tight.

Theory predicted that the Mach disc would occur at about 3.3 mm behind the sampling orifice when argon was used as a plasma gas at a flow of 1000 cm^3 min^{-1}. However, studies by Gray[140] and Luan et al.[141] indicated that subsidiary barrel shocks and Mach discs form downstream of the primary Mach disc when $P_0/P_1 < 80$ for an argon ICP. Because the pressure in the torch and the expansion region can change quite considerably when different plasma gases are used (e.g. in this study a plasma formed with helium at a flow rate of 3 cm^3 min^{-1} was investigated), the skimmer, which was a conventional nickel skimmer for a VG PlasmaQuad II with a 0.7 mm orifice, was mounted on a copper plate which could be moved back and forth by adding or removing copper spacing washers. Hence, the sampler/skimmer spacing could be optimised empirically.

Ideally the distance from the skimmer to the analyser should be as short as possible. However, even over a short distance the extracted ion beam can diverge rapidly. To combat this, two charged cylindrical ion lenses were placed behind the skimmer to transport and focus the ions from the skimmer tip to the remaining ion lenses. The downstream end of the expansion stage was machined with a 40mm KF flange which was connected to a gate valve (VAT Vacuum Products Ltd, Finchley, London, UK) using a viton O-ring and a customised brace. The gate valve was then connected to the analyser section of a Hewlett Packard MSD (HP 5970 MSD, Hewlett Packard, Stockport, Cheshire, UK), completing the vacuum stages of the instrument. Diagrams of the expansion interface are shown in Figures 3.2- 3.5.

3.2.3 Ion Optics

Once the ions have entered the skimmer tip, it is necessary to extract and focus the ions to the analyser. The ion focusing lenses are crucial for the overall sensitivity of the instrument because scattered ions will not be detected. Ion focusing is achieved by subjecting the charged ions to constant electric fields. These electric fields have an accelerating effect on the ions, but if the field strength is too high, ions may be accelerated to such an extent that their residence time in the analyser is not sufficient for effective mass analysis.

In order to construct an effective ion optical array it was necessary to calculate the path taken by ions in the electrostatic fields. To do this, several assumptions must be made about the conditions, electric fields, and ion interactions:

i) an ion is a free particle with a positive charge;

ii) ionic velocities are small in comparison with the speed of light;

iii) the density of the ion beam is not great enough to induce space charge (ion-ion repulsions);

iv) the presence of the ions brings about no appreciable change to the electrostatic fields they are subjected to;

v) vacuum conditions are assumed to be adequate to give the ions the necessary mean free path.

The movement of a charged body through an electric field is defined by Newton's second law of motion, which states that:

The rate of change of momentum of a body is proportional to the resultant applied force, and is in the same direction as this force.

$$F = ma \qquad\qquad a = \frac{dv}{dt} \qquad\qquad 3.9$$

where F is the force, m the mass of the ion, v is the velocity and a the acceleration of the body. Firstly it is necessary to calculate the potential variations across the electric field and the effects of these potentials on the ion trajectories.

Electrostatic lenses, placed in a vacuum chamber and set at specific potentials, will affect the surrounding space by causing a gradient of equipotentials in the regions between different lenses. These equipotentials are the refracting surfaces of electrostatic ion optics, and are analogous to the lateral refracting surfaces of glass lenses in ordinary light optics. The potential distributions between lenses can be calculated using LaPlace's conditions and relaxation methods[142]. For a two dimensional array, a grid of equal sized boxes is created. The potential at any one box can be calculated from its four nearest neighbours, by the equation

$$V_0 = \frac{1}{4}(V_1 + V_2 + V_3 + V_4)$$ 3.10

Where V_0 is the newly calculated potential of the central grid and V_1 to V_4 are the potentials of its four neighbours.

	V_1	
V_2	V_0	V_4
	V_3	
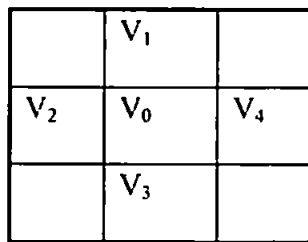
So by choosing the starting point to be an electrode of known potential, the potential of all points between the electrodes can be calculated by applying equation 3.10 to all lattice points repeatedly until the change in the lattice point potential is successively less than a pre-set value. The smaller this set figure the longer the relaxation calculations will take, but the more accurate the potential array will become. For even greater accuracy a lattice with even smaller intervals may be chosen[142].

Once the potential (volts) of each point inside the electrostatic array is known, it is possible to trace the path of ions through the array by using Snell's law,

$$N \sin \alpha = N' \sin \alpha' \qquad\qquad 3.11$$

Where N is the refractive index of the medium in front of the lens, N' is the refractive index of the lens, α is the angle of the incident ion and α' is the angle of the refracted ion. The spaces between equipotentials V_1 and V_2, V_2 and V_3, V_3 and V_4, etc., are assumed to be regions of constant refractive indices,

$$N_1 = \sqrt{V_1}, \qquad N_2 = \sqrt{V_2}, \qquad N_3 = \sqrt{V_3}, \text{ etc. }^{[143]}$$

The angle of the ion incidence, α_1, with the first equipotential, V_1, may be measured with a protractor. The corresponding angle of refraction, α_1', can then be calculated using Snell's law and plotted on the other side of the equipotential. The paths between equipotentials are drawn as straight lines. The same procedure is applied to α_2 and α_2' at the equipotential V_2, and so on[142].

The calculation of the equipotentials for the a 25cm long array consisting of six ion lenses would be a time consuming process in itself without having to trace the trajectories and calculate the velocities of individual ions. Because of the complexity of the ion velocity equations and the time consuming repetitiveness of the calculations, a computer simulation program was used to aid in the ion optic design. The computer program (SimIon version 4.0, Argonne National Laboratory, USA) calculates the voltage of the equipotentials in the array by the method described above. The ion trajectories and velocities are then calculated and plotted. To do this the program must first be given the position and voltage of each electrostatic lens. This is achieved by setting designated grid potentials as constant voltage positions with the same geometry as the lenses. For the ion trajectories to be calculated, the computer requires the starting position of the ion, its incident angle, the kinetic energy and

mass to charge ratio of the ion. Once these variables have been entered into the program the ion trajectory can be calculated. Using this program it was possible to experiment with differing lens designs, changing the lens potential and geometry, until all the inputted ions passed through the length of the array and into the quadrupole through the entrance lens. However, this model does not account for field fringing effects and the effects of space charge in the ion beam. In order to compensate for such effects on the ion beam, the entrance angle of the ions into the electrostatic array was varied and the model tested for a series of different mass ions, with differing ion kinetic energies. Figure 3.6 shows the ion trajectories for ions entering the optimised ion optics at ± 20° off-axis. Hence, it was possible to design an ion optical array which consisted of two extraction lenses behind the skimmer and three ion focusing lenses just prior to the quadrupole.

3.2.4 Mass Spectrometer

The Hewlett Packard mass selective detector (HP-MSD) and its data handling computer station was originally designed to be interfaced to a gas chromatograph (GC), via a split jet separator. Once the sample entered the vacuum housing of the quadrupole it was ionised by an electron impact source and the ions were focused into the quadrupole by a set of three electrostatic lenses, which were controlled by the data handling software. The quadrupole has a mass range from 10 to 800 m/z and the software is designed for rapid multi-ion scanning in a time resolved manner to facilitate qualitative mass spectral analysis. For quantitative analysis, a selected ion monitoring function is also available.

The HP-MSD is a bench top instrument of proven capability and was, therefore considered an ideal analyser for the LP-ICP. However, it was necessary to make several

modifications to the instrument in order to couple the LP-ICP and ion extraction interface with the HP-MSD.

To enable ions from an external ionisation source to be transmitted freely into the mass analyser, certain electrical and mechanical modifications were made to the MSD. First, the jet separator interface was removed and the entrance to the quadrupole vacuum chamber was widened and welded with a 40mm KF type vacuum flange. This enabled the new ion expansion interface to be connected to the analyser section using a viton O-ring and a 40mm KF vacuum flange brace.

Inside the vacuum chamber, the repeller lens was removed along with the EI source filaments and electron focusing magnets. The ion lens mounting block was replaced with a new block which contained a wider central channel for ions to pass through. Three ion focusing lenses were incorporated prior to the quadrupole entrance lens to focus ions from the external source. Because an EI source was no longer present, it was no longer necessary to heat the vacuum chamber, so the heater power supply was disconnected as the heat would have destroyed the O-rings used to seal the new interface.

The power supplies for the lenses varied, with the four lenses inside the analyser housing being computer controlled and the two lenses behind the skimmer being controlled manually. Table 3.2 gives details of the voltage ranges for the individual lenses. This lens system had no photon stop because the detector in the mass analyser used is offset so was shaded from any photon noise. Also, the low pressure plasma studied in this work gave rise to very little photon noise. A schematic diagram of the ion lens array is shown in Figure 3.6.

Table 3.2   Details of ion lenses and voltage ranges for the LP-ICP-MS ion optical

array.

Lens element	Voltage range (V)	Computer control
L1	0 to -200	no
L2	+5 to -20	no
L3	0 to +10	yes
L4	0 to -255	yes
L5	0	yes
Entrance	0 to -255	yes

The Hewlett Packard 5970 MSD has a sophisticated systems check written into the data handling software which will disable all mass spectrometer functions if a fault is detected in the system. The removal of the EI source was seen as a major fault and so this part of the diagnostic logic had to be disarmed. This was done simply by grounding a pin on a logic chip which confused the computer into thinking the EI source was present and hence causing it to function normally. A diagram of the final instrument set-up is shown in Figure 3.7.

3.3 OPTIMISATION AND EVALUATION

3.3.1 Ion Lens and Analyser Optimisation

In order to generate a useful analytical signal, a solution of perfluorotributylamine (PFTBA, Fluka Chemicals, Gillingham, UK) which was contained in a vial attached to the side-arm of the low pressure plasma torch, was introduced to the low pressure plasma via a molecular leak (Fig. 3.7). PFTBA was chosen because the software on the MSD computer is typically configured to use the three molecular fragment ion peaks from PFTBA, at 69, 219 and 502 m/z, to tune the quadrupole and ion optics. This enabled the mass calibration and resolution settings of the quadrupole, and the ion lens voltage settings, to be optimised.

The initial operating conditions for the low pressure plasma are given in Table 3.3, and Fig. 3.8a shows the three mass peaks selected for tuning the quadrupole. It can be seen from the peak shape and width that good resolution and calibration were achieved using the customised instrument. A total mass spectrum for PFTBA is shown in Fig. 3.8b, and data pertaining to the major peaks is given in Table 3.4. Prior to conversion to a LP-ICP source, the EI mass spectrum for PFTBA was acquired using the instrument, and the abundances of the major peaks are also given in Table 3.4. The major difference between the data for the

Quadrupole
(10-800 m/z)

Ion
Optics

Slide
Valve

Vacuum electrical feedthrough

Rotary Pump

Low Pressure Sampler

Detector

GC
COLUMN

Turbo molecular pump

Rotary pump

Modified
Torchbox

MSD
Computer
Workstation

PFTBA
Solution

rf
Generator

Ion Sampling Interface

87
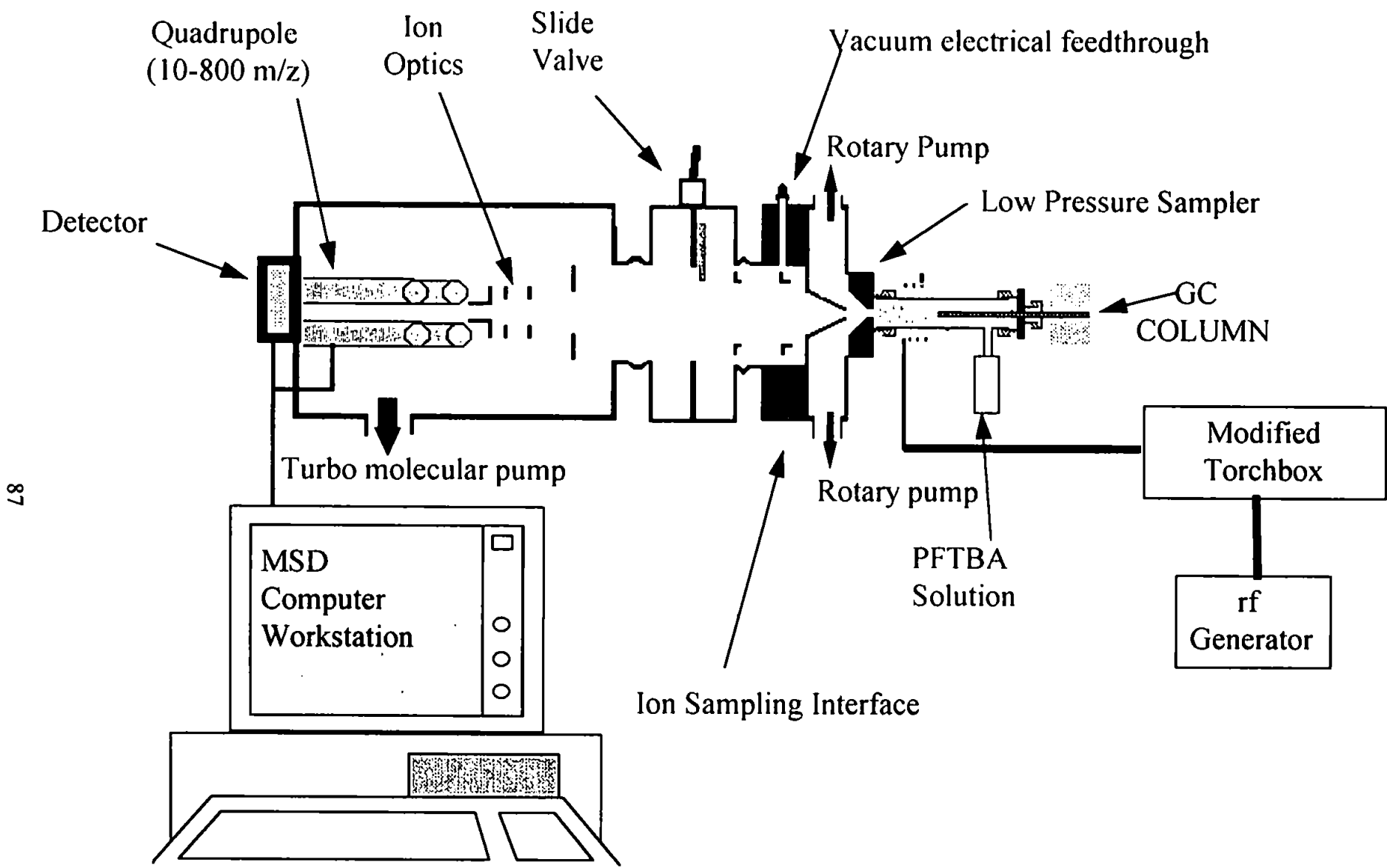
Figure 3.7   Schematic diagram of the GC-LP-ICP-MS.

Table 3.3   Operating conditions used for the initial studies with the LP-ICP-MS system.

Mass Spectrometer	Modified Hewlett Packard MSD
Plasma	
Forward power (W)	6
Reflected power (W)	0
Pressure (Torr)	
Torch	0.2
Interface	0.03
Analyser	2×10^{-5}
Ion lenses (V)	
L1	-75
L2	-10
L3	+1
L4	-64
L5	0
Entrance	-45
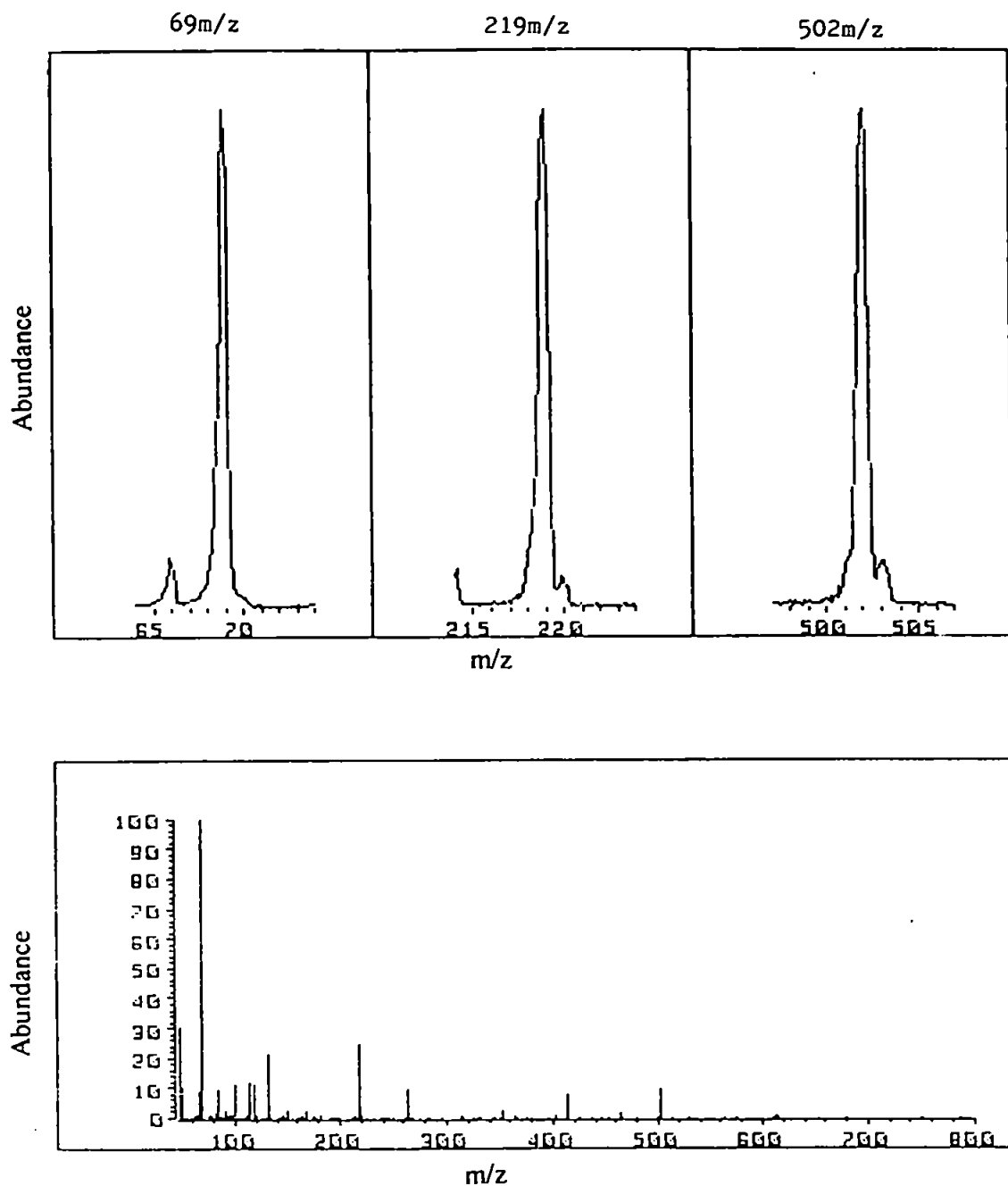
Figure 3.8   Mass spectrum of PFTBA: a) selected mass fragments at 69 , 219, and 502 m/z;
and b), mass spectrum from 45 to 800 m/z.

Table 3.4   Major peaks in the mass spectrum of PFTBA between 45 and 800 m/z, obtained using LP-ICP-MS.

m/z	Abundance		Relative abundance	
	LP-ICP-MS	EI	LP-ICP-MS	EI
69	1,547,264	1,825,280	100	100
219	383,680	1,100,288	24.80	60.28
502	141,184	223,808	9.12	12.26

two sources was the higher abundance of ions at m/z 219 and 502 obtained using the EI source, although the abundances can be varied quite considerably using either ionisation source. Once the MSD had completed its optimisation procedure for the quadrupole and ion lenses, lenses L1 and L2 were adjusted manually to yield maximum signal for the three chosen masses.

3.3.2 Skimming Distance and Plasma Power

Once the instrument had been set-up and the lenses and quadrupole settings tuned to give maximum signals for the PFTBA signals, optimisation of the skimmer/sampler spacing and plasma forward power was performed. The skimmer/sampler spacing was altered by placing copper spacing rings behind the skimmer mounting plate. Figures 3.9 a-c show 3 dimensional surface plots of signal intensity versus skimmer/sampler spacing and forward power, for the three fragment ions of PFTBA at 69, 219, and 502 m/z respectively. Each data point is an average of ten readings with the coefficient of variance at the maximum signal intensity being between 9 and 11 %. The experiment was repeated and the observations were found to be reproducible.

Maxima in signal intensity occurred at two skimming distances, namely 6 mm and 8 mm downstream of the sampler orifice, with comparable signal intensities observed at each of the maxima. Gray[140] has shown that, as the expansion stage pressure increases, the barrel shock downstream of the sampler shortens, and the Mach disc gets closer to the sampling orifice. The same author also found that, for $P_0/P_1 = 76$, several shock regions and Mach discs, could be observed downstream of the primary shock region. These observations have recently been confirmed by Luan et al.[141]. In the present study at $P_0 = 0.2$ Torr and $P_1 = 0.03$ Torr, and $D_0 = 2.0$ mm, the position of the Mach disc was calculated to be $X_m = 3.5$ mm. The presence of two maxima in signal intensity downstream of the Mach disc,

a)

90°

113°

Vacuum line

60°

45°

Electric feedthrough

135°

0°

180°

315°

225°

293°

Vacuum line

150°

270°

A:40 mm

G:67.4 mm

H:69.4 mm

E:89 mm

b)

90°

60°

45°

Electric feedthrough

135°

0°

180°

315°

225°

150°

270°

A:40 mm

B:41.2 mm

C:55 mm

E:89 mm
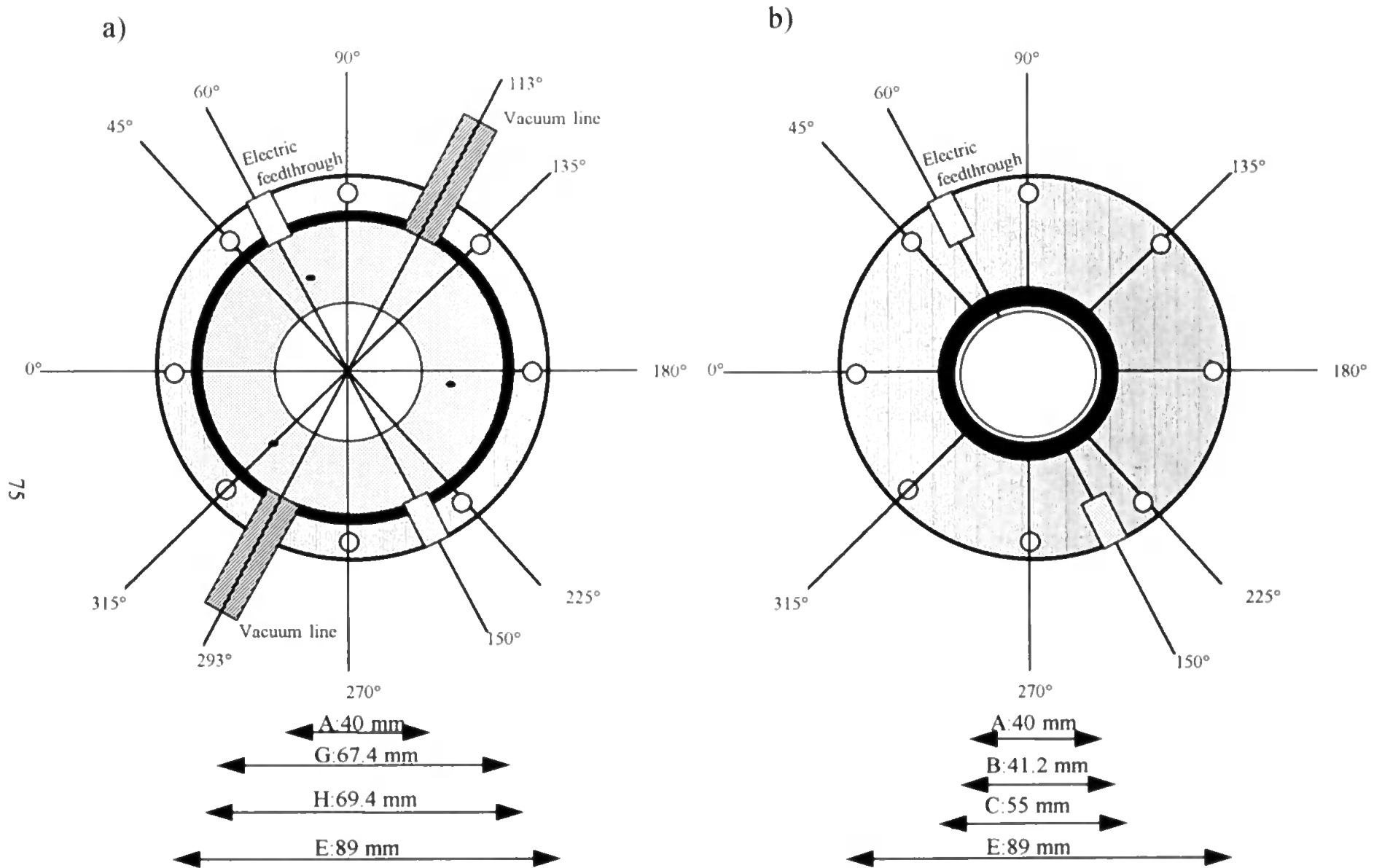
Figure 3.2   Diagram of the ion sampling interface; a) top view; b) bottom view.

Seating for ion optical lenses

3mm

2mm

Vacuum pump port

Screw tap for
skimmer mounting plate

E:89mm

D:80mm

H:69.4mm

G:67.4mm

F: 57.5mm

Seating for o-ring vacuum seal

7mm

13mm

15mm

10mm

26mm

7mm

39mm

35mm

13mm

2mm

3mm

A: 40mm

B: 41.2mm

1.2mm

C: 55mm

D: 80mm

E: 89mm

M4 bolt tap

Vacuum electrical feedthrough
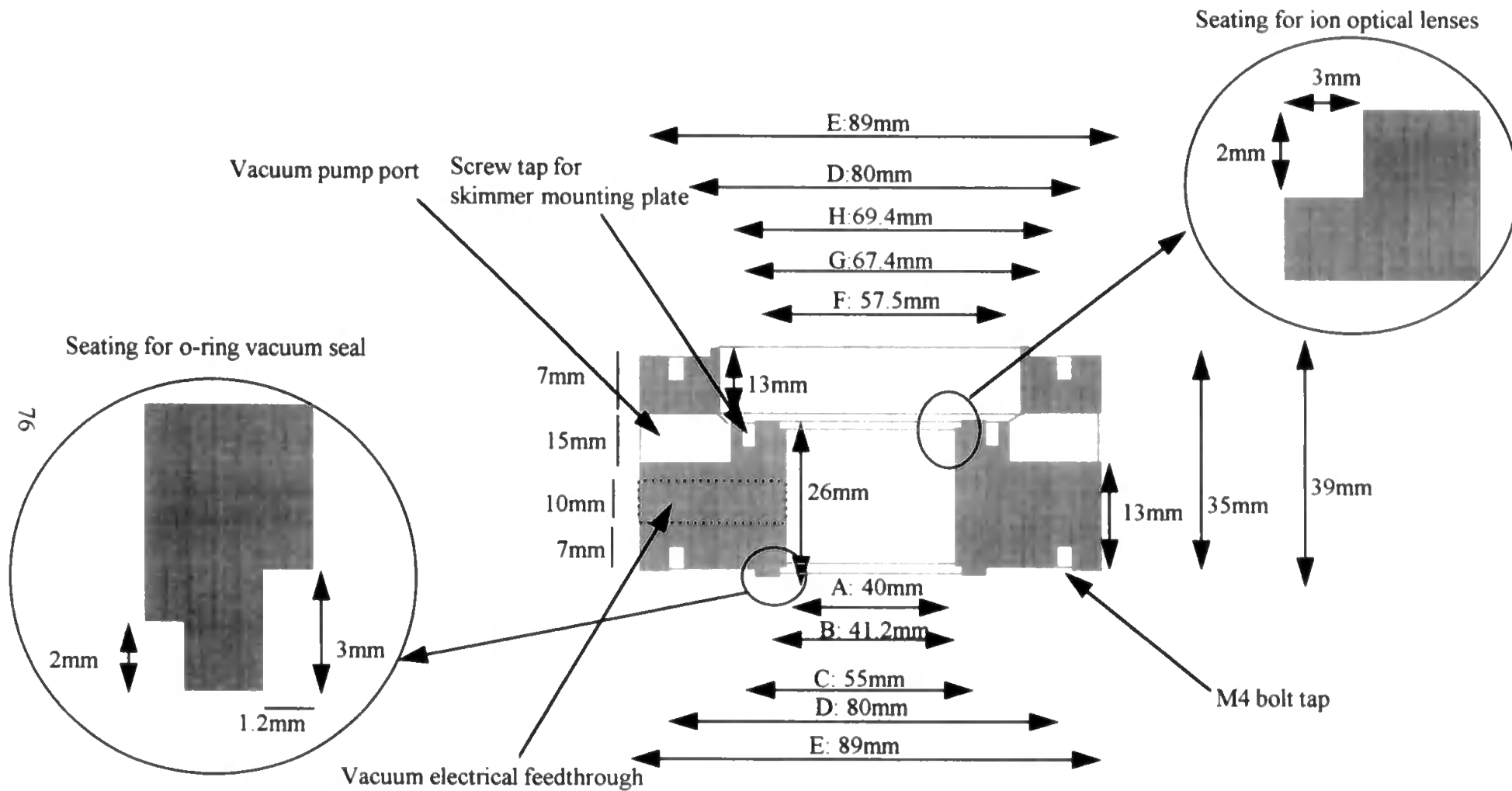
Figure 3.3   Diagram of the ion sampling interface; side view

a)

90°

45°

135°

0°

180°

315°

225°

77

270°

40mm

67.4mm

69.4mm

80mm

89mm

b)

90°

45°

135°

0°

180°

315°

225°

270°

33mm

45mm

50mm

80mm

89mm
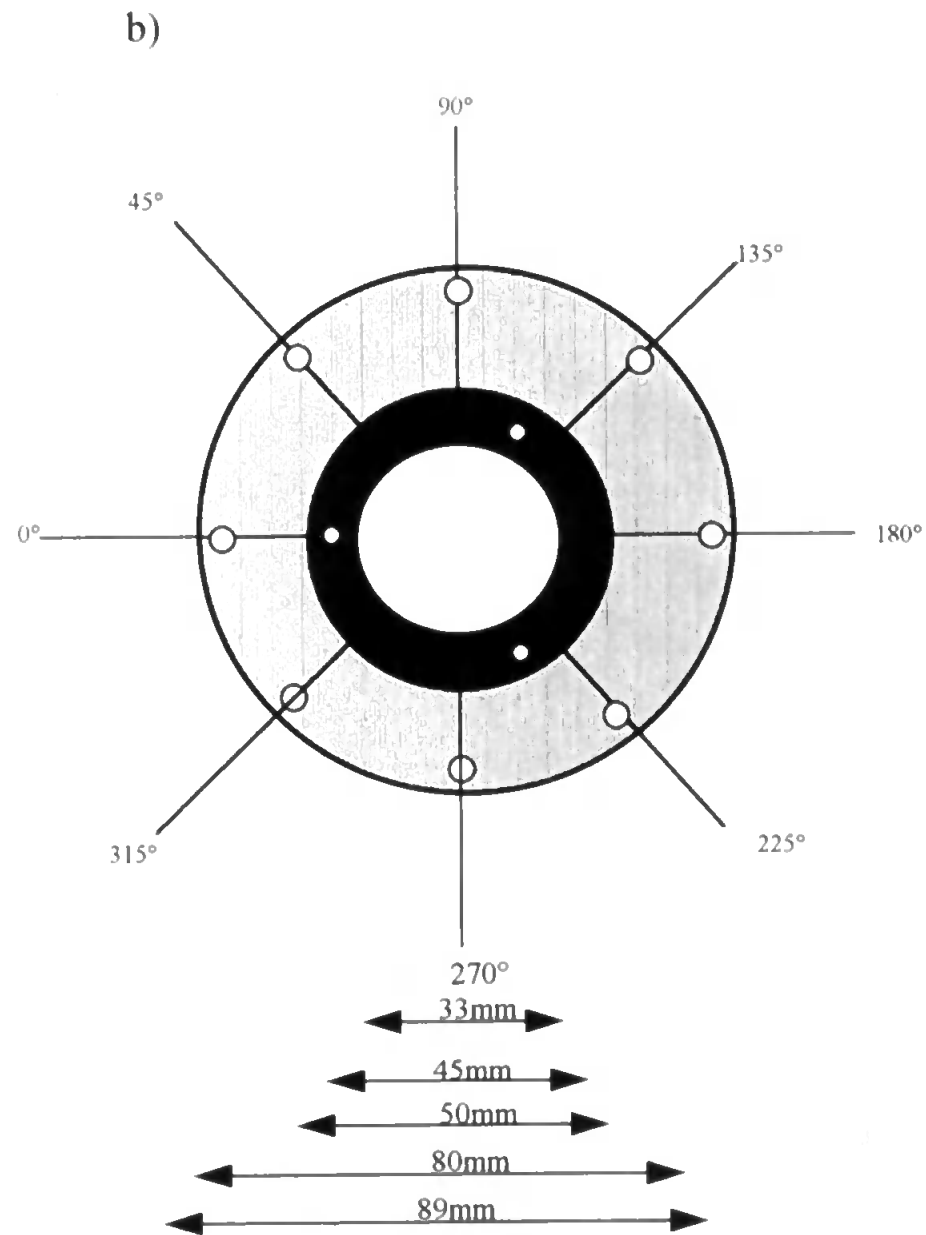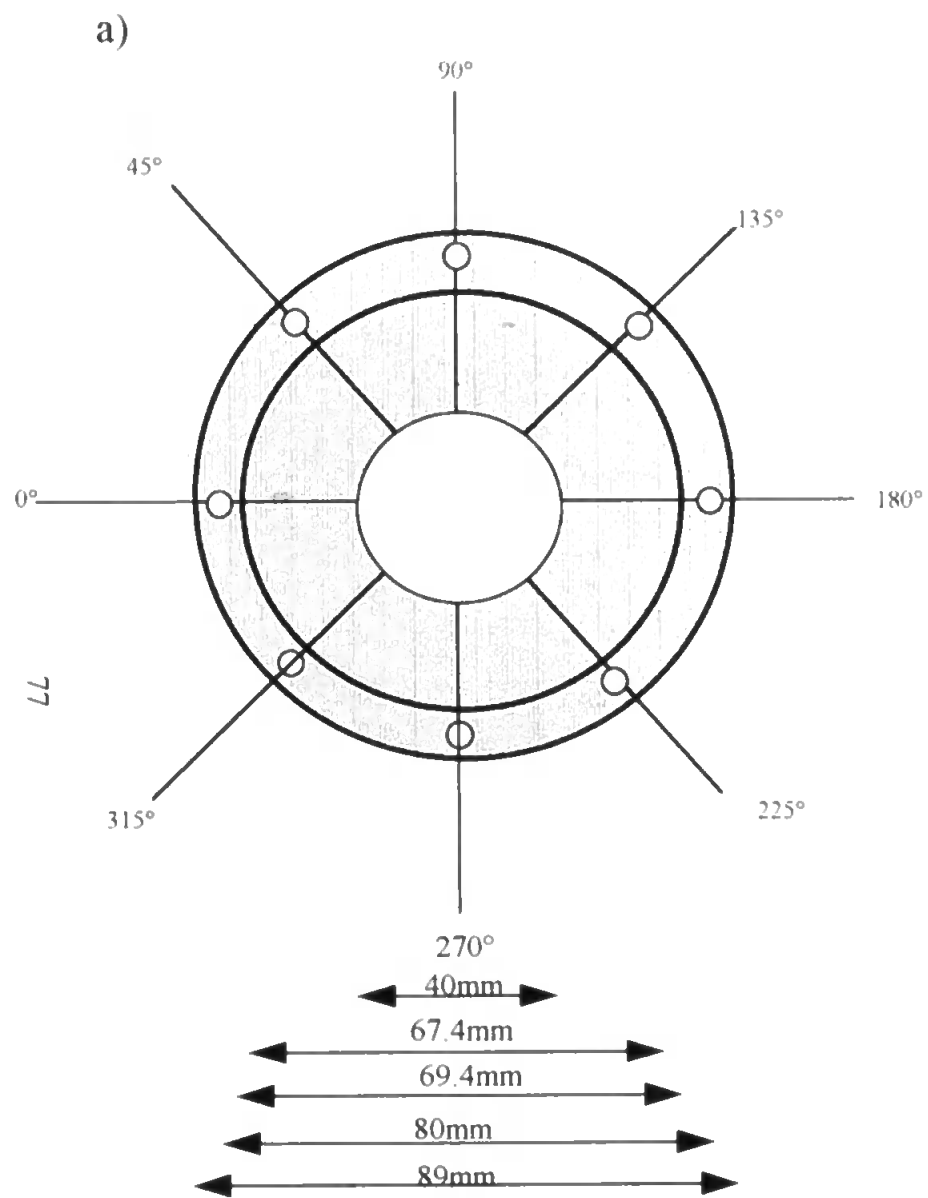
Figure 3.4   Diagram of the front plate of ion sampling interface; a) bottom view; b) top view
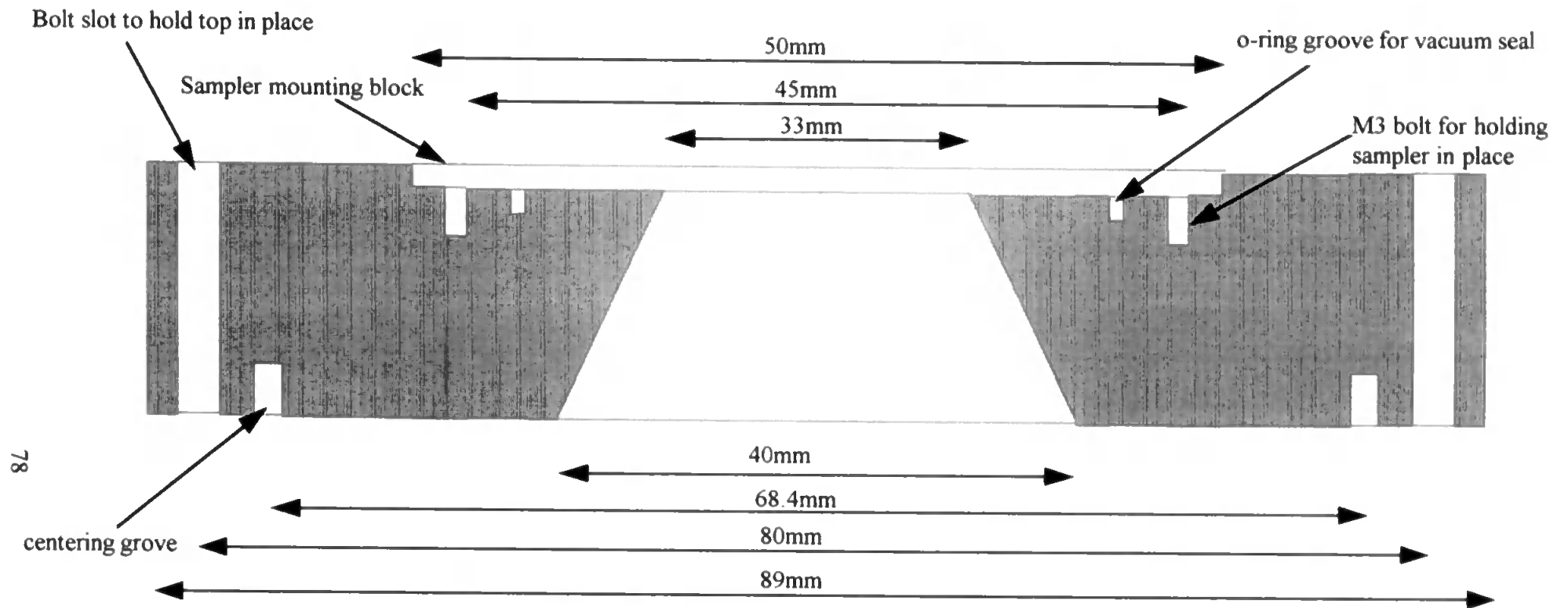
Figure 3.5   Diagram of the front plate of the ion sampling interface; side view

Skimmer and mounting plate
(0V)

L3: +1V

L1: -75V   L2: -10V

L4: -64V   L5: 0V   Entrance lens:
-45V

83
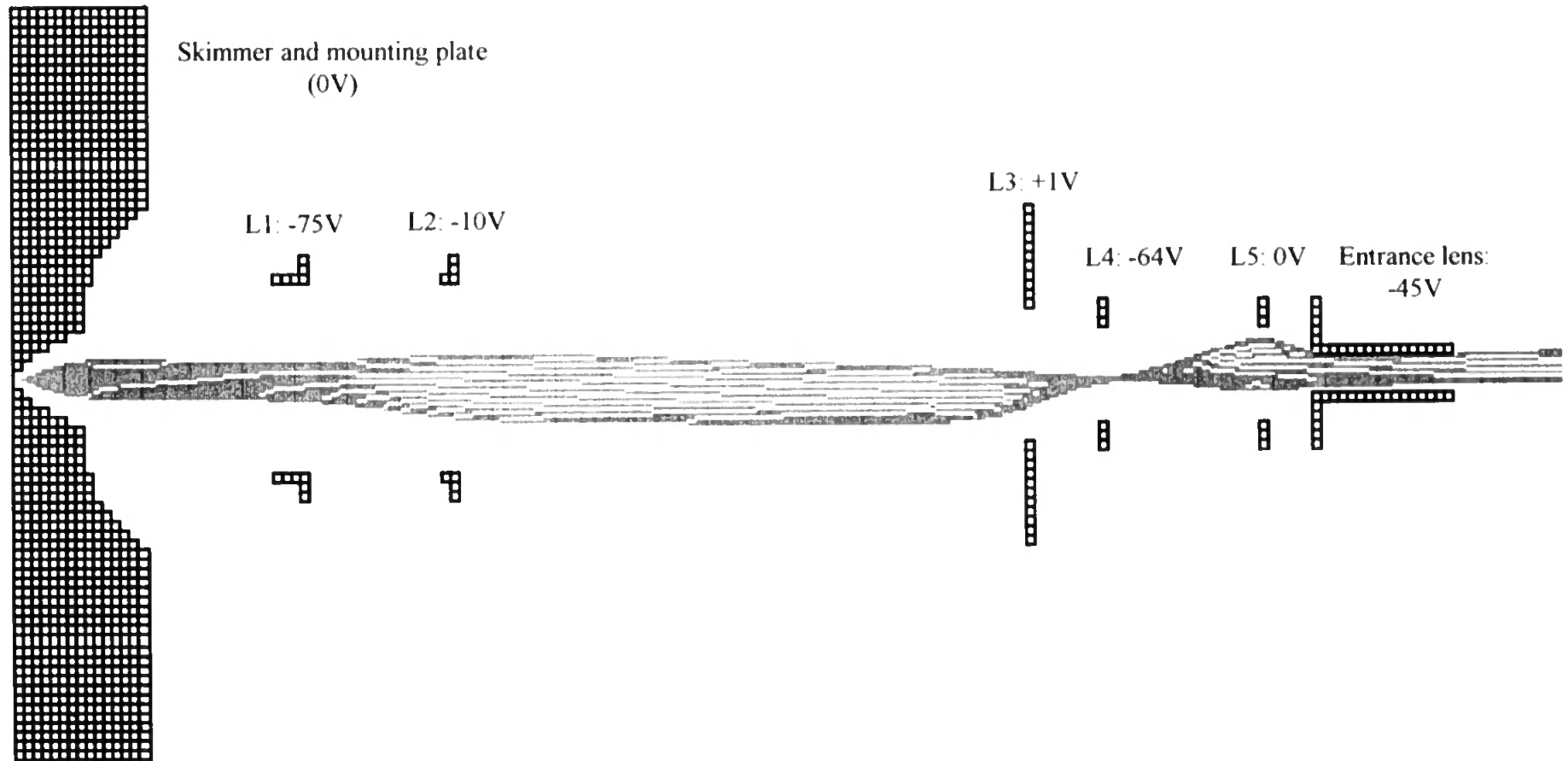
Figure 3.6   SimIon plot of ion trajectories for ions, with an average ion kinetic energy of 10 eV, through the ion optical array
designed for use in the customised LP-ICP-MS instrument with optimum voltage settings.
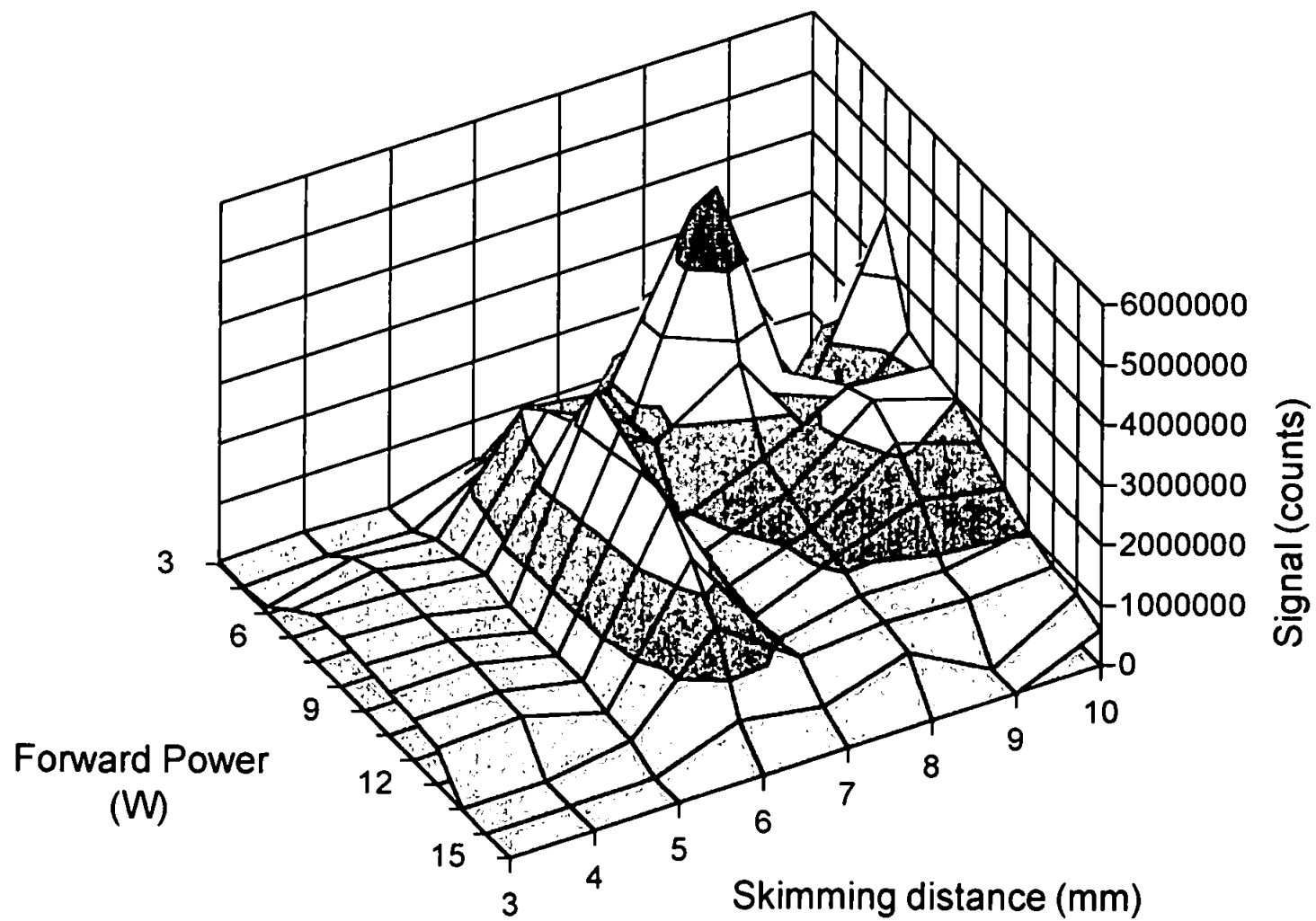
Figure 3.9 (a)   3D plot showing the effect of plasma power and skimming distance on the signal intensity for PFTBA at 69 m/z.
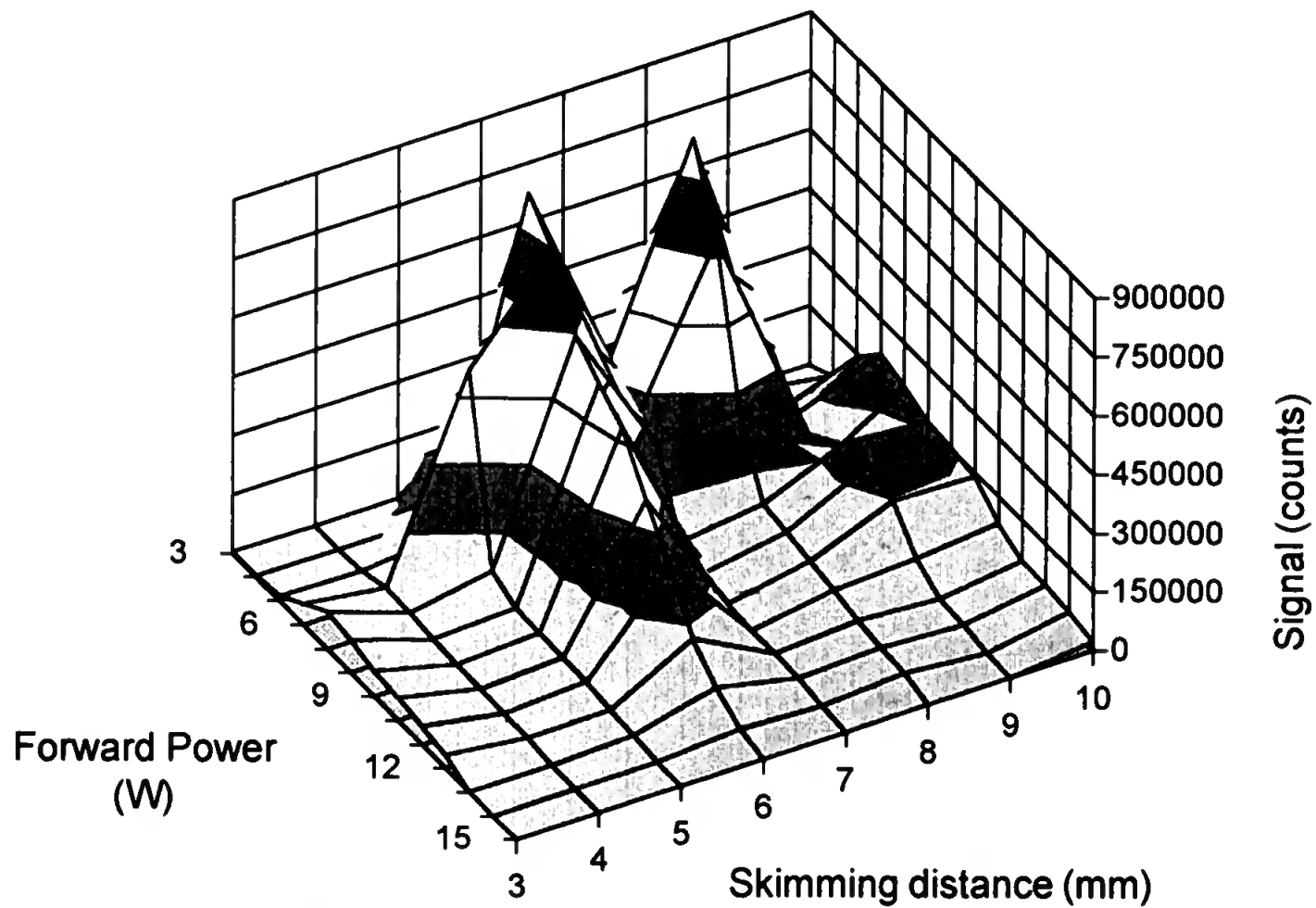
Figure 3.9 (b) 3D plot showing the effect of plasma power and skimming distance on the signal intensity for PFTBA at 219 m/z.
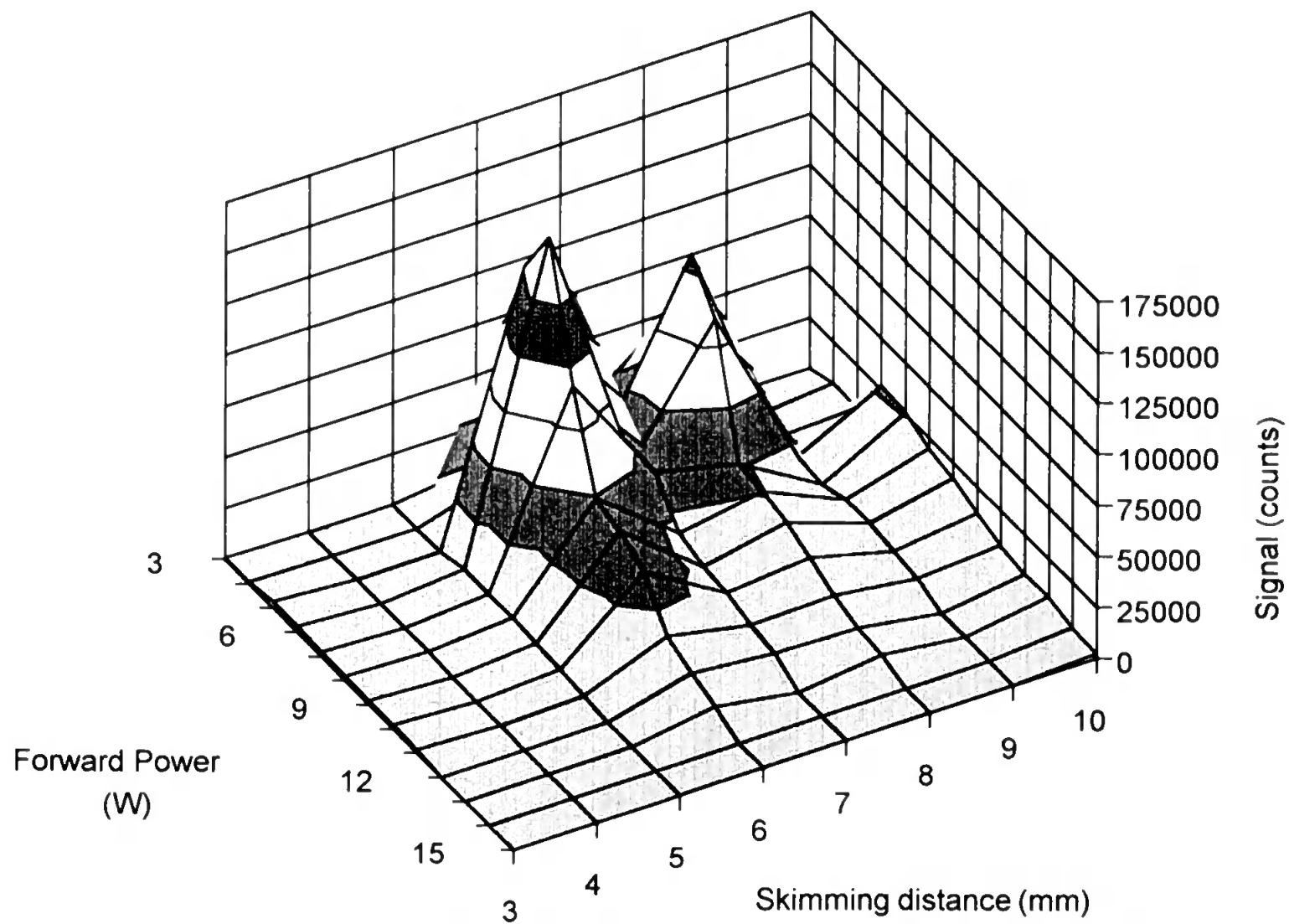
Figure 3.9 (c)   3D plot showing the effect of plasma power and skimming distance on the signal intensity for PFTBA at 502 m/z.

observed in this work, suggests that the fragment ions were formed not in the plasma itself but in the expansion stage, possibly in regions associated with one or two Mach discs downstream of the sampler orifice. At 3.5 mm, the theoretical position of the Mach disc, a maximum in signal intensity was not observed, however, the observations of Gray[140] suggest that the Mach disc becomes progressively larger in relation to the barrel shock as the P_0/P_1 ratio is reduced, so it may possibly extend out to 6 mm downstream of the sampler orifice. Visual observation of the expansion process was achieved by replacing the copper expansion chamber with a glass one. However, this provided little information as the shock regions were not visible to the naked eye.

The power which yielded maximum signal was between 6 and 8 W, although this depended somewhat on which fragment ion and skimming distance was chosen (Fig. 3.10 a-b). At a skimming distance of 6 mm the signal intensity for the fragment ions at 219 and 502 m/z dropped rapidly above 6 W (Fig. 3.10a). The signal intensity for the fragment ion at 69 m/z also decreased as the power increased, but not as sharply, suggesting that the high mass fragments were further fragmented, adding to the signal observed at 69 m/z. This is indicative that the source operate in a tuneable fashion. At a skimming distance of 8 mm the power which yielded maximum signal intensity was very similar for the three fragment ions (Fig. 3.10b).

3.3.3 Analytical Utility

Previous studies showed that the low pressure plasma was an effective atomic ionisation source. In this work the analytical utility of the instrument with regard to the formation of molecular fragment mass spectra was investigated, as this was considered to be the more challenging application. In order to introduce analytically useful masses of analyte, a gas
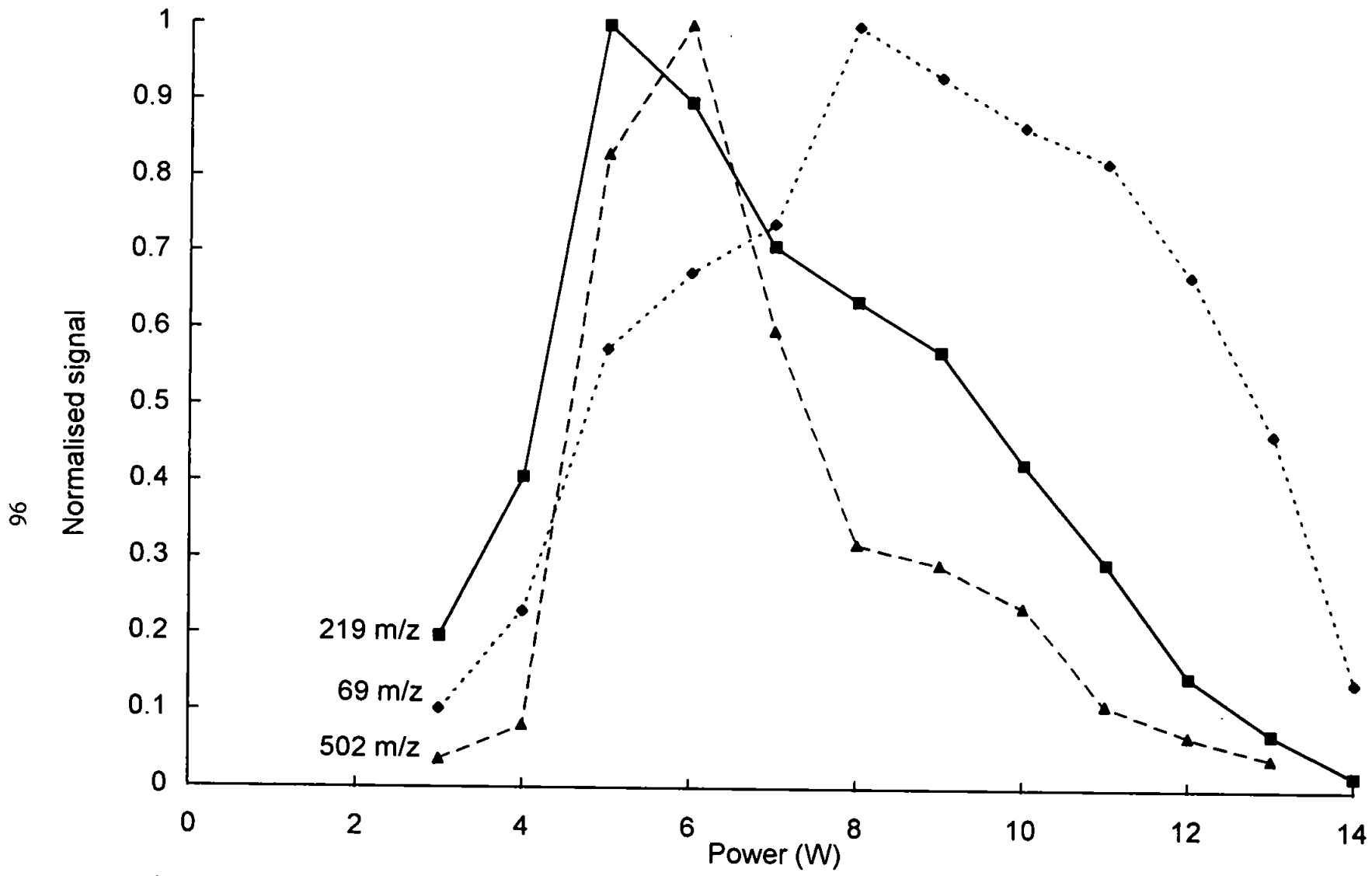
Figure 3.10 a)   Plot of normalised signal intensity against plasma power for fragment ions of PFTBA at 69, 219, and 502 m/z at a skimming distance of 6mm.
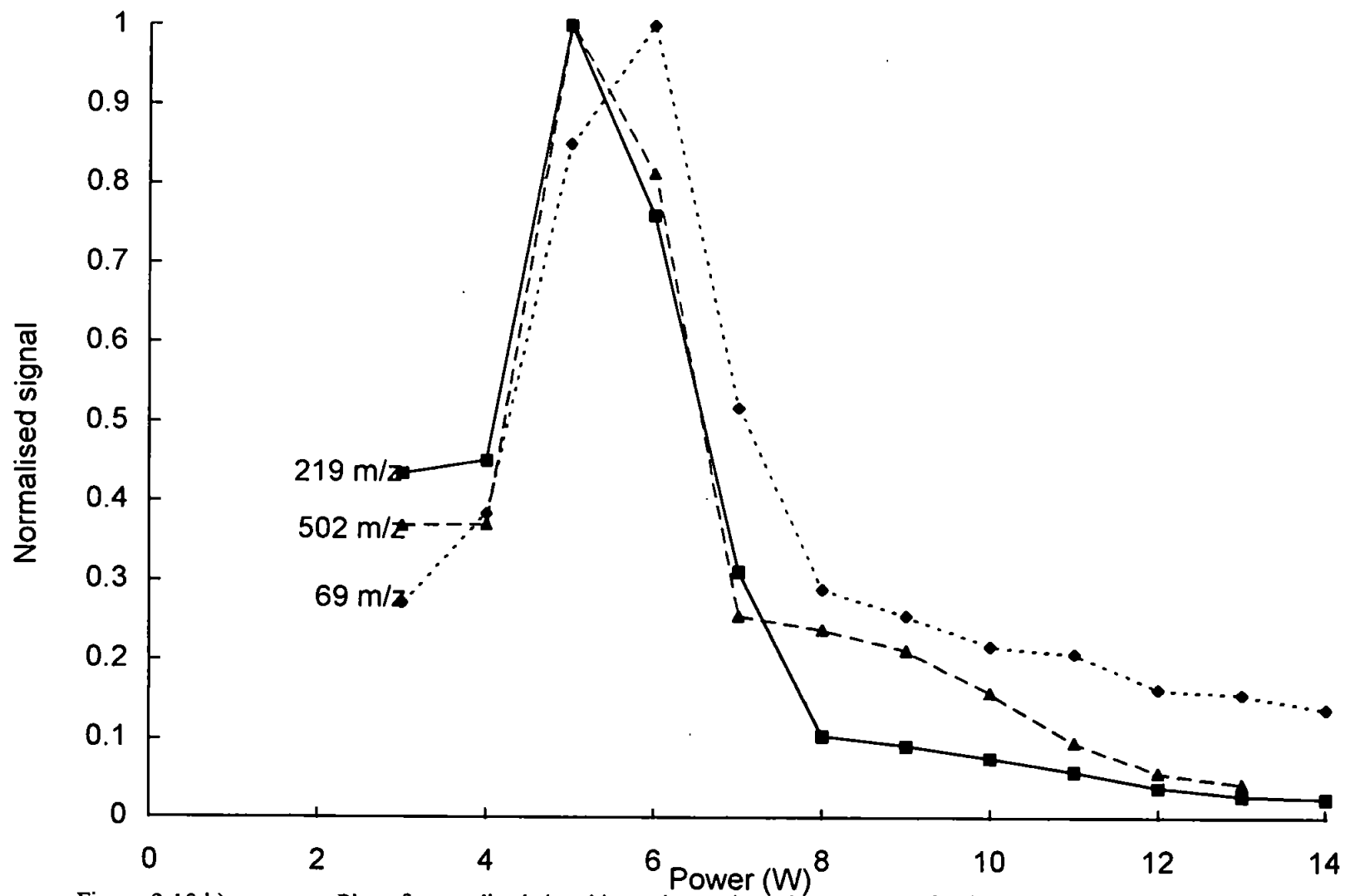
Figure 3.10 b)   Plot of normalised signal intensity against plasma power for fragment ions of PFTBA at 69, 219, and 502 m/z at a skimming distance of 8mm.

chromatograph was interfaced with the rear of the LP-ICP torch, via a heated transfer line, as shown in Fig. 3.7, with operating conditions given in Table 3.5.

Using this set-up 1.0 μL of a 50 μg ml^{-1} solution of halobenzenes in pentane was injected on-column, and the GC ramped from 40 to 200 °C at 20 °C min^{-1}. Figure 3.11 shows a total ion chromatogram (TIC) for this injection, and the mass spectra of the respective analyte compounds are shown in Fig. 3.12a-c. The mass spectra were similar to mass spectra obtained for the same analytes using an EI source on the same instrument before conversion, with the same parent ion peaks (Figs 2.7 to 2.9). However, as shown in the power and skimming distance studies (Figs. 3.9a-c), the abundance of each fragment can be altered by changing the plasma power. The results of selective ion monitoring (SIM) for the molecular ion peaks of each analyte are shown in Fig. 3.13. The signal to noise ratio suggests that the technique could easily be used for trace analysis, although the use of this instrument for such an application may be limited because the detector is configured in analogue mode, whereas a pulse counting detector would be preferable. While trace level analysis of molecular species would be possible, several problems still existed. The plasma was sustained with the eluent gas of the GC. The carrier gas flow through the GC column was controlled using a constant-pressure, constant-flow unit (Carlo Erba, Fisons Instruments, Crawley, Sussex, UK) which should reduce gas flow fluctuations when ramping the oven temperature. The device enabled the plasma to remain ignited throughout a chromatographic run, but the plasma stability was poor, causing fluctuations in the analytical signal. Also, it was still not possible to obtain a linear calibration, nor detect molecular ions below 50 ng on-column as was seen to be a threshold value for molecular ion formation.

Table 3.5   Operating conditions used for the analytical utility studies with the LP-ICP-MS instrument.

Mass Spectrometer	Modified Hewlett Packard MSD
Plasma	
Forward power (W)	6
Reflected power (W)	0
Pressure (Torr)	
Torch	0.2
Interface	0.03
Analyser	2×10^{-5}
Gas Chromatograph	
Injector	Cold on-column
Column	DB5 30 m x 0.32 mm
Carrier gas	Helium
Carrier flow (ml min^{-1})	3
Injection volume (μl)	1
Oven temperature (°C)	40-200 @ 20°C min^{-1}
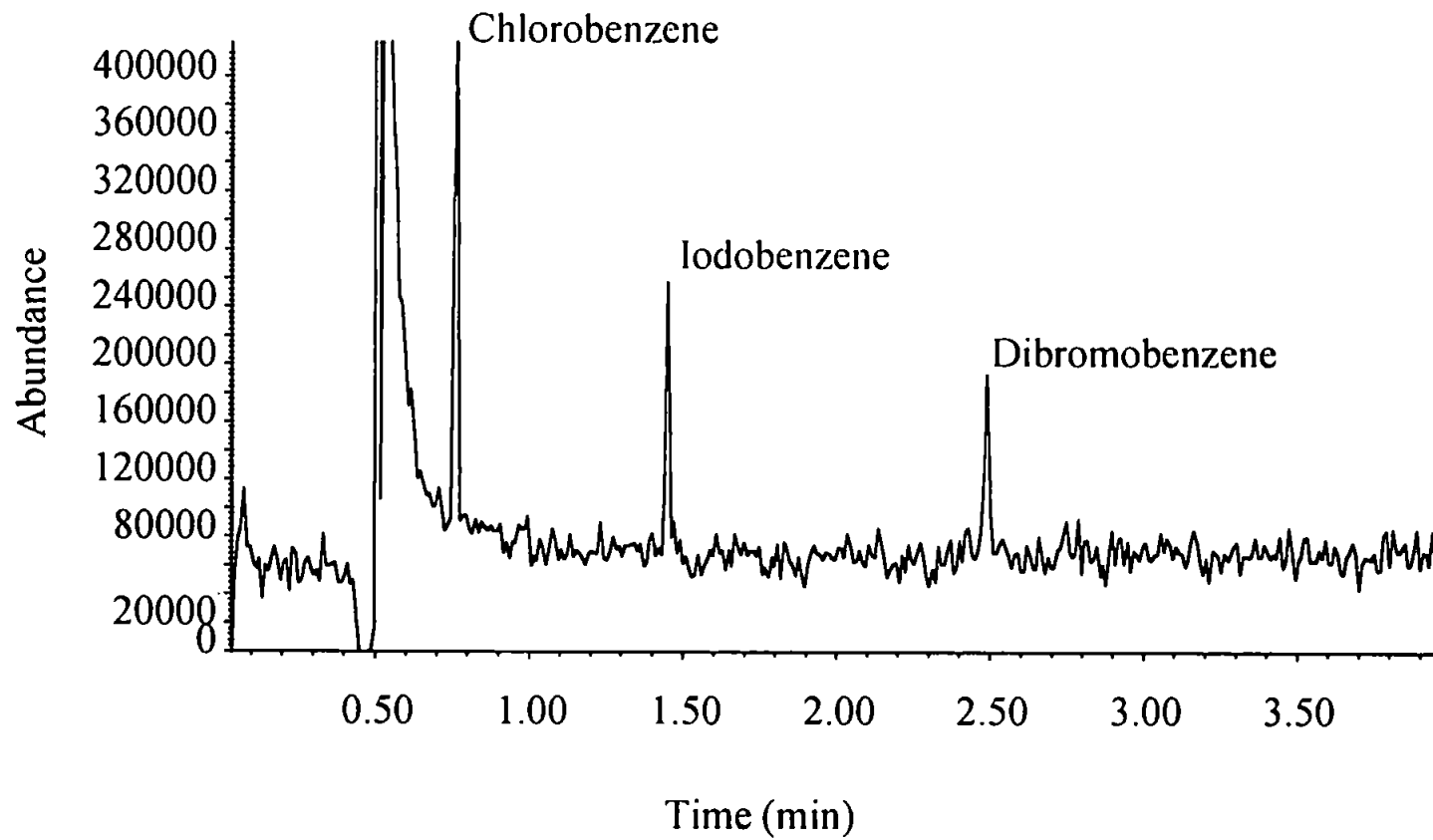
Figure 3.11 Total ion chromatogram for 50 ng on-column of a halobenzene mixture.
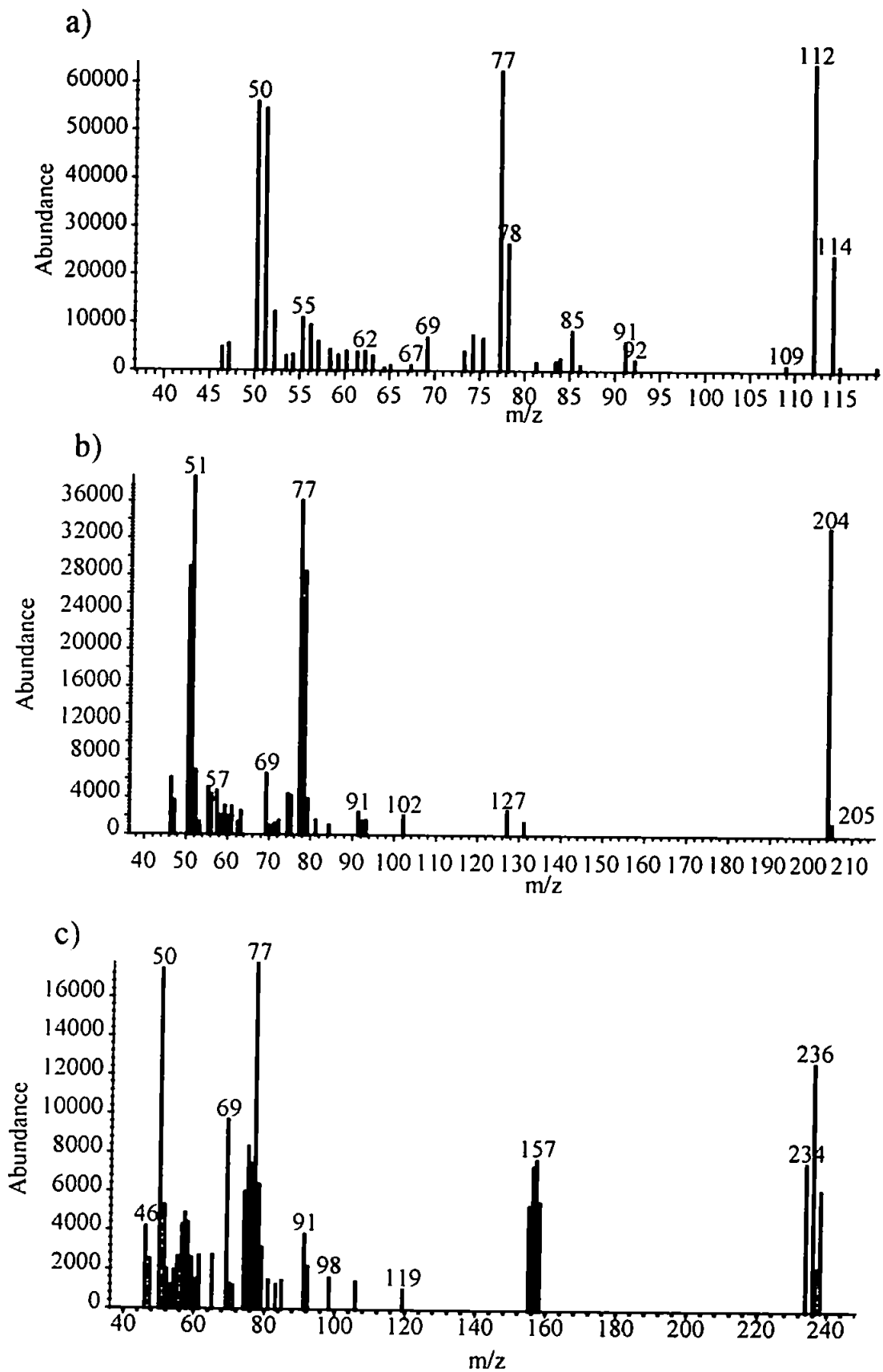
Figure 3.11 Mass spectra for: (a) chlorobenzene; (b) iodobenzene; and (c) dibromobenzene.

101
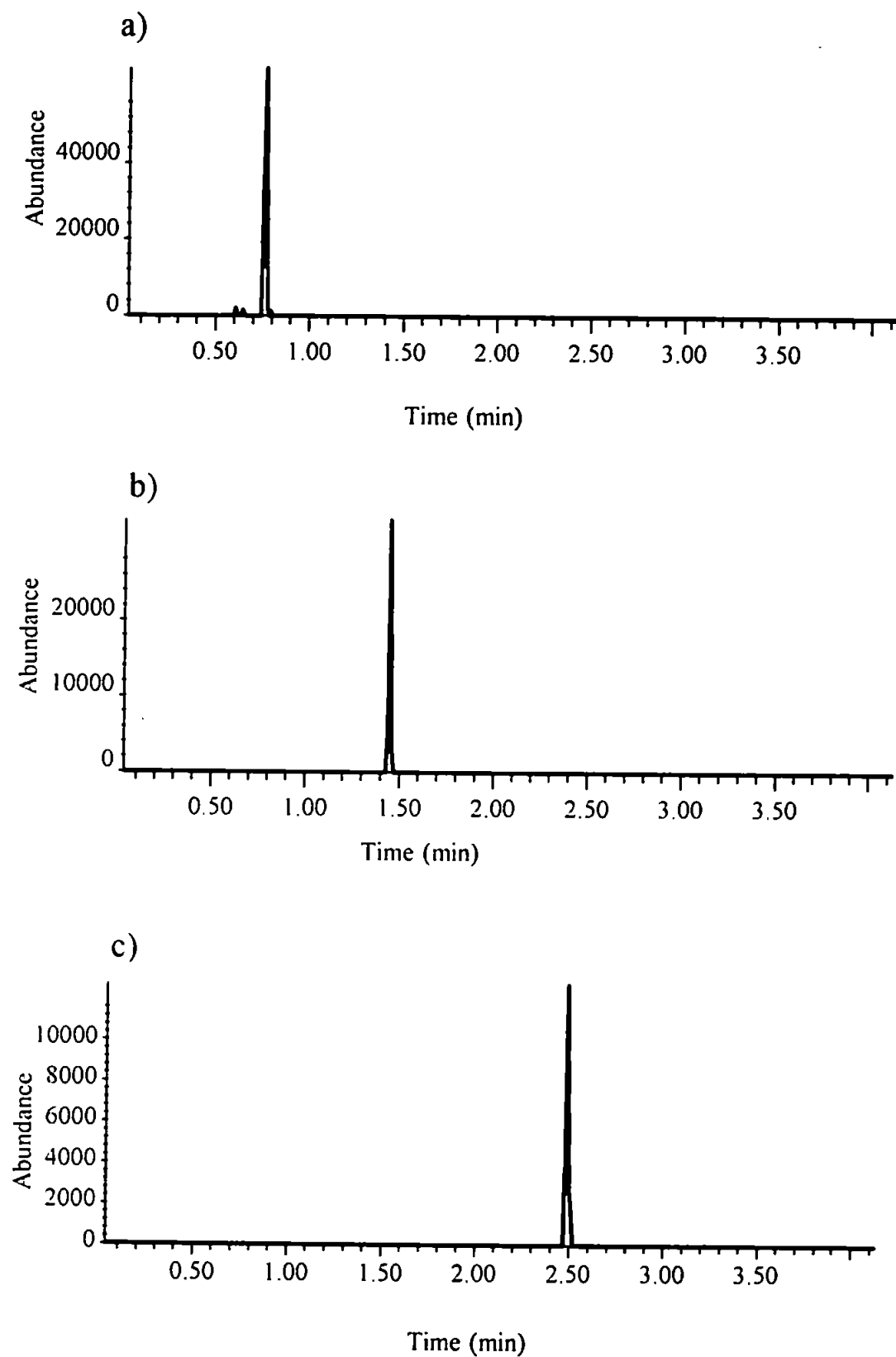
Figure 3.12 Selected ion chromatograms for: (a) chlorobenzene, 112 m/z; (b) iodobenzene, 204 m/z; and (c) dibromobenzene, 236 m/z.

3.4 CONCLUSIONS

The customised instrument partly alleviated the problems associated with the use of commercial ICP-MS for low pressure plasma work, and showed great promise for further development. Such an instrument is more economical to operate compared with conventional ICP-MS and helium MIP systems, and can potentially be operated in both atomic and molecular modes. This will also reduce capital costs because a single instrument with a single source could provide a wide range of mass spectral information, both element selective detection and detection of fragment and molecular ions.

The similarities in ion signal intensities between the LP-ICP source and the EI source shows that effective ion transmission was occurring, suggesting that the ion optical design was effective. The skimming of the plasma seemed to deviate from established theory, but, an optimum skimming distance for the molecular species was determined nevertheless, and was constant across the mass range studied. The appearance of two maxima in the skimming profiles suggested that a number of different ionisation processes were occurring and this is discussed in detail in Chapter 5. The plasma power profiles were indicative of the LP-ICP operating in a tuneable mode, allowing the operator to designate the degree of fragmentation.

Problems associated with the formation of molecular and fragment ions from analytes, introduced via GC, still existed and are addressed in the next chapter.

Chapter 4

ADDITION OF REAGENT GASES

CHAPTER 4 - ADDITION OF REAGENT GASES

4.1 INTRODUCTION

In Chapter 3 it was shown that a 3 ml min^{-1} helium LP-ICP-MS, sustained at 6W, is capable of producing molecular and fragment ions of organohalide compounds. However, while studies with perfluorotributylamine (PFTBA) and selective ion monitoring (SIM) of the halogen species, suggest that the custom made instrument was capable of trace molecular analysis, this was not possible in practice. The plasma seemed to be unstable which led to unreproducible signals for the molecular ions. The cause of these problems may be that the plasma was sustained with GC carrier gas alone. Even with a constant-pressure, constant-flow device controlling the carrier gas for the GC, small fluctuations in gas flow may have occurred when ramping the GC oven temperature. One obvious method to alleviate such problems would be to introduce a post column make-up gas to stabilise the plasma.

To date, analytical figures of merit for various low pressure plasma sources have been determined using the source only in its atomic mode[35,110,120](i.e. with element selective detection). The detection limits for organohalides determined using different instrument set-ups are shown in Table 4.1. The limits range from 0.1 pg to low nanogram range depending on the source and detector used. While some of these sources have been used to produce molecular ions,[35,83,85,87,110,111] no detection limits for such have been reported. In order to obtain molecular spectra, large quantities of the analyte have been introduced into the source thus, these sources have not been capable of providing molecular fragment ion information at trace levels. Limits of detection for the Hewlett Packard instrument, prior to conversion, with an electron impact source are also reported in Table 4.1 for comparison.

The appearance of molecular and fragment ions of analytes introduced to the LP-ICP-MS at high concentration, as observed in Chapter 3, suggests that the partial pressure of the

Table 4.1   Figures of merit for halobenzene species using element selective detection in

the atomic mode.

Instrument	Plasma gas	Analyte	Ion monitored m/z	Limit of detection (pg)	Reference
GC-LP-ICP-MS	Ar	chlorobenzene	$^{35}Cl^+$	500	110
	Ar	iodobenzene	$^{127}I^-$	25	
	Ar	bromobenzene	$^{79}Br^+$	50	
GC-LP-MIP-MS	He	chlorotoluene	$^{35}Cl^+$	22	35
	He	iodobenzene	$^{127}I^+$	0.1	
	He	bromononane	$^{79}Br^+$	3.5	
GC-MIP-MS	He	chlorobenzene	$^{35}Cl^-$	9.2	35
	He	iodobenzene	$^{127}I^-$	1.5	
	He	bromooctane	$^{79}Br^-$	1.08	
GC-MIP-AES	He	Cl		39	120
	He	Br		10	
	He	I		not given	

analyte in the LP-ICP is a contributing factor in molecular fragment ion formation. This would explain the non linear relationship between concentration and molecular ion signals in the LP-ICP. The mechanisims by which the high levels of analyte are influencing the ionisation process are considered of utmost importance, as these may hold the key for the use of such low pressure plasmas as tuneable sources.

In this chapter the problems associated with the non linear nature of calibration, for molecular fragment ions, in a LP-ICP have been addressed. Initial studies on the use of reagent gases in the LP-ICP suggest that by altering the composition of the plasma gas alone, it is possible to utilise the LP-ICP as a soft ionisation source, yielding spectra similar to those of a CI source, or as a harsh ionisation source which provides only elemental information, such as an atmospheric ICP. Furthermore, the source can be operated in a tuneable mode between hard and soft ionisation regimes.

4.2 EXPERIMENTAL

4.2.1 Low Pressure Plasma Mass Spectrometer

The design and construction of the LP-ICP-MS has been described fully in Chapter 3. However, a slight modification to the plasma gas supplies was performed to enable a reagent and make-up gas to be added. This modification was the addition of a 6.4 mm Ultra-Torr "T" vacuum union which was placed between the PFTBA vial and the side arm of the plasma torch. The make-up and reagent gases were added to the plasma torch via this T-piece.

The amount of added nitrogen and isobutane was controlled using a scaled metering valve. The flow rate of the reagent gas through the valve was measured at atmospheric pressure, for a series of needle valve settings, and flow of gas through the orifice of the needle valve,

106

operating under low pressure conditions, was calculated using Poiseuille's relationship[143].

Helium make-up gas was introduced using a 100 ml min⁻¹ mass flow controller (Unit
Instruments, Dublin, Ireland) in place of the needle valve. A diagram of the new gas inlet
system can be found in Figure 4.1. The instrument operating conditions are shown in Table
4.2.

4.2.2 Data Acquisition Parameters

Data were acquired on a Hewlett Packard MS workstation, with HP59970A (Version 3.1)
software, which was interfaced to the MSD. The ions were detected using two different MS
operating modes. For structural information of the analytes, the instrument was operated in
scanning mode, where the mass range 60 - 800 m/z was monitored. For the quantitative
determination of the analytes the instrument was operated in selective ion monitoring (SIM)
mode. In this mode of operation the molecular, halogen, and phenyl ion of the analytes was
monitored.

4.2.3 Reagents and Standards

Standards were diluted in pentane (HPLC grade, Rathburn Chemicals, Scotland, UK) to the
required concentration. Chlorobenzene, iodobenzene and dibromobenzene were obtained
from Aldrich Chemicals (Gillingham, UK). Nitrogen (99.9%) and isobutane (99%) were
obtained from Air Products (Cheshire, UK).

4.3 RESULTS AND DISCUSSION

To date LP-ICPs have been sustained with mainly argon or helium gas. The 1 l min⁻¹ argon
LP-plasma has been utilised for the production of atomic mass spectra, totally atomising
analytes introduced to the source via a GC[35,105,110,111]. The helium LP-ICP has been used as
a dual mode ionisation source producing both atomic or molecular ion mass spectra,
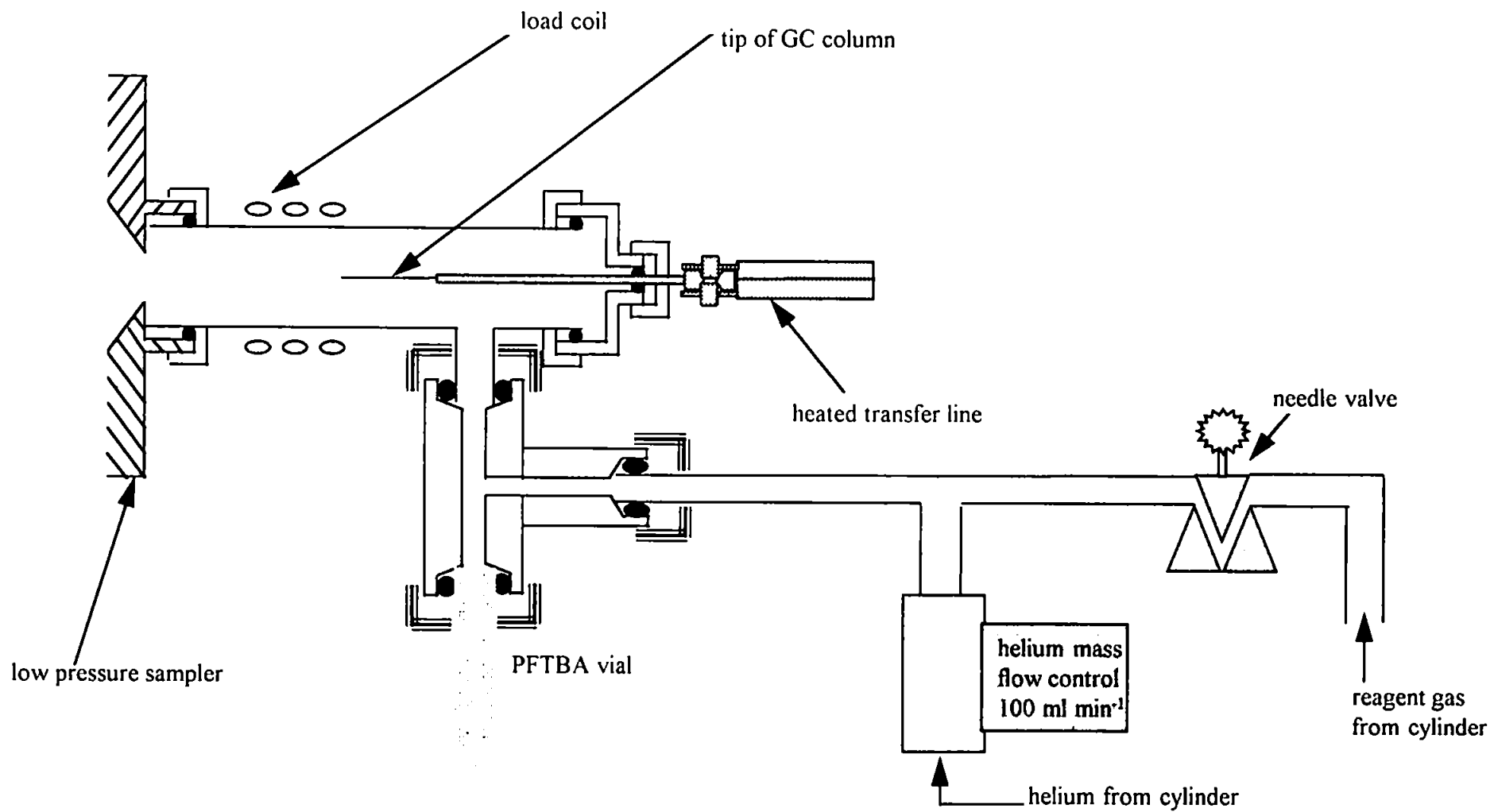
Figure 4.1 Diagram of the low pressure ICP-MS interface for reagent gas addition

load coil

tip of GC column

heated transfer line

needle valve

low pressure sampler

PFTBA vial

helium mass
flow control
100 ml min⁻¹

reagent gas
from cylinder

helium from cylinder

Table 4.2   Operating conditions used for the initial studies with the LP-ICP-MS system.

Mass Spectrometer	Modified Hewlett Packard MSD
Plasma	
Forward power (W)	6
Reflected power (W)	0
Reagent Gases (ml min^{-1})	
Nitrogen	0 - 4.5
Isobutane	0-1.2
Helium	2 - 9
Pressure (Torr)	
Torch	0.2
Interface	0.01
Analyser	<1 x 10^{-6}
Gas Chromatograph	
Injector	Cold on-column
Column	DB5 30m x 0.32 mm
Carrier flow (ml min^{-1})	3
Injection volume (µl)	1
Oven temperature (°C)	40-120 @ 20°C min^{-1}

depending on the gas flow, plasma power, and torch pressure used[35,106,110,111]. However, for the fragmentation studies, relatively large amounts of analyte (>50 ng on-column) were necessary to facilitate the fragment ion formation. Also, the response obtained from the fragments produced by the LP-ICP was not related linearly to the analyte concentration. These two phenomena suggest that the analyte plays a major role in the fragmentation and ionisation process, i.e. the analytes were self-ionising above a certain concentration. In order to investigate this phenomenon it was decided to evaluate the effect of reagent gases on molecular and fragment ion formation.

4.3.1 Nitrogen Addition

4.3.1.1 Optimisation of Skimming Distance and Power

Between 0 and 4.5 ml min^{-1} of nitrogen was added to a 3 ml min^{-1} helium plasma via the side arm tube of the quartz torch. It would be expected that the helium/nitrogen plasma would differ in temperature from a helium only LP-ICP, due to the differing thermal conductivity and ionisation potential of nitrogen compared with helium. If a change in the plasma gas kinetic temperature occurred, then the ion flux through the sampler and skimmer would also change (Equation 3.1 and 3.7). The physical processes that describe this phenomenon have been described in Chapter 3. It has been shown that for a LP-helium ICP the experimental optimum pressure and flow conditions were different to those calculated using theory, hence it was decided to optimise the ion sampling conditions experimentally. For the optimisation study PFTBA was introduced into the helium/nitrogen LP-ICP. Three fragment ions of PFTBA, at 69, 219, and 502 m/z respectively, were monitored continuously while the plasma forward power and the sampler/skimmer spacing were changed. Figure 4.2 a-c shows the resulting plots of the signal intensity, versus skimmer/sampler spacing and forward power, for these fragment ions. The points labelled 'A' correspond to maxima on each plot. The plots are shown in two dimensions only to help

Figure 4.2 Surface contour plots showing the effect of plasma power and skimming
distance on the signal intensity of PFTBA at: (a) 69 m/z; (b) 219 m/z and
(c) 502 m/z. The points labelled 'A' indicate intensity maxima.
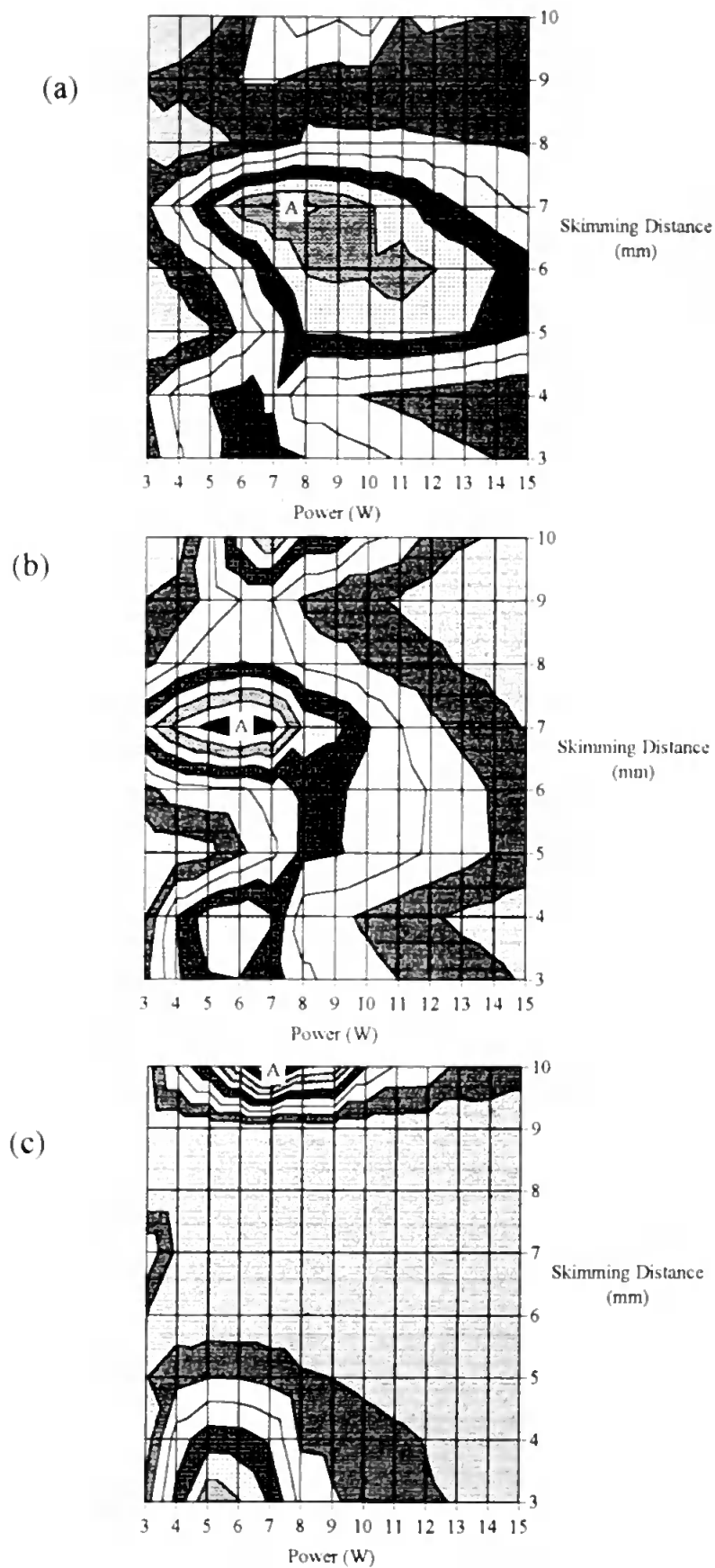
111

reveal the pertinent features. If the plots were to be shown in three dimensions they would reveal plots with three distinct peaks the central peaks, being the most intense for the 69 and 219 m/z fragment ions (point 'A'). This phenomenon has been described in chapter 3 for a helium only LP-ICP-MS, and suggests that several 'shock' regions form behind the sampler. For the helium/nitrogen plasma the fragment ions at 69 and 219 m/z (Figure 4.2 a and b) gave rise to maximum signal intensity at a skimming distance of 7 mm, with less intense peaks at 4 and 10 mm. However, the fragment ion at 502 m/z (Figure 4.2 c) yielded no maxima between 5-9 mm and instead yielded maxima at 3 mm and 10 mm. This may be because the higher mass fragment at 502 m/z, underwent a different ionisation process compared with the lower mass fragments, or was ionised in a different part of the plasma or interface. The occurrence of the maximum signal intensity at 3 mm skimming distance for the 502 m/z fragment suggests that this ion is formed in the low pressure plasma itself, or within the first 3 mm of the expanding jet of sampled gas. Whereas, the 69 and 219 m/z fragments yield maxima at 7 mm skimming distance. This indicates that these ions may not be formed in the plasma but may undergo fragmentation and ionisation in the expansion interface. This is indicative of a secondary discharge being present in the expansion interface. Alternatively, the helium/nitrogen plasma may simply cause the molecular ion at 502 m/z to fragment further into smaller molecular species. Chapter 5 will deal with the ionisation process in more detail.

It is also evident that the optimum plasma operating power differed greatly depending on the skimming distance and fragment ion studied. Figure 4.3 shows the effect of power on the signal intensity for fragment ions of PFTBA with a sampler/skimmer distance of 7 mm. At this skimming distance the optimum power for 219 m/z ion was 6 W and that for the 69 m/z fragment was at the highest power, between 7 and 8 W. However, the 502 m/z ion showed a rapid decrease in signal as the power was increased from 2 W suggesting that as
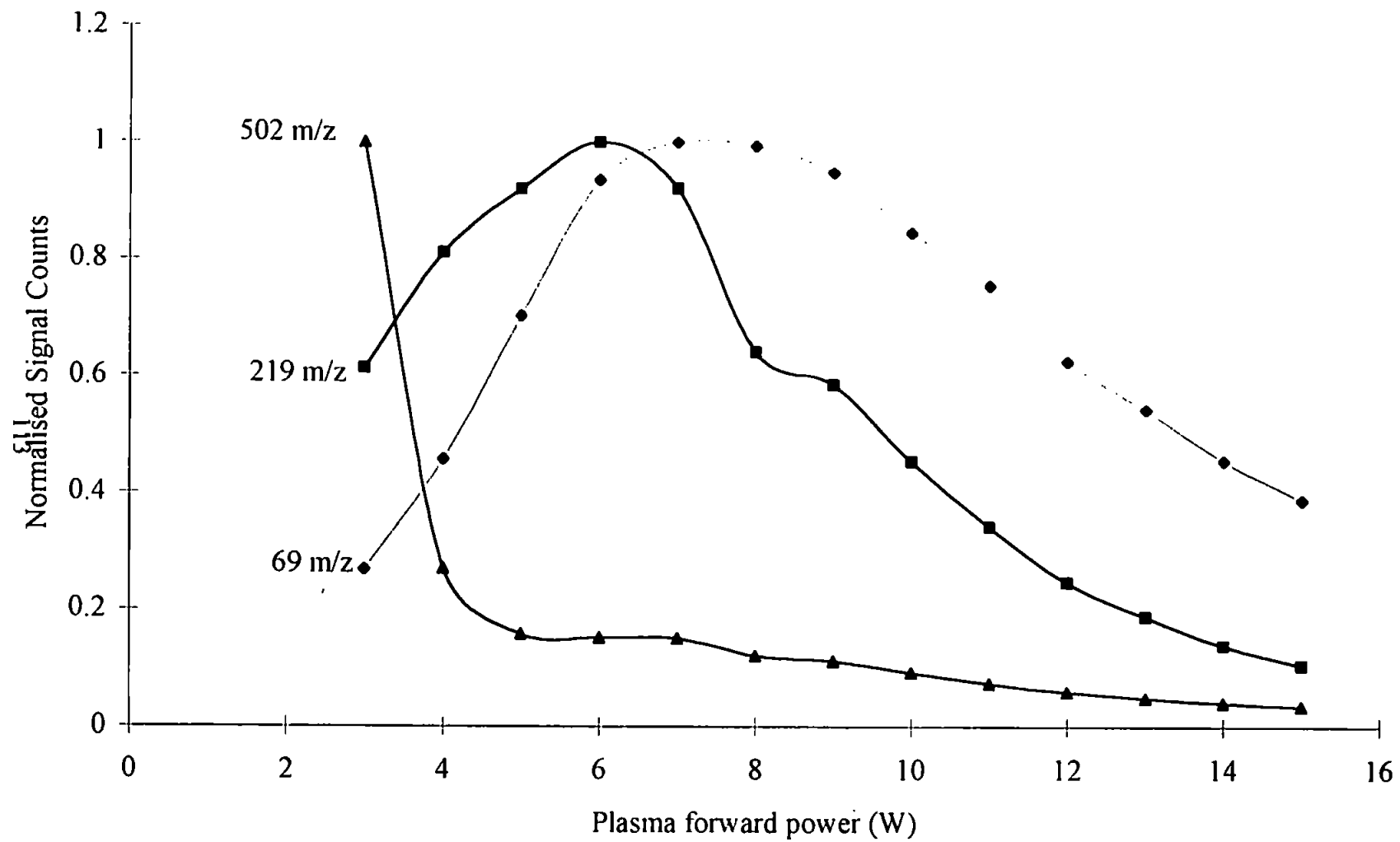
Figure 4.3 Plot of normalised signal intensity versus plasma power for the fragment ion of PFTBA at; 69, 219, and 502 m/z, at 7mm skimming distance.

the power was increased, the 502 m/z fragment of PFTBA was quickly broken down. The increase in the 219 and 69 m/z signal for the PFTBA suggests that the 502 m/z ion was further fragmented, hence increasing the signals of the lighter fragments. Above 8W forward power even the smaller molecular fragments began to disintegrate, which should add to the atomic ion signals, though these could not be monitored because of the high background signals between 12 and 32 m/z.

4.3.1.2 Optimisation of Gas Flows

Optimisation of the helium carrier gas flow and the nitrogen reagent gas flow for the production of stable molecular ions was performed when introducing discrete 10 ng injections of chlorobenzene into the plasma via the GC. The molecular ion for chlorobenzene (112 m/z) and the phenyl ion (77 m/z) were monitored continuously for three repeat 1 µl injections of the 10ng/µl standard. The helium carrier gas flow rate had little effect on the chlorobenzene signal (Figure 4.4) up to 7 ml min^{-1}, with both the phenyl and molecular ions remaining fairly constant in intensity between 2 and 5 ml min^{-1}. However, as the carrier gas flow was increased the signals became increasingly unstable, indicated by the increased standard deviations of the chlorobenzene signals, shown in Figure 4.4. The optimum carrier flow rate was 3 ml min^{-1}. The signal for the molecular ion decreased above 6 ml min^{-1} helium. This could be due to the extra gas increasing the electron and ion number density, and thermalising the plasma. This would lead to a greater number of collisions between the analyte and electrons, which in turn, would lead to increased fragmentation of the analyte causing a reduction in the molecular signals. On addition of 7 ml min^{-1} of helium, the molecular ion decreased whereas the phenyl ion signal increased, which may be caused by the molecular ion fragmenting and adding to the phenyl ion signal. However, the precision was poor so it was not possible to draw a firm conclusion. Above 7 ml min^{-1}
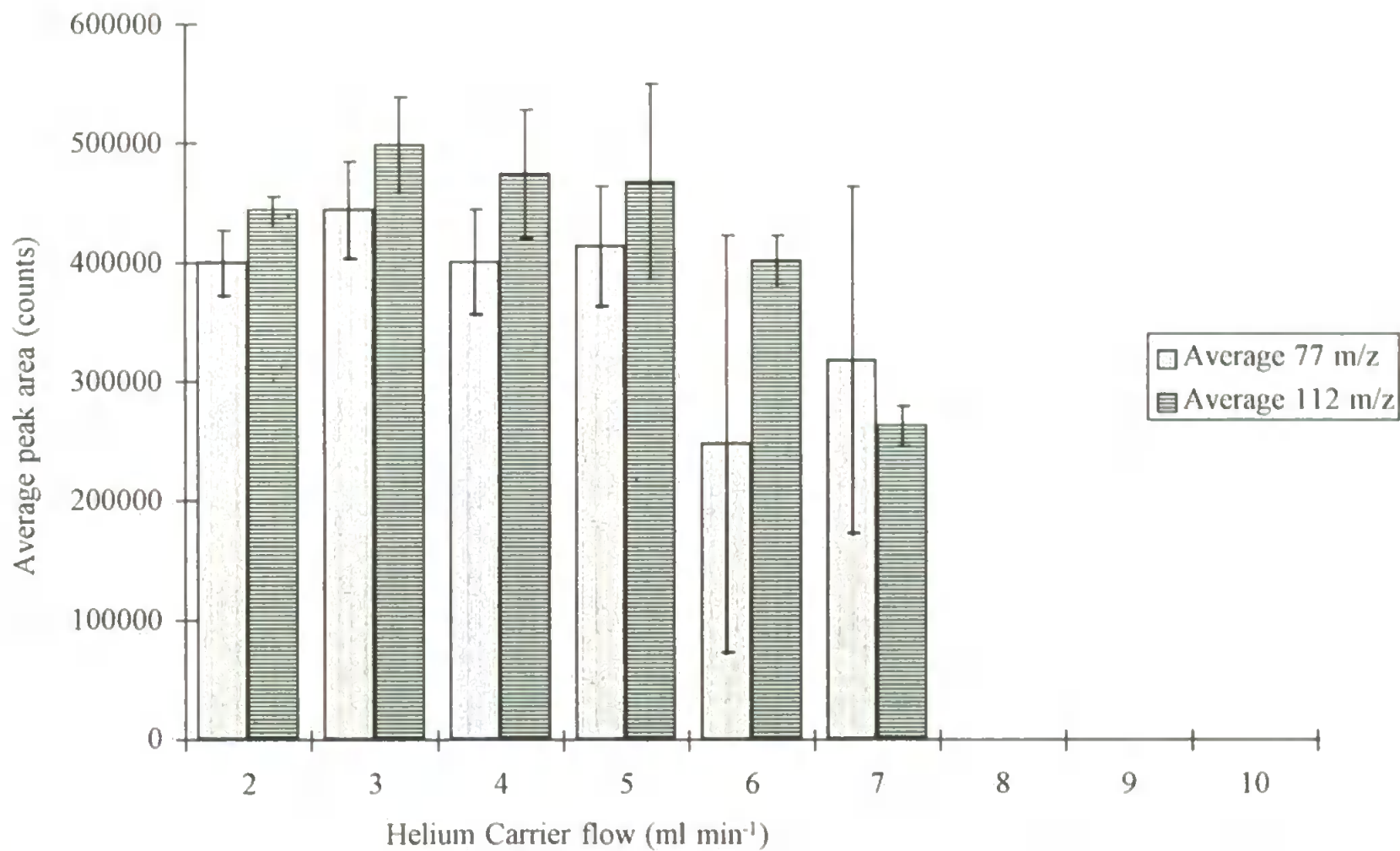
Figure 4.4   Effect of helium carrier gas flow rate on the signal intensity of a 10 ng on-column injection of chlorobenzene, in a nitrogen/helium LP-ICP.

helium the phenyl and molecular ion signals disappeared, which could be because the ions became totally atomised, yielding only atomic information.

The effect of the nitrogen gas added to a 3 ml min⁻¹ helium plasma, on the chlorobenzene signal is shown in Figure 4.5. The signal for the molecular ion peak at 112 m/z for chlorobenzene was relatively unaffected by the nitrogen as the signal remained fairly constant up to 2.1 ml min⁻¹. With nitrogen flows above 2.1 ml min⁻¹ the signal for both the molecular ion and the phenyl ion decreased by over 50%. Again this may be due to the increased electron and ion density in the plasma causing further fragmentation of the analyte. A point of interest is the stability of the analyte signals, even above a combined gas flow of 7 ml min⁻¹. This suggests that the unstable signals obtained on adding helium carrier gas were due to degradation of chromatographic efficiency, or that the lower thermal conductivity of nitrogen compared with helium may have stabilised the LP-ICP. The improved stability is shown in Figure 4.6, which shows ten, 100 pg on-column, repeat injections of chlorobenzene, while keeping the oven at 40°C. This isothermal repeated injection run yielded a coefficient of variance of 8%. This was considered acceptable since, manual on-column injection can have a coefficient of variance as high as 10% at this sample volume.

4.3.1.3 Figures of Merit

Once the optimisations were completed, an investigation of the analytical figures of merit was performed. Optimised operating conditions and figures of merit are shown in Tables 4.2 and 4.3 respectively. The figures of merit were obtained by selective ion monitoring for the molecular ion of chlorobenzene (112 m/z). The detection limit of 2 pg shows that the LP helium-nitrogen plasma is capable of producing molecular and fragment ions at ultra trace levels thereby facilitating qualitative and quantitative analysis. Also the nitrogen addition

116
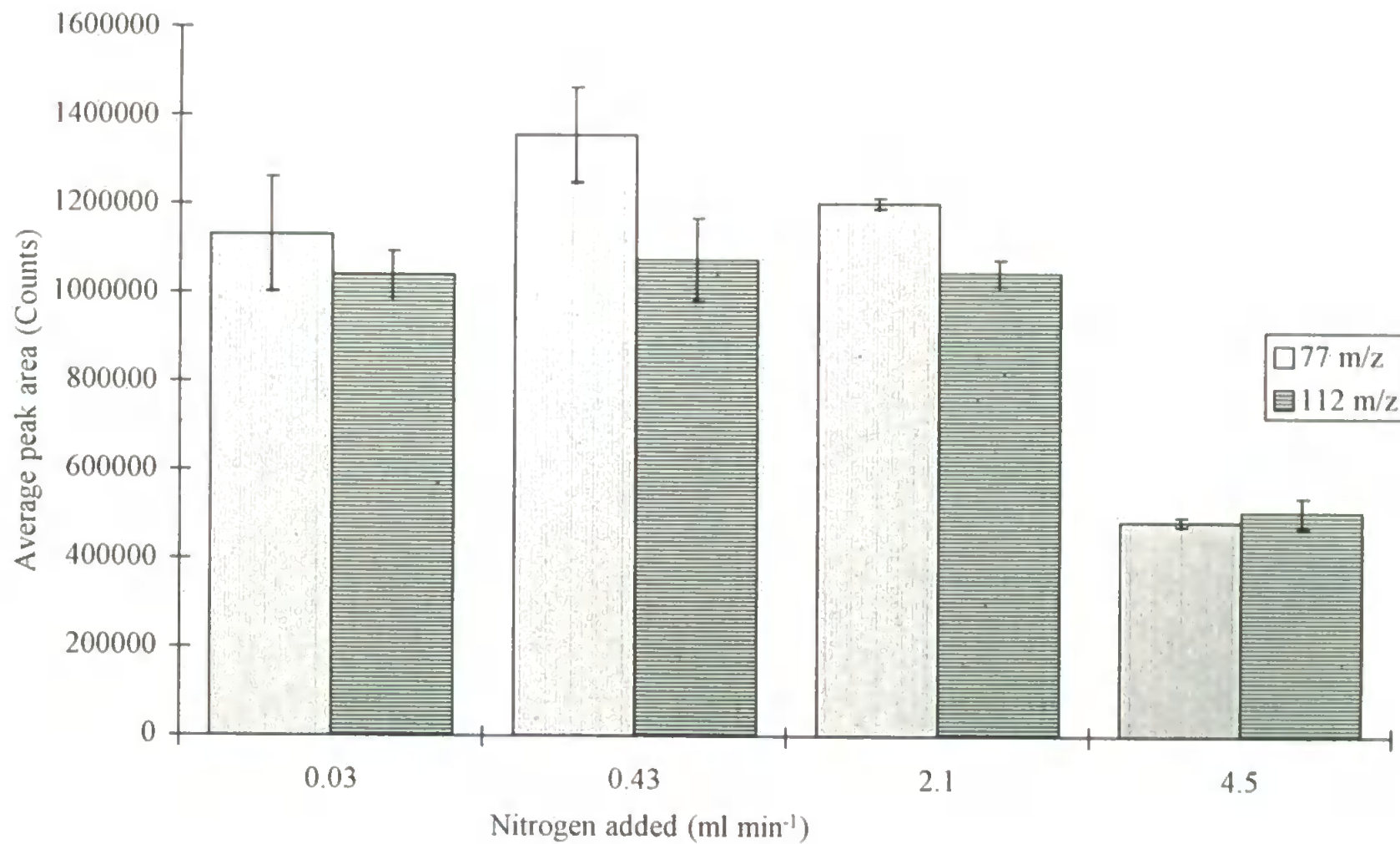
Figure 4.5   Effect of nitrogen make-up gas flow rate on the signal intensity of 10 ng on-column injection of chlorobenzene, in a 3ml min⁻¹ helium LP-ICP.

Table 4.3   Analytical figures of merit for chlorobenzene using a 0.43 ml min^{-1} nitrogen,

3 ml min^{-1} helium LP-ICP.

Single Ion Monitoring- Mass Monitored	112 m/z
Linear range studied (decades)	3
Slope / counts pg^{-1}	99
r^2(regression coefficient)	0.985
Slope of Log-log plot	1.012
Detection limit[a] / pg	2
RSD[b] (%)	8.5

a) LOD= 3σ/slope

b) RSD(%) for 5 replicate 10 pg injection
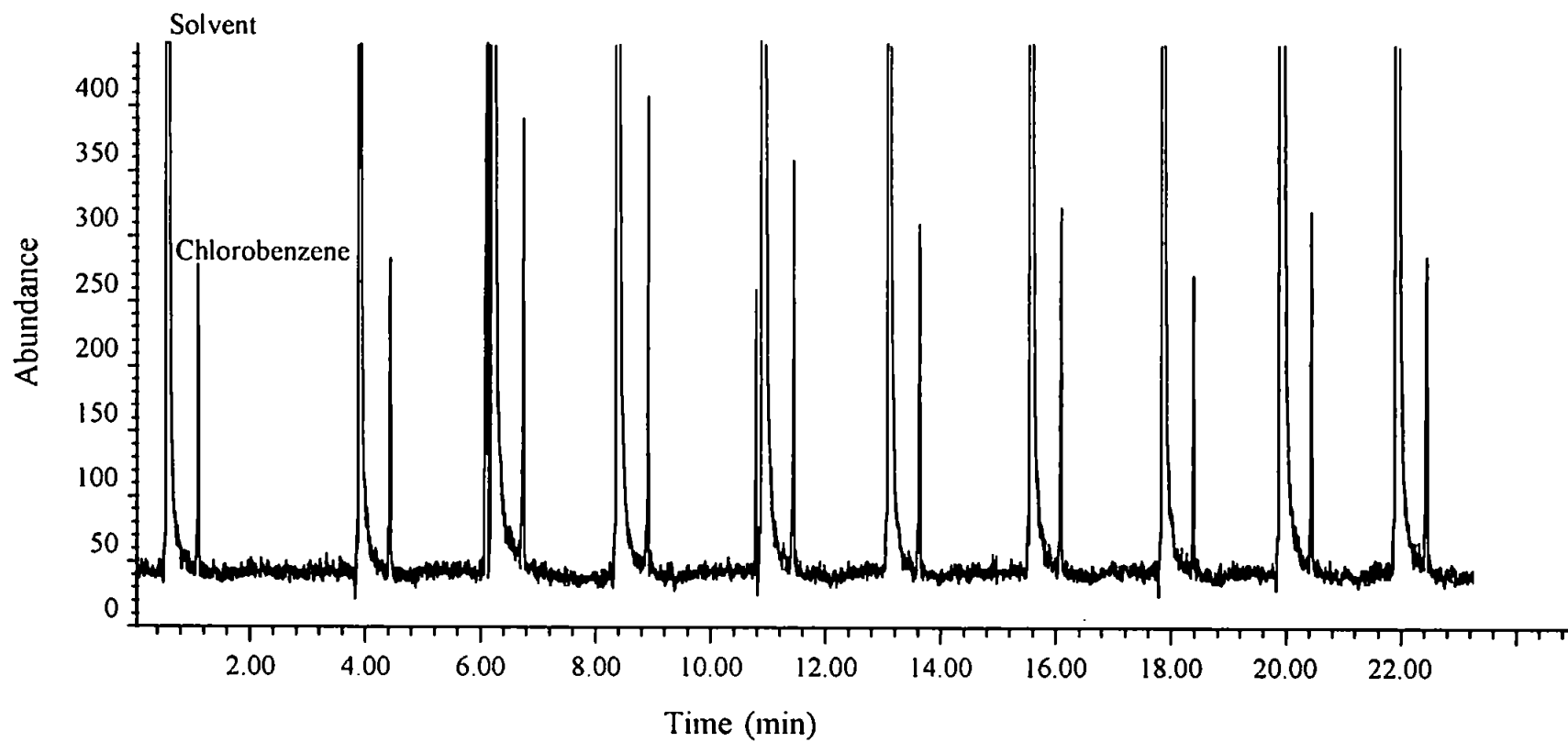
Figure 4.6   Selective ion chromatogram (112 m/z) of ten repeat injections of 100 pg on-column of chlorobenzene.

improved the linear range of calibration, with calibration over three orders of magnitude possible (Figure 4.7). This is a vast improvement compared with the helium only LP-ICP-MS for which calibration was not possible. Figure 4.8 shows a SIM chromatogram at 112 m/z for a 100 pg on-column injection of chlorobenzene illustrating the excellent signal to noise ratio obtained.

These results suggested that the addition of nitrogen to the LP-ICP-MS would cure the problems encountered previously. However for analytes with retention times greater than 2 minutes, only the atomic signals were observed. This was thought to be due to the influence of the tail of the solvent peak on chlorobenzene because of the short retention time of the latter. In order to try and mimic the effect of the solvent tail throughout the chromatographic run it was decided to investigate the use of isobutane as the reagent gas.

4.3.2 Isobutane Addition.

Between 0 and 1.5 ml min^{-1} of isobutane was added to the LP helium plasma in a similar manner to nitrogen, and its effect on the molecular, phenyl, and atomic ion signals for a series of halobenzenes was investigated. The analytes were injected, approximately 10 ng each on-column, as a mixed standard. Figure 4.9a shows the effect of the isobutane on the signals for 10 ng on-column injection of chlorobenzene. The atomic ion signal for chlorine has not been shown because fragment ions from the reagent gas interfered with ion signals below 58 m/z. With a 3 ml min^{-1} helium only plasma, the molecular ion of chlorobenzene was the parent ion. On the addition of the reagent gas both molecular ion and phenyl ion signals were increased greatly. However, as the reagent gas partial pressure was increased further the phenyl ion peak disappeared leaving only the molecular ion (Figure 4.9a). This is consistent with the isobutane/helium plasma acting as a conventional CI source where the partial pressure of the reagent gas often determines the analyte spectra obtained[3]. Unlike the

120
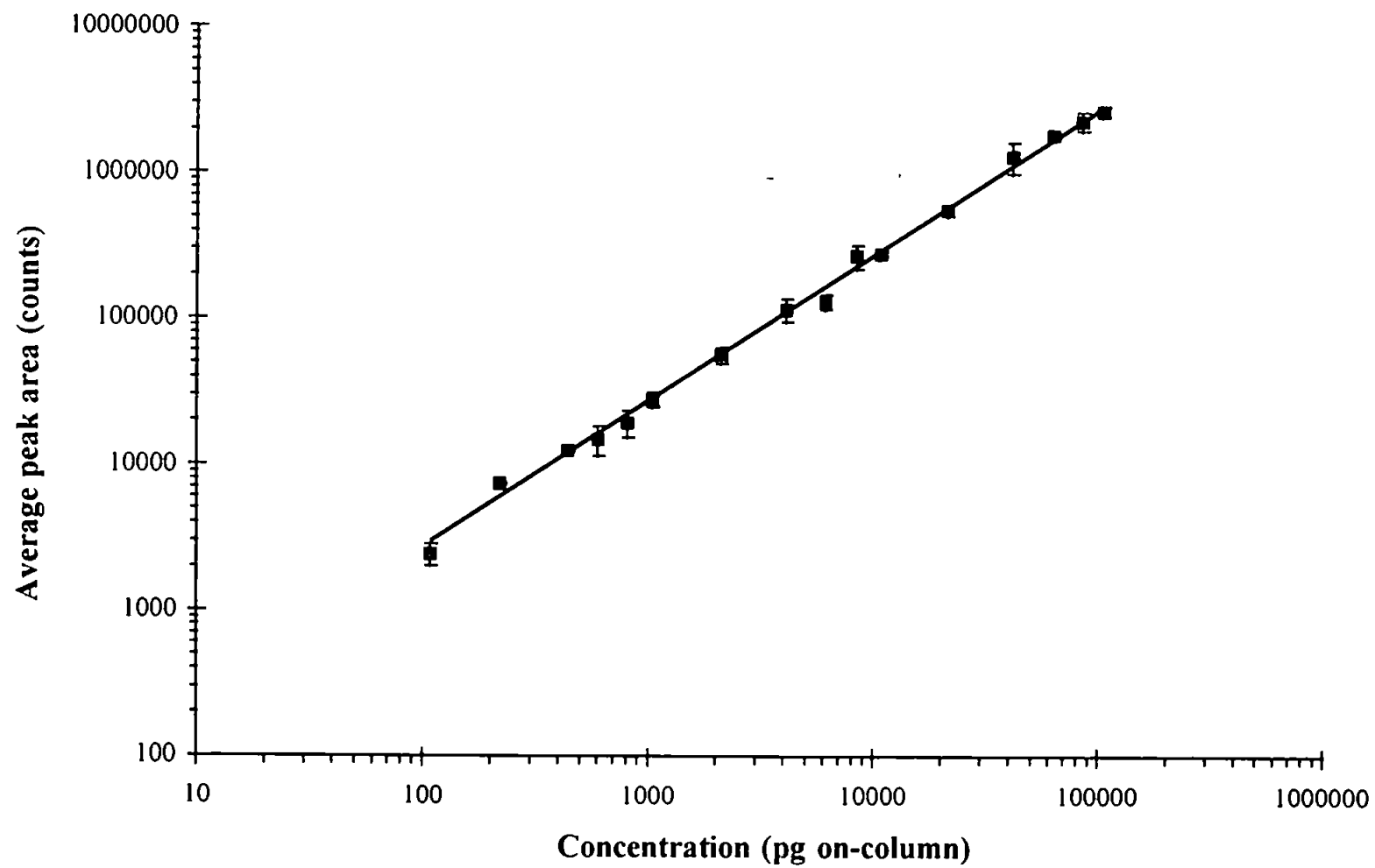
Figure 4.7   Linear calibration range for chlorobenzene using a 6W, nitrogen/helium (0.43/3.0 ml min⁻¹) LP-ICP.
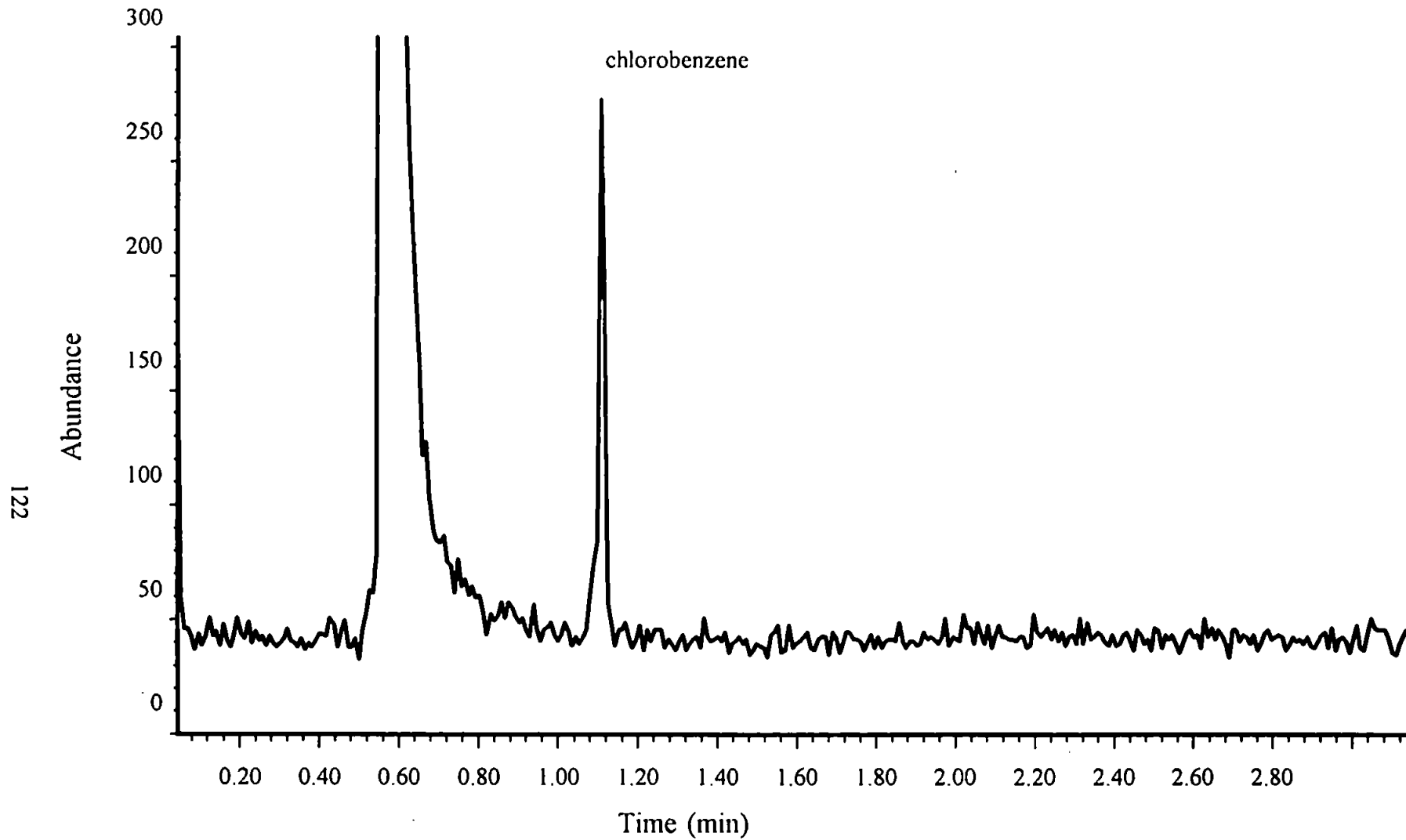
Figure 4.8   Chromatogram of a 100 pg on-column injection of chlorobenzene for a helium/nitrogen (3.0/0.43 ml min⁻¹) LP-ICP using selected ion monitoring at 112 m/z.

Figure 4.9 Effect of isobutane make-up gas flow on the signal intensity of the molecular and fragment ions of (a) chlorobenzene; (b) iodobenzene; and (c) dibromobenzene, in a 3 ml min^{-1} helium LP-ICP.
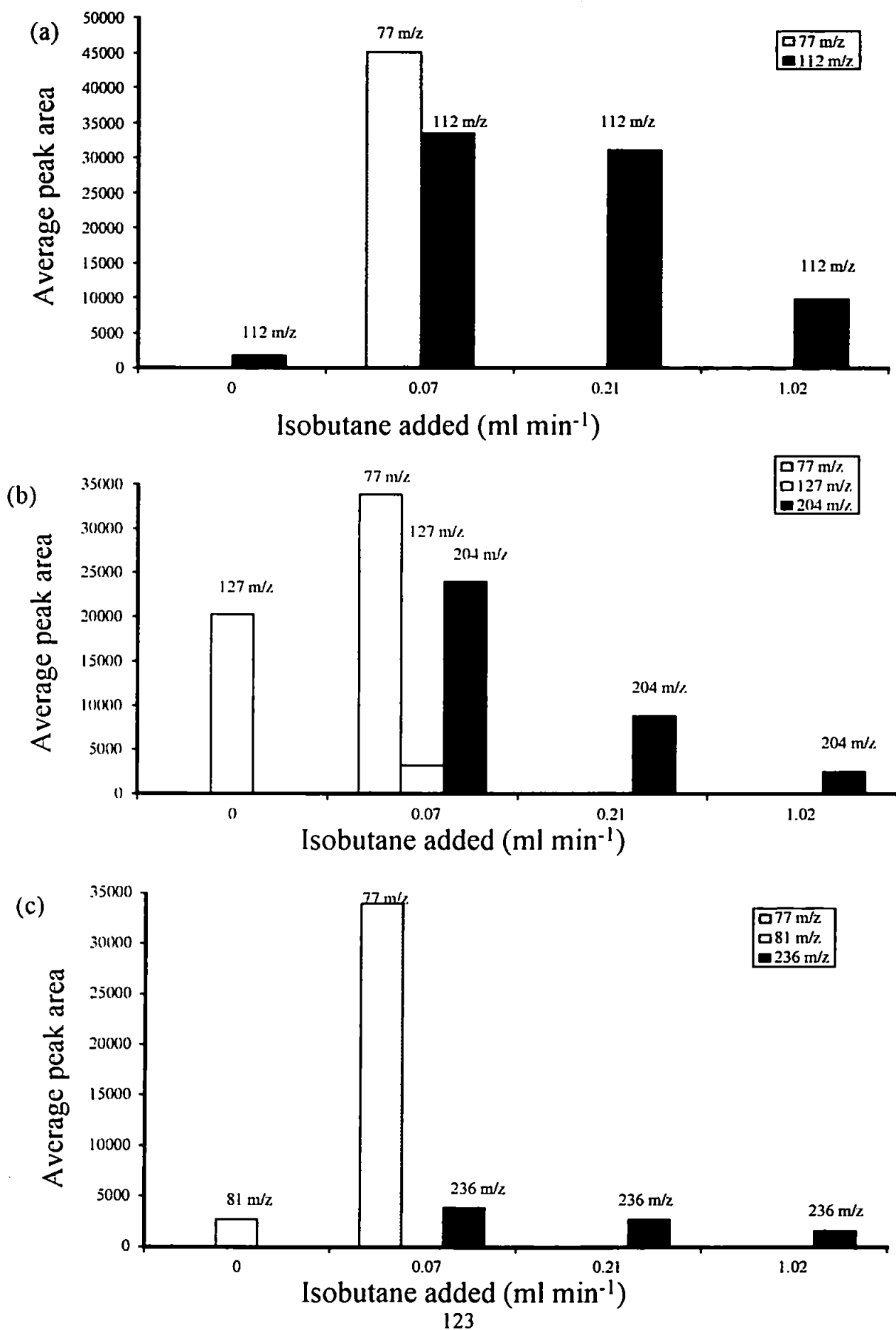
nitrogen reagent gas, the effects of isobutane were consistent throughout the chromatographic run. Figure 4.9b and c show the effect of isobutane on iodobenzene and dibromobenzene which had retention times of 1.1 and 2.0 minutes respectively. For the 3 ml min^{-1} helium plasma, with a 10 ng on-column injection, the only ions that were observed were the atomic signals for the halogens. When 0.07ml/min of isobutane reagent gas was added the phenyl and molecular ions were observed. This yielded spectra very similar to those obtainable by EI source MS. On the addition of more isobutane the phenyl and atomic halogen ion signals were no longer observed and only the compound molecular ion remained, yielding spectra similar to that expected from CI source MS. However, on the addition of greater than 1 ml min^{-1} isobutane, the molecular ion signals started to reduce in intensity. The halogen and phenyl ions of the analytes did not increase on the reduction of the molecular ions. This suggests a reduction in the ionising capability of the source, because if the ionising capability increased one would expect to see corresponding increases in the signals for the lower mass fragment ions as the molecular ion decomposed.

Figure 4.10 shows a total ion chromatogram, for a 10 ng on-column injection of chlorobenzene, iodobenzene and dibromobenzene, obtained using a 0.07 ml min^{-1} isobutane/ 3ml min^{-1} helium LP-ICP. The resulting mass spectrum for each compound is shown in Figure 4.11 a-c. The predominant ionisation mechanism for isobutane in CI is proton transfer. However, the mass spectra of the halobenzenes studied (Figure 4.11 a-c) show little sign of protonation with the MH$^-$ peak being less than one third the intensity of the M$^-$, and in the case of the iodobenzene no MH$^+$ peak was visible. This, along with the reduction in molecular and fragment ion signals caused by increasing the isobutane partial pressure, suggests that the isobutane was not behaving as a proton transfer reagent gas. Also, no quasimolecular ions, such as M$^+$ + 57 m/z, were observed. On the addition of 0.07 ml min^{-1} of isobutane the major reagent ion was 57 m/z. This is consistent with the loss of a
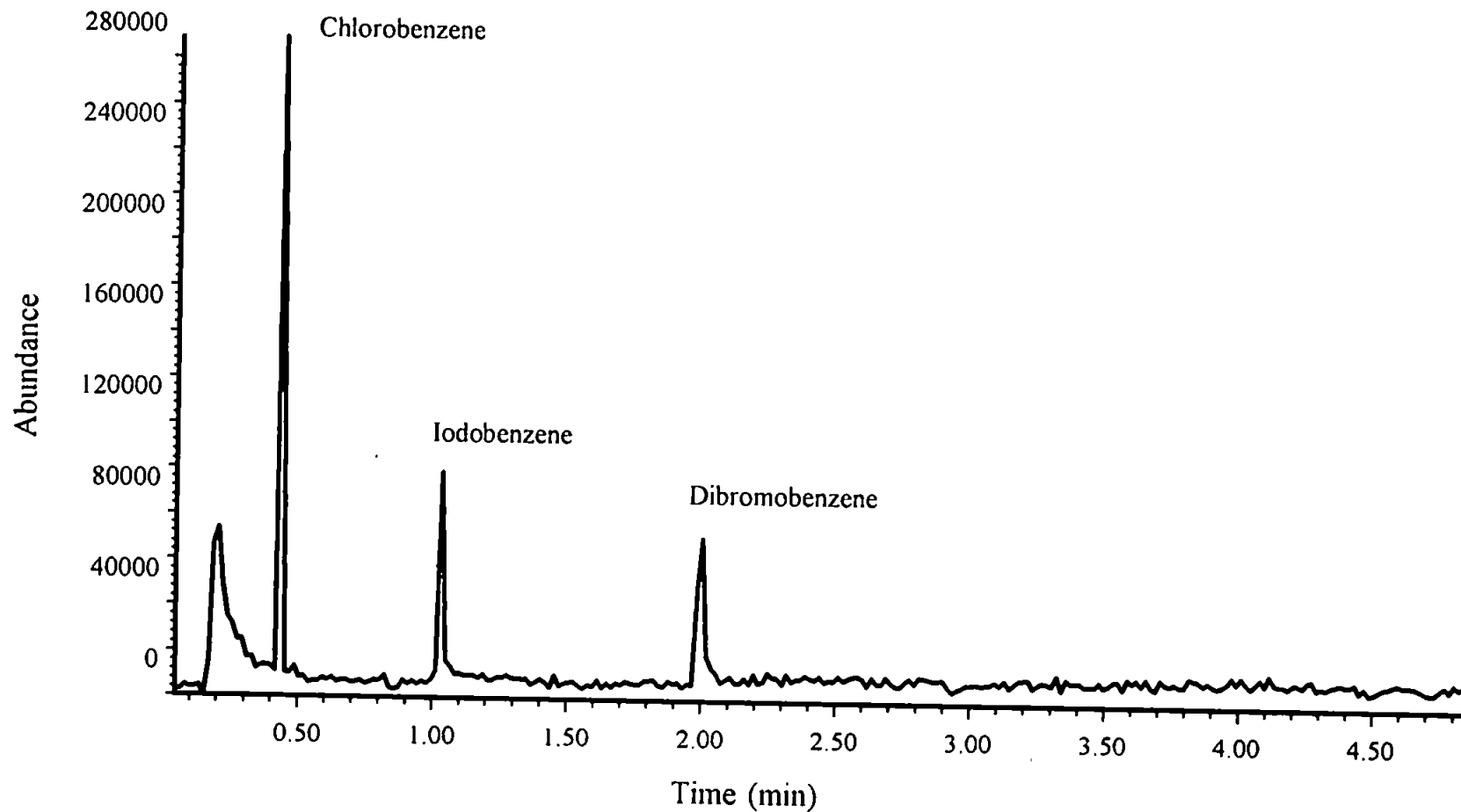
Figure 4.10 Total ion chromatogram for a 10 ng on-column injection of chlorobenzene, iodobenzene and dibromobenzene for a helium/isobutane (3.0/0.07 ml min⁻¹) LP-ICP

Figure 4.11 Mass spectra scans obtained from an isobutane/helium (0.07/3.0 ml min^{-1}) LP-ICP for 10 ng on-column injection of (a) chlorobenzene; (b) iodobenzene; and (c) dibromobenzene.
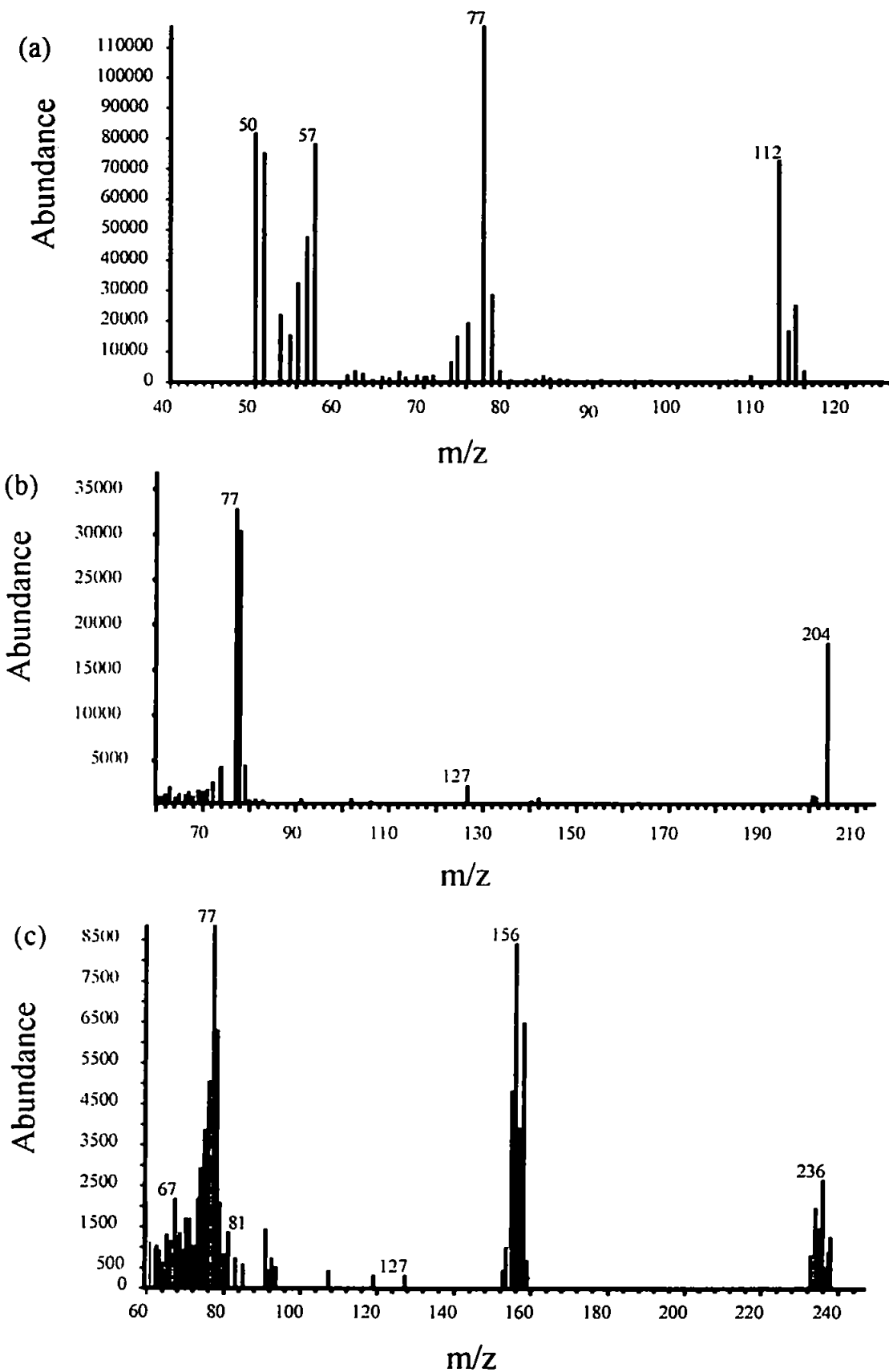
proton from the isobutane, however, it has already been shown that protonation of the analytes was not the dominant ionisation process. As the reagent gas concentration was increased the most abundant reagent ion changed from 57 m/z to 43 m/z, which is consistent with the loss of a methyl group from isobutane. This suggests that as more isobutane was added the plasma ionisation processes were getting harsher, because greater fragmentation was observed. However, Figure 4.9 shows that analyte fragmentation exhibited the opposite trend, with only the molecular ion being detected on increasing the isobutane added. An alternative explanation may be that the ionisation process of the helium plasma was suppressed by the presence of the isobutane, and that as more isobutane was added a greater amount of energy was required to form the reagent ions, thereby leaving less energy to ionise the analyte and resulting in molecular ion production only.

This suggests that the source was not acting as a conventional CI source and that a number of ionisation mechanisms were taking place. This is consistent with other plasma sources where a number of non-equilibrium properties are used to describe the plasma ionisation characteristics. Most plasmas do not exhibit thermal equilibrium at atmospheric pressure, let alone at reduced pressure. Charge transfer is a well known ionisation mechanism in helium plasmas, involving helium metastables, ions and atoms, and if ionisation was occurring via charge transfer in a helium/isobutane plasma, one would expect a small degree of fragmentation and ionisation due to the low ionisation potential of isobutane (10.57eV)[144]. Charge transfer from isobutane to the analyte species can be investigated by reagent ion monitoring[9,145,146]. This is possible because the charge transfer reaction results in the reagent ion forming a neutral species, so a decrease in reagent ion intensity would be expected as analyte enters the LP-ICP. Figure 4.12 shows the selective ion chromatograms of the halogen species and the reagent ion of isobutane. This shows no drop in reagent ion signal suggesting that charge exchange from isobutane is unlikely.

127
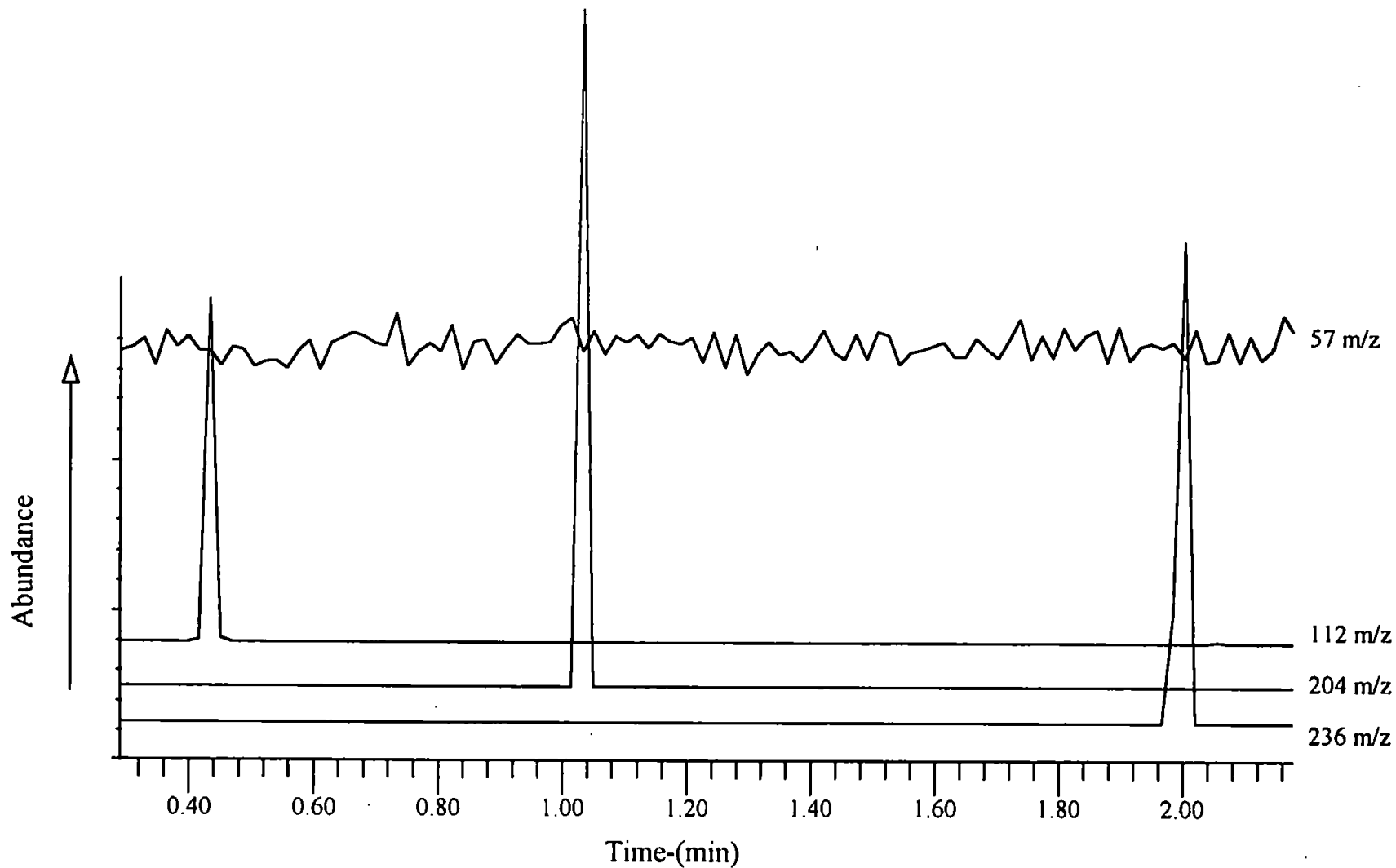
Figure 4.12 Selective ion monitoring for the molecular ion of chlorobenzene (112 m/z), iodobenzene (204 m/z), dibromobenzene (236 m/z) and the reagent ion of isobutane (57 m/z), for a 6W isobutane/helium LP-ICP.

These results suggest that isobutane played no active role in the ionisation process, therefore an isobutane CI process can be ruled out. However the effects of the isobutane are clearly visible on the molecular ion signals. Another explanation for this may be that the isobutane is influencing the helium plasma ionisation processes. The addition of methane to glow discharge sources has been used to investigate the role of Penning ionisation in the source[147,148]and it has been shown that the addition of the molecular gas reduces the number of metastable species in the GD. Such a reduction in metastables has resulted in a reduction in analyte atomic ions. The effect of the molecular gas is to act as a transport route for the metastable to reach the ground state which results in the emission of a low energy electron. The occurrence of such a process in the LP-ICP would explain the phenomenon observed here. In a helium only plasma, Penning ionisation would cause ionisation of the analyte yielding atomic ion signals. The absence of such a process would normally lead to a drop in analyte ionisation. However, the resulting electrons, produced by quenching the metastable species, will be quickly accelerated by the rf field and will gain enough energy to cause electron impact ionisation of the analytes. Such a process would explain the similarities between the observed mass spectra from the LP-ICP-MS and those produced by an electron impact source.

The figures of merit for the helium/isobutane plasma operating in the molecular mode are shown in Table 4.4 with typical calibration graphs shown in Figure 4.13. The detection limits obtained would be considered average for a modern EI-MS. However in molecular MS, selective ion monitoring is used for quantitative analysis. The base peak in the analyte spectrum is chosen as the selected ion for quantitative analysis. The very nature of this type of analysis suggests that detection limits in the molecular mode are totally dependent on the individual compound to be analysed. Compounds that exhibit little fragmentation or yield a single intense fragment ion will have considerably lower limits of detection than one which

Table 4.4   Analytical figures of merit for chlorobenzene, iodobenzene and

dibromobenzene, using a 0.25ml min^{-1} isobutane, 3 ml min^{-1} helium LP-ICP.

Analyte	Chlorobenzene	Iodobenzene	Dibromobenzene
Selected ion monitoring- mass monitored	112 m/z	204 m/z	236 m/z
Linear range studied (decades)	3	3	3
Slope/ counts ng^{-1}	84645	28405	4905
r^2 (regression coefficient)	0.9925	0.9848	0.9925
Log-log slope	0.85	0.74	0.70
Detection limit[a] / pg	100	140	229
RSD[b] (%)	12	6	5

a) LOD= 3σ/slope

b) RSD(%) for 5 replicate 380 pg injection
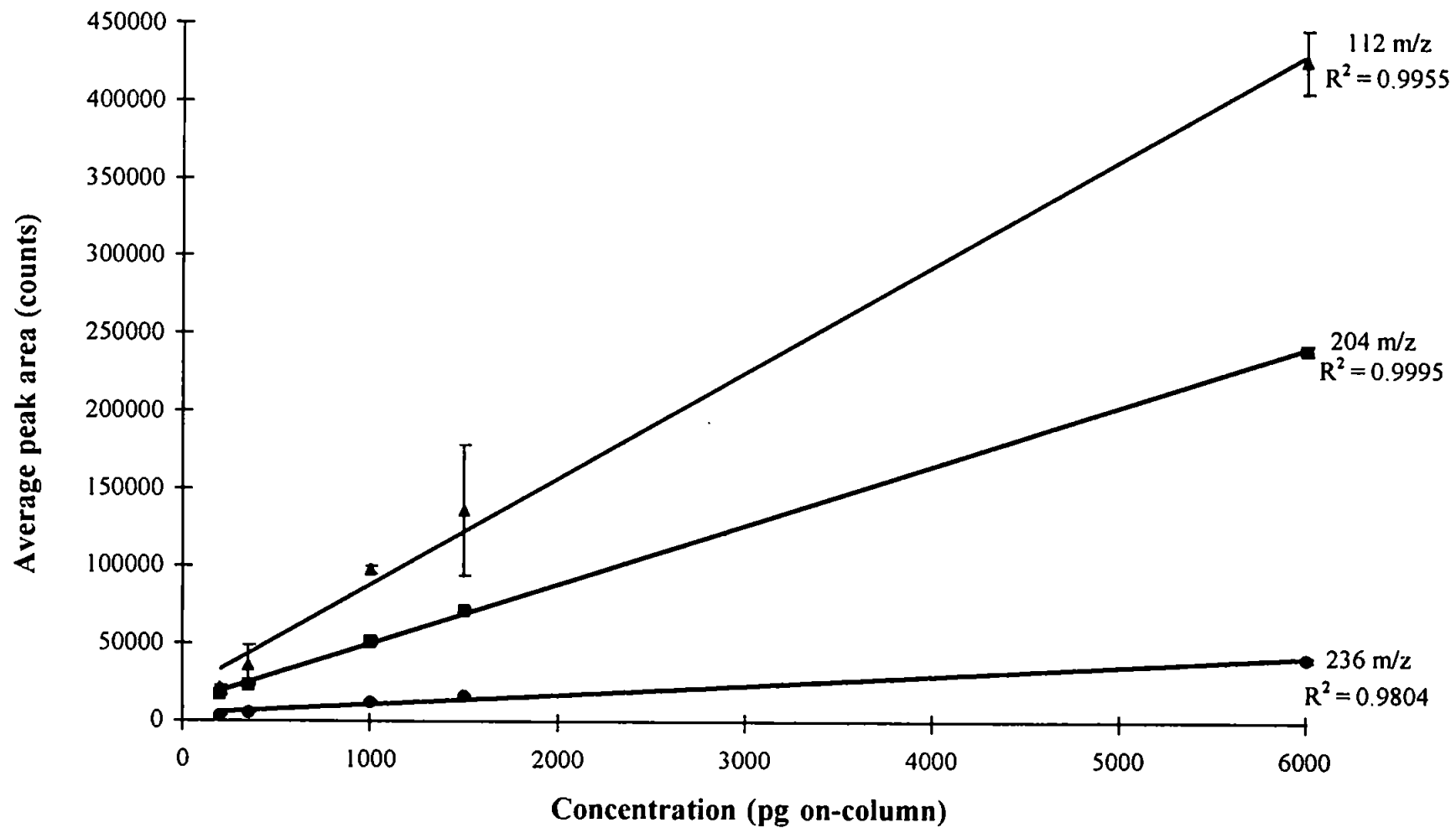
Figure 4.13 Calibration graphs for a 6W helium/isobutane (3.0/0.07 ml min^{-1}) LP-ICP for chlorobenzene (112m/z), iodobenzene (204m/z) and dibromobenzene (236m/z).

fragments easily yielding many less intense fragment ions. Therefore, a better representation of how the limits of detection obtained by the LP-ICP-MS compare with EI-MS, is to use the limit of detection reported by the manufacturer of the MSD used in this study. A detection limit of 10 pg for methyl stearate, which yields an intense molecular fragment ion at 128 m/z, has been reported[149]. The limits of detection for the LP-ICP-MS operating in the molecular mode, reported in Table 4.4, were obtained using selected ion monitoring of the molecular ion. It can be seen in Figures 4.11 a-c that the molecular ion is not the base peak of the compounds studied, as this was the phenyl ion at 77 m/z in all spectra. The base peak was not chosen as the selected ion in this instance as the LP-ICP has been shown to be a tuneable source, therefore it would be possible to influence the abundances of the fragment ions in the spectra, with the lowest limits of detection expected when the source was operated in the atomic mode. Therefore, it was necessary to prove that qualitative information was available from low levels of analyte.

4.3.3 Helium Addition

In the initial studies performed using a LP helium ICP the dependence of molecular ion formation on the analyte concentration suggested that a chemical ionisation process dominated in the plasma. If the helium was acting as a reagent gas for conventional CI the expected dominant ionisation process would be charge transfer. The rate of charge transfer is dependent on the partial pressure of reagent gas and analyte in the source. The survival of molecular ions in a charge transfer source is also dependent on the internal energy of the ion. If the internal energy is large (>5 eV) a great deal of fragmentation would be expected. The internal energy of a molecular ion can be calculated using equation 4.2[3];

$$E_{int} = RE(X^+) - IP(M) \qquad (4.2)$$

Where; $RE(X^-)$ is the recombination energy of the reagent ion (24.6 eV for helium) and $IP(M)$ is the ionisation potential of the analyte molecule. This would lead to an internal

energy of over 13eV for the molecular ions of the halobenzene series studied, with ionisation potentials between 9 and 11eV. Hence, extensive fragmentation of the analyte molecules would be predicted using a dense helium plasma. However, in conventional CI-MS, it is not unusual to observe molecular ions of organic molecules with ionisation potentials less then 10eV, when using helium as the reagent gas. Therefore, the presence of the rf magnetic field may induce collisional energy exchange between excited electrons and the analyte, increasing the ionisation power of the plasma. Hence, by increasing the helium partial pressure in the LP-ICP, the rate of charge exchange would increase. This should lead to greater fragmentation, and eventually atomisation of the analyte molecules, leaving only the atomic ions to be detected. This suggests the possibility of utilising a low flow helium LP-ICP-MS for atomic MS.

To test this hypothesis a helium make up gas was added to the plasma gas, via the side arm of the LP torch. The effect of this extra gas on analyte atomic signals for dibromobenzene is shown in Figure 4.14. It can be seen that the addition of gas increased the analyte atomic signal until at 7 ml min^{-1} the atomic signal decreased slightly. A 6 ml min^{-1} helium LP-ICP was then studied for the production of elemental mass spectra for iodobenzene and dibromobenzene. Figure 4.15 a-b show the resulting mass spectra (60-240 m/z) of a 50 ng on-column injection of the standards, proving the existence of only the atomic signals for the iodine (127 m/z) and bromine (79 and 81 m/z) even at this relatively high concentration. This shows that the 6 ml min^{-1} helium plasma operating at only 6W forward power can atomise and ionise the halobenzenes. Figure 4.16 a and b show extracted ion chromatograms for 50 ng on-column injection of iodobenzene and dibromobenzene at 127 and 81 m/z respectively. The chromatograms show extensive peak tailing which is thought to be due to the analyte atomic ion interacting with the wall of the plasma torch, whereas
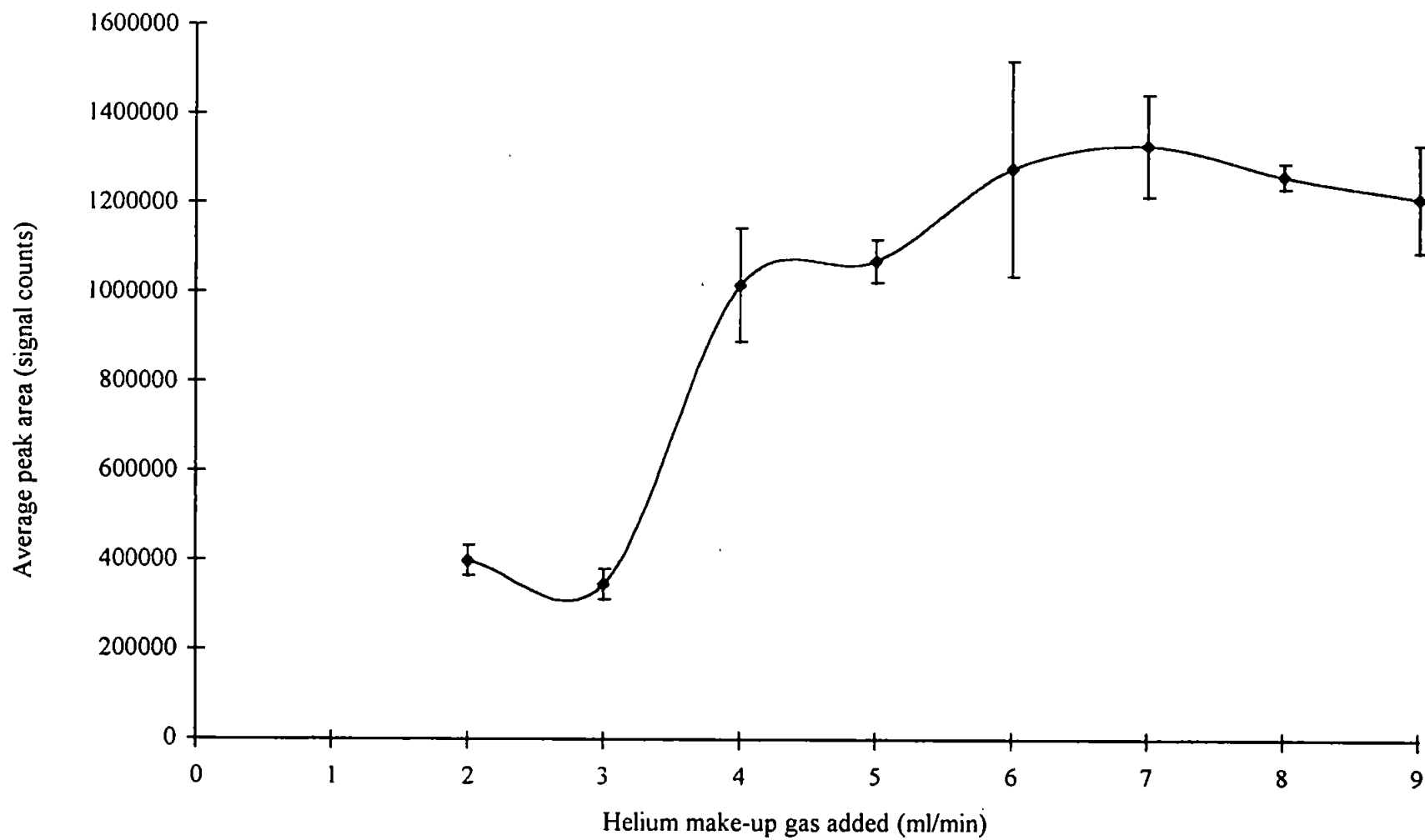
Figure 4.14 Effect of make-up gas on the signal for bromine (81 m/z) from a 10 ng injection of dibromobenzene for a 6W LP-ICP-MS.

Figure 4.15 Mass spectra obtained for a 6 ml min⁻¹ helium LP-ICP for a 50 ng
on-column injection of (a) iodobenzene and (b) dibromobenzene.

(a)

(b)
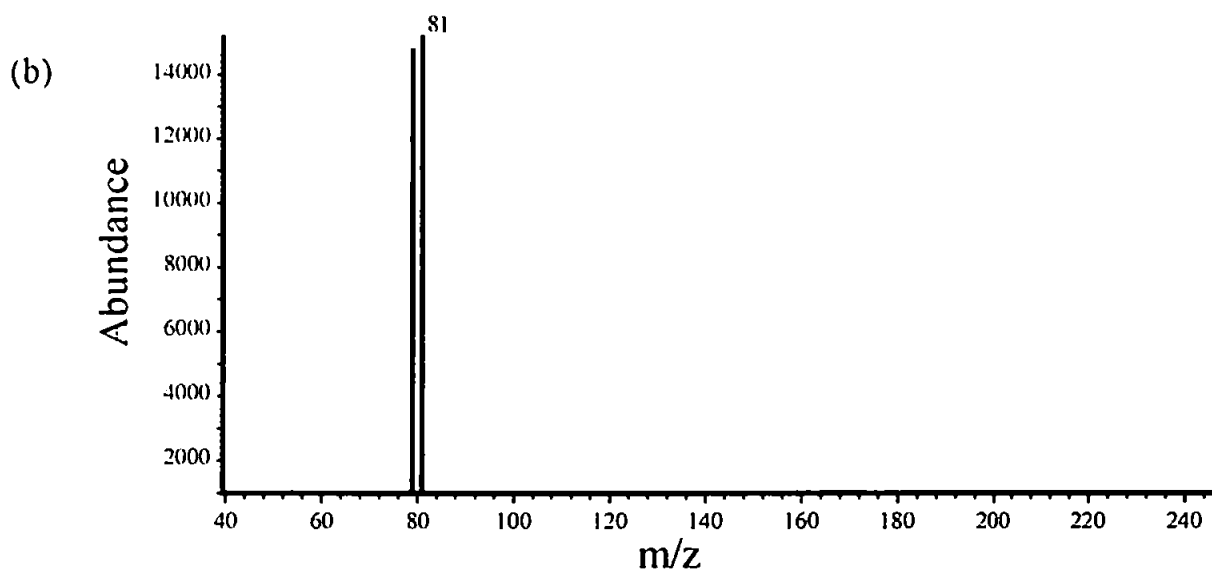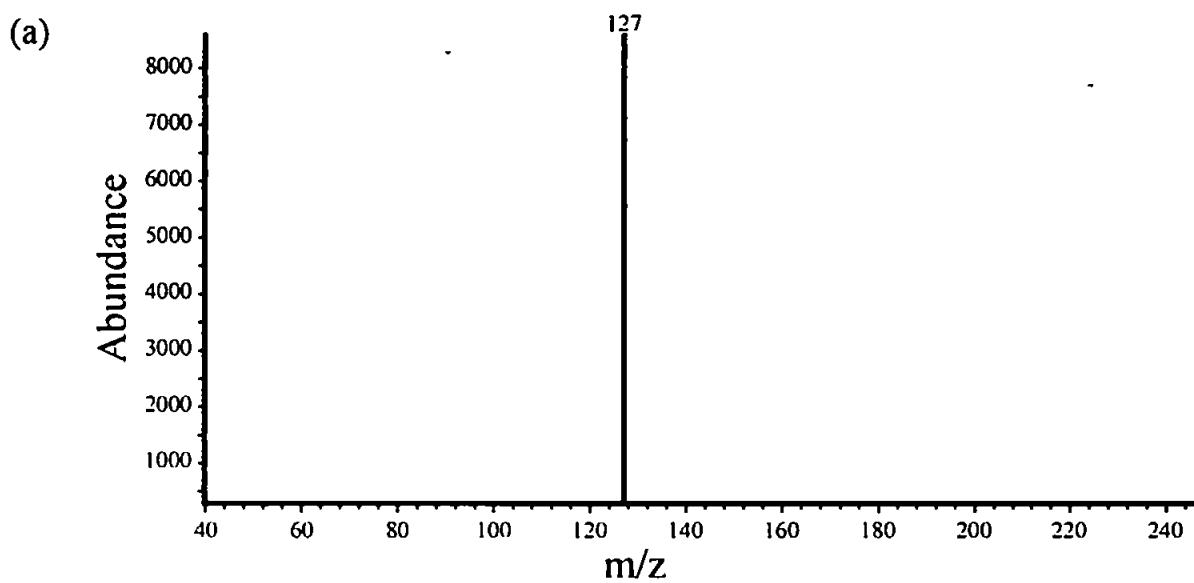
Figure 4.16 Extracted ion chromatogram for a 50 ng on-column injection
of (a) iodobenzene and (b) dibromobenzene.
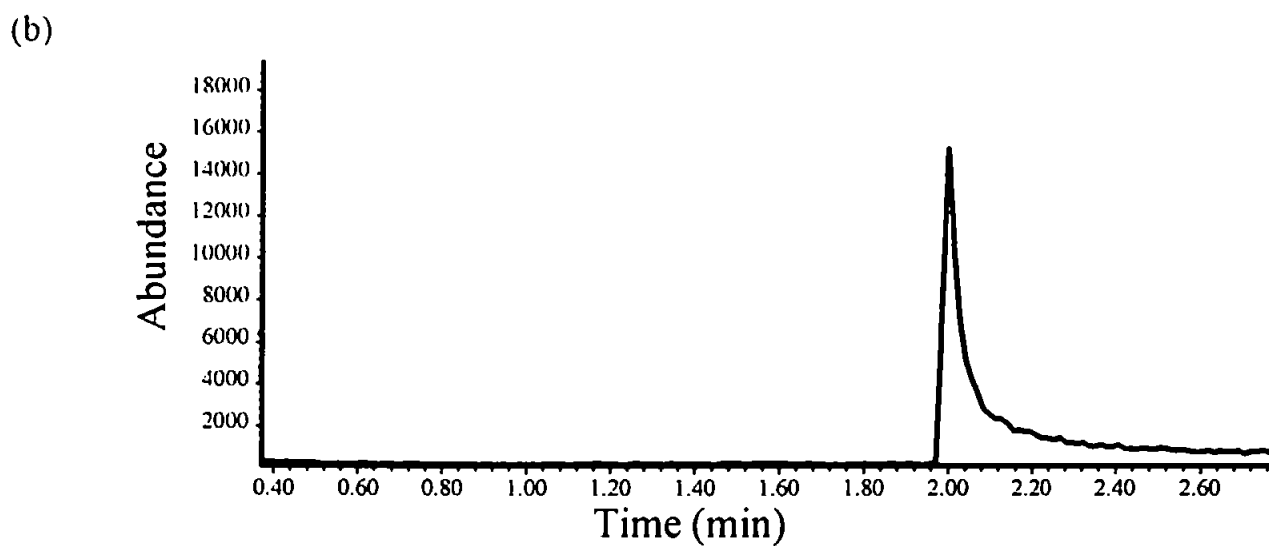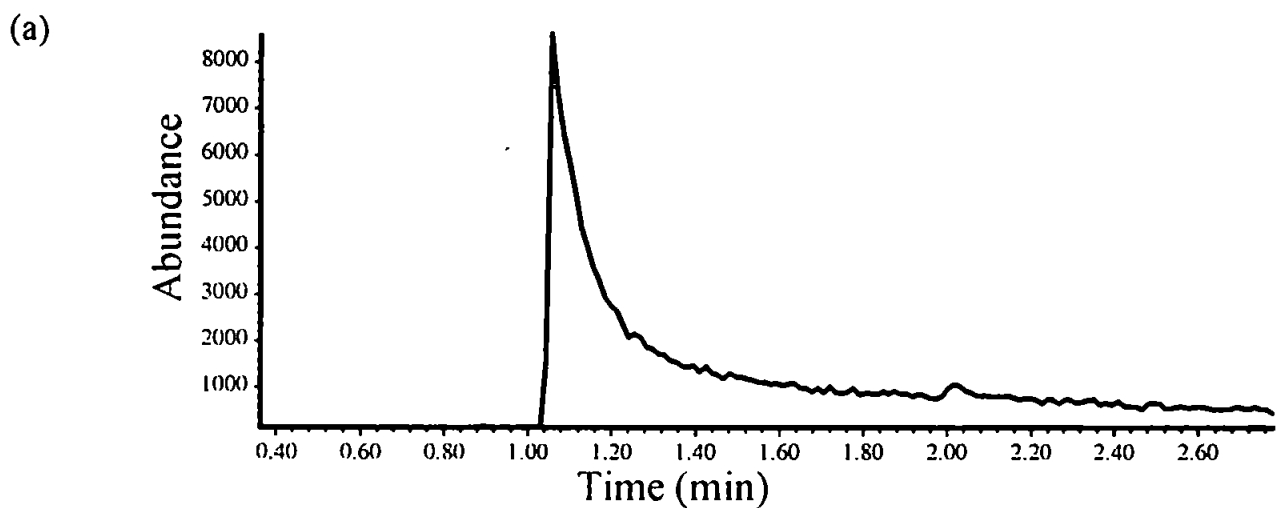
this does not occur for the molecular ion signals using the same chromatographic conditions (see Figures 3.11 and 3.12).

The figures of merit for the 6 ml min^{-1} helium only LP-ICP-MS are shown in Table 4.5, with calibration graphs shown in Figure 4.17. The detection limits and stability obtained are comparable with a previous study[110], where a 1 l min^{-1} argon LP-ICP was interfaced with a commercially available ICP-MS. It is interesting to note that in the previous study[110] no peak tailing for the atomic species was observed. With a 1 l/min argon LP-ICP there is a distinct central channel evident, much like a conventional atmospheric pressure ICP. However, unlike an atmospheric pressure ICP this is thought to be formed by the pressure drop at the 2 mm diameter sampler orifice pulling a central channel out of the plasma. This effectively pulls the analyte ions into the centre of the plasma and away from the torch walls. At very low gas flows and pressures this effect is not observed, so it is likely that the analyte interacts more with the walls of the torch.

4.4 CONCLUSIONS

The GC-LP-ICP-MS has been shown to be capable of providing a tuneable degree of fragmentation for a series of halobenzene compounds. The problems associated with poor linear calibration range and high detection limits for the molecular ions have been solved by the use of reagent gases.

The addition of small amounts of nitrogen to the LP-ICP increased the stability of the plasma and the detection limits for the molecular fragments of chlorobenzene were greatly improved. However, this effect did not extend to the other halobenzene compounds studied.

Table 4.5   Analytical figures of merit for Iodobenzene and dibromobenzene using a 6

ml min^{-1} helium LP-ICP.

Analyte	Iodobenzene	Dibromobenzene
Single ion monitoring , mass monitored	127 m/z	79 m/z
Linear range studied (decades)	3	3
Slope/ counts pg^{-1}	235	129
r^2 (regression coefficient)	0.999	0.999
Log-log slope	0.890	0.881
Detection limit[a] / pg	4	76
RSD[b] (%)	8	12

a) LOD= 3σ/slope

b) RSD(%) for 5 replicate 100 pg injection

Figure 4.17 Calibration graphs for a 6 ml min^{-1} helium LP-ICP: (a) dibromobenzene (79 m/z) and (b) iodobenzene (127 m/z).
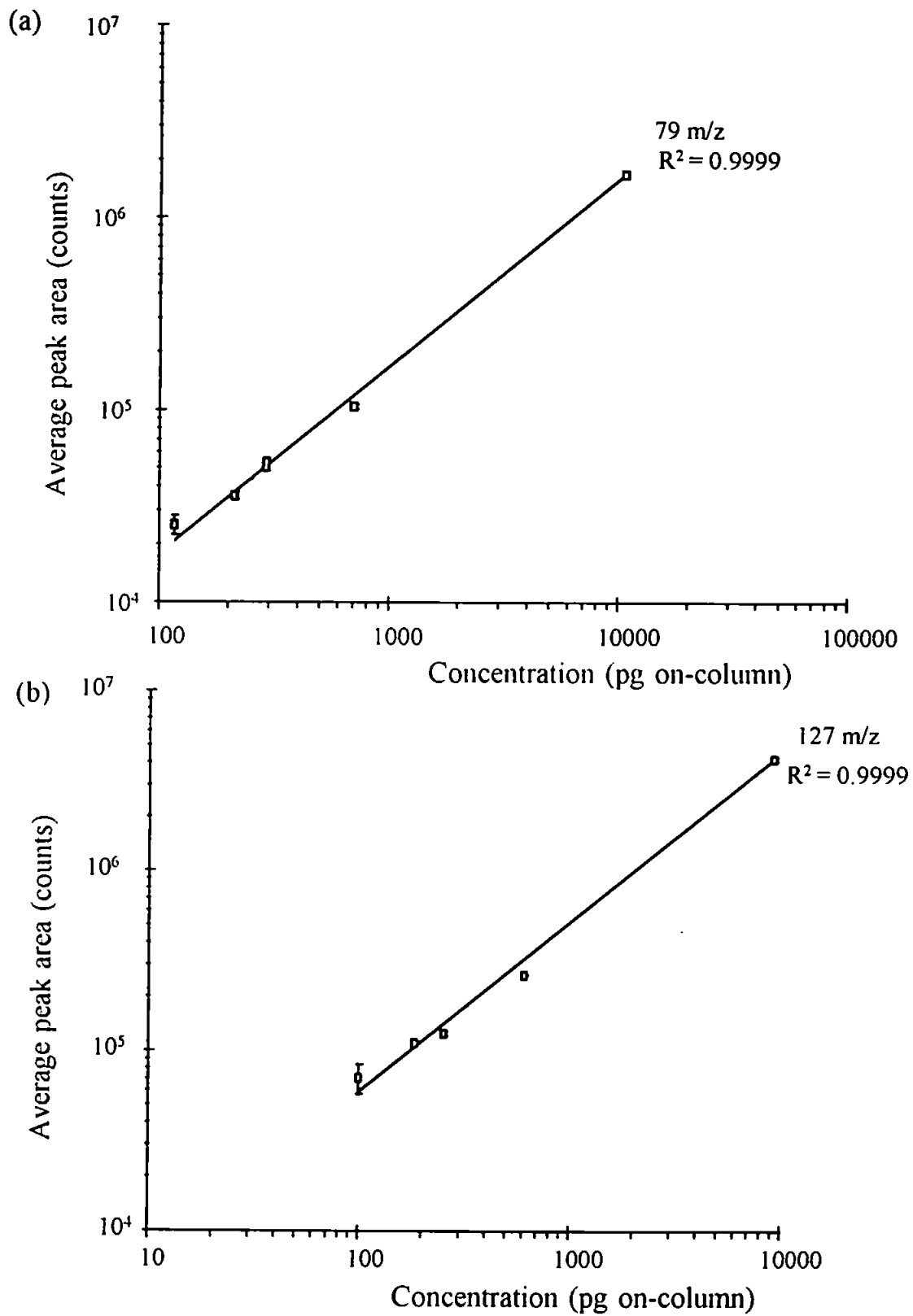
The addition of isobutane enhanced all the analyte molecular and fragment ion signals. The iso-butane did not seem to be acting as it would in a conventional CI source because proton transfer reactions were minimal. However, isobutane seemed to reduce the ionisation energy of the plasma, yielding only molecular ions of the analytes, as it would in CI source MS, at low level concentrations.

A low pressure plasma sustained at 6 W and utilising only 6 ml min^{-1} of helium has been used to atomise both iodobenzene and dibromobenzene totally, producing atomic mass spectra. This proves that a GC-LP-ICP MS is capable of providing different degrees of fragmentation for a series of halobenzenes.

Chapter 5

FUNDAMENTAL STUDIES

CHAPTER 5: FUNDAMENTAL STUDIES

5.1 INTRODUCTION

The measurement of the fundamental properties of plasma sources for atomic spectrometry has played a major role in their successful development as powerful analytical tools. The fundamentals of plasma sources can be basically described in terms of the temperature and population density measurements of the respective species within the plasma. This would be a simple matter if plasma sources existed in complete thermal equilibrium (CTE), where a single temperature could be used to describe the plasma. However, plasma sources do not exhibit CTE, therefore the measurement of each excited species, such as gas kinetic temperature (T_{gas}), ionisation temperature (T_{ion}), excitation temperature (T_{exc}) and electron temperature (T_e) along with the number density measurements of ions, neutrals and electrons are often required to characterise a plasma fully. The measurement of such species in atmospheric pressure argon ICPs[23,34] and MIPs[31] has been critically reviewed previously.

Most diagnostic methods involve the measurement of radiation emitted by atomic or molecular species in conjunction with fundamental equations which are derived from the Boltzmann, Saha, or other equilibrium relationships. However, because these relationships rely somewhat on thermal equilibrium, an argument of local thermal equilibrium (LTE) has been adopted to justify the use of such measurement techniques in atmospheric pressure plasmas. These techniques have been used successfully to spatially map excited species in atmospheric pressure plasmas[150-151], however, agreement between different laboratories is often dependent on the exact plasma operating conditions along with the thermionic species studied. These are often the major contributing factors to interlaboratory disagreement on plasma temperatures[34].

In plasma emission spectroscopy radiation of excited, ionised, and neutral species may be measured, however, in mass spectrometry only ions can be detected. Therefore the fundamentals of interest in mass spectrometry are those influencing ion formation and sampling, and information pertaining to these effects can partially be obtained by making measurements of the ion kinetic energies and floating potential of the plasma ion source.

Electron number density (n_e) measurements of atmospheric pressure plasmas often form the backbone on which other temperature measurements are calculated. One of the reasons for this is that n_e measurements can be obtained from atmospheric pressure plasmas without the assumption of LTE. One common method of doing this is to measure the Stark broadening of the H_β line, which has yielded n_e measurements of 10^{14} to 10^{15} cm^{-3} for most atmospheric pressure ICPs and MIPs[34], however, this technique is not practical for use with low pressure plasmas[88,152] because the electron number density measurements calculated using Stark broadening are only practical for plasmas with number densities greater than 10^{13} cm^{-3}. This is attributed to the high signal levels required to minimise uncertainties in line width measurements. Such high signal levels are not normally present in LP sources. This requires the addition of large amounts of hydrogen, altering the plasma composition and leading to incorrect fundamental measurements. Hence, many fundamental parameters in low pressure plasmas have been determined using electrically conducting probes.

The use of Langmuir probes in atmospheric pressure ICP-MS has almost exclusively been applied to characterising the ion extraction and sampling process[156,161]. This is due to the high gas kinetic temperature exhibited by atmospheric pressure plasmas, which can cause the probe tips to oxidise and/or melt, and any thermionic emissions from the probe tip at elevated temperature can lead to incorrect probe measurements. Nevertheless, the feasibility

of using a double probe assembly has been investigated for n_e and T_e measurements in an atmospheric argon ICP[153].

The effect of plasma potential on the formation of a secondary discharge in the ion sampling interface has been investigated using a Langmuir probe which was slowly swept through the plasma to stop the probe tip from melting[154]. It was shown that, as the plasma potential increased, the number of doubly charge ions increased and the number of argon-associated polyatomic ions decreased. It was thought that the presence of a secondary discharge in the sampling interface was causing this phenonomon[154]. The effect of load coil geometry and earthing position on plasma potential, and hence the intensity of the secondary discharge, was monitored by using a floating Langmuir probe[155]. These investigations led to probe measurements being obtained inside the interface region of an ICP-MS with plasma potential, n_e and T_e being determined[156,161]. More recently a floating Langmuir probe was used to measure the plasma potential of a helium low pressure ICP-MS. The effects of water cooling and electrically shielding the plasma torch were observed to have a pronounced effect on the plasma potential, which ranged from 20 V without shielding to 3.5 V with electrical shielding[162].

Langmuir probe measurements have been used to obtain T_e, n_e, ion number density (n_i), and plasma potential measurements of low pressure glow discharges (GDs)[163-168]. The successes of this approach can be partially attributed to the role of particle collisions in low pressure plasmas, which dominate the analyte excitation process and the formation of metastable species[88,147,148]. This effectively enables the fundamental parameters which govern ion formation in low pressure plasmas to be characterised by Langmuir probe measurements. Probe measurements have recently been used to characterise an argon diode GD source and an argon and neon Grimm type GD[170].

Ion kinetic energy measurements are important for the characterisation of plasma sources used for mass spectrometry because a spread in energies will often affect the sensitivity or resolution of the mass analyser. A quadrupole is the most common analyser used in plasma source MS, and a decrease in resolution is normally observed using this type of analyser when ions of a particular m/z exhibit a wide spread in kinetic energies. This is rather detrimental because quadrupoles are normally only capable of unit mass resolution. Ion kinetic energy measurements can be made by placing a retarding potential on the front of the mass analyser, increasing the potential gradually, and obtaining an ion stopping curve. Stopping curves for ions extracted from an argon ICP have been obtained, at different operating conditions, by applying a DC bias to the quadrupole mass analyser. The DC bias was ramped and the plot of ion signal against the quadrupole DC offset yielded the stopping curve, which was differentiated to obtain the ion kinetic energy[171]. Ion kinetic energies have also been obtained by placing a small orifice retarding plate in front of the mass analyser. Again stopping curves were obtained by ramping the DC offset of the retarding plate[173].

Douglas[34] described the application of a three lens ion stopping grid for ion kinetic energy measurements. In this paper the author described the necessity for removing any ion optics up-stream of the measurement grid. This was deemed necessary due to the accelerating effect of the optics which would alter the ion energies. This system was later used by Tanner[174]. In the first instance ion kinetic energies were measured in order to characterise the extent of a secondary discharge at different plasma operating conditions[171]. However, Fulford and Douglas[172] have investigated the relationship between ion mass and ion kinetic energy, and have shown that the ion kinetic energy increases linearly with ion mass in accordance with the energy imparted by the ion sampling process in addition to the plasma potential. More recently ion kinetic energy measurements and ion sampling theory have been used to calculate the gas kinetic temperature of the sampled plasma[174, 68].

5.2 THEORY

The principles behind Langmuir probe measurements are not complex and measurements are simple to obtain in practice. A conducting wire when placed in a plasma, which is itself a conducting media, should reach the floating potential of the plasma assuming no net charge is applied to the probe wire. If the probe is biased, either positively or negatively with respect to the plasma potential, the charged species in the plasma will be attracted to or repelled from the probe surface. If another electrode is placed in the plasma and the current monitored across the two electrodes, information about the charged species within the plasma can be elucidated.

The application of an external potential to the probe causes a space charge envelope to develop around the probe. If the probe is driven to a negative potential, only electrons with sufficient kinetic energy will carry current from the probe to the second electrode. However, if the probe is driven further negative, all electrons will be repelled from it, so that any current flowing across the system will be due solely to the ions in the plasma. A similar process occurs for ions when the probe is driven positive with respect to the plasma potential, and at a high enough potential the current will be due solely to the electrons. Since the mobility of the electrons in the plasma is greated than that of the ions, the current obtained by the probe when it is positive is much greater then when it is negative[169]. Therefore, by sweeping the voltage from a negative to a positive potential, a plot of voltage versus current, should yield an 'S' shaped plot with the plateau at the bottom being the ion saturation region, the plateau at the top being the electron saturation region, and the region between the two being known as the electron retardation region (Figure 5.1). It is from these characteristic current-voltage (I-V) plots that the plasma n_i, T_e, and n_e are calculated.
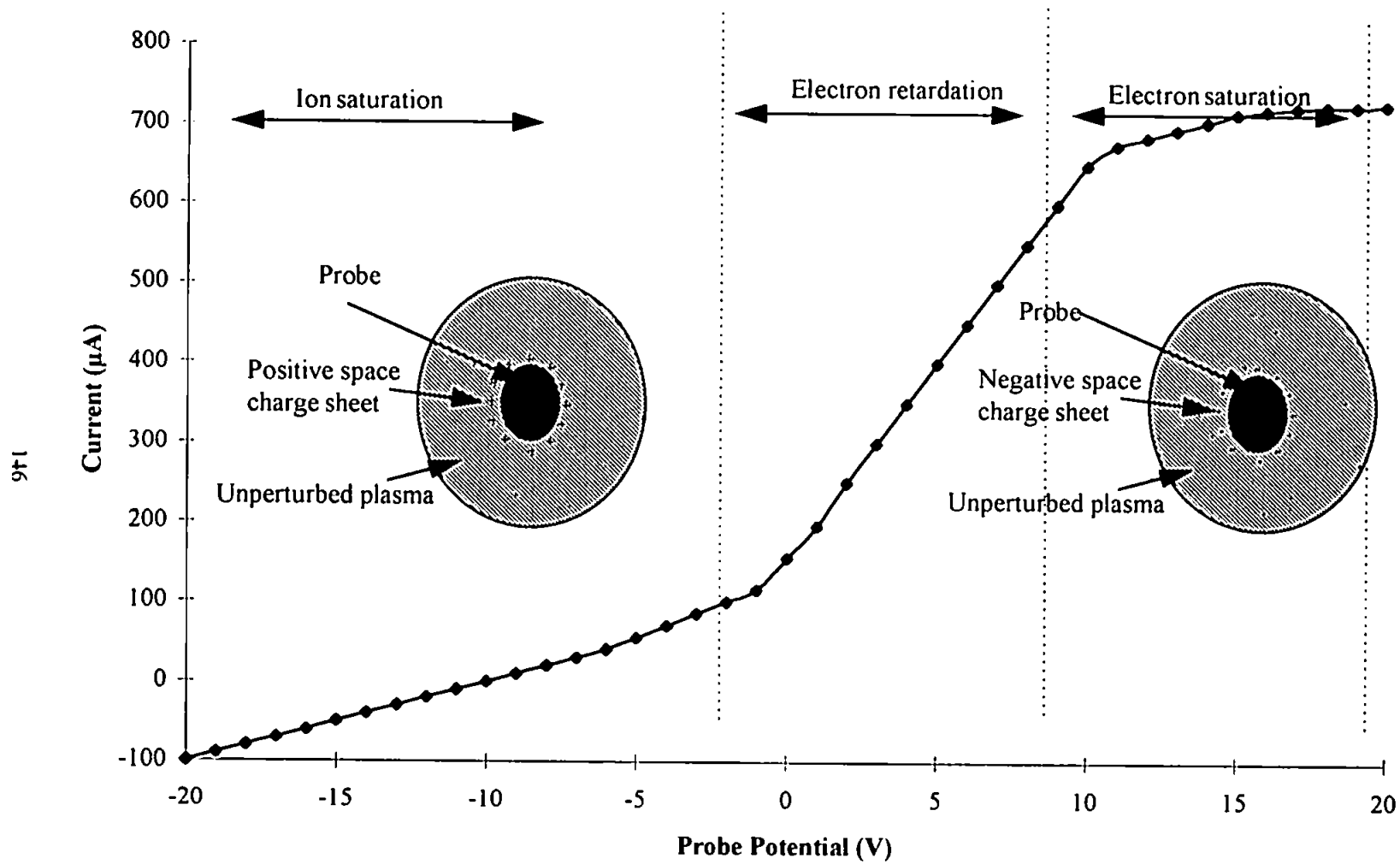
Figure 5.1   Ideal current - voltage plot, showing the three stages of probe charge.

However, to do this certain assumptions about the charged species in the plasma have to be made:

i) the distribution of electrons in the plasma is Maxwellian,

ii) the probe length is much greater than its radius, so end effects do not influence current measurements,

iii) the presence of the probe in the plasma does not disturb the plasma significantly,

iv) ions are considered mono-energetic,

v) the probe is considered to be orbit motion limited *i.e.* ions do not adopt trapped circular trajectories around the probe but are either attracted to or are repelled away from the probe,

vi) charged particle trajectories do not effect the collection efficiency of the the probe.

For an orbital-motion limited probe, the ion number density is directly related to the current reaching the probe and the probe voltage by:

$$I_+ = A n_i e \left(\frac{-e V_p}{8M} \right)^{0.5} \qquad (5.1)$$

where I_- is the ion current in amps, M is the ion mass in kg, A is the surface area of the probe in m^3, e is the electronic charge in coulombs and V_p is the potential experienced by the probe (*i.e.* the applied probe potential relative to the local plasma potential in volts). However, this method of calculation is reliant on an accurate measurement of the local plasma potential, so, in order to account for this, a method of determining n_i by use of a linear regression method has been described[169], where equation 5.1 is rearranged to:

$$(I_+)^2 = \left(\frac{A^2 n_i^2 e^2}{8M} \right) \left(e V_s - e V_{ap} \right) \qquad (5.2)$$

Where, V_s is the local plasma potential and V_{ap} is the applied probe potential. A plot of $(I_+)^2$ against $(eV_s\text{-}eV_{ap})$ is linear in the ion saturation region and n_i is determined from the slope of this plot. Using equation 5.2, the ion current at local plasma potential can also be determined from this plot. Theoretically, this should be zero, however, residual ion currents above the local plasma potential can lead to inaccurate T_e measurements. Therefore the ion current contribution to the electron retardation current must be calculated in order for accurate T_e measurements to be made.

5.2.1 Electron Temperature

Assuming a Maxwellian distribution of electrons in the plasma the electron temperature is obtained from the Boltzmann relationship[164].

$$I_e = I_0\, exp\left(\frac{eV_p}{kT_e}\right) \qquad (5.3)$$

Where I_e is the electron current (*i.e.* the current monitored in the electron retardation region minus the residual ion current), V_p is the applied probe potential and k is the Boltzmann constant. By taking the natural log of equation 5.3 the following is obtained:

$$ln\,I_e = ln\,I_0 + \left(\frac{eVp}{kT_e}\right) \qquad (5.4)$$

Therefore, T_e can be calculated from the slope of the semi-log plot of $ln\,I_e$ against V_p in the electron retardation region of the I-V curve. When the probe potential is positive with respect to the plasma potential the current density becomes saturated, because no electrons are repelled from the probe. This causes the upper region of the semi-log plot to curve and plateau off. Therefore, it is possible to use the semi-log plot to determine the local plasma potential, which is indicated by the knee in the plot. An alternative method of calculating the local plasma potential has been described by Fang and Marcus[169]. This uses the fact that the maximum increase in current per unit of potential squared occurs at the plasma potential.

Therefore a derivative plot of the I-V curve will reach its maximum at the local plasma potential. This has been suggested as a simple and more effective method of measuring the plasma potential, which is much less prone to error[169]. Once the plasma potential has been determined the electron number density can be calculated from the electron current at the local plasma potential using:

$$I_0 = Aen_e \left(\frac{kT_e}{2\pi m} \right)^{0.5} \qquad\qquad (5.5)$$

Where I_0 is the current measured at the local plasma potential and m is the electron mass in kg.

5.3 EXPERIMENTAL

5.3.1 Langmuir Probe Measurements

A Langmuir probe was constructed (Glass blowing workshop, University of Plymouth, UK) by vacuum sealing a 10cm length of 1.16 mm diameter tungsten wire into a 3.175 mm o.d. silica tube, which acted as an insulator for the majority of the wire. A small length of wire, 5 mm, protruded from one end of the silica tube. The wire tip was dipped in concentrated nitric acid (Aristar grade, Fisher Chemicals, Loughborough, UK) to remove any outside layer that may have been present. This acted as the probe tip which was submerged in the plasma. The other end of the wire protruded 2 cm out of the silica tubing. This was also cleaned in nitric acid and was then connected through a current meter (AVO, Megger Instruments, Dover, UK) to the power supply circuit.

A ±80 V DC power supply was constructed in house using two variable voltage power supply units (Farnell Instruments Ltd., Wetherby, Yorkshire, UK). The positive terminal of the first power pack was connected to one input terminal of a 10 kΩ, 3W wire-wound potentiometer (Colvern Ltd., Romford, UK). The negative terminal was connected through

the low pressure sampler on the frontplate of the ion extraction interface to ground. The negative terminal of the second power supply was connected to the second input terminal of the potentiometer. The positive terminal was connected to ground through the low pressure sampler. Both power supplies were set to give a maximum output of 80 V DC, resulting in a variable voltage of ±80V being available on the output terminal of the potentiometer. The output terminal of the potentiometer was connected to the probe through a current meter. The voltage across the probe circuit was monitored with a voltage meter (AVO, Megger Instruments, Dover, UK). A diagram of the Langmuir probe, power supply circuit and torch set-up is shown in Figure 5.2.

In order to enable the low pressure plasma to be monitored by the probe the conventional low pressure plasma torch was replaced with a 14 cm long 12.7 mm o.d. quartz tube with two 6.4 mm o.d. side arms (H. Baumbach and Co. Ltd., Suffolk, UK). The side arms were located 35 mm from both ends of the quartz tubing. The load coil of the LP-ICP-MS was rewound around the centre of the torch, between the two side arms. The torch was vacuum sealed to the low pressure sampler of the LP-ICP-MS using an Ultra-Torr fitting. The GC transfer line was then connected to the back of the torch using a Swagelok fitting with a graphite ferrule. The helium make up gas was connected to the side arm nearest the GC inlet with an Ultra-Torr fitting. The Langmuir probe was then connected to the second side arm with an Ultra-Torr fitting. The probe tip was place in the centre of the low pressure plasma torch, 5 mm above the load coil. Operating conditions for the probe and plasma are shown in Table 5.1.

The I-V plots were obtained by increasing the voltage manually, in 2V steps, whilst monitoring the resulting current across the circuit. This was repeated at different plasma forward powers and helium gas flow rates.
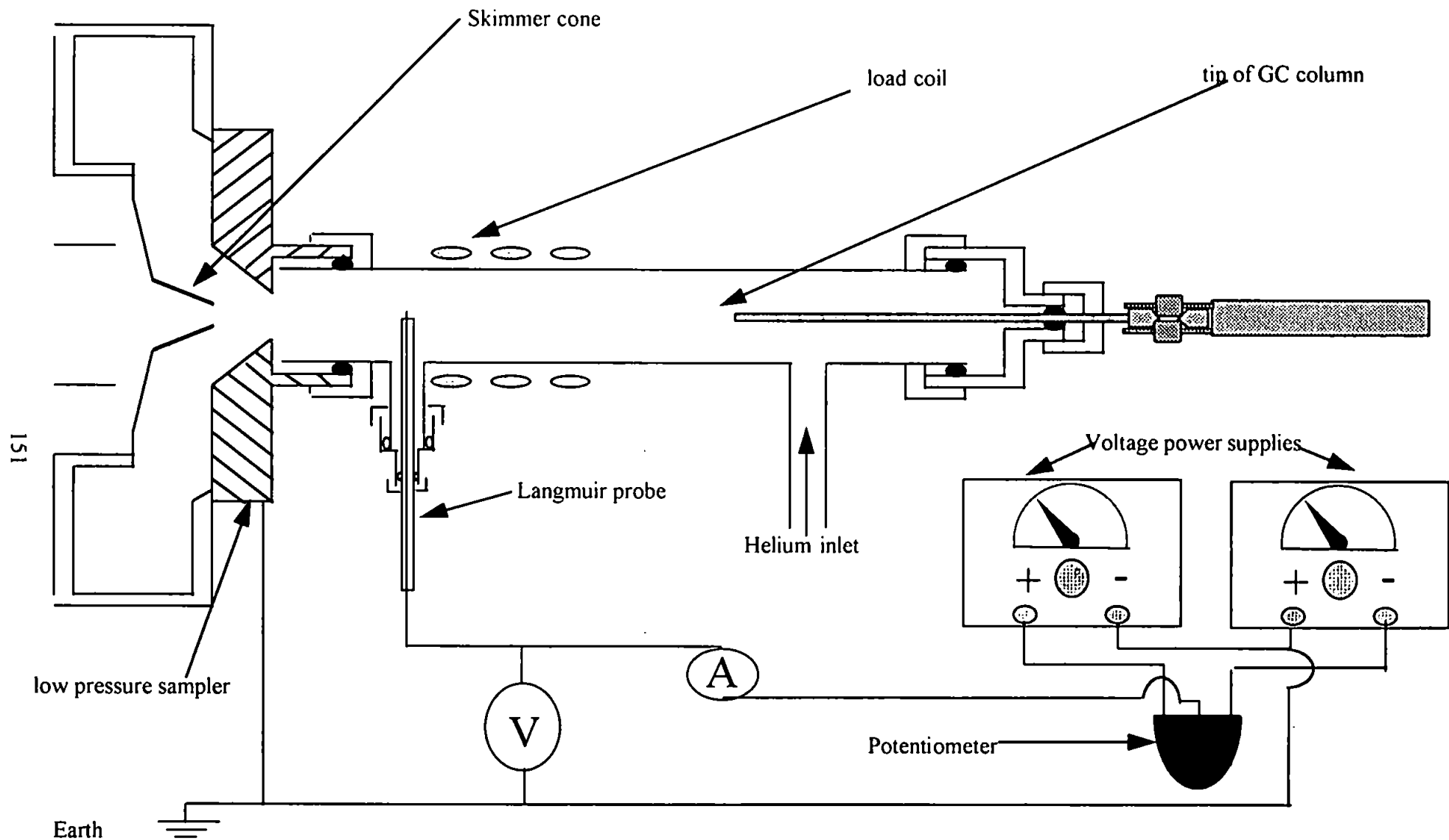
Figure 5.2   Diagram of the instrumental set-up for Langmuir probe measurement of the LP-ICP-MS

Table 5.1   Operating conditions for Langmuir probe measurements on LP-ICP-MS.

Langmuir probe	
Material	Tungsten
Potential (V)	-80 to +80
Plasma	
Forward power (W)	3-21
Reflected power (W)	0
Pressure (Torr)	
Interface	0.03-0.5
Plasma gas	
Helium flow (ml min^{-1})	3-15

5.3.2 Ion Kinetic Energy Measurements

Ion kinetic energy measurements were made by plotting ion stopping curves for the three fragment ions of perfluorotributylamine (PFTBA, Fluka Chemicals, Gillingham, UK). The PFTBA was introduced into a 6 ml min^{-1} helium LP-ICP, via a PTFE sample vial with a molecular leak which was attached to the gas inlet side arm of the low pressure torch. In order to ensure that the energy obtained by the ions was that gained from the plasma and the ion sampling processes only, the first two ion lenses were removed from the instrument. Ion stopping curves were obtained by using the third ion lens as an energy barrier. This lens, which was computer controlled, was ramped from 0 to +10V with the resulting ion current, for the 69m/z, 219m/z and 502m/z fragment ions of PFTBA, being monitored by the mass spectrometer. The ion currents were monitored at 0.2V intervals and the ion stopping curves were plotted by the MSD workstation software. The instrument operating conditions for the ion kinetic energy measurements are shown in Table 5.2.

5.4 RESULTS AND DISCUSSION

5.4.1 Langmuir Probe Measurements

The observed current-voltage plots for a 3 to 15 ml min^{-1} helium LP-ICP, operated at different plasma forward powers, are shown in Figures 5.3-5.7. The plots show the characteristic 'S' shape with the three separate regions, ion saturation, electron retardation, and electron saturation becoming more pronounced as the plasma forward power was increased. This was due to the increase in electron and ion number densities with increasing plasma power. It was from these plots that the overall plasma characteristics were determined. The overall current measured by the probe circuit was in microamps, which is considerably less than that observed in other low pressure discharges, which generally have

Table 5.2   Operating conditions used for the ion kinetic energy studies with the LP-

ICP-MS system.

Mass Spectrometer	Modified Hewlett Packard MSD
Plasma	
Forward power (W)	6 to 8
Reflected power (W)	0
Pressure (Torr)	
Torch	0.2
Interface	0.03
Analyser	2×10^{-5}
Ion lenses (V)	
L1	Removed
L2	Removed
L3	0 to +10
L4	0
L5	0
Entrance	0
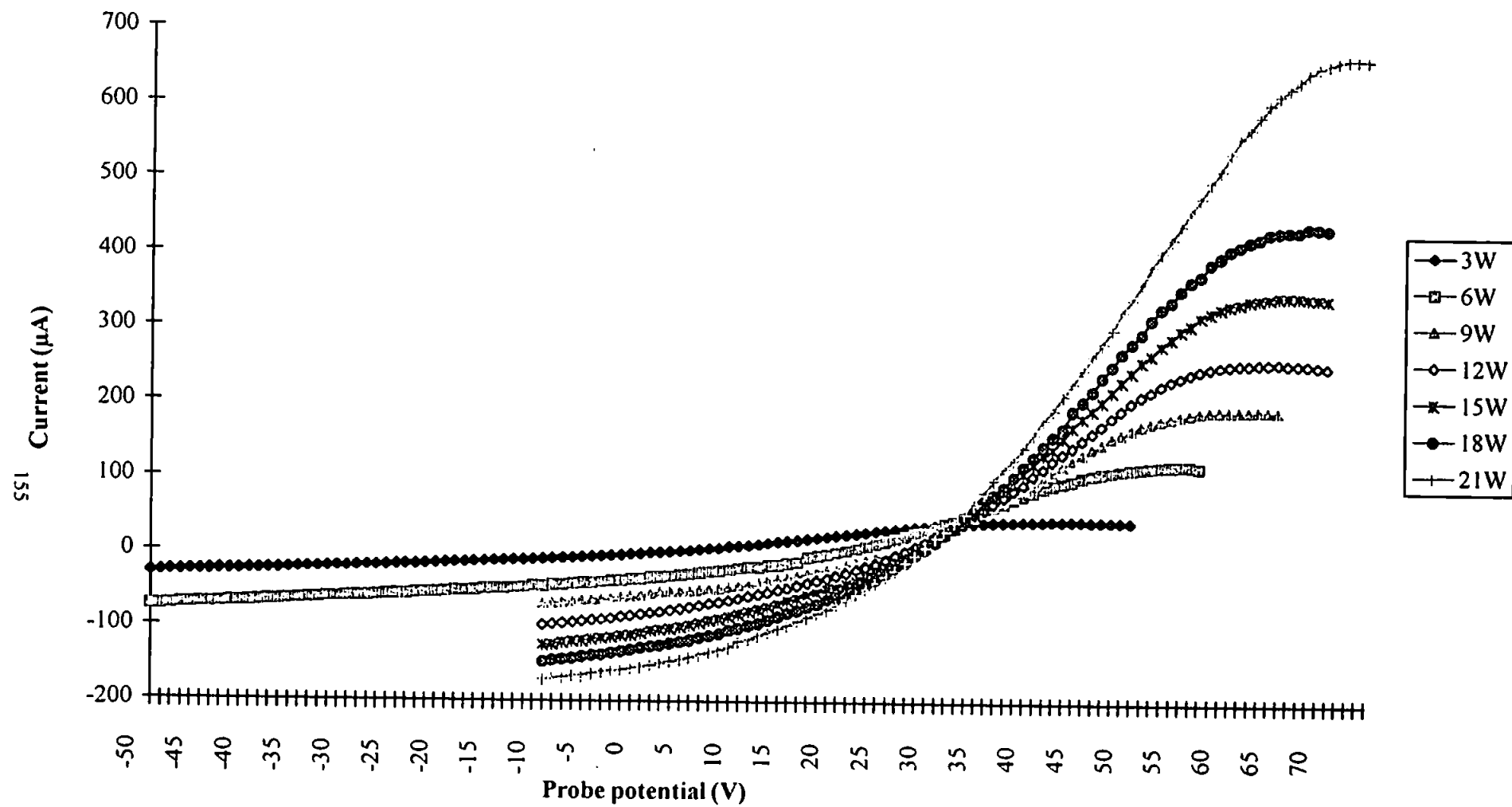
Figure 5.3   Characteristic current-voltage plots for a 3 ml min⁻¹ helium LP-ICP at selected plasma forward powers.
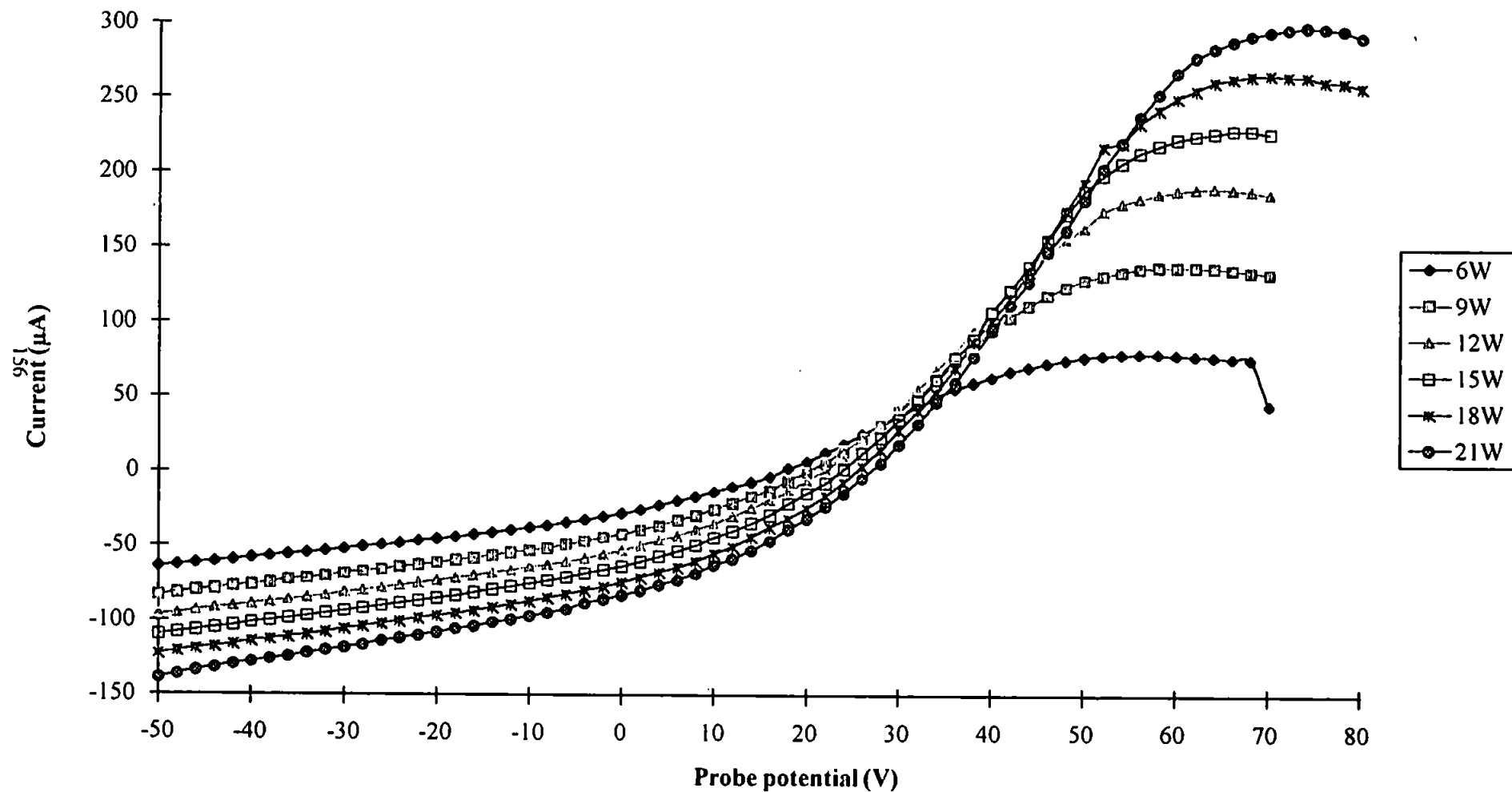
Figure 5.4   Characteristic current-voltage plots for a 6 ml min^{-1} helium LP-ICP at selected plasma forward powers.
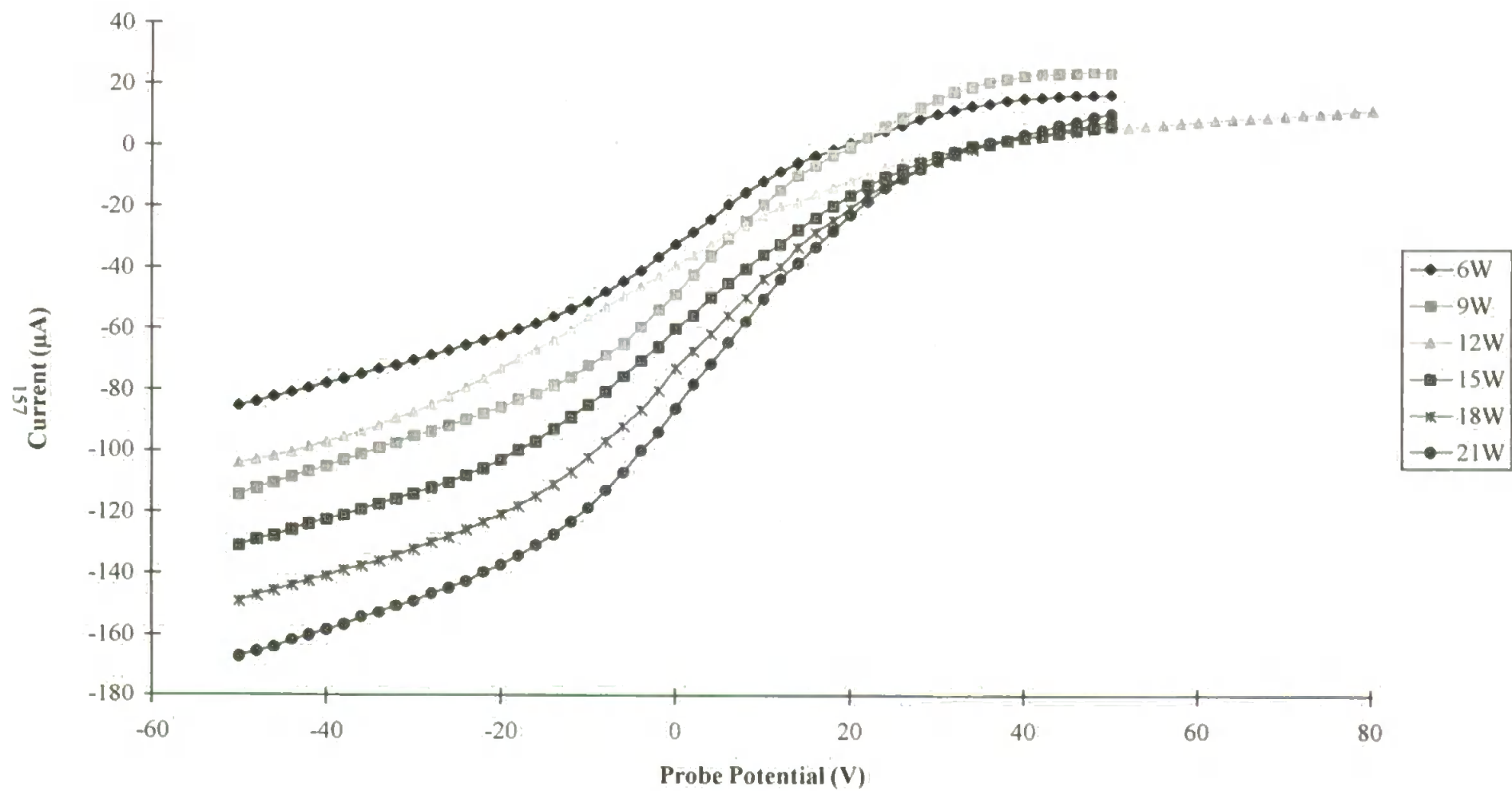
Figure 5.5   Characteristic current-voltage plots for a 9 ml min⁻¹ helium LP-ICP at selected plasma forward powers.
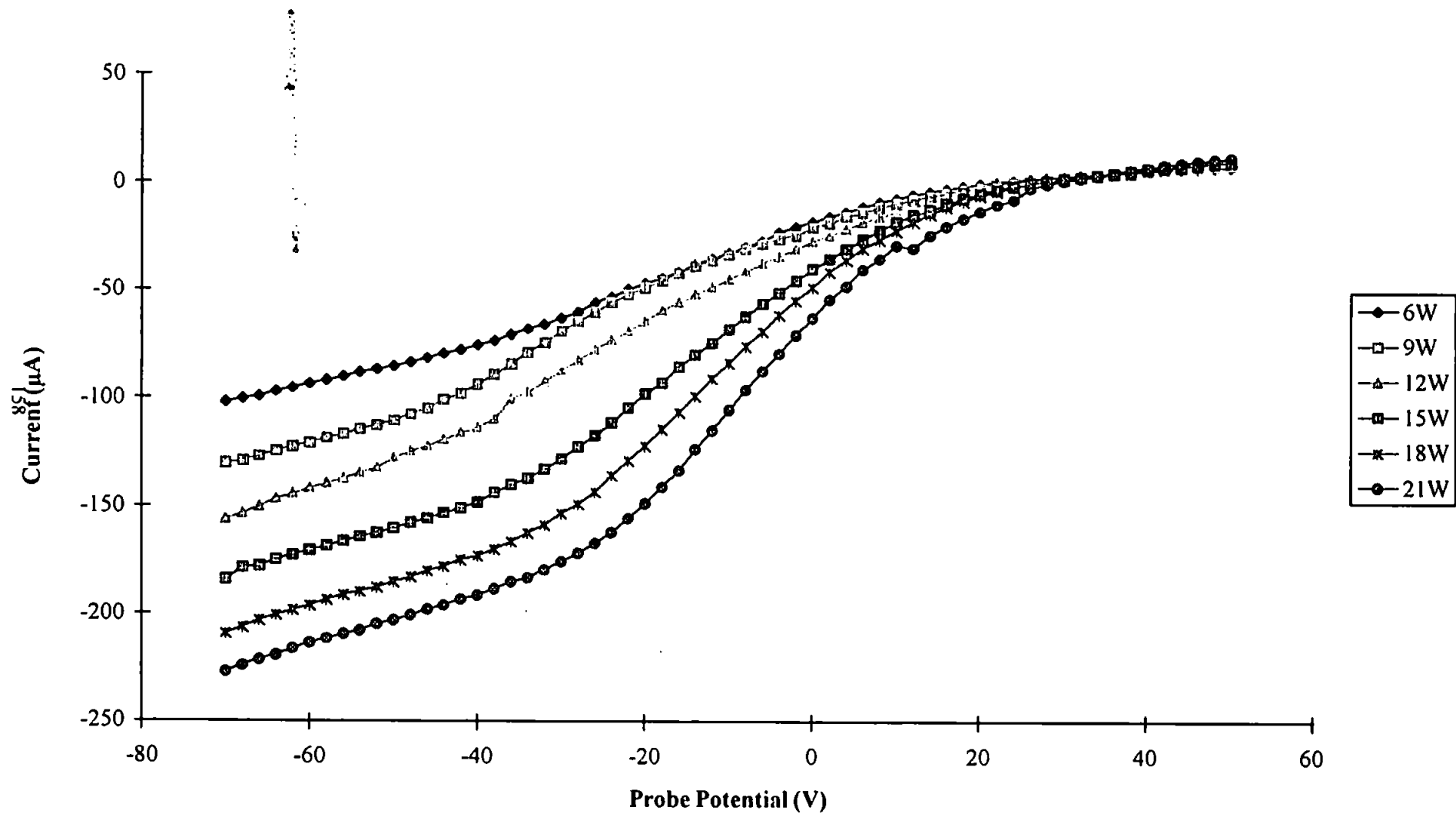
Figure 5.6 Characteristic current-voltage plots for a 12 ml min⁻¹ helium LP-ICP at selected plasma forward powers.
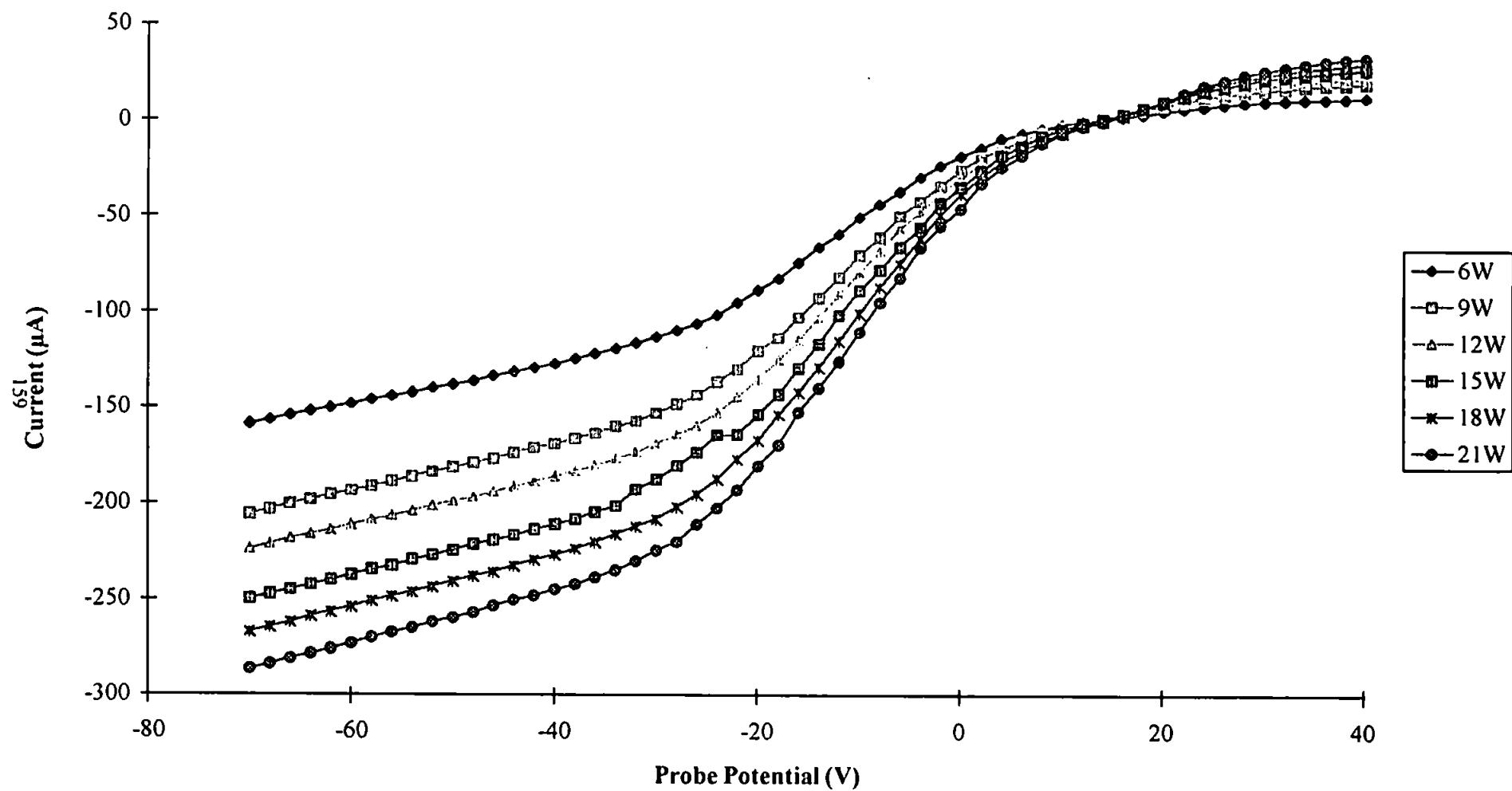
Figure 5.7   Characteristic current-voltage plots for a 15 ml min^{-1} helium LP-ICP at selected plasma forward powers.

currents in the milliamp region[88,164,169]. However, this can be attributed to the lower powers and pressures used in this study, and that many of the previous probe studies were performed on low pressure glow discharges. The current readings were logged manually with the current being measured to the nearest microamp. The current remained stable during the experimental readings, as long as the voltage remained constant, with between run variances at selected probe potentials being less than 1%.

For the 3 ml min^{-1} LP-ICP the current-voltage plot obtained at 3W exhibited only a slight increase in current with increasing probe potential, this is indicative of the low levels of excited species in the 3W LP-ICP. The plots for 3 and 6 ml min^{-1} exhibited a continuously increasing current with plasma power. However, above 9 ml min^{-1} the plasma electron saturation current seemed to reach a limit which increased only slightly with increasing plasma power. This limiting current is due solely to the electrons in the plasma and would seem to suggest that the electron density did not increase above a certain gas flow (i.e. pressure). However, at these elevated flow rates the plasma size increased and touched the torch walls, which may have caused a decrease in electrons flowing to the LP sampler electrode as electrons may flow to the torch wall instead.

Another consideration in assessing the reliability of single Langmuir probe plasma measurements, is that the probe remained fixed in position throughout the measurement process. In GD sources this would be disadvantageous as sputtered atoms will coat the probe, thereby changing its surface area. This changes the dimensions of the space charge envelope around the probe and interferes with probe measurements. This is not a consideration for the LP-ICP as no sputtered electrode exists, however, the plasma changed physical size as the power and flow rates were varied. The probe was, therefore, placed in the centre of the plasma as this was deemed to be essential. Also important to note is that

the LP-ICP used in this study was a ball like plasma, which did not exhibit the annular shape normally associated with an atmospheric pressure plasma. This reduced the complexity of the probe measurements as central channel cooling effects did not have to be considered.

The local plasma potential was easily found from the maximum of a second derivative plot of the current-voltage plot. An example of such a plot is shown in Figure 5.8a. The local plasma potential varied from +19.5 V to +50 V for the 3 and 6 ml min^{-1} plasmas, increasing with plasma power and gas flow. Such high plasma potentials have been associated with large secondary discharges in the ion sampling interface in the past[34,162,171,172,174]. Table 5.3 shows the observed plasma potential obtained for the LP-ICP at different operating parameters. Yan et al.[162] have attributed the high plasma potentials (+20 V) observed in a helium LP-ICP, sustained in a water cooled torch, to the enhanced capacitive coupling into the LP plasma caused by the water jacket. However, the large potentials observed in this study suggest that the low pressures used may contribute to the high potentials observed due to capacitive coupling. While capacitive coupling and the presence of secondary discharges in atmospheric pressure ICP-MS is considered disadvantageous, it has been suggested that the enhanced capacitive coupling in LP-ICPs enhances analyte signals, for elements with high ionisation potentials, due to the increased electron energy afforded by the capacitive coupling[107]. Above 9 ml min^{-1} the plasma potential changed sign with a negative potential being observed. This coincided with the plasma changing physical form, from a small ball, which extended from the tip of the load coil to the LP sampler cone, to an elongated plasma which filled the whole LP torch making it resemble a fluorescent strip light bulb. This may be indicative of the plasma coupling into the Swagelock fitting at the rear of the LP torch. Therefore the current would flow from the probe to the rear of the torch instead of the LP sampler. When this occurred all analyte signals were lost.

161
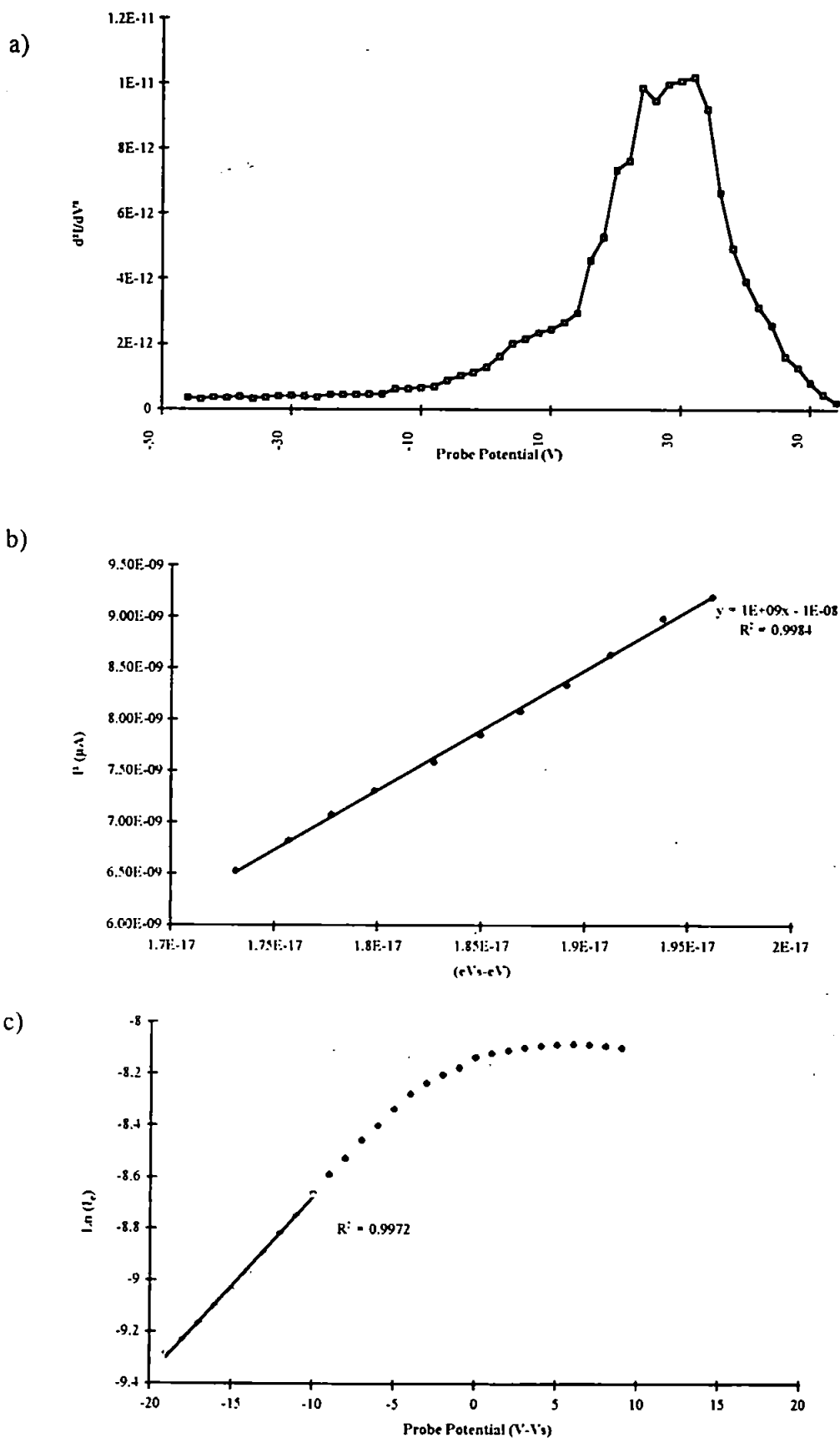
Figure 5.8   Characteristic plots for a 9 W 6 ml min⁻¹ helium plasma; a) second derivative plot; b) plot of I^2 against (eVs-eV) for the determination of n_i; c) semi-log plot for the determination of T_e.

Table 5.3   Plasma potentials for the low pressure inductively coupled plasma at different plasma power and flow rates.

Helium flow (ml min^{-1})	Plasma power (W)						
	3	6	9	12	15	18	21
3	19.5	33	37.5	43	43	44.5	50.5
6	30	38	40	44	48	50	50
9	8	6	0	0	0	0	0
12	-20	-32	-38	-20	-18	-16	0
15	-14	-12	-14	-12	-10	-10	0

The ion number densities were obtained from equation 5.2 and the plots such as that shown in Figure 5.8b. The intercept of this linear plot can also be used to determine the ion current contribution to the overall current at the local plasma potential. Theoretically this should be zero, but any ion current contributions to the overall current in the electron retardation region can cause serious errors in T_e and n_e calculations if not taken into account. The linear relationship observed for all ion current plots was considered proof that the probe was indeed orbit motion limited and that, assuming a Maxwellian distribution of electrons, the current measured by the probe was caused solely by its potential and the surrounding charged species[169].

An example of the semi-log plots used to determine the electron temperature is shown in Figure 5.8c. The example shown has a large linear section with the first ten points in the electron retardation region used to indicate the electron temperature. However, many plots above 6 ml min^{-1} exhibited a much smaller linear region of only 5 points. All plots exhibited the characteristic curvature at increased probe potential, representing electron saturation of the probe surface. The plot shown is a semi-log plot of current against the probe potential relative to the plasma potential. Therefore, the knee of this curve should occur at zero, indicating agreement between the second derivative method of plasma potential calculation and the method of using the intersection between the two linear sections of the semi-log plot. The plot shows a difference of ≈ 1 V between the two methods which can cause uncertainties, of up to 7%, in n_e calculations. Both methods of determination are thought to be equally correct with the preference of method being left to the investigator[164, 169].

The relationships between ion number density and plasma forward power, for 3 to 15 ml min^{-1} helium low pressure plasmas, are shown in Figures 5.9a-5.13a. The ion number density increased, from 5×10^8 to 5×10^9 cm^{-3}, with increasing plasma power and flow rate. For the 3 ml min^{-1} plasma (Fig. 5.9a), n_i was seen to increase rapidly in an almost linear

fashion. This is consistent with the plasma forward power increasing the capacitive coupling into the LP-ICP hence producing more excited electrons and greater ionisation. If electron impact was the dominant source of ions, such a sharp rise in n_i would be expected. However, as the flow rate was increased (Figs 5.9a-5.13a) the effect of plasma forward power on ion formation became less pronounced with n_i increasing only slightly for the 15 ml min^{-1} (Fig. 5.13a) LP-ICP. This suggests that electron impact is not the dominant ionisation process, however the behaviour of the electron number density and energy must also be taken into account, as described below.

The effect of plasma forward power on T_e at the respective plasma flow rates is shown in Figures 5.9b - 5.13b. For the 3ml min^{-1} LP-ICP the electron temperature was seen to change little with increasing power, however, the 6 ml min^{-1} LP-ICP showed an increase in T_e with increasing plasma power. Such an increase in electron energy was consistent with electron impact ionisation causing the rapid increase in n_i observed in the 3 and 6 ml min^{-1} plasmas. The electron temperature for the 9 ml min^{-1} plasma was seen to drop with increasing forward power, whilst above 9 ml min^{-1} the plasma forward power was seen to have little effect on the value of T_e. This may be suggestive of electron impact playing a limited role in ionisation at higher flow rates as n_i is seen to continue rising even though T_e was falling. However, an explanation for this was shown by the electron number densities (Figures 5.9c- 5.13c).
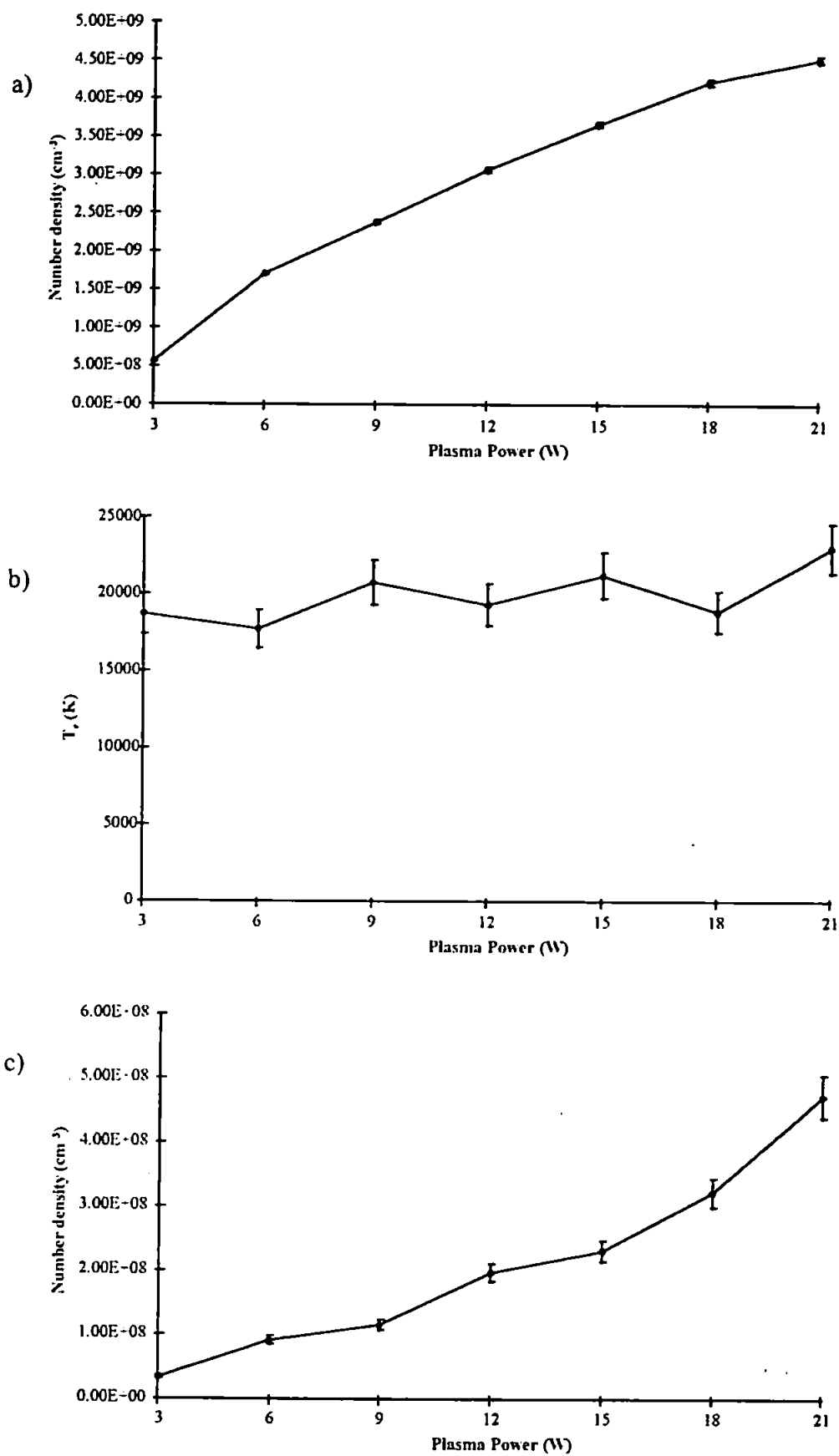
Figure 5.9 Effect of plasma forward power on a) ion number density; b) electron temperature; and c) electron number density, for a 3 ml min^{-1} helium LP-ICP

166
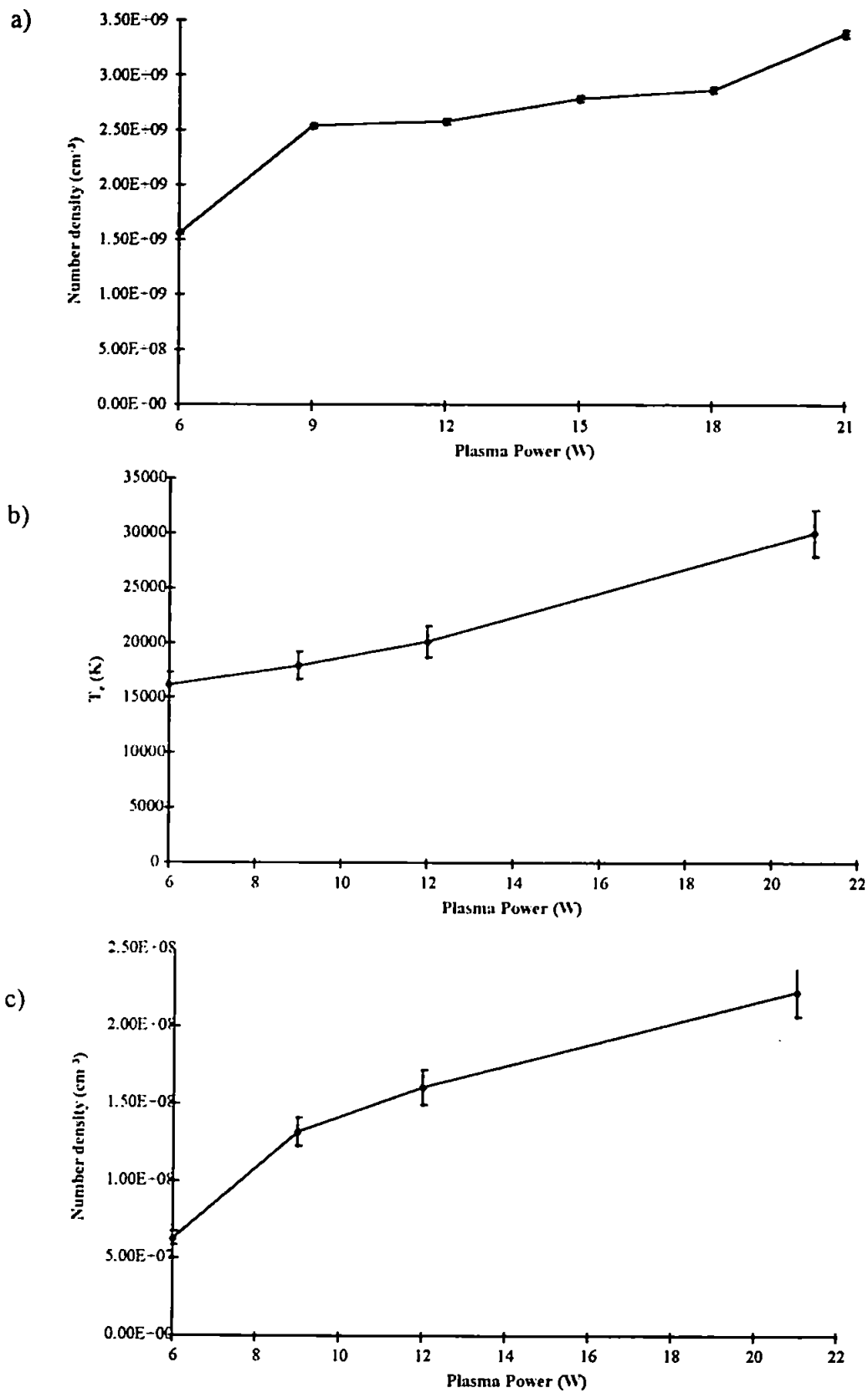
Figure 5.10 Effect of plasma forward power on a) ion number density; b) electron
temperature; and c) electron number density, for a 6 ml min⁻¹ helium LP-ICP
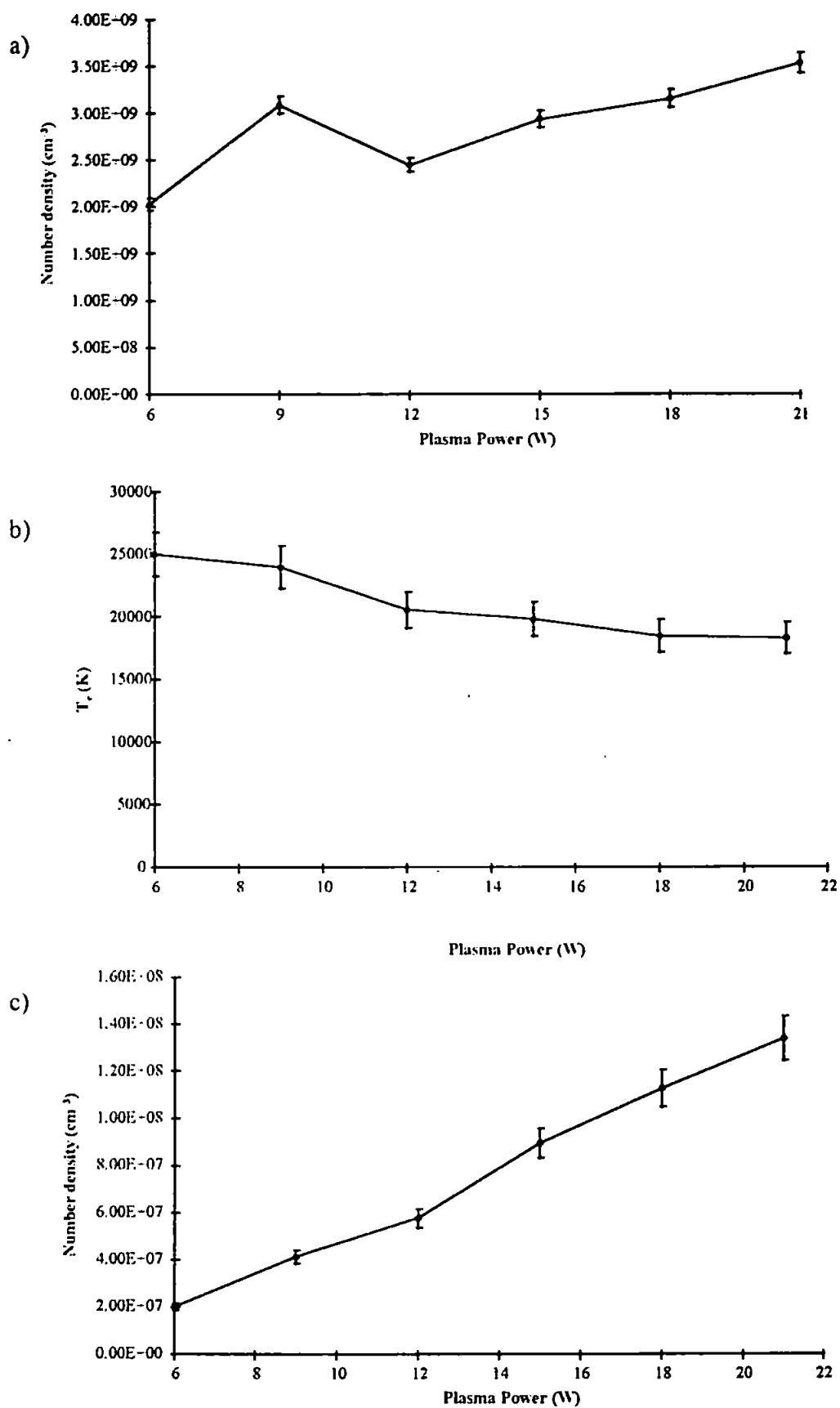
Figure 5.11 Effect of plasma forward power on a) ion number density; b) electron temperature; and c) electron number density, for a 9 ml min⁻¹ helium LP-ICP
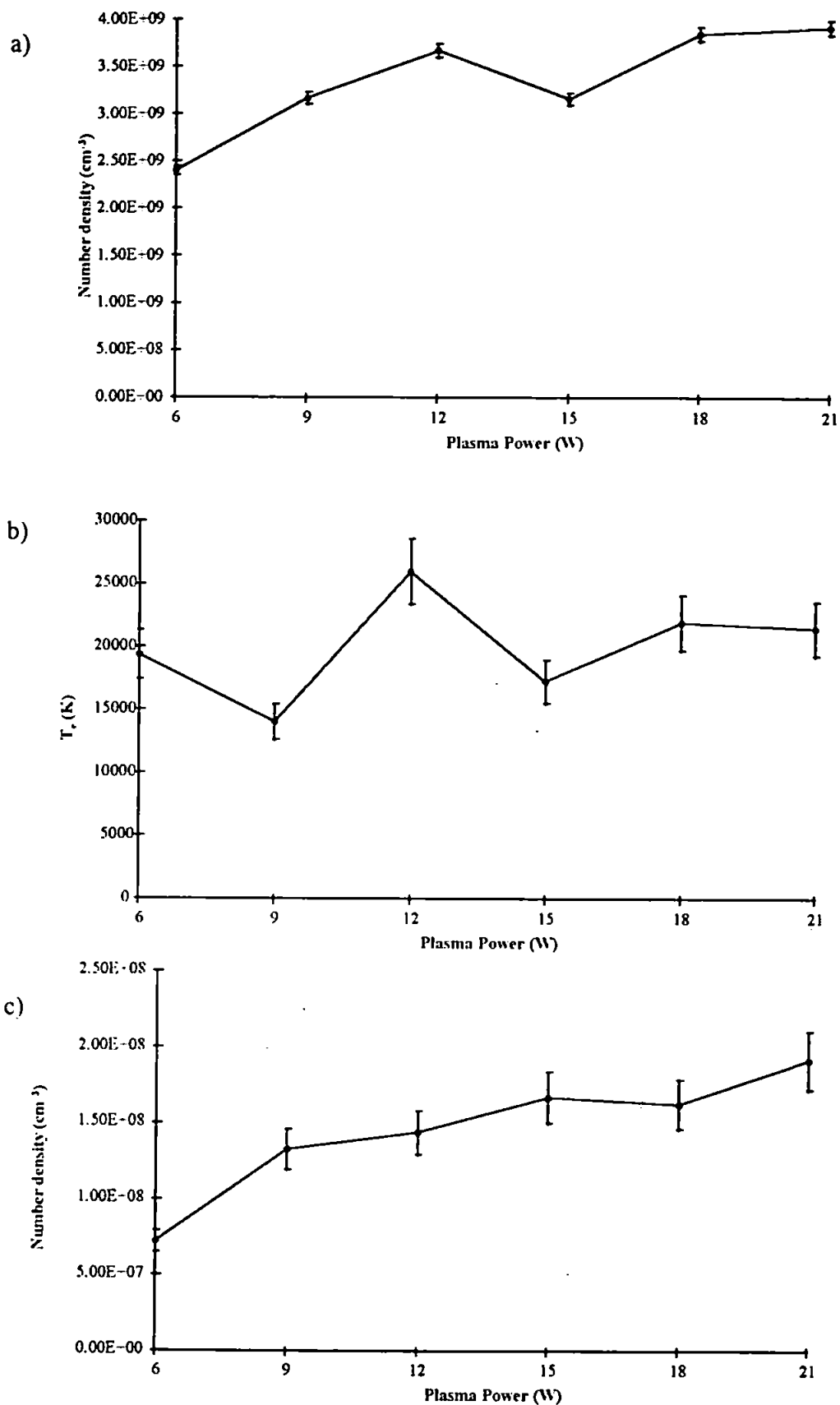
Figure 5.12 Effect of plasma forward power on a) ion number density; b) electron temperature; and c) electron number density, for a 12 ml min⁻¹ helium LP-ICP
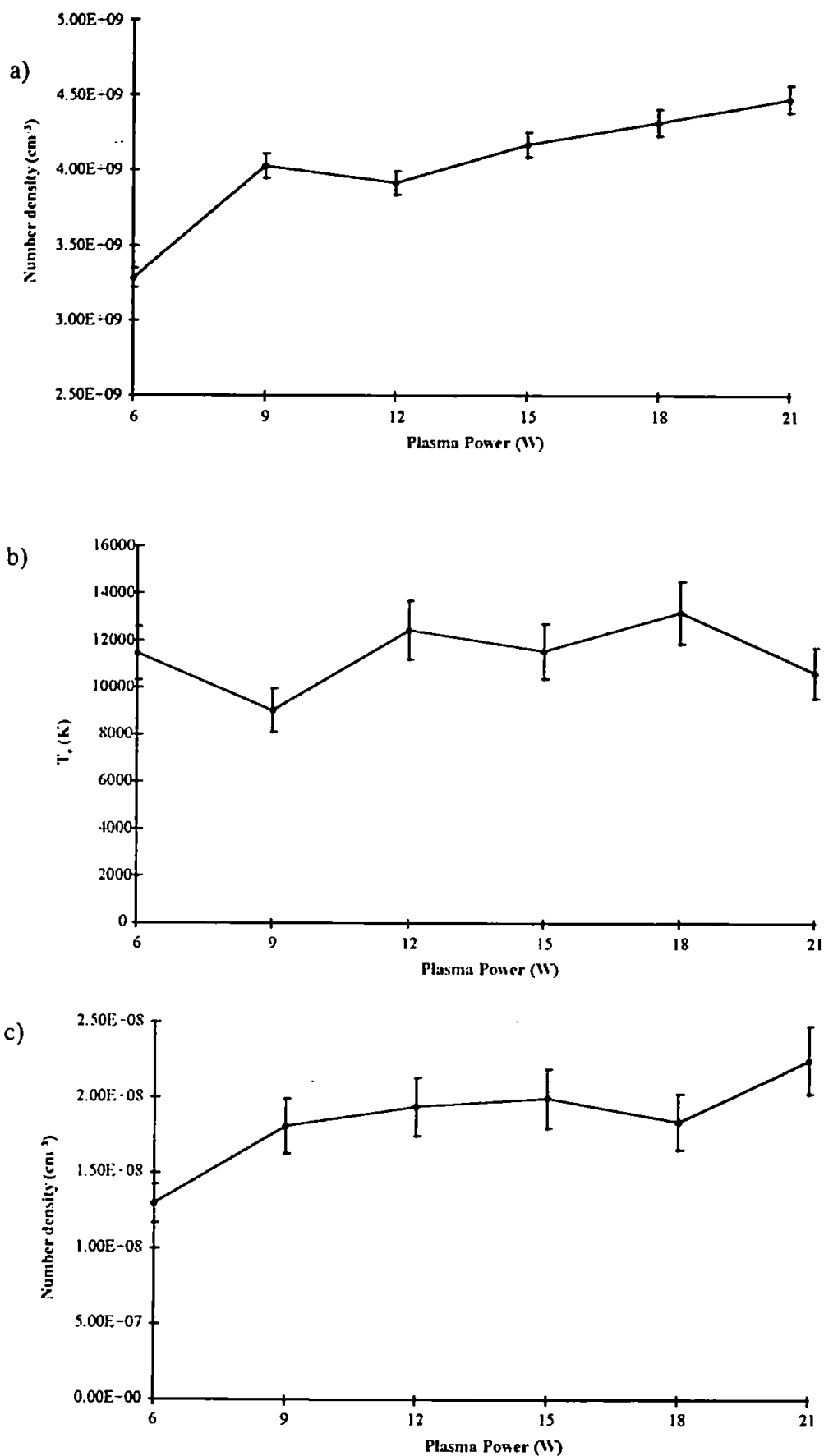
Figure 5.13 Effect of plasma forward power on a) ion number density; b) electron temperature; and c) electron number density, for a 15 ml min⁻¹ helium LP-ICP

The electron number densities exhibited an increasing trend with increasing plasma power, for all the flow rates studied (Figures 5.9c-5.13c). This may explain the slight increase in n_i with power for the 9 - 15 ml min^{-1} plasmas, as the reduction in T_e may have been compensated for by the rise in n_e. This would occur since there is a Maxwellian distribution of electron energies, the fall in T_e (*i.e.* the fall in the energy of the electron) was compensated by a rise in n_e (*i.e.* the net effect was a rise in the number of high energy electrons). The overall observed n_e was considerably lower than other low pressure plasmas[169], however comparison is difficult because a variety of sources and measurement techniques have been used. The results of temperature measurements performed by other workers on a variety of other low pressure plasmas are summarised in Table 5.4.

The electron energy is considerably higher than many other reported GD sources, so the LP-ICP may possess sufficient energy for the ionisation of organic compounds (IP $\approx$9 eV), but it would be unlikely that the ionisation of the halogens (IP 10.5 - 13 eV) and helium (IP 24.6 eV) would occur with such low energy electrons[9]. Secondary electron groups are commonplace in GD sources and often have energies an order of magnitude greater than the thermal electron group[88]. If such a group was present in the LP-ICP source, ionisation may occur by electron impact. However, such a secondary group was not detected by the Langmuir probe in this instance. Therefore, Penning ionisation is considered to be the major mechanism of ionisation for helium and the halogens in the LP-ICP-MS.

The effect of helium gas flow, and therefore pressure, on plasma characteristics can be seen more clearly from Figures 5.14 - 5.16. The ion number density varied little with gas flow, although it exhibited a minimum at 6W in most cases, and thereafter a slight increasing trend (Fig. 5.14). The electron temperature showed a decrease with plasma gas flow (Figure 5.15), albeit very slight, which can be attributed to the increasing collisions experienced by

Plasma Source	Fill Gas	Plasma Power	Pressure (Torr)	Measurement method	T_e (K)	n_e (10^{12}cm^{-3})	Reference
MIP	Argon	25 W	3.0	Double Probe	21680	15	88
MIP	Helium	25 W	3.0	Double probe	51941	10.5	88
MIP	Argon/Mercury	25 W	3.0	Double probe	31651	19.5	88
RF	Argon	50 W	2.0	Double probe	43013	1	169
RF	Neon	50 W	2.0	Double probe	54955	0.85	169
RF	Argon/Thallium	50 W	2.0	Double probe	39999	2.0	88
RF	Argon/Titanium	50 W	2.0	Double probe	36984	0.15	88
RF	Argon	50 W	2.0	Double probe	27941	0.80	88
GD Al (discharge tube)	Helium/Mercury	8 mA	4.0	Single Langmuir probe	579	0.82	169
GD Al (discharge tube)	Helium/Mercury	8 mA	12.0	Single Langmuir probe	811	0.22	169
GD Cu	Argon	10 mA x 620 V	2.0	Single Langmuir probe	3130	0.16	169
GD Cu	Argon	10 ma x 530 V	3.0	Single Langmuir probe	3130	0.16	169
GD Grimm type lamp	Argon	40 mA x 800 V	15.3 cm^3 min^{-1}	Hβ Method	927	203	88
GD Grimm type lamp	Argon	60 mA x 800 V	29.1 cm^3 min^{-1}	Hβ Method	1159	287	88
GD Grimm type lamp	Argon	80 mA x 800 V	35.5 cm^3 min^{-1}	Hβ Method	1275	319	88
GD Grimm type lamp	Argon	40 mA x 1000 V	17.5 cm^3 min^{-1}	Hβ Method	811	201	88
RF	Helium	6 W	0.2	Single Langmuir probe	17931	0.0000412	this work
RF	Helium	9W	0.2	Single Langmuir probe	20090	0.0000536	this work

Table 5.4   Fundamental parameters for low pressure plasma discharges (adapted from reference 88 and 169)
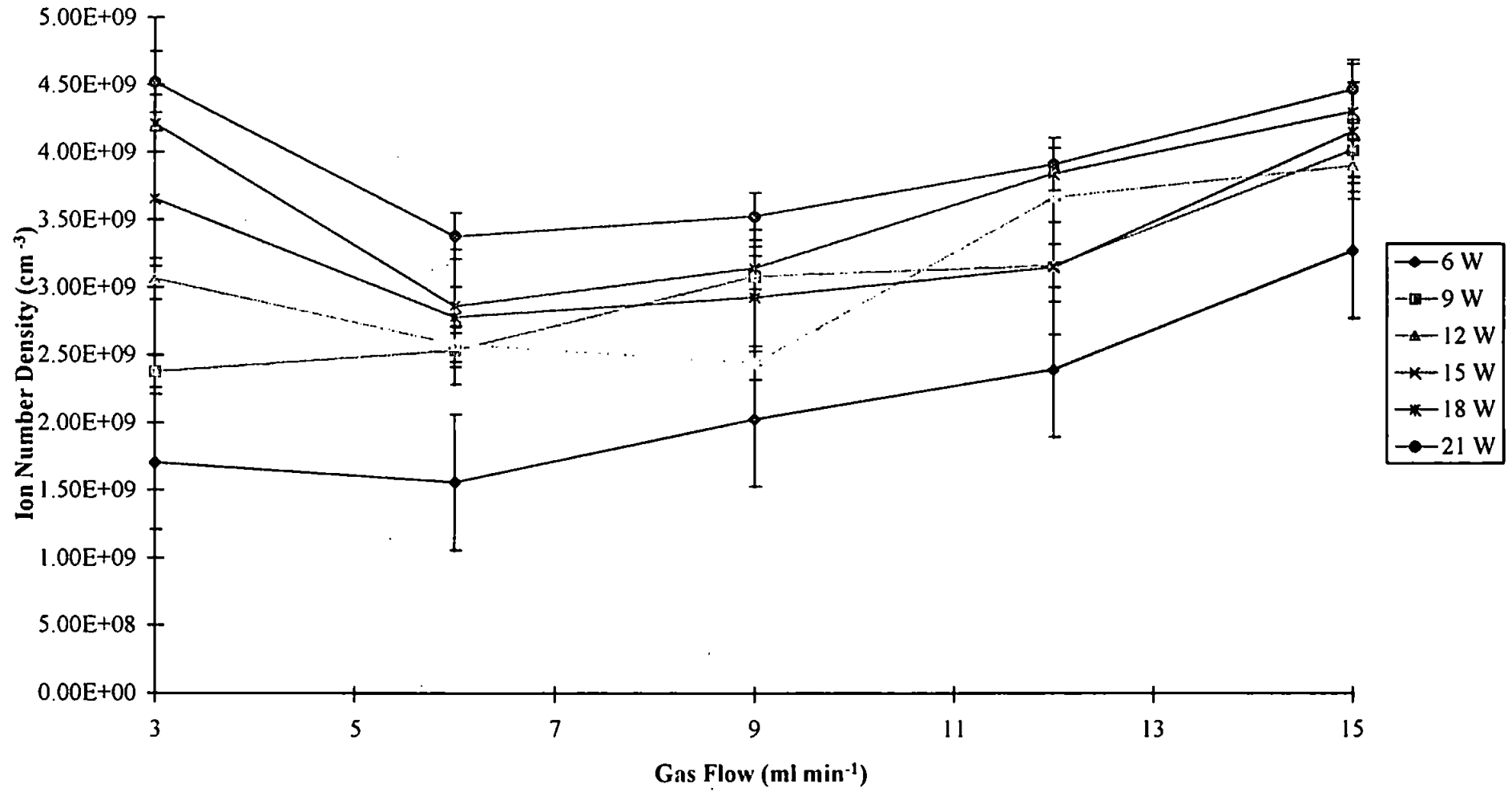
Figure 5.14 Effect of helium plasma gas flow on ion number density for a LP-ICP at selected plasma powers.
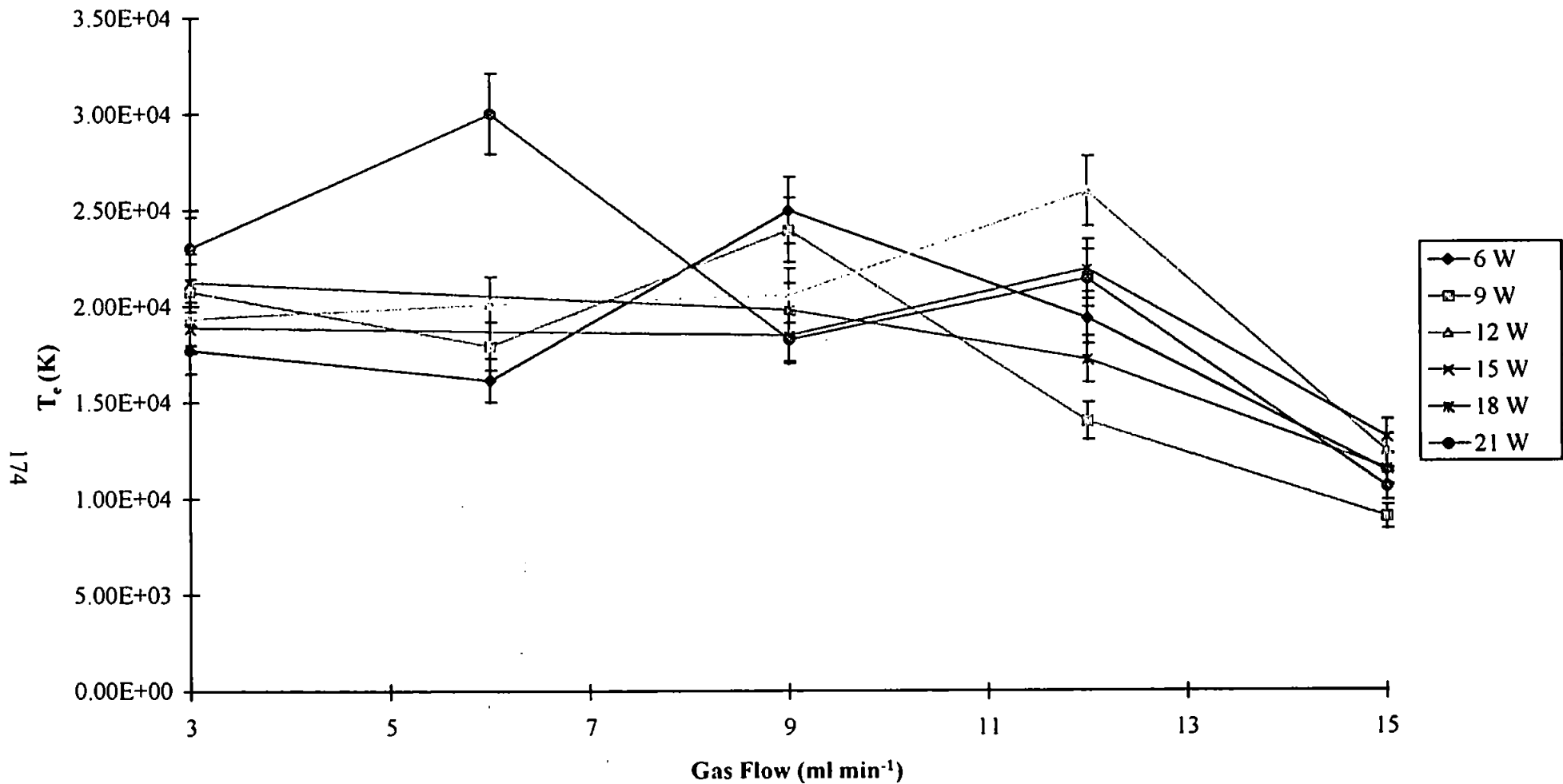
Figure 5.15 Effect of helium plasma gas flow on electron temperature for a LP-ICP at selected plasma powers.
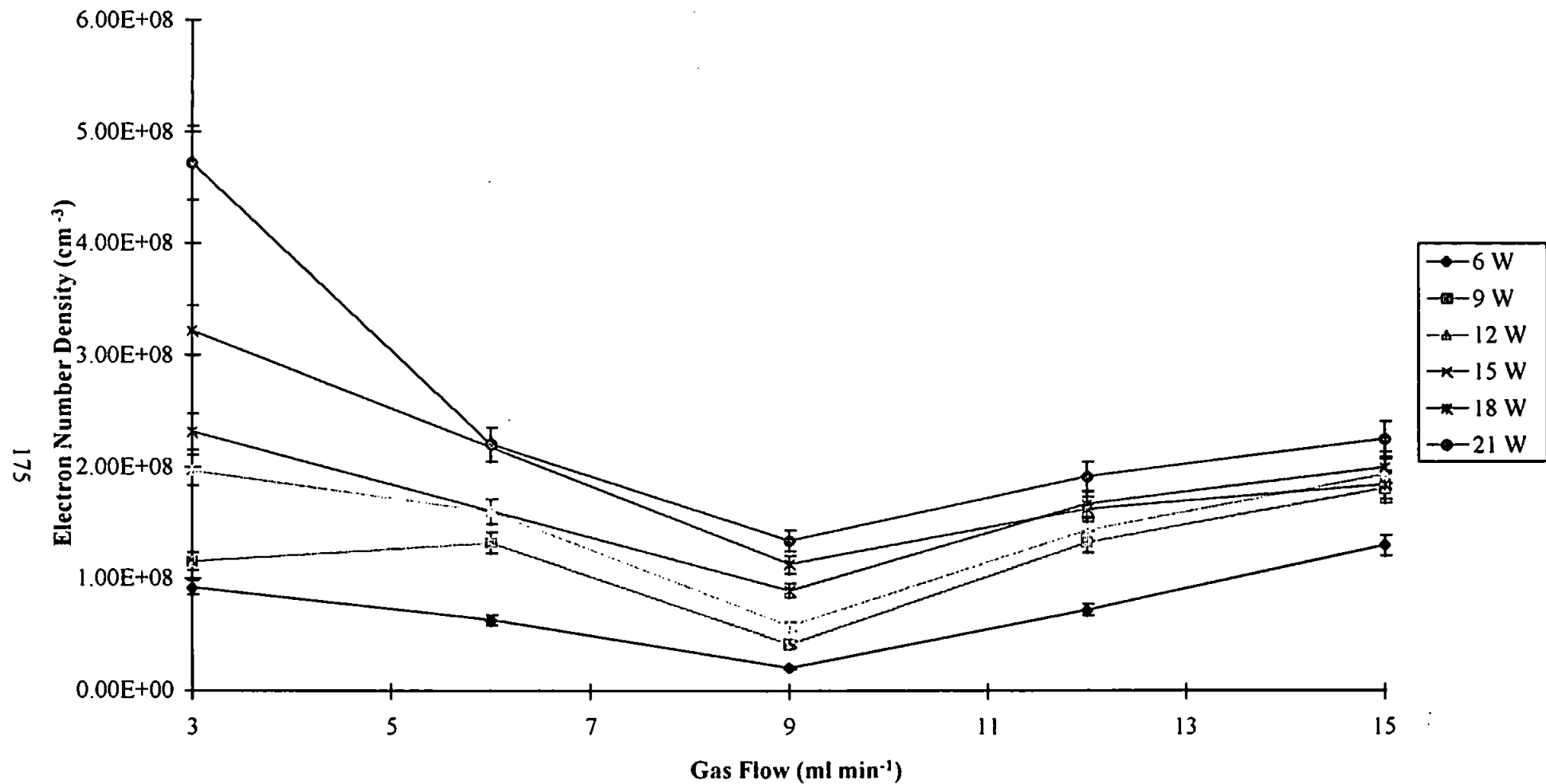
Figure 5.16 Effect of helium plasma gas flow on electron number density for a LP-ICP at selected plasma powers.

the electrons as the torch pressure increased. The electron number density exhibited a fall up to 9 ml min^{-1}, and thereafter a rise with increasing flow. This is the opposite trend to that which one would expect from similar experiments performed on GD sources[88,169,170]. One explanation for such trends is the change in the plasma's physical shape as the gas flow was increased above 9 ml min^{-1}.

In an attempt to distinguish between the different ionisation processes in a helium only LP-ICP-MS and a helium/isobutane LP-ICP-MS, Langmuir probe measurements were also performed on the latter. As isobutane was bled into the helium plasma, the probe quickly became coated with a brown film. This coating rendered the current-voltage plots meaningless, as the probe surface area changed and the probe was effectively insulated by the deposit.

5.4.2 Ion Kinetic Energy Measurements

In order for the helium low pressure ICP to be used as an effective ion source it is necessary for the kinetic energy spread of the ions to be over a narrow range, since a wide range of ion kinetic energies would lead to difficulty in tuning the mass calibration on the quadrupole, and if the spread of kinetic energy at an individual mass was large it may prove difficult to maintain good peak resolution. The ion kinetic energies of the three fragment ions of PFTBA at 69, 219, 502 m/z, were calculated from the respective ion stopping curves for the 6W plasma, shown in Figure 5.17. The curves suggest that, for the 6W helium plasma, the ion kinetic energies were quite similar. Derivative plots for these curves are shown in Figure 5.18, indicating that the mean ion kinetic energies for the three mass fragments were 2.1, 1.2 and 1.7 eV, for 69, 219, and 502 m/z respectively; and that the spread in the kinetic energies was less then 1.5 eV, which should lead to well resolved peaks for all three mass fragments. This was indeed the case.

Figure 5.17 Ion stopping curves for the three mass fragments of PFTBA, at 69, 219, and 502 m/z, for a 6W helium LP-ICP.

Fulford and Douglas[172] have described how the ion kinetic energies of ions, extracted through a molecular beam type interface, should increase linearly in relationship to the mass as described by:

$$E_s = \frac{M}{M_{gas}}\left(\frac{5}{2}kT_{gas}\right) + P \qquad (5.6)$$

which is due to the translational energy imparted by the ion sampling process. Where E_s is the ion kinetic energy, M is the mass of the ion, M_{gas} is the mass of the plasma gas, k is the Boltzmann constant, T_{gas} is the gas kinetic temperature of the sampled plasma (K), and P is the plasma potential (V). Tanner[174] later used this linear relationship to determine T_{gas} and the plasma potential of an atmospheric pressure argon ICP. The relationship was applied to both sampled atomic and polyatomic ions, with both showing a linear increase in energy with mass. However, the polyatomic ions showed lower energies than atomic ions of the same mass. Such a linear relationship did not exist for the LP-ICP sampling process as all the observed ions had similar energies (Fig 5.18). Additionally, since the observed plasma potentials were of the order of 30 V for a 6W plasma one would expect the ions to have higher kinetic energies than those observed (i.e. 1.2 - 2.1 eV). This suggests that the ions did not undergo supersonic expansion, which could mean one of two things:

i)   the pressure differential across the low pressure sampler was not great

        enough for supersonic gas sampling;

ii)   ions were formed in the sampling interface, rather than the torch.

Further evidence that not all fragment ions were formed in the LP-ICP, is found in the calculated gas kinetic temperature for the LP-ICP using equation 5.6 (Table 5.5). While LP plasmas can be formed at or just above room temperature, the calculated temperature from the 219 and 502 m/z fragments, which are well below room temperature, suggest they were
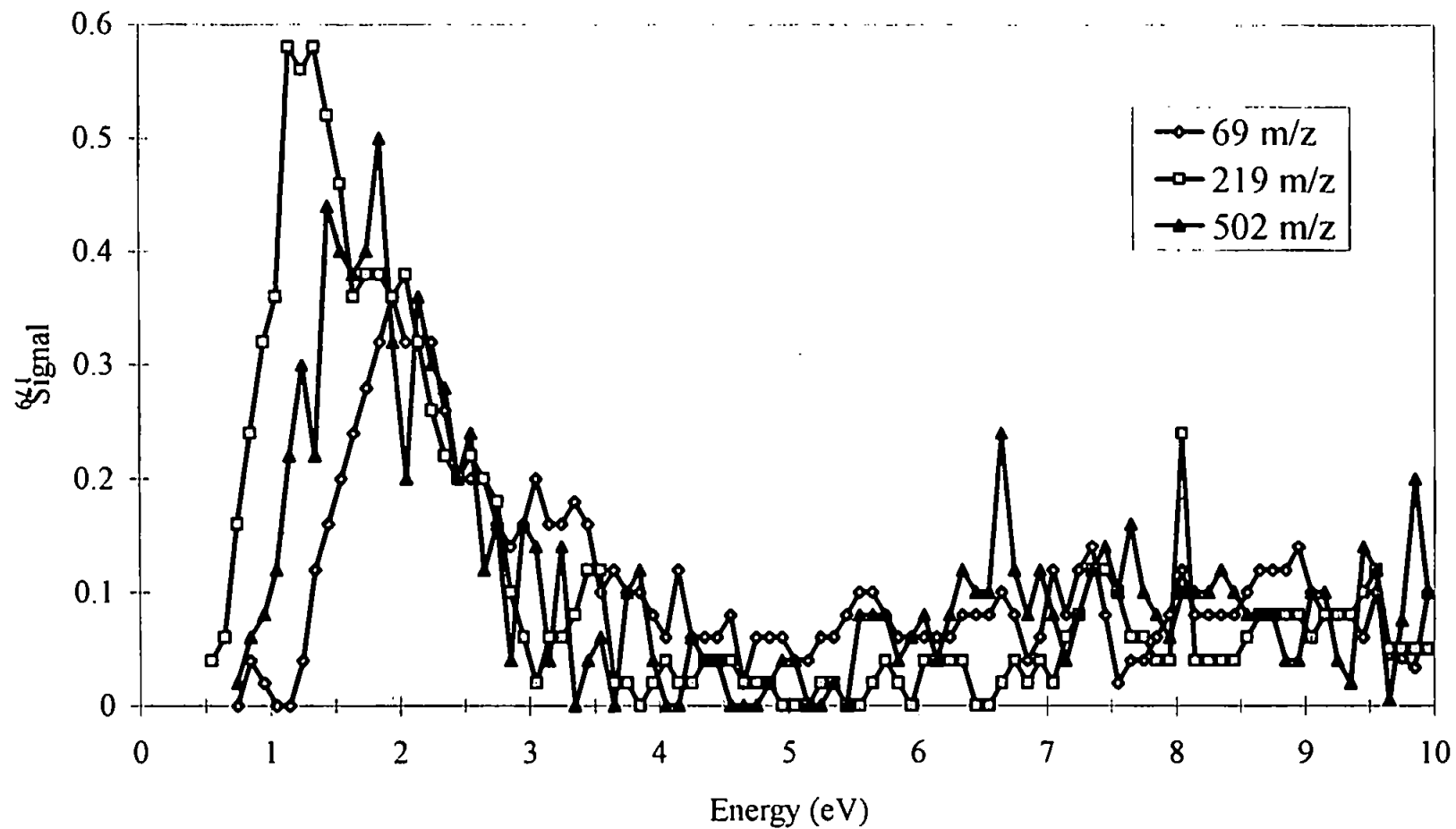
Figure 5.18 Derivative plot of the ion stopping curves for three mass fragments of PFTBA, at 69, 219, and 502 m/z, for a 6W helium LP-ICP.

Table 5.5   Calculated plasma gas kinetic temperature from ion kinetic energy

measurements.

Ion Mass (m/z)	Ion kinetic energy (eV)	Gas kinetic temperature (K)
69	2.1	505
219	1.2	127
502	1.8	66

not formed in the plasma, or did not undergo a supersonic expansion. The 69 m/z fragment yields a temperature closer to that which one would expect of a LP-ICP. However, the temperature of the LP-ICP has been indicated by passing a capillary tube, containing a melting point apparatus reference compound (Azobenzol m.p. 341K), into the low pressure plasma via a vacuum seal. The compound was placed in a 6 ml min^{-1} helium plasma. The plasma power was slowley raised from 3 W to 21 W. The compound started to melt at 21W, suggesting the lower power plasma used in these studies had a T_{gas} of less than 340K.

Tanner[174] has also discussed how ions, when formed in sampler boundary layers and shock wave structures would exhibit similar ion kinetic energies. Tanner used this theory to explain the similarities in ion energies for simple polyatomics, formed by recombination reactions in the boundary layer of a shock wave structure, and this may also be the reason for the similarities in ion energy obtained here, i.e. that ionisation is caused by a secondary discharge in the expansion interface. Such a discharge is likely because of the high plasma potential observed for the LP-ICP.

The ion stopping curves for PFTBA fragment ions formed in an 8 W helium LP-ICP are shown in Figure 5.19. It can be seen from this plot that there is no linear relationship between ion mass and energy. The mean ion energies increased with power, as did the spread in energy. Such increases in energy in an atmospheric argon ICP have been described by Olivares and Houk[171] and have been attributed to a secondary discharge in the expansion interface. Therefore, the increase in energy and energy spread with power may be considered as further evidence that a secondary discharge existed, and hence was playing a role in fragment ionisation in the LP-ICP-MS.
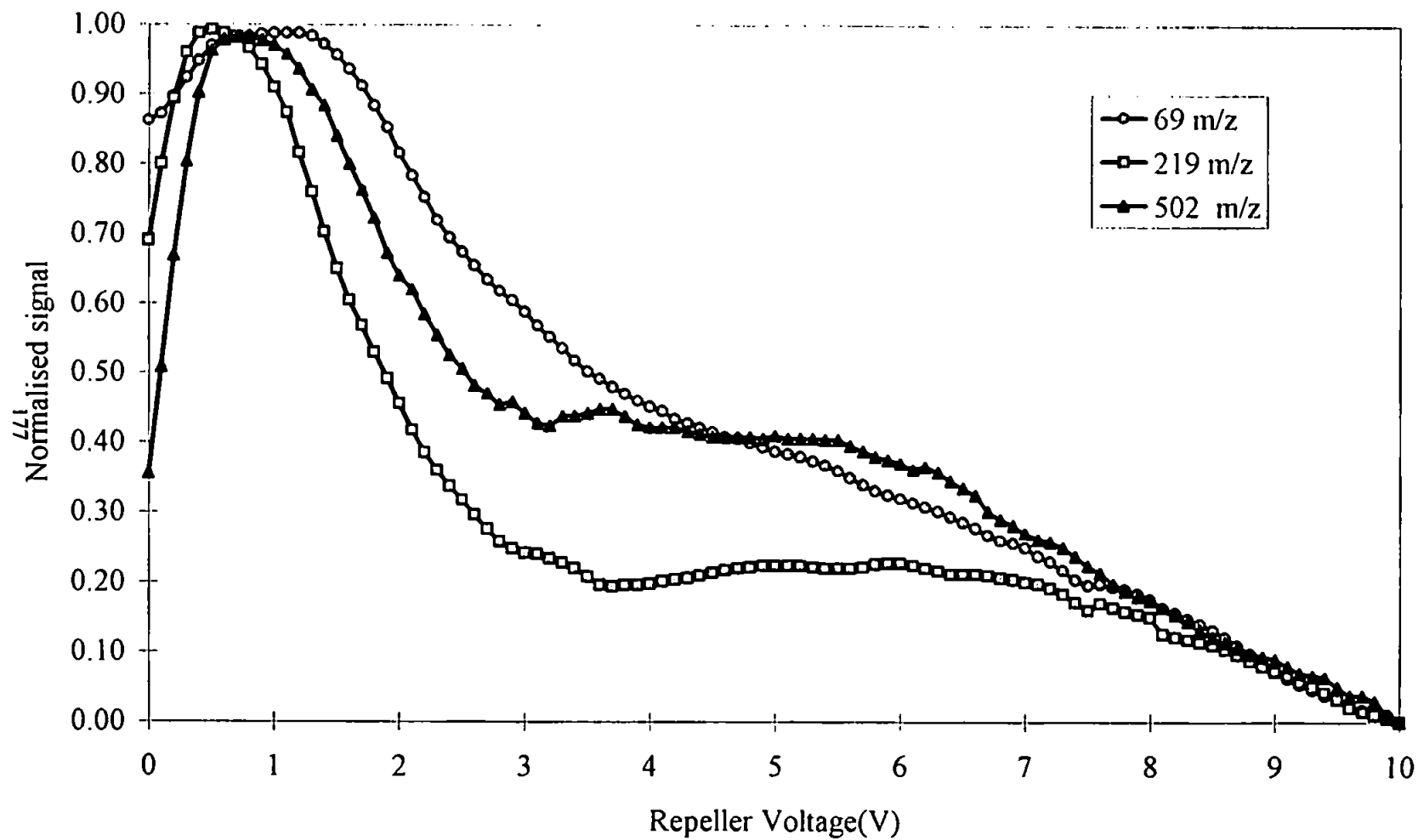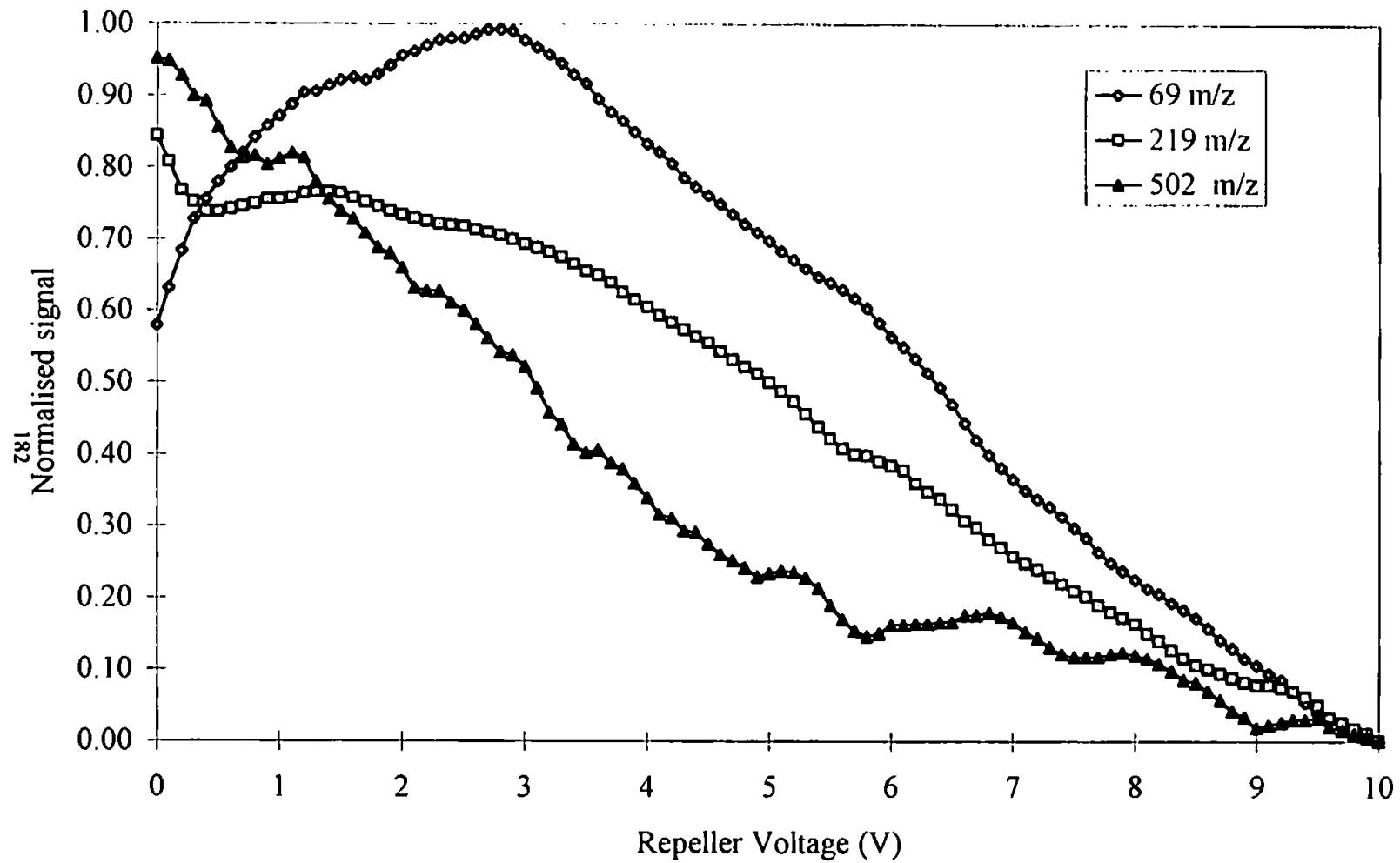
Figure 5.19 Ion stopping curves for the three mass fragments of PFTBA, at 69, 219, and 502 m/z, for a 8W helium LP-ICP.

5.5 CONCLUSIONS

The large plasma potentials observed are concurrent with secondary discharges in the expansion interface of plasma source mass spectrometers. The existence of a secondary discharge would seem to be confirmed by the increased spread in the ion kinetic energies as the power was increased. However, the role of this discharge in analyte ionisation is difficult to assess. The values for n_i, n_e and T_e are considered low in comparison to other low pressure sources. This can be attributed to the lower pressures used in this study.

The low gas kinetic temperature, calculated from the ion kinetic energies, indicated that the large fragment ions of PFTBA, at 219 m/z and 502 m/z, did not undergo supersonic expansion. This suggests that ionisation occurred in a secondary discharge in the expansion interface.

Chapter 6

DETERMINATION OF TETRAETHYLLEAD IN A STANDARD REFERENCE FUEL BY LOW PRESSURE-INDUCTIVELY COUPLED PLASMA-MASS SPECTROMETRY

CHAPTER 6 - DETERMINATION OF TETRAETHYLLEAD IN A STANDARD REFERENCE FUEL BY LOW PRESSURE-INDUCTIVELY COUPLED PLASMA-MASS SPECTROMETRY.

6.1 INTRODUCTION

The coupling of element specific detectors to chromatographic systems has greatly enhanced the ability of analysts to provide trace level information on a wide variety of organometallic species. However, these highly specific and selective detectors have a number of unattractive features. First, much of the instrumentation used for trace level multielement analysis has high capital and running costs. These running costs can be justified when performing multielement analysis on aqueous samples which are directly introduced into the instrument, yielding analysis times of less than 1 minute. However, the addition of a chromatographic separation technique greatly increases the analysis time per sample making the speciation of trace metals a costly exercise. Also, by using such detection systems much of the chemical information available to the analyst is lost because the metal species are totally atomised. Hence a ready supply of certified reference compounds and standards of known organometallic species are required to enable species identification by comparison of retention time. This is disadvantageous because the analysis of individual standards is a time consuming and costly affair, and for many organometallic species such standards simply don't exist. Therefore, any instrumentation capable of providing both quantitative trace level element specific information and qualitative identification of unknown species, without having to rely on the running of standards but with reduced capital and running cost, would be welcomed.

For many years alkyllead compounds have been added to petrol as antiknocking agents[175]. While this practice has decreased in recent years, organolead species are still prevalent in

the environment. Many organolead species are know neurotoxins, which can enter the body orally and trans-dermally, and therefore are of interest for clinical reasons. The determination of organolead species by GC-MIP-AES, in core samples from polar ice caps and high mountain glaciers has formed the basis for the archiving of historical automobile pollution, and the study has shown clear links between the increased use of leaded petrol and organolead species being found in the environment[175]. Also highlighted in this study was the wide variety of species derived from the natural breakdown of tetraalkyllead compounds.

Organolead species have also been found in wine samples, and this serves as an excellent example of how such species enter the human food chain[176]. Hence such studies can provide invaluable information on the fate of polluting and naturally occurring trace metals in the environment, the use of which will be essential for future environmental impact assessments.

The analysis of organolead species has been previously performed by low pressure inductively coupled plasma mass spectrometry[110]. In this instance a 1 l min^{-1} argon LP-ICP was used and only atomic information was obtained. The main aim of this chapter is to assess the ability of LP-ICP-MS to provide further species information enabling unequivocal identification of the organometallic species without resorting to a comparison of retention time.

6.2 EXPERIMENTAL

Mixed standards of tetraethyllead (99% Aldrich chemicals, Gillingham, UK) were freshly prepared by weight in pentane (Rathburn Chemicals, Scotland, UK). A 15 ng μl^{-1} solution was then used to optimise the instrumental parameters, with three separate injections being

made at each instrument setting. The instrumental parameters used for the analysis of the alkyllead species in a standard reference fuel are shown in Table 6.1.

The instrument response was first calibrated for tetraethyllead using the three most intense fragment ions in the mass spectrum, at 208, 237 and 295 m/z. The concentration of lead in a reference fuel (NBS SRM 1637 II) was then determined by direct injection of 1 μl of reference material onto the column of the gas chromatograph.

A full scan mass spectrum of the tetraethyllead standard and reference fuel was obtained by using the same plasma and GC conditions as above, however, the mass spectrometer was set to full scan mode, continuously scanning a mass range between 100 and 500 m/z. The resulting spectrum was then compared to a library spectrum obtained from a Hewlett Packard 5970 GC-MS workstation.

6.3 RESULTS AND DISCUSSION

The column head pressure (*i.e.* helium carrier gas flow) was optimised first. Such an optimisation was essential because the analyte eluted close to the solvent front, which has been shown to affect the spectra observed (section 4.3). The effect of column head pressure on a 15 ng on-column injection of tetraethyllead is shown in Figure 6.1. The optimum head pressure, yielding the highest total ion count, was 60 KPa. This resulted in a column carrier gas flow of 4 ml min^{-1} at 120 °C. Also shown in Figure 6.1 are the relative intensities of the fragment ions, which changed little with increasing flow rate. This suggested that the increase in gas flow did not cause further fragmentation of the analyte as was previously observed for the halobenzene species (Chapter 4).

Table 6.1   Operating conditions for the analysis of tetraethyllead using low pressure-inductively coupled-plasma source-mass spectrometry.

Mass Spectrometer	Modified Hewlett Packard MSD
Quantitative analysis	
selected ions monitored (m/z)	208, 237 and 295
Qualitative analysis	
Scan range (m/z)	100 to 500
Plasma	
Forward power(W)	6
Reflected power(W)	0
Helium make-up gas flow rate (ml min^{-1})	3
Isobutane flow rate (ml min^{-1})	1.8
Pressure (Torr)	
Torch	0.2
Interface	4×10^{-2}
Analyser	$< 10^{-6}$
Gas Chromatograph	
Injector	cold on-column
Column	DB1, 30 m length, 0.32 mm o.d., 0.25 μm film thickness
Carrier gas	Helium
Head Pressure (KPa)	60
Carrier flow (ml min^{-1})	4
Injection Volume (μl)	1
Oven temperature($^{\circ}$C)	120 isothermal
Transfer line temperature ($^{\circ}$C)	120
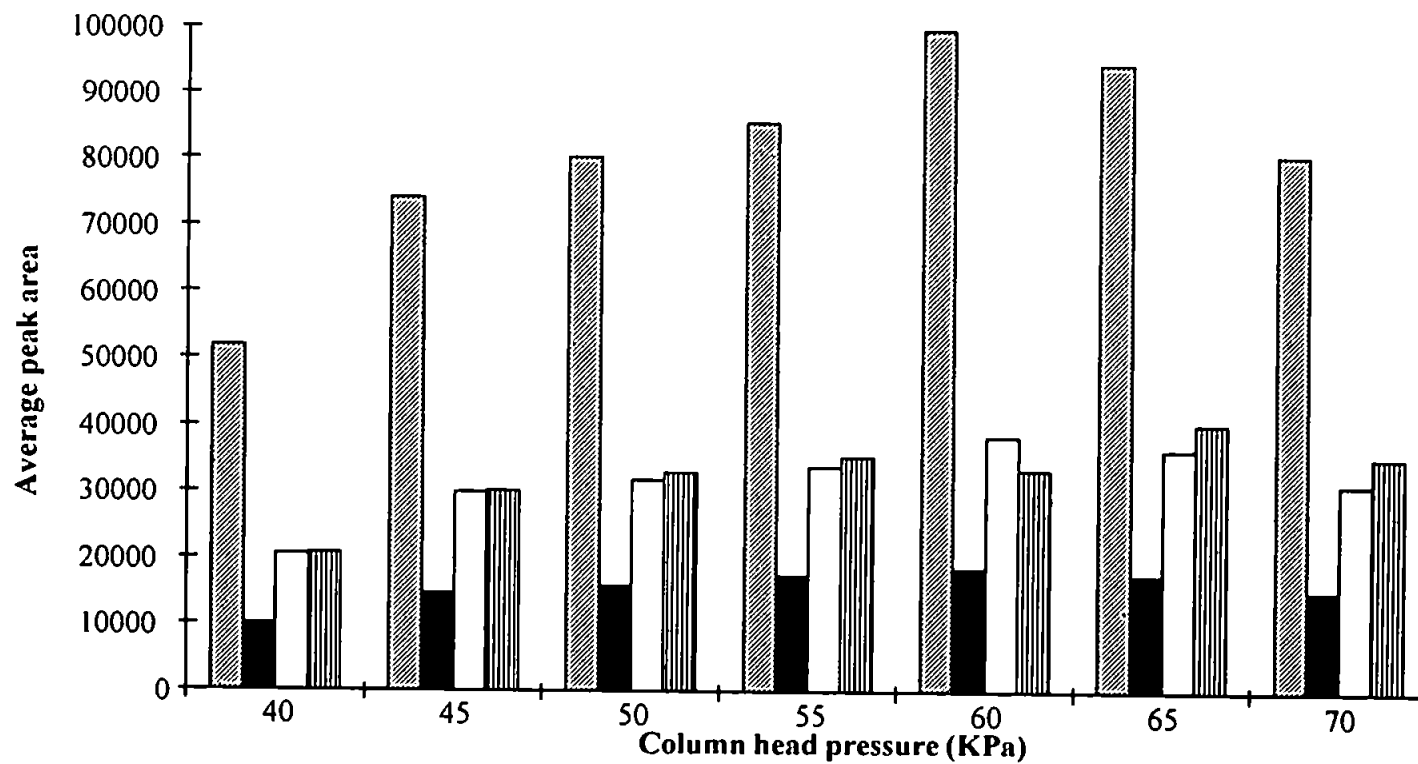
Figure 6.1   The effect of column head pressure (KPa) on the signal for tetraethyllead, ▨Total ion count, ■208 m/z, ☐ 237 m/z and ▥ 295 m/z.

The effect of plasma forward power on analyte signal is shown in Figure 6.2. For the halobenzenes (Chapter 4) lower power favoured the production of the most intense molecular signals, however, in this case a reduction in the intensity of the molecular fragments did not coincide with an increase in the atomic signal for lead. This is further evidence that penning ionisation may be playing an important role in the formation of atomic ions, because it is more likely that the halogens, with higher ionisation potentials, will be ionised by charge transfer from the helium metastable species, whereas, metals, such as lead, with lower ionisation potentials will not be ionised by charge transfer because of the mismatch in energies.

No fragment ions were observed in the absence of isobutane reagent gas. The effect of increasing reagent gas concentration is shown in Figure 6.3. The lowest gas flow resulted in the most intense ion signals, however, unlike the halobenzene species, the molecular ion was not observed for tetraethyllead, and the larger fragment ions of tetraethyllead did not increase in intensity with increased isobutane flow.

The addition of a helium make-up gas to the plasma was essential to maintain good plasma stability and to keep the plasma sustained while the solvent eluted from the GC column. The effect of the added helium on the analyte signal is shown in Figure 6.4. An almost linear decrease in sensitivity was observed with increased helium gas flow. Fragmentation of the molecular fragments yielding higher atomic signals for lead was not observed.

Calibration curves are shown in Figures 6.5a and 6.5, constructed by plotting total ion signal and the signals for the individual fragment ions versus tetraethyllead concentration respectively. The calibration exhibited good linearity. Analytical figures of merit, based on the total ion counts for tetraethyllead using the above optimised plasma conditions are
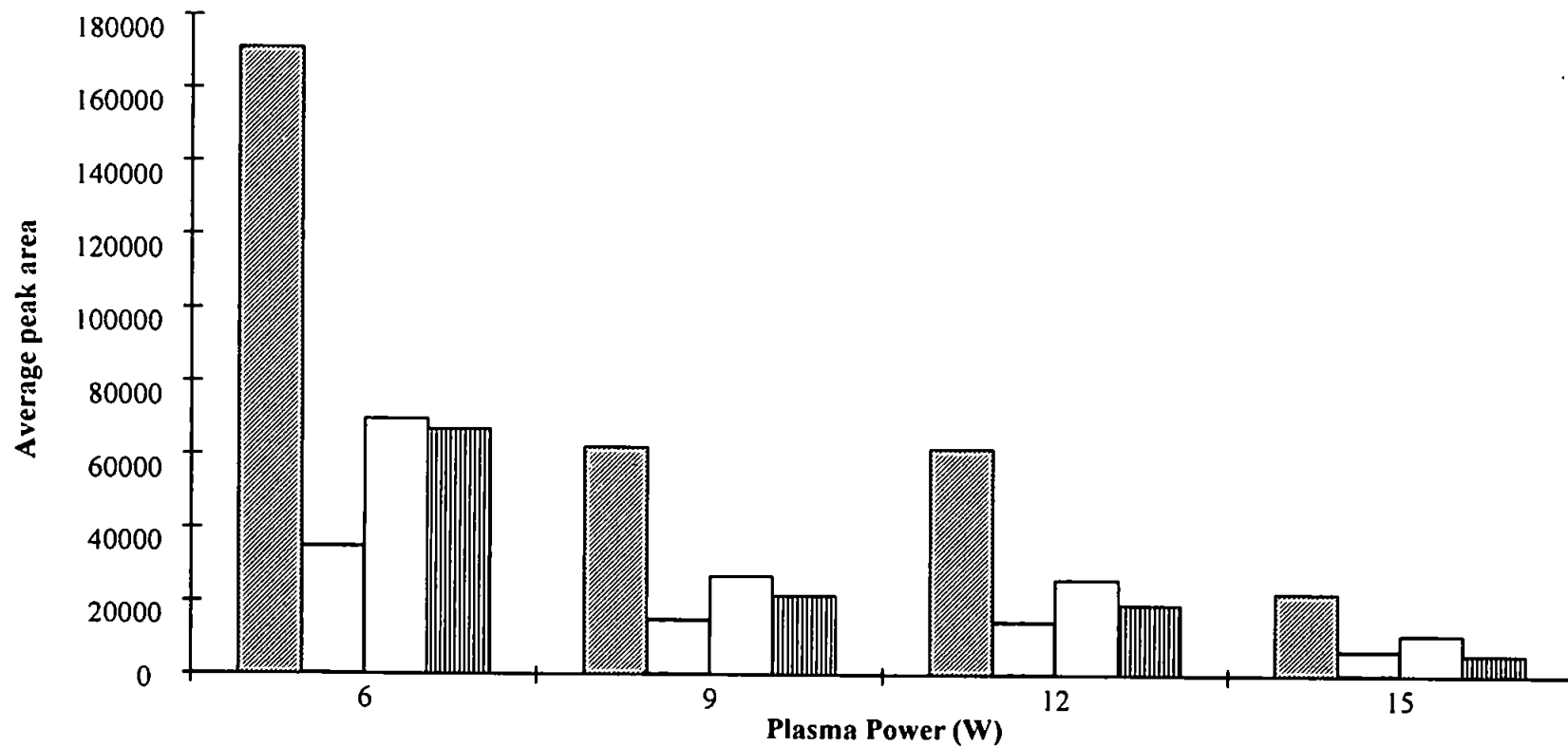
Figure 6.2   The effect of plasma forward power (W) on the signal for tetraethyllead, ▨ Total ion count, ☐ 208 m/z, ☐ 237 m/z and ▥ 295 m/z.
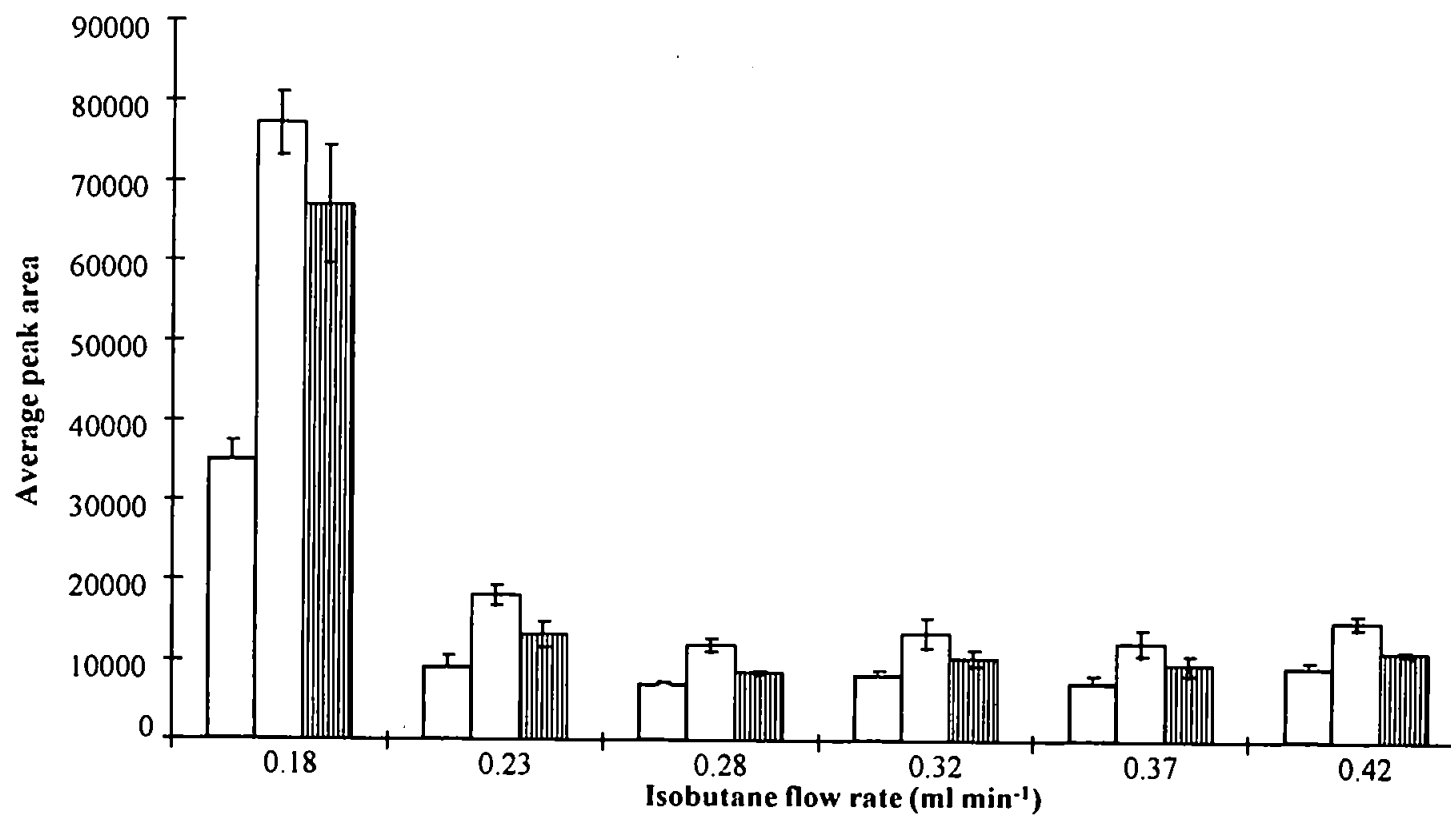
Figure 6.3   The effect of isobutane flow rate (ml min⁻¹) on the signal for tetraethyllead,□ 208 m/z, □ 237 m/z and ▥ 295 m/z.
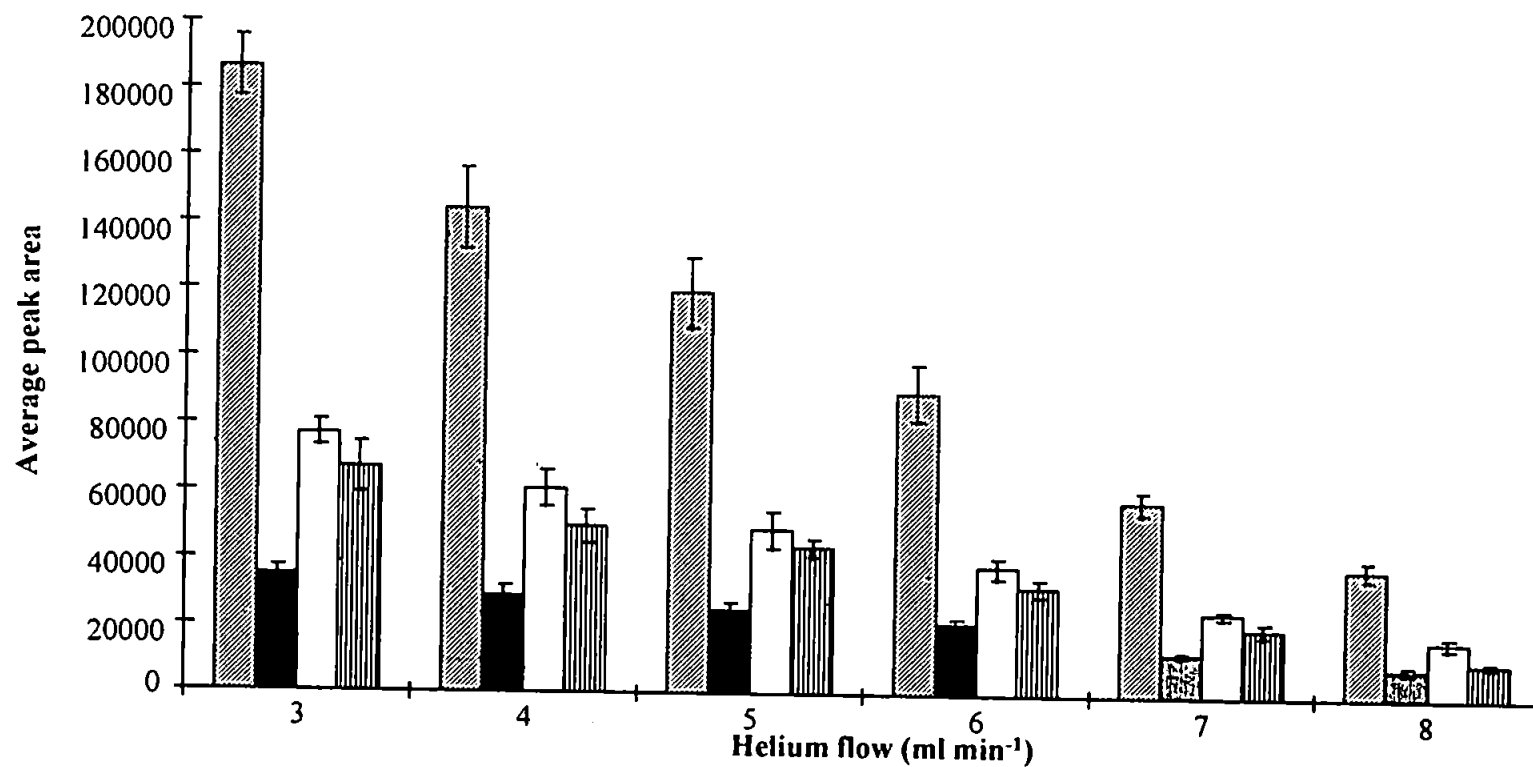
Figure 6.4   The effect of helium make-up gas flow (ml min^{-1}) on the signal for tetraethyllead, ▨ Total ion count, ■ 208 m/z, ☐ 237 m/z and ▥ 295 m/z.

a)

$y = 23833x - 4616.5$

$R^2 = 0.9996$

b)

237 m/z

$y = 9726.4467x - 1926.4574$

$R^2 = 1.0000$

295 m/z

$y = 8245.1994x - 1894.9906$

$R^2 = 1.0000$

208 m/z

$y = 4860.4x - 949.61$

$R^2 = 0.9999$
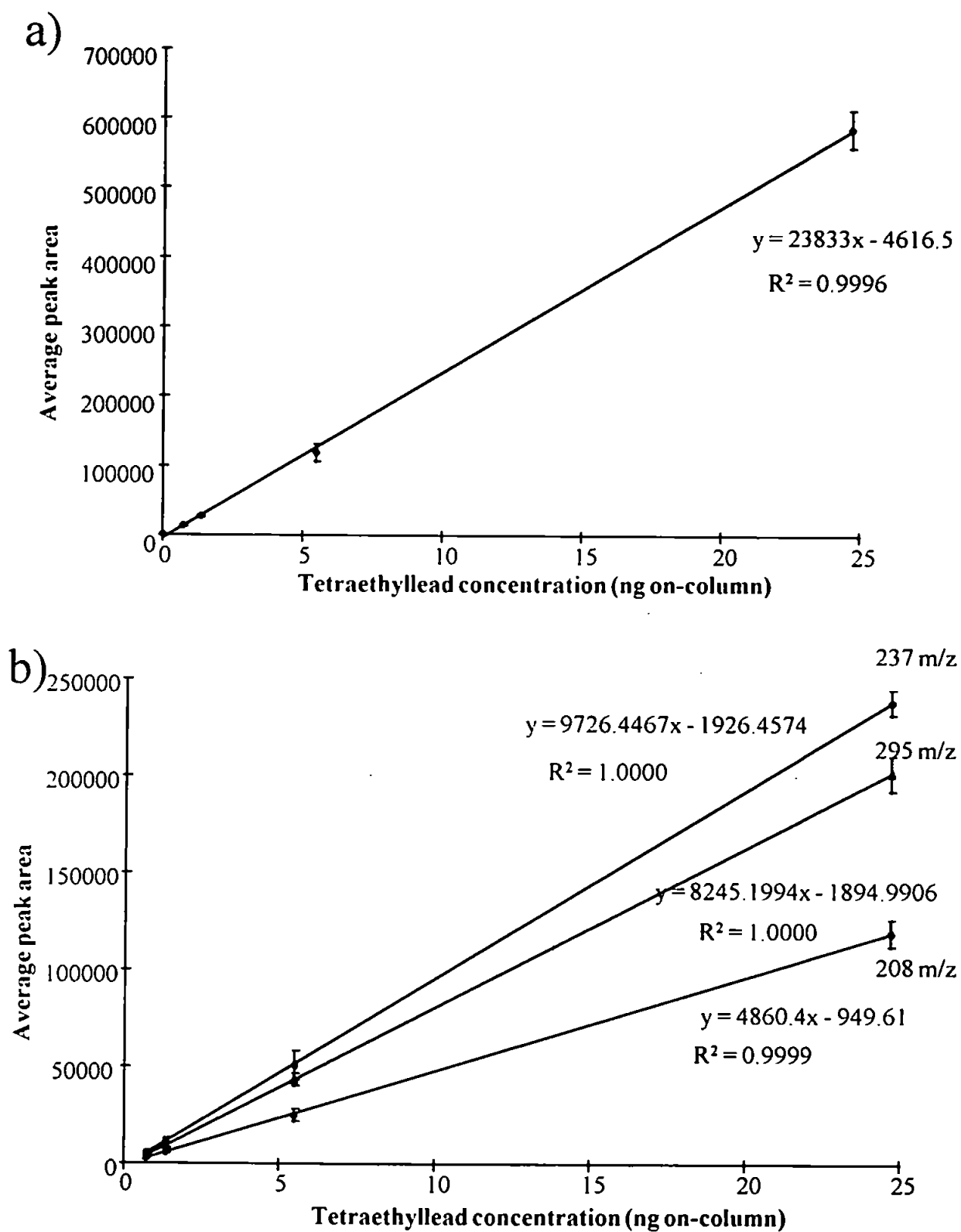
Figure 6.5   Calibration curves for tetraethyllead for a) total ion signal; b) signals for

fragment ions at m/z 208, 237 and 295.

shown in Table 6.2. The calculated limit of detection was 7 picograms, which approximates the limit of detection for a Hewlett Packard mass selective detector operating in the electron impact mode, as stated by the instrument manufacture[149]. Four consecutive on-column injections of 0.7 ng of tetraethyllead are shown in Figure 6.6, demonstrating the stability and reproducibility of the low pressure plasma.

Results for the determination of tetraethyllead in NBS SRM 1637 II reference fuel are shown in Table 6.3. The fuel has been certified for total lead, however, previous studies using GC-ICP-MS have detected only one lead species in the reference fuel[177]. The determined concentration of lead was in good agreement with the certified value.

A total ion chromatogram for the analysis of the standard reference material is shown in Figure 6.7a. The lighter hydrocarbon fraction of the petrol eluted rather quickly (< 1 min) from the DB1 GC column, leaving the tetraethyllead well separated from these fractions. The presence of tetraethyllead was verified by the mass spectrum of the chromatographic peak (Figure 6.7b). The molecular ion for tetraethyllead at 324 m/z was not observed (Figure 6.7b), however, the peaks at 295 and 267 and 237 m/z were consistent with the loss of successive ethyl groups (29 m/z) from the molecule, and the lead isotopes were observed between 204 and 208 m/z. The mass spectrum for a 10 ng injection of tetraethyllead is shown in Figure 6.8a and the EI library spectra for tetraethyllead is shown in Figure 6.8b. Comparison of the spectra unequivocally identifies the lead species in the standard reference materiel as tetraethyllead.

Table 6.2   Figures of merit for tetraethyllead calibration using low pressure inductively coupled plasma source mass spectrometry.

Selected ions (m/z)	208,237 and 295
Linear range studied	10^2
Slope (counts ng^{-1})	23833
R^2	0.9996
Limit of detection (ng)[a]	0.007
RSD %[b]	7

a) 3 standard deviations of 10 readings take at the blank level.
b) 4 readings at 0.7 ng on-column.
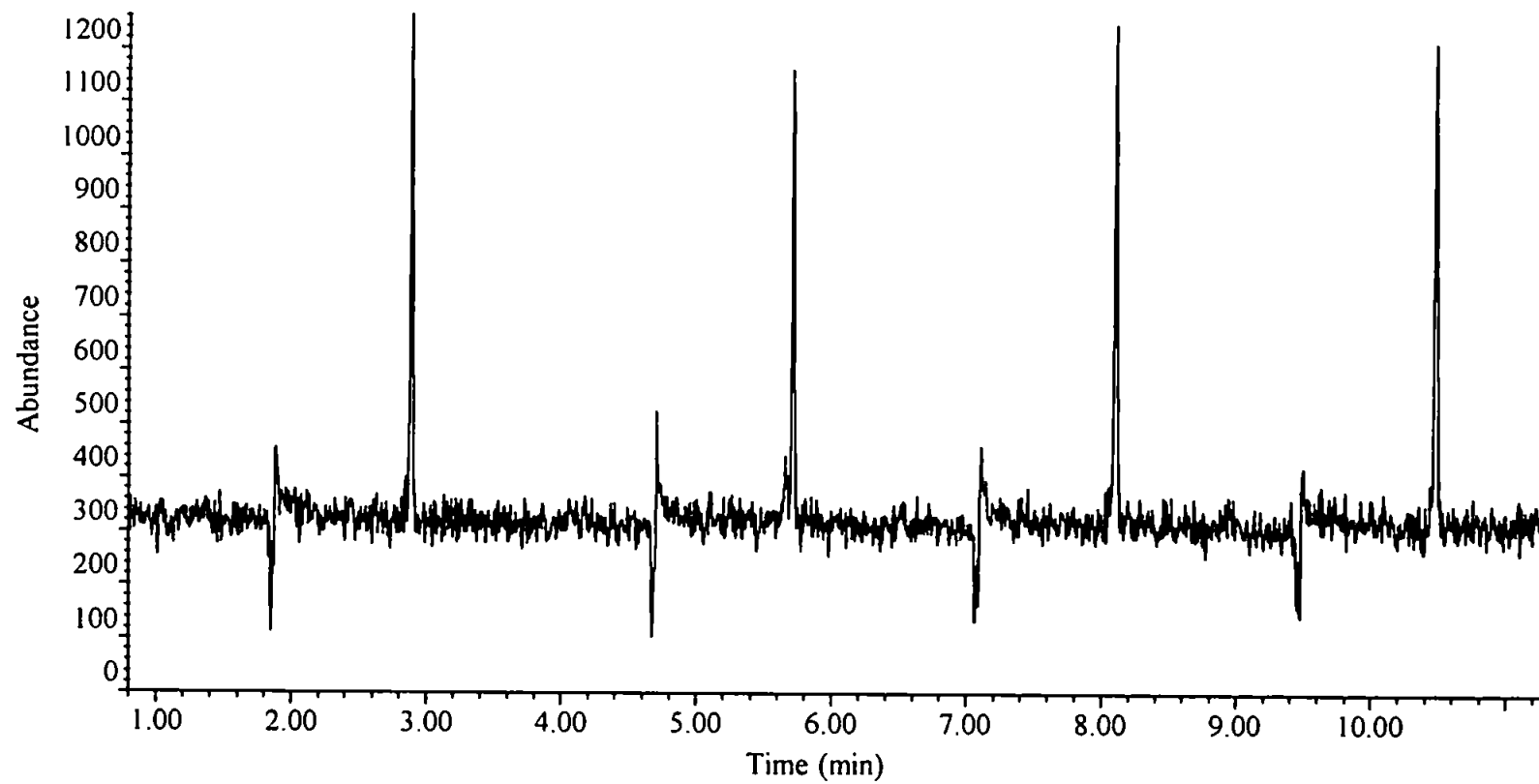
Figure 6.6   **Chromatogram of four consecutive injections of tetraethyllead (0.700 ng on-column).**

Table 6.3   Determination of tetraethyllead in standard reference fuel, NBS SRM 1637

II, by low pressure inductively coupled plasma source mass spectrometry.

Determined concentration as Tetraethyllead ($\mu g\ ml^{-1}$)	Determined concentration as lead ($\mu g\ ml^{-1}$)	Certified value for lead ($\mu g\ ml^{-1}$)
20.36 ± 1.59	13.06 ± 0.91	12.9 ± 0.07
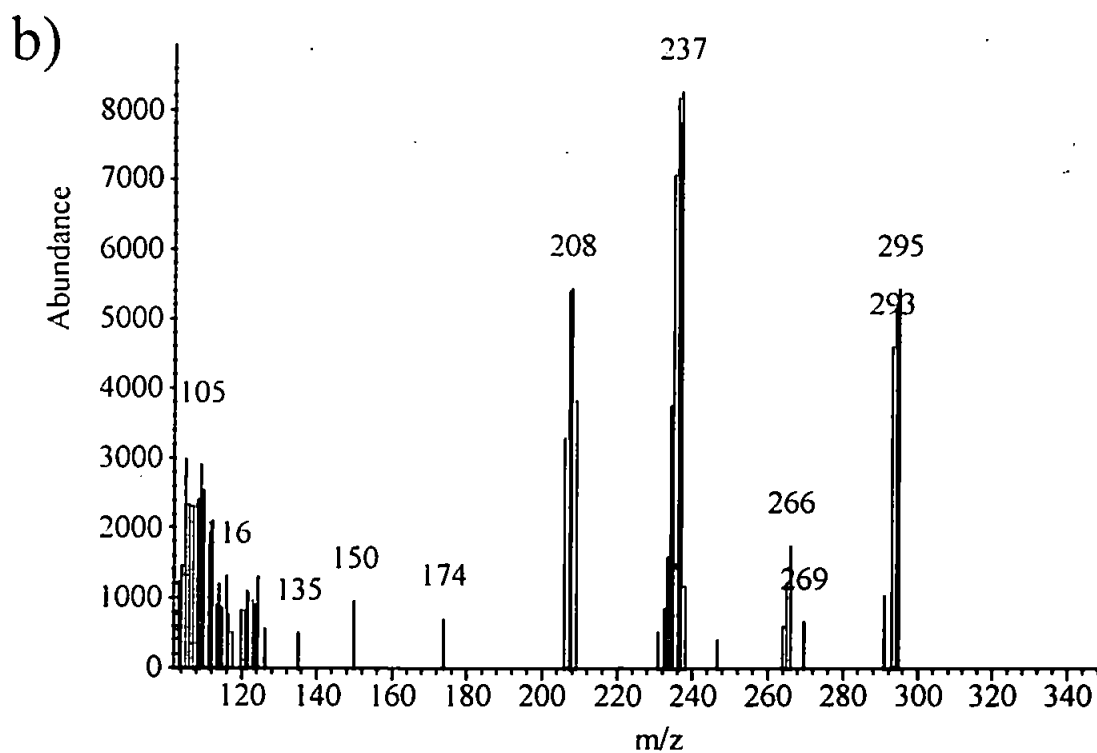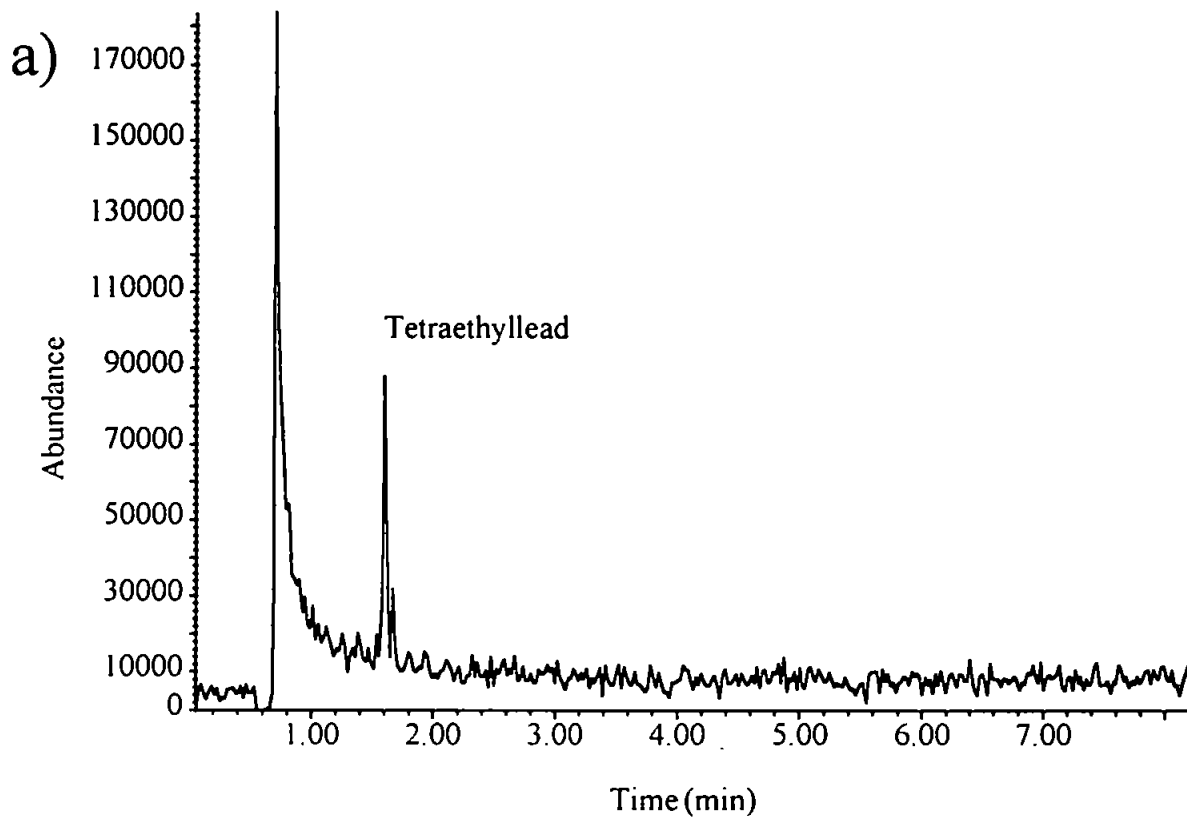
Figure 6.7   1 μl on-column injection of NBS SRM 1637 II: a) total ion chromatogram;

b) mass spectrum
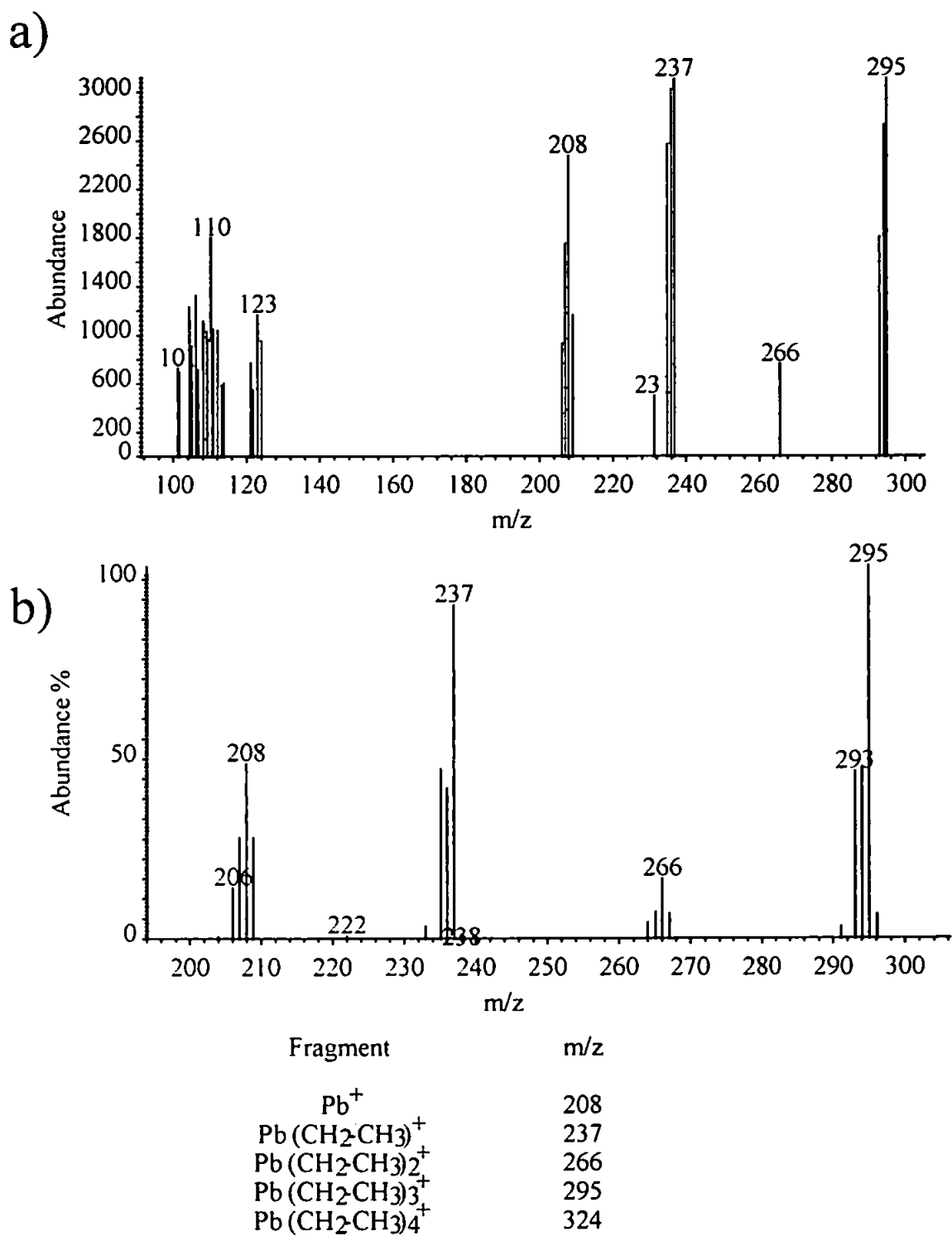
Figure 6.8 Mass spectrum for tetraethyllead obtained using:a) LP-ICP-MS;

b) EI source library.

Fragment	m/z
Pb^+	208
$Pb(CH_2-CH_3)^+$	237
$Pb(CH_2-CH_3)_2^+$	266
$Pb(CH_2-CH_3)_3^+$	295
$Pb(CH_2-CH_3)_4^+$	324

6.4 CONCLUSIONS

Low pressure ICP-MS was used for the qualitative and quantitative determination of tetraethyllead in fuel. The molecular mass spectrum for tetraethyllead was very similar to that of an EI source library spectrum. The LP-ICP could not be used to obtain atomic only spectra, as was previously observed for the halide species. It was possible to obtain atomic spectra for tetraethyllead with an alternative low pressure-plasma source (Chapter 2), however the prototype instrument used for this study did not have the differentially pumped vacuum chamber design of a conventional ICP-MS and could, therefore, not cope with the 1 l min^{-1} flow necessary. The ionisation of the halogens but, not lead, in the LP-ICP may be indicative of a penning ionisation process occurring in the helium-only plasma, and this is possibly the major ionisation process for helium low pressure plasma sources.

Chapter 7

CONCLUSIONS AND SUGGESTIONS FOR FUTURE WORK

CHAPTER 7-CONCLUSION AND SUGGESTIONS FOR FUTURE WORK

7.1 CONCLUSIONS

A low pressure inductively coupled plasma ionisation source, capable of providing both atomic and molecular information, has been designed, constructed, optimised and used for the determination of organo-halides and organo-metaillics. Detection limits were comparable to those obtained by EI-MS.

Initial studies using a commercially available ICP-MS indicated that it was possible to produce atomic and molecular fragments using a LP-ICP, sustained with both argon and helium, however, certain problems remained. One major disadvantage was the inability to form a stable, LP helium plasma at very low powers (6W). Also, the quadrupole mass filter had an upper mass transmission value of 255m/z, thereby preventing the detection of large molecular fragment ions.

A customised instrument was designed and constructed to solve the problems identified when using the commercially available ICP-MS. Optimisation of the skimming conditions was performed, and results suggested that a multiple shock structure existed behind the sampler orifice, and that a number of ionisation processes were occurring in the LP plasma. Power optimisation studies demonstrated the potential for operation of the low pressure plasma in a tuneable mode, with higher mass fragments breaking down to smaller fragment ions at higher plasma forward powers.

Molecular gases were added to the LP-ICP resulting in an increase in the intensity of the molecular ion signals. In particular the use of isobutane was found to be beneficial, mass spectra similar to EI and CI mass spectra being observed when this gas was added to the

plasma at different concentrations. Ionisation mechanisms such as proton transfer, normally associated with isobutane, and charge exchange were ruled out as the likely ionisation mechanisms in the LP-ICP, suggesting that the isobutane affected the population density of excited species and "thermalised" the plasma. When isobutane was removed entirely, total atomisation of organohalide compounds was observed.

Langmuir probe studies revealed the existence of a large plasma potential. This plasma potential indicated the presence of a secondary discharge in the expansion interface, a supposition confirmed by skimming distance studies. This discharge may play an important role in analyte ionisation. The low electron number densities observed in the LP-ICP confirmed the diffuse nature of the plasma. The electron temperature was quite high for such a diffuse plasma, but this can be attributed to the reduced pressure since the electrons will have a greater mean free path compared to a denser plasma.

The low gas kinetic temperature observed indicated that the low pressure plasma was not in local thermal equilibrium and that thermal atomisation of the organic compounds was unlikely to have occurred. The electron energy measured in the plasma was considerably less than that in an EI source and it was therefore thought unlikely to cause fragmentation of the molecules, hence, the only remaining explanation was charge transfer from excited plasma species such as helium metastables (Penning ions) and excited helium atoms.

The ion kinetic energies measured suggested the presence of a secondary discharge. No relationship between ion mass and ion kinetic energy was observed indicating the absence of an adiabatic expansion and suggesting the possible existence of several shock structures. Hence, it is possible that ionisation occurred in one of a number of shock wave structures.

Finally the LP-ICP-MS was used for the determination of tetraethyllead in reference fuel. The instrument provided both quantitative and qualitative analysis with the molecular mass spectra obtained providing conclusive proof of the presence of tetraethyllead.

Total fragmentation of the organolead compound was not achieved using the customised low pressure helium plasma, however, this was previously achieved using a 1 1 min^{-1} LP-ICP-MS modified from a commercial instrument.

7.2 FUTURE WORK

The instrument constructed in this work was a proto-type and was ideal for the initial investigation of a LP-ICP as a tuneable ionisation source. The instrument was constructed using old instrumentation and readily available technology. If such an instrument was to be commercialised, a compact benchtop design would be possible. The addition of an extra evacuated stage would enable the use of higher flow rate LP-ICPs. Due to the dense nature of the higher flow rate plasmas, a photon stop may need to be incorporated in the ion lens array. Alternatively the use of an ion-trap mass analyser may alleviate some of these problems, as they can operate at intermediate pressures.

A much more detailed assessment of the ionisation process occurring in the LP-ICP is an essential future study if LP-ICPs are to be used routinely. The role of Penning ionisation could be further assessed by the use of laser studies combined with population density measurement by atomic emission studies. The use of a laser tuned to the excitation wavelength of the helium metastable species will cause the metastables to excite and then return to the ground state. This would require a tuneable Dye laser operating in the vacuum ultra violet region of the electromagnetic spectrum. The role of the secondary discharge also needs to be assessed and this could be achieved by spatially mapping the discharge with

with a Langmuir probe placed inside the expansion interface, and by reduction of the local plasma potential using a shield torch or central tapped load coil.

The LP-ICP-MS needs to be assessed for the determination of a wide range of analytes with the analysis of more sample types. Also the evaluation of different chromatographic interfaces for LP-ICP-MS should be considered an essential future development, because gas chromatography has limitations in the type of analytes that can be placed on the column. The low thermal temperature and the fragile nature of the plasma deployed in this study may make liquid sample introduction difficult, however the use of thermospray or particle beam sample introduction may be possible.

REFERENCES

REFERENCES

1   Willard, H.H., Merritt, L.L., Dean, A.J., and Settle, A.F., *Instrumental Methods of Analysis*, 7th Ed. Wadsworth, California (1988), Chapter 16.

2   Melton, C.E., *Principles of Mass Spectrometry and Negative Ions*, Marcel Dekker, New York (1970).

3   Chapman, J.R., *Practical Organic Mass Spectrometry*, 2nd Ed. John Wiley & Sons, Chichester UK (1993).

4   Flesch, G.D., and Svec. H.J in, *International Review of Science (Mass Spectrometry) Physical Chemistry*, Series 2, Vol.5, Ed. by Buckingham, A.D., and Maccol, A., Butterworths & Co., London (1975).

5   Todd, J.F.J., and Lawson, G. in, *International Review of Science (Mass Spectrometry) Physical Chemistry*, Series 2, Vol.5, Ed. by Buckingham, A.D., and Maccol, A., Butterworths & Co., London (1975).

6   Davis, R. and Frearson, M., *Mass Spectrometry*, Analytical Chemistry by Open Learning (ACOL), John Wiley and Sons, Chichester UK (1987).

7   Karasek, F.W, and Clement,R.E., *Basic Gas Chromatography - Mass Spectrometry, Principles and Techniques*, Elsevier Science Publishing Company, New York (1988).

8   Skoog, D.A., and Leary,J. J., *Principles of Instrumental Analysis*, 4th Ed. Sanders College Publishing, New York (1992).

9   Munson, B., *Anal.Chem.*, 1977, **49**, (9), 772a.

10   Lattimer, R.P., and Schulten, H.R., *Anal.Chem.*, 1989, **61**, (21), 1201a.

11   Cotter, R.J., *Anal. Chem.*, 1988, **60**, (13), 781a.

12   Grant, E.R., and Cooks, R.G., *Science*, 1990, **250**, 61.

13   Lodding, A. in, *Inorganic Mass Spectrometry*, Chapter 4, Ed. by Adams, F., Gijbels, R., and Van Grieken, R., John Wiley and Sons, Chichester UK, (1988).

14   Busch, L.K., and Cooks, R.G., *Science*, 1982, **218**, 247.

15   Rinehart, K.L., *Science*, 1982, **218**, 254.

16   Fenn, J.B., Mann, M., Meng, C.K., Wong, S.F., and Whitehouse, C.M., *Science*, 1989, **246**, 64.

17   Gray, A.L., *Analyst*, 1975, **100**, 289.

18   Gray, A.L., *Anal. Chem.*, 1975, **47**, 600.

19   Gray, A.L., *Anal. Proc.*, 1994, **31**, 369.

20   Houk, R.S., Fassel, V.A., Flesch, G.D., Svec, H.J., Gray, A.L., and Taylor, C.E., *Anal. Chem.*, 1980, **52**, 2283.

21   Gray, A.L., *Spectrochimica. Acta*, 1985, **40B**, 1525.

22   Houk, R.S., *Anal. Chem.*, 1986, **58**, (1), 97a.

23   Montaser, A., and Van Howe, *CRC Critical Reviews in Analytical Chemistry*, 1987, **18**, 1, 45.

24   Hieftje, G.M., and Norman, L.A., *Int. Journ. Mass. Spectrom. Ion. Proc.*, 1992, **118/119**, 519.

25   Blades, M.W., *Appl. Spectrosc.*, 1994, **48**, (11), 12a.

26   Colodner, D., Salters, V., and Duckworth, D.C., *Anal. Chem.*, 1994, **66**, (21), 1079a.

27   Sheppard, B.S., and Caruso, J.A., *J. Anal. At. Spectrom.*, 1994, **9**, 145.

28   Horlick, G., *J. Anal. At. Spectrom.*, 1994, **9**, 593.

29   Broekaert, J.A.C., *Mikrochim. Acta*, 1995, **120**, 21.

30   Olesik, J.W., *Anal. Chem.*, 1996, **68**, 469a.

31   Jin, Q., Duan, Y., Olivares, J.A., *Spectrochim. Acta*, 1997, **52B**, 131.

32   Harrison, W.M., Barshick, C.M., Klingler, J.A., Ratliff, P.H., and Mei, Y., *Anal. Chem.*, 1990, **62**, (18), 943a.

33   Gray, A.L. in, *Inorganic Mass Spectrometry*, Chapter 6, Ed. by Adams, F., Gijbels, R., and Van Grieken, R., John Wiley and Sons, Chichester UK, (1988).

34   Montaser, A., and Golightly, D.W., *Inductively Coupled Plasmas in Analytical Atomic Spectrometry*, 2nd Ed., VCH Publishers Inc., New York, 1992

35   Evans, E.H., Giglio, J.J., Castillano, T.M., and Caruso, J.A., *Inductively Coupled and Microwave Induced Plasma Sources for Mass Spectrometry*, Royal Society of Chemistry, Cambridge, 1995.

36   Fisher, A.S., and Ebdon. L. in, *Advances in Atomic Spectroscopy, Vol. 3*, Chapter 1, Ed. by Sneddon, J., JAI Press Inc.(1997).

37   King, F.L., and Harrison, W.W., in *Glow Discharge Spectroscopies*, Ed. by Marcus, R.K., Plenum Press, New York, (1993).

38   Reed, T.B., *J. Appl. Phys.*, 1961, **32**, 821.

39   Reed, T.B., *J. Appl. Phys.*, 1961, **32**, 2534.

40   Reed, T.B., *Int. Sci. Tech.*, 1962, **6**, 42.

41   Greenfield, S., Jones, I.L.W., and Berry, C.T., *Analyst*, 1964, **89**, 713.

42   Smith, T.R., Bonner Denton, M., *Appl. Spectrosc.*, 1989, **43**, 1385.

43   Fannin, H.B., Seliskar, C.J., and Miller, D.C., *Appl. Spectrosc.* 1987, **42**, 621.

44   Houk, R.S., Svec, H.J., and Fassel, V.A., *Appl. Spectrosc.*, 1981, **35**, 380.

45   Crain, J.S., Smith, F.G., and Houk, R.S., *Spectrochim. Acta*, 1990, **45B**, 249.

46   Seliskar, C.J., Miller, D.C., and Fleitz, P.A., *Appl. Spectrosc.*, 1987, **41**, 658.

47   Blades, M.W., and Caughlin, B.L., *Spectrochim. Acta*, 1985, **40B**, 579.

48   Caughlin, B.L., and Blabes, M.W., *Spectrochim. Acta*, 1985, **40B**, 987.

49   Caughlin, B.L., Blades, M.W., *Spectrochim. Acta*, 1985, **40B**, 1539.

50   Evans, E.H., and Giglio, J.J., *J. Anal. At Spectrom.*, 1989, **4**, 299.

51   Liu, K., Kovacic, N., and Barnes, R.M., *Spectrochim. Acta*, 1990, **45B**, 145.

52   Yang, P., and Barnes, R.M., *Spectrochim. Acta*, 1989, **44B**, 1093.

53   Yang, P., and Barnes, R.M., *Spectrochim. Acta*, 1989, **44B**, 1081.

54   Yang, P., and Barnes, R.M., *Spectrochim. Acta*, 1990, **45B**, 157.

55   Yang, P., and Barnes, R.M., *Spectrochim. Acta*, 1990, **45B**, 167.

56   Barnes, R.M., Kovacic, N., and Meyer, G.A., *Spectrochim. Acta*, 1985, **40B**, 907.

57   Meyer, G.A., and Barnes, R.M., *Spectrochim. Acta*, 1985, **40B**, 893.

58   Kovacic, N., Meyer, G.A., Ke-Ling, L., and Barnes, R.M., *Spectrochim. Acta.*, 1985, **40B**, 903.

59   Ishii, I., Tan, H., Chan, S., and Montaser, A., *Spectrochim. Acta*, 1991, **46B**, 901.

60   Chan, S., Tan, H., and Montaser, A., *Appl. Spectrosc.*, 1989, **43**, 92.

61   Cai, M., Ishii, I., Clifford, R.H., and Montaser, A., *Spectrochim. Acta*, 1994, **49B**, 1081.

62   Chan, S., Van Hoven, R.L., and Montaser, A., *Anal. Chem.*, 1986, **58**, 2342.

63   Koppenaal, D.W., and Quinton, L.F., *J. Anal. At. Spectrom.*, 1988, **3**, 667.

64   Chan, S., and Montaser, A., *Spectrochim. Acta*, 1985, **40B**, 1467.

65   Chan, S., and Montaser, A., *Spectrochim. Acta*, 1987, **42B**, 591.

66   Tan, H., Chan, S.K., and Montaser. A., *Anal. Chem.*, 1988, **60**, 2542.

67   Nam, S.H., Masamba, W.R.L., and Montaser, A., *Spectrochim. Acta*, 1994, **49B**, 1325.

68   Zhang, H., Nam, S.H., Cai, M., and Montaser, A., *Appl. Spectrosc.*, 1996, **50**, 4, 427.

69   Evans, E.H., and Ebdon, L., *J. Anal. At. Spectrom.*, 1989, **4**, 299.

70   Evans, E.H., and Ebdon, L., *J. Anal. At. Spectrom.*, 1990, **5**, 425.

71   Montaser, A., Chan, S.K., and Koppenaal, D.W., *Anal. Chem.*, 1987, **59**, 1240.

72   Chambers, D.M., Carahan, J.W., Jin, Q., and Hieftje, G.M., *Spectrochim. Acta*, 1991, **46B**, 1745.

73   Heppner, R.A., *Anal.Chem.*, 1983, **55**, 2170.

74   Workman, J.M., Brown, P.G., Miller, D.C., Seliskar, C.J., and Caruso, J.A., *Appl. Spectrosc.*, 1986, **40**, 6, 857

75   Satzger, R.D., Fricke, F.L., Caruso, J.A., *J. Anal. At. Spectrom.*, 1988, **3**, 319.

76   Greenway, G.M., and Barnett, N.W., J. Anal. At. Spectrom., 1989, **4**, 783.

77   Suyani, H., Creed, J., Caruso, J., and Satzger, R.D., *J. Anal. At. Spectrom.*, 1989, **4**, 777.

78   Brill, J.H., Narayanan, B.A., and Mc Cormick, J.P., *Appl. Spectrosc.*, 1991, **45**, 1617.

79   Olson, L.K., and Caruso, J.A., *Spectrochim. Acta*, 1994, **49B**, 7.

80   Story,W.C., and Caruso, J.A., *J. Anal. At. Spectrom.*, 1993, **8**, 571.

81   Story, W.C., Olsen, L.K., Shen, W-L., Creed, J.T., and Caruso, J.A., *J. Anal. At. Spectrom.*, 1990, **5**, 467.

82   Creed, J.T., Davidson,T.M., Shen, W-L., and Caruso, J.A, *J. Anal. At. Spectrom.*, 1990, **5**, 109.

83   Olsen, L.K., Story, W.C., Creed, J.T., Shen, W-L., and Caruso, J.A, *J. Anal. At. Spectrom.*, 1990, **5**, 471.

84   Hooker, B., and DeZwaan, J., *Anal. Chem.*, 1989, **61**, 2207.

85   Poussel, E., Mermet, J.M., Derauz, D., and Beaugrand, C., *Anal. Chem.*, 1988, **60**, 923.

86   Lunzer, F., Garcia, R.P., Garcia, N.B., Sanz-Medel, A., *J. Anal. At. Spectrom.*, 1995, **10**, 311.

87   Shen, W.L., and Satzger, R.D., *Anal. Chem.*, 1991, **63**, 1960.

88   Marcus, R.K., in *Glow Discharge Spectroscopies*, Ed. by Marcus, R.K., Plenum Press, New York, 1993.

89   Schelles, W., Maes, K.J.R., De Gendt, S., and Van Grieken, R.E., *Anal. Chem.*, 1996, **68**,1136.

90   Marcus, R.K., *J. Anal. At. Spectrom.*, 1993, **8**, 935.

91   Shick, C.R., DePalma, P.A., and Marcus, R.K., *Anal. Chem.*, 1996, **68**, 1, 2113.

92   Olson, L.K., Belkin, M., and Caruso, J.A., *J. Anal. At. Spectrom.*, 1996, **11**, 491.

93   Lauritsen, F.R., Choudhury, T.K., Dejarme, L.E., and Cooks, R.G., *Anal. Chim. Acta*, 1992, **266**, 1.

94   Carazzato, D., and Bertrand, M.J., *J. Am. Soc. Mass. Spectrom*, 1994, **5**, 305.

95   McLuckey, S.A., Goeringer, D.E., Asano, K.G., Vaidyanathan, G., and Stephenson, J.L., *Rapid. Commun. Mass Spectrom.*, 1996, **10**, 287.

96   You, J., Depalma, P.A., and Marcus, R.K., *J. Anal. At. Spectrom.*, 1996, **11**, 483.

97   Zhao, J., Zhu., J., and Lubman, D.M., *Anal. Chem.*, 1992, **64**, 1426.

98   Fannin, H.B., and Seliskar, C.J., *Appl. Spectrosc.*, 1987, **41**, 1216.

99   Fleitz, P.A., and Seliskar, C.J., *Appl. Spectrosc.*, 1987, **41**, 4, 679.

100   Wolnik, K.A., Miller, D.C., Seliskar, C.J., and Fricke, F.L., *Appl. Spectrosc.*, 1985, **39**, 930.

101   Miller, D.C., Seliskar, C.J.,and Davidson, T.M., *Appl. Spectrosc.*, 1985, **39**, 13.

102   Seliskar, C.J., and Warner, D.K., *Appl. Spectrosc.*, 1985, **39**, 181.

103   Miller, D.C., Fannin, H.B., Fleitz, P.A., and Seliskar, C.J., *Appl. Spectrosc.* 1986, **40**, 611.

104   Smith, T.R., and Denton, M.B., *Spectrochim. Acta*, 1985, **40B**, 1227.

105   Evans, E.H., and Caruso, J.A., *J. Anal. At. Spectrom.*, 1993, **8**, 427.

106   Castillano, T.M., Giglio, J.J., Evans, E.H., and Caruso, J.A., *J. Anal. At. Spectrom.*, 1994, **9**, 1335.

107   Yan, X., Tanaka, T., and Kawaguchi, H., *Appl. Spectrosc.*, 1996, **50**, 182.

108   Yan, X., Tanaka, T., and Kawaguchi, H., *Spectrochim. Acta*, 1996, **51B** , 1345.

109   Castillano, T.M., Giglio, J.J., Evans, E.H., and Caruso, J.A., *J. Anal. At. Spectrom.*, 1997, **12**, 383.

110   Evans, E.H., Pretorius, W., Ebdon, L., and Rowland, S., *Anal. Chem.*, 1994, **66**, 3400.

111   Pretorius, W.G., PhD Thesis (University of Plymouth) 1994.

112   Faubert, D., Paul, G.J.C., Giroux, J., and Bertrand, M.J., *J. Mass Spectrom. Ion Processes.*, 1993, **124**, 69.

113   Kohler, M., and Schlunegger, U.P., *Rapid. Commun. Mass Spectrom.* 1993, **7**, 1113.

114   Kohler, M., and Schlunegger, U.P., *J. Mass Spectrom.*, 1995, **30**, 134.

115   Chong, N.S., and Houk, R.S., *Appl. Spectrosc.* 1987, **41**, 66.

116   Kim, A.W., Foulkes, M.E., Ebdon, L., Hill, S.J., Patience, R.L., Barwise, A.G., and Rowland, S.J., *J. Anal. At. Spectrom.*, 1992, **7**, 1147.

117   Kim, A., Hill, S., Ebdon, L., and Rowland, S., *J. High. Res. Chrom.*, 1992, **15**, 665.

118   Hill, S.J., Bloxham, M.J., and Worsfold, P.J., *J. Anal. At. Spectrom.*, 1993, **8**, 499.

119   Prange, A., and Jantzen, E., J. Anal. At. Spectrom. 1995, **10**, 105.

120   Uden, P.C., *J. Chromatogr. A*, 1995, **703**, 393.

121   Foulkes, M.E., PhD Thesis (Polytechnic South West) CNAA, 1989.

122 O'Hanlon, K.L., PhD Thesis (University of Plymouth) 1996.

123 Darke, S.A., Long, S.E., Pickford, C. J., and Tyson, J.F., *J. Anal. At. Spectrom.*, 1989, **4**, 715.

124 Campargue, R., *J. Chem. Phys.*, 1970, **52**, 1795.

125 Campargue, R., *J. Phys. Chem.*, 1984, **88**, 4466.

126 Olivares, J.A., and Houk, R.S., *Anal. Chem.*, 1985, **57**, 2674.

127 Niu, H., and Houk, R.S., *Spectrochim. Acta*, 1996, **51B**, 779.

128 Vaughan, M.A., Horlick, G., and Tan, S.H., *J. Anal. At. Spectrom.*, 1987, **2**, 765.

129 Vaughan, M.A., and Horlick, G., *Spectrochim. Acta*, 1990, **45B**, 1301.

130 Cleland, T.J., Bonchin-Cleland, S.L., Olson, L.K., Meeks, R.F., Caruso, J.A., *Spectrochim. Acta*, 1995, **50B**, 873.

131 Gillson, G.R., Douglas, D.J., Fulford, J.E., Halligan, K.W., and Tanner, S.D., *Anal. Chem.*, 1988, **60**, 1472.

132 Tanner, S.D., *Spectrochim. Acta*, 992, **47B**, 809.

133 Vijgen, L.J., and Kruit, P., *Nuclear Inst. Method In Physics Research.*, 1992, **B64**, 378.

134 Tanner, S.D., Douglas, D.J., and French, J.B., *Appl. Spectrosc.*, 1994, **48**, 1373.

135 Tanner, S.D., Cousins, L.M., and Douglas, D.J., *Appl. Spectrosc.*, 1994, **48**, 1367.

136 Burgoyne, T.W., Hieftje, G.M., and Hites, R.A., *Anal. Chem.*, 1997, **69**, 3, 485.

137 Barnett, D.A., and Horlick, G., *J. Anal. At. Spectrom.*, 1997, **12**, 497..

138 Douglas, D.J., and French, J.B., *J. Anal. At. Spectrom.*, 1988, **3**, 743.

139 Hoglund, A., and Rosengren, L.G., *Int, Journ. Mass. Spectom. Ion. Proc.*, 1984, **60**, 173.

140   Gray, A.L., *J. Anal. At. Spectrom.*, 1989, **4**, 371.

141   Luan, S., Ming, H., and Houk, R.S., *J. Anal. At. Spectrom.*, 1996, **11**, 247.

142   Klemperer, O., and Barnett, M.E., *Electron Optics*, Cambridge Monographs on Physics, Cambridge University Press. (1971).

143   Atkins, P.W., *Physical Chemistry*, 4th Ed, Oxford University Press, Oxford, UK. 1990.

144   *Handbook of Chemistry and Physics*, CRC Press, 65th Ed, Boca Raton, Florida, 1984-1985.

145   Hatch, F., and Munson, B., *Anal. Chem.*, 1977, **49**, 1, 169.

146   Polley, C.W., and Munson, B., *Anal. Chem.*, 1981, **53**, 308.

147   Smith, R.L., Serxner, D., and Hess, K.R., *Anal. Chem.*, 1989, **61**, 1103.

148   Serxner, D., Smith, R.L., and Hess, K.R., *Appl. Spectros.*, 1991, **45**, 10, 1656.

149   HP5970 Mass Selective Detector, Hardware manual, Publication No. 05970-90049, Hewlett Packard, California, USA.

150   Kornblum, G.R., and De Galan, L., *Spectrochim. Acta*, 1977, **32B**, 71.

151   Furuta, N., Nojiri, Y., and Fuwa, K., *Spectrochim. Acta*, 1985, **40B**, 423.

152   Zyrnicki, W., *Fresenius J. Anal. Chem.*, 1996, **355**, 461.

153   Pei-Qi, L., Pei-Zhong,G., Tie-Zheng, L., and Houk, R.S., *Spectrochim. Acta*, 1988, **43B**, 273.

154   Gray, A.L., Houk, R.S., and Williams, J., *J. Anal. Atom. Spectrom.*, 1987, **2**, 13.

155   Houk. R.S., Schoer, J.K., Crain, J.S., *J. Anal. Atom. Spectrom.*, 1987, **2**, 283.

156   Lim, H.B., and Houk, R.S., *Spectrochim. Acta*, 1990, **45B**, 453.

157   Lim, H.B., Houk, R.S., and Crain, J.S., *Spectrochim. Acta*, 1989, **44B**, 989.

158   Niu, H., Luan, S., Pang, H, Houk. R.S., *Spectrochim. Acta*, 1995, **50B**, 1247.

159   Niu, H., and Houk, R.S., *Spectrochim. Acta*, 1994, **49B**, 1283.

160 Niu, H.S., Hu, K., and Houk, R.S., *Spectrochim. Acta*, 1991, **46B**, 805.

161 Chambers, D.M., Poehlman, J., Yang. P., and Hieftje, G.M., *Spectrochim. Acta*, 1991, **46B**, 741.

162 Yan, X., Huang, B., Tanaka, T., and Kawaguchi, H., *J. Anal. At. Spectrom.*, 1997, **12**, 697.

163 Llewellyn-Jones, F., *The Glow Discharge and an Introduction to Plasma Physics*, John Wiley and Sons, New York, 1966.

164 Allen, J.E., in *Plasma Physics*, Ed. by Keen, B.E., Institute of Physics, London, 1974.

165 Howatson, A.M., *An Introduction to Gas Discharges*, Chapter 7, 2nd Ed., Pergamon Press, Oxford, 1976.

166 Bittencourt, J.A., *Fundamentals of Plasma Physics*, Chapter 11, Pergamon Press, Oxford, 1986.

167 Papoular, R., *Electrical Phenomena in Gases*, App 1, Iliffe Books Ltd, London, 1965.

168 Laframboise, J.G., University of Toronto, Institute of Aerospace Studies, Report No. 100, 1966.

169 Fang, D., and Marcus, R.K., *Spectrochim. Acta*, 1990, **45B**, 1053.

170 Bogaerts, A., Quentmeier, A., Jakubowski, N., and Gijbels, R., *Spectrochim. Act.*, 1995, **50B**, 1337.

171 Olivares, J.A., and Houk, R.S., *Appl.Spectorsc.*, 195, **39**, 1070.

172 Fulford, J.E., and Douglas, D.J., *Appl. Spectrosc.*, 1986, **40**, 971.

173 Chambers, D.M., and Hieftje, G.M., *Spectromchim. Acta*, 1991, **46B**, 761.

174 Tanner, S.D., *J. Anal. Atom. Spectrom.*, 1993, **8**, 891.

175 Lobinski, R., *Analyst*, 1995, **120**, 615.

176   Adams, F.C., *LC-GC Int.*, 1994, **7**, 694.

177   Kim, A.W., PhD Thesis (University of Plymouth), 1993.

APPENDIX

Papers Published

Feasibility Study of Low Pressure Inductively Coupled Plasma Mass Spectrometry for Qualitative and Quantitative Speciation

GAVIN O'CONNOR, LES EBDON AND E. HYWEL EVANS*

Department of Environmental Sciences, University of Plymouth, Drake Circus, Plymouth, Devon, UK PL4 8AA

HONG DING, LISA K. OLSON AND JOSEPH A. CARUSO

Department of Chemistry, University of Cincinnati, Cincinnati, OH 45221-0172, USA

Low-pressure ICPs (LP–ICPs) formed with helium have been utilized as ion sources for MS. In the first part of the paper a description is given of a plasma operated at 90 W forward power, used to ionize organotin and organolead compounds introduced by GC, with detection limits of 11, 2 and 14 pg obtained for tetraethyltin (TEtSn), tetrabutyltin (TBuSn) and tetraethyllead (TEtPb), respectively. The same plasma operated at 45 W forward power yielded fragment ions of TEtSn and TBuSn. In the second part, a customized mass spectrometer for use with an LP–ICP is described. The optimum power for the generation of fragment ions of perfluorotributylamine (PFTBA) was found to lie between 5 and 8 W. Two optima for skimming distance were observed, at 6 and 8 mm downstream of the sampler orifice. Mean ion kinetic energies for fragment ions of PFTBA at 69,219 and 502 m/z were 1.2, 1.7, and 2.1 eV, respectively, at 6 W forward power, but increased when the power was increased to 8 W. Molecular and other fragment ions were observed for chloro-, iodo- and dibromobenzenes introduced using GC.

Keywords: *Low-pressure inductively coupled plasma; helium plasma; mass spectrometry; element-selective detection; molecular ion*

The requirement for information about the chemical composition and structure of organic compounds has led to the development of numerous instrumental techniques. For example, the elemental composition of organometals can be determined by ICP-MS, while structures can be elucidated by techniques such as electron impact MS (EI-MS) and nuclear magnetic resonance (NMR) spectrometry. Additionally, an extra degree of specificity can be afforded by coupling separation techniques such as LC or GC to the above spectrometric instruments.

Mass spectrometer ion sources essentially fall into two categories, *i.e.*, those which create molecular species and fragment ions, such as conventional electron impact (EI), chemical ionization (CI) and fast atom bombardment (FAB), and those which create atomic species, such as ICPs and MIPs. Coupled with suitable chromatographic inlets these have led to the development of two of the major instrument classes found in virtually all modern analytical laboratories. However, no existing mass spectrometer ion source allows routine monitoring of both atomic and molecular species, particularly in a tuneable mode.

For trace metal speciation, element-selective detectors, coupled with chromatography of one form or another, have been used successfully to quantify organometallic compounds

at sub-pg levels.[1] However, qualitative identification of the compounds has relied on comparison of chromatographic retention times, and it has proved impossible to identify unknown peaks without the use of a complementary technique. This effectively limits the analysis to the determination of known compounds.

A major advantage of element-selective detection is the ability to calibrate for an unknown compound with a known compound containing at least one element in common. This is possible because the compounds are completely broken down to their constituent atoms, and then ionized and/or excited to facilitate either optical or mass spectrometric detection of monatomic ions. Hence, the signal intensity does not depend on the nature of the compound, but only on the nature of the element chosen for detection. If it were possible to operate a single instrument as an element-selective detector and a qualitative analyser, this would allow compounds to be identified qualitatively in one mode of operation and determined quantitatively in another, and would provide a powerful technique for the determination of a wide range of compounds, both known and unknown.

MIPs, operated under reduced pressure, have previously been investigated as possible sources for fragment ions of organic compounds.[2–4] However, these experiments were generally performed by introducing the pure compound, or headspace vapour, so were not representative of analysis at trace levels.

Atmospheric pressure ionization (API) sources have also been developed utilizing an MIP[5] or GD.[6] The latter workers noted that the predominant ions produced using the API source were the molecular (M⁺) and (M+1)⁺ ions, while the same GD source used under reduced pressure produced molecular ions accompanied by fragmentation. However, these workers used continuous sample introduction, and no work was performed with transient signals.

Recently, Evans and co-workers have developed a low-pressure ICP (LP–ICP) as an ion source for MS,[7–9] which is capable of providing information about both the elemental composition and molecular structure of the analyte. In particular, Evans *et al.*[9] have operated a low-pressure helium ICP at powers of between 4 and 40 W and 1 mbar (1 bar = 10^5 Pa) pressure to produce molecular ions and fragmentation spectra similar to an EI source for organometallic and halogenated species introduced by GC. On increasing the power and pressure the degree of fragmentation was increased until complete fragmentation, and hence element-selective detection, was achieved at a power of 150 W and pressure of 10 mbar, with detection limits in the 10–100 pg range for a variety of organohalogen and organometallic compounds. Clearly, this demonstrates the potential of the technique as a dual mode detector.

---

* To whom correspondence should be addressed.

UTILIZATION OF A COMMERCIAL ICP-MS INSTRUMENT

Experimental

Instrumentation

The ICP-MS instrument used was a VG PlasmaQuad I (VG Elemental, Winsford, Cheshire, UK). The original torch-box was designed for an atmospheric pressure argon ICP, so it did not have a sufficient tuning range to impedance match low pressure plasmas. Hence, the tuning range was extended by increasing the vacuum capacitance approximately four-fold, thereby reducing the high reflected power to zero for helium LP–ICP operation at 100 W forward power.

The low-pressure torch was a quartz tube 145 mm long, with 6 mm o.d. and 4 mm i.d. One end of the torch was connected to a GC interface with an Ultra-Torr fitting and the other end was connected to a modified aluminium sampler (Fig. 1). The sampler–skimmer spacing was reduced by approximately 2 mm using spacers behind the skimmer plate. Additional pumping at the expansion stage was provided by a 1500 l min^{-1} E1M-80 rotary vacuum pump (Edwards High Vacuum, Crawley, Sussex, UK). The pressure achieved with this interface in the absence of any helium flow was 7.0×10^{-2} mbar, and 4.4×10^{-1} mbar with a helium flow of 562 cm^3 min^{-1}. The gas chromatograph was a Hewlett-Packard Model 5700A. The capillary column (40 m × 0.32 mm i.d.) had an SE 54 non-polar stationary phase (J&W Scientific, Austin, TX, USA). The transfer line from the GC outlet to the interface T was a 1/8 in o.d. copper tube through which a 0.32 mm i.d. deactivated fused silica capillary column was inserted to transfer the GC eluent. The transfer line was heated with a heating tape powered with a variable transformer (Fisher Scientific, Pittsburgh, PA, USA) and the helium plasma gas line was heated to the same temperature as the GC transfer line using the same type of heating device. The heated transfer and gas lines were necessary for complete and reproducible transfer of GC analytes and to minimize any temperature disturbance at the mixing T. A four-way valve (Valco, Anspec, Ann Arbor, MI, USA) was employed for venting in some of the experiments. Two mass-flow controllers capable of flows of up to 3000 and 25 cm^3 min^{-1} (Tylan General, Torrance, CA, USA), respectively, were utilized to regulate the plasma gas and GC make-up gas flows. EI-MS spectra of the organotin compounds were provided by Jim Carlson (Department of Chemistry, University of Cincinnati) from a computer data base, or obtained experimentally using a GC–MS instrument (6890 Series, Hewlett-Packard, Palo Alto, CA, USA).

Reagents

Tetraethyltin (TEtSn), tetrabutyltin (TBuSn) and tetraethyllead (TEtPb) compounds (Aldrich, Milwaukee, WI, USA) were used to prepare standard solutions, and a Lead in Fuel SRM was used for analysis (SRM 2715, NIST, Gaithersburg, MD, USA). Methanol and hexane (Fisher Scientific, Fair Lawn, NJ, USA) were used for solution preparation for the tin and lead compounds, respectively. Stock solutions (1000 µg g^{-1}) were prepared from the alkylmetal compounds as m/m concentration of the metal moiety. Fresh analytical solutions were prepared daily from these stock solutions.

Results and Discussion

Optimization of Operating Conditions

Operating conditions for the GC instrument were similar to those used in previous studies. Briefly, the initial oven temperature was held at 80 °C for 2 min, then increased to 290 °C at a rate of 32 °C min^{-1}. However, the temperature of the GC injection port proved to be important for the quantitative recovery of TBuSn. As shown in Fig. 2 the signal-to-noise ratio (S/N) increased substantially with increasing injection port temperature before starting to plateau at 400 °C.

The position of the capillary termination just behind the load coil of the ICP had to be adjusted carefully to obtain good S/Ns. As shown in Fig. 3, there was an optimum distance between the capillary outlet and the load coil. Shortening the length of the torch by 10 mm resulted in a 62–180% increase in S/N [Fig. 3(d)]; however, shortening the quartz tubing any further [Fig. 3(e)] resulted in unstable signals, possibly owing

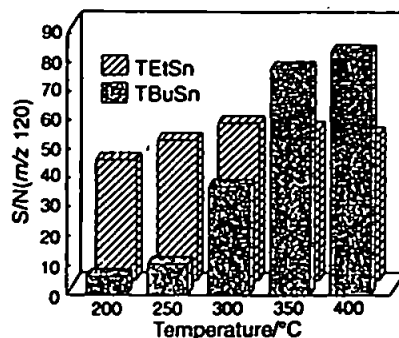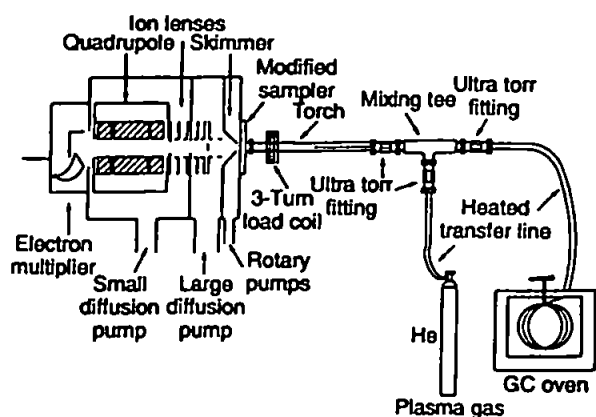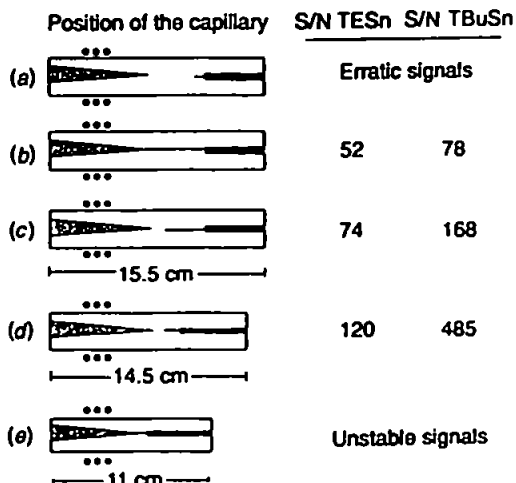Fig. 2 Effect of GC injection port temperature on S/Ns for TEtSn (▨) and TBT (□)

Fig. 3 Effect of the position of the GC capillary and length of the LP–ICP torch on S/Ns for TBuSn and TEtSn

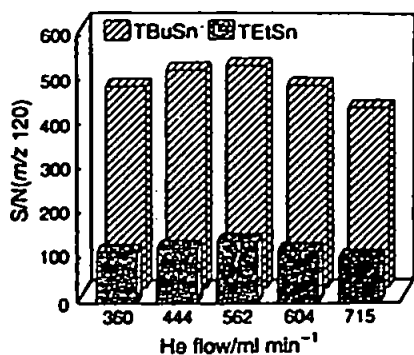Fig. 1 Modifications to an atmospheric ICP-MS instrument for use with an LP–ICP source

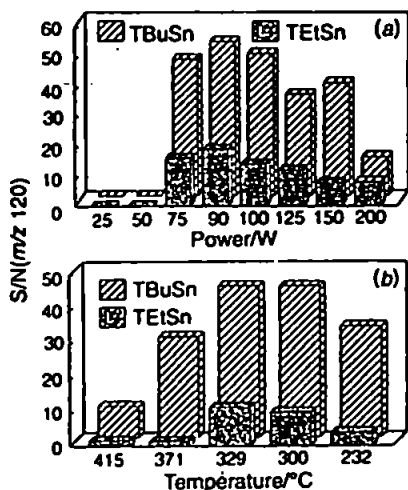Fig. 4 Effect of He outer plasma gas flow on S/Ns for TEtSn (▨) and TBuSn (▩)

Fig. 5 Effect of (a) forward power and (b) transfer line temperature on S/Ns for TEtSn (▨) and TBuSn (□)

to interference between the metal sheath of the capillary and the load coil.

For total metal determination, the forward power, helium plasma gas flow and GC transfer line temperature were optimized to yield the best S/Ns for m/z 120. The helium plasma gas flow did not affect the S/N greatly over a range of 285–652 cm³ min⁻¹ (Fig. 4), but the influence of forward power and transfer line temperature were more significant (Fig. 5). The optimal ranges of forward power and transfer line temperature required for good S/Ns were 75–90 W and 300–390 °C, respectively. Optimal operating conditions for the low-pressure plasma are listed in Table 1.

Good S/Ns were observed for 100 pg injections of TEtSn and TBuSn (Fig. 6), although the TEtSn peak was broader than the TBuSn peak because it was affected by the solvent front. A calibration was successfully performed, with at least three orders of magnitude linear dynamic range, less than 5% RSD for both compounds, and detection limits of 19 and 11 pg for TEtSn and TBuSn, respectively. Figures of merit are summarized in Table 2. Peaks were also observed at m/z 135

Table 1 Operating conditions for the low-pressure inductively coupled plasma

Forward power/W	90
Reflected power/W	2
He outer plasma gas flow/cm³ min⁻¹	562
Expansion stage pressure/mbar*	4.4×10^{-1}
Transfer line temperature/°C	325

* 1 bar = 10^{-5} Pa.
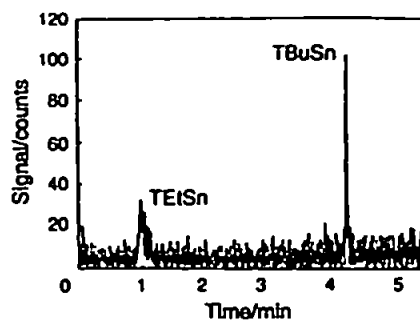
Fig. 6 Separation of 100 pg each of TEtSn and TBuSn by GC-LP-ICP-MS with element-selective detection at m/z 120 and without solvent venting

and 150 for both TEtSn and TBuSn (Fig. 7). These were thought to be due to Sn–CH₃ at m/z 135 and Sn–(CH₃)₂ at m/z 150, although peak intensities were low, and high concentrations of the analyte compounds (20 and 50 ng, respectively) had to be used. The molecular ion for TEtSn at m/z 236 was not observed and that for TBuSn at m/z 348 was beyond the scanning range of the mass spectrometer.

Solvent venting was performed with a Valco four-way valve in order to improve the quality of GC separation by removing the solvent. The gas chromatograph was operated under atmospheric pressure for the first minute, then the column outlet was connected to the low-pressure plasma by switching the valve. A helium GC make-up gas at a flow of 5 cm³ min⁻¹ was used to compensate for the difference in the helium flow in the plasma when the chromatograph was operated at atmospheric pressure. Solvent venting improved the detection limits from 19 and 11, to 7 and 2 pg, for TEtSn and TBuSn, respectively (Table 2). The same operating conditions were used for the determination of TEtPb, for which figures of merit are also given in Table 2.

Analysis of SRMs

The chromatogram obtained for the determination of TEtPb in the NIST SRM 2715 Lead in Fuel is shown in Fig. 8. The SRM was diluted two-fold with hexane before analysis. The lead concentration was found to be 838 ± 2 µg g⁻¹ of Pb in the form of TEtPb compared with the certified value which is 784 ± 4 µg g⁻¹ of Pb in the form of TEtPb. The value found was outside the confidence limits of the certified value, exhibiting positive bias. The reason for this is not known, although

Fig. 7 Single-ion monitoring at (a) m/z 135, 20 ng injection and (b) m/z 150, 50 ng injection, for fragment ions of TEtSn and TBuSn

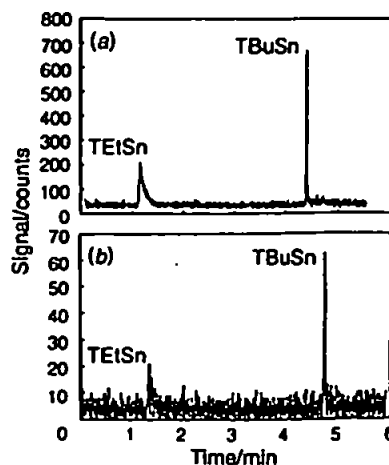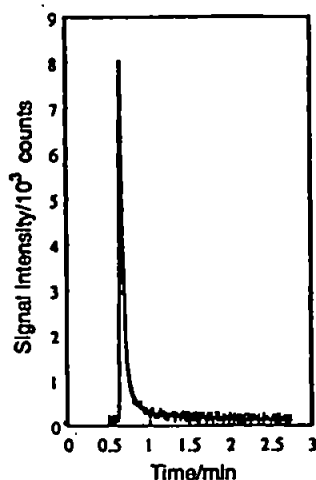| Parameter	TEtSn		TBuSn		TEtPb	
	Venting	Without venting	Venting	Without venting	Venting	Without venting
Linear dynamic range	10^3	10^3	10^3	10^3	10^2	10^2
r^2[*]	0.9999	0.9997	0.9962	0.9999	0.9997	0.9976
Slope of log–log plot	1.013	0.9986	0.9321	0.9983	0.9842	0.9001
RSD (%)	4.7	1.2	4.0	3.1	5	7.1
Detection limit/pg	19	11	7	2	6	14

[*] r^2 = regression coefficients.

Fig. 8 Chromatogram for the analysis of NIST SRM 2715 Lead in Fuel, by GC–LP–ICP-MS, using element-selective detection at m/z 208

Fig. 10 Effect of forward power on signal intensity for fragment ions at: (a) m/z 150 and (b) m/z 235

the TEtPb standard could have degraded somewhat given the lability of this organometallic species.

Fragmentation studies

Mass spectra of TEtSn and TBuSn were also obtained at a forward power of 45 W instead of the usual 90 W. The signal intensity at m/z 135 was greatest at a forward power of 75 W for both TEtSn and TBuSn (Fig. 9). However, higher mass fragments such as those at m/z 150 and 235 were favoured at lower forward powers ($\approx$45 W), as shown in Fig. 10 (a) and (b). The most predominant fragments were those of lower mass, such as elemental tin and monomethyltin. The spectra of TEtSn and TBuSn were similar, as is shown in Fig. 11. This was consistent with the observation of Heppner,[2] suggesting that the compounds were fully ionized in the plasma, and the fragments are recombinants of the ions rather than fragments from the original molecules. Hence, fragmentation did not occur in an analogous manner to an EI or CI source under these operating conditions.

At higher analyte concentrations, more high mass fragments

Fig. 11 Mass spectra obtained by GC–LP–ICP-MS for 20 ng each of TEtSn and TBuSn, showing the most probable assignments of the fragment ions

(i.e., m/z 170 and 200) were observed (Fig. 12). Greater amounts of analyte may require more energy for ionization, hence fragmentation was incomplete under these conditions, and these ions could reflect the structure of the original compound more accurately. EI spectra are shown in Figs. 13 and 14, and compared with the spectra obtained with the LP–ICP it is obvious that the plasma conditions were still not 'soft' enough to produce similar fragmentation patterns to EI spectra. In short, the forward power and partial pressure of analyte influences the degree of fragmentation, and even lower power and pressure could favour the formation of molecular and fragment ions rather than recombinants. Recently, an LP–ICP
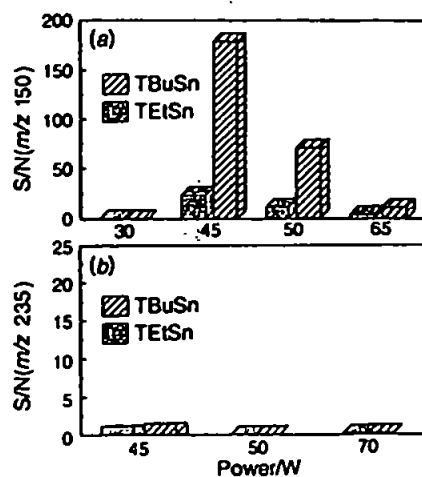

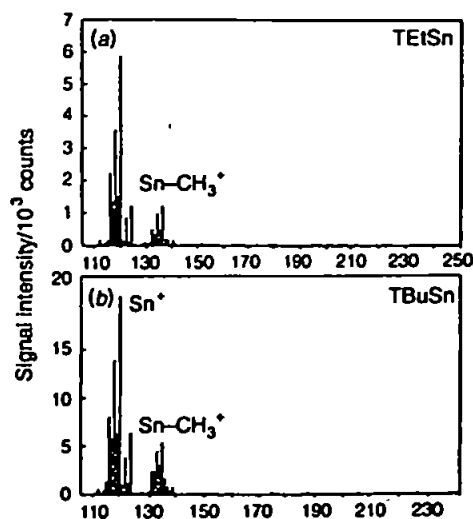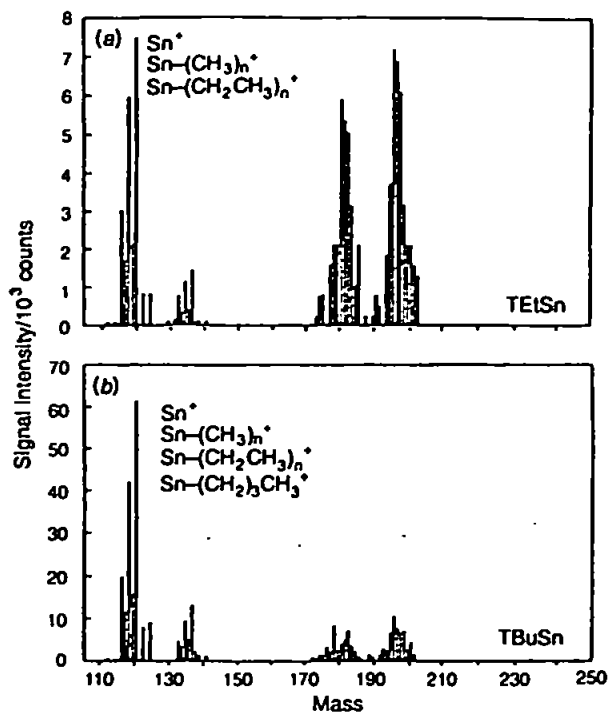Fig. 9 Effect of forward power on signal intensity for fragment ions at m/z 135

Fig. 12 Mass spectra obtained by GC–LP–ICP-MS for 500 ng each of TEtSn and TBuSn, showing the most probable assignments of the fragment ions

sustained at 5 W using only the GC helium flow as the plasma has been developed,[9] and the results suggest that lower power and pressure do indeed favour the formation of molecular ions. The instrumentation has now been developed further and results are reported in the next part of this paper.

Conclusions

Elemental quantitation, and some limited fragmentation, has been achieved with a single instrumental configuration. Optimization of the ion sampling and skimming process and the power between 1 and 15 W, and the utilization of a mass spectrometer with a greater mass range, is required. These aspects have been addressed in the next part of this paper, which describes the development of a customized LP–ICP-MS instrument.

UTILIZATION OF A CUSTOMIZED LP–ICP-MS INSTRUMENT

To date, only commercially available ICP-MS instruments have been modified and used as low-pressure plasma mass spectrometers. However, a number of disadvantages are inherent in this and have been addressed, as detailed below.

Generation of an LP–ICP

Commercial ICP-MS instruments were originally designed to form argon plasmas at gas flow rates of between 15 and 17 l min^{-1} and forward powers of between 1300 and 1500 W. Most commercial instrument manufacturers use a 1.5 kW rf generator with a matching network designed to couple rf power into an atmospheric argon plasma. With such a generator it is impossible to form a stable low-pressure helium plasma at low power, and the matching network is inappropriate for low-pressure plasmas in almost all gases. Hence, a 1.5 kW, 27.12 MHz rf generator was modified to give a stable output between 1 and 300 W, and a new rf matching network

was purchased (RF Applications, Eastbourne, East Sussex, UK) to enable coupling of rf power from the modified generator into the low-pressure plasma source.

The LP–ICP torch consisted of a 140 mm long quartz tube of ½ in o.d., with a ¼ in o.d. side-arm through which the plasma gas could be introduced. The low-pressure sampling cone was machined from aluminium (Machine Shop, University of Plymouth) and had a 2 mm orifice and an Ultra-Torr fitting for a ⅛ in pipe, so it was possible to form a vacuum seal between the low-pressure torch and sampler. The low-pressure torch was interfaced at the rear end with a gas chromatograph (PU 4550, Pye Unicam, Cambridge, UK) fitted with an on-column injector, by way of a heated transfer line held at a temperature of 250 °C. The GC capillary extended through the transfer line and into the torch, the vacuum seal being made using a combination of Ultra-Torr and Swagelock fittings with graphite ferrules. This configuration has been described previously in more detail.[9]

Customization of the Mass Spectrometer

Another disadvantage associated with using a commercial ICP-MS instrument is that it is designed for elemental analysis, so the quadrupole mass range only scans up to 255 m/z. This would be a great disadvantage for the determination of organometallic or other high relative molecular mass compounds because the molecular ion peak would appear above m/z 255. In order to overcome these problems a dedicated instrument was constructed by conversion of a Hewlett-Packard Mass Selective Detector (HP-MSD) for use with an LP–ICP ion source. The HP-MSD is ideal for such an application because it is a compact, bench-top instrument of proven capability, with a mass range of between 10 and 800 m/z. However, it was necessary to make several major modifications to the instrument in order to couple the LP–ICP and extract and focus ions from this source. These modifications are described below.

Ion sampling interface

The theory underlying the design of ion-sampling interfaces for plasma MS has been developed and discussed in length by other workers,[10–14] so it will not be repeated here.

The Hewlett-Packard 5970a MSD is normally operated as a GC–EI-MS, so it required modification to enable it to accept ions produced by an external ion source. Hence, a new ion-sampling interface was constructed using established theory as a guide.

The position of the first Mach disc down stream from the sampler orifice is expressed as[11]

$$X_M = 0.67 D_0 \left(\frac{P_0}{P_1} \right)^{1/2} \quad (1)$$

where X_M is the position of the Mach disc downstream of the sampler orifice, P_1 is the pressure in the expansion stage, P_0 is the pressure in the source and D_0 is the diameter of the sampler orifice. In order for a representative sample to be obtained from the plasma the skimmer orifice must be placed upstream of the first Mach disc. Initial studies[9] suggested that the Mach disc would occur at about 3.6 mm behind the sampling orifice when argon was used as the plasma gas at a flow of 1000 cm^3 min^{-1}. Hoglund and Rosengren[13] stated that the flow conditions appropriate to eqn. (1) prevail when the pressure ratio across the sampler orifice is greater than two, or analytically for an ideal gas when:

$$\frac{P_0}{P_1} \geqslant \left[\frac{\gamma+1}{2} \right]^{n/n-1} \quad (2)$$

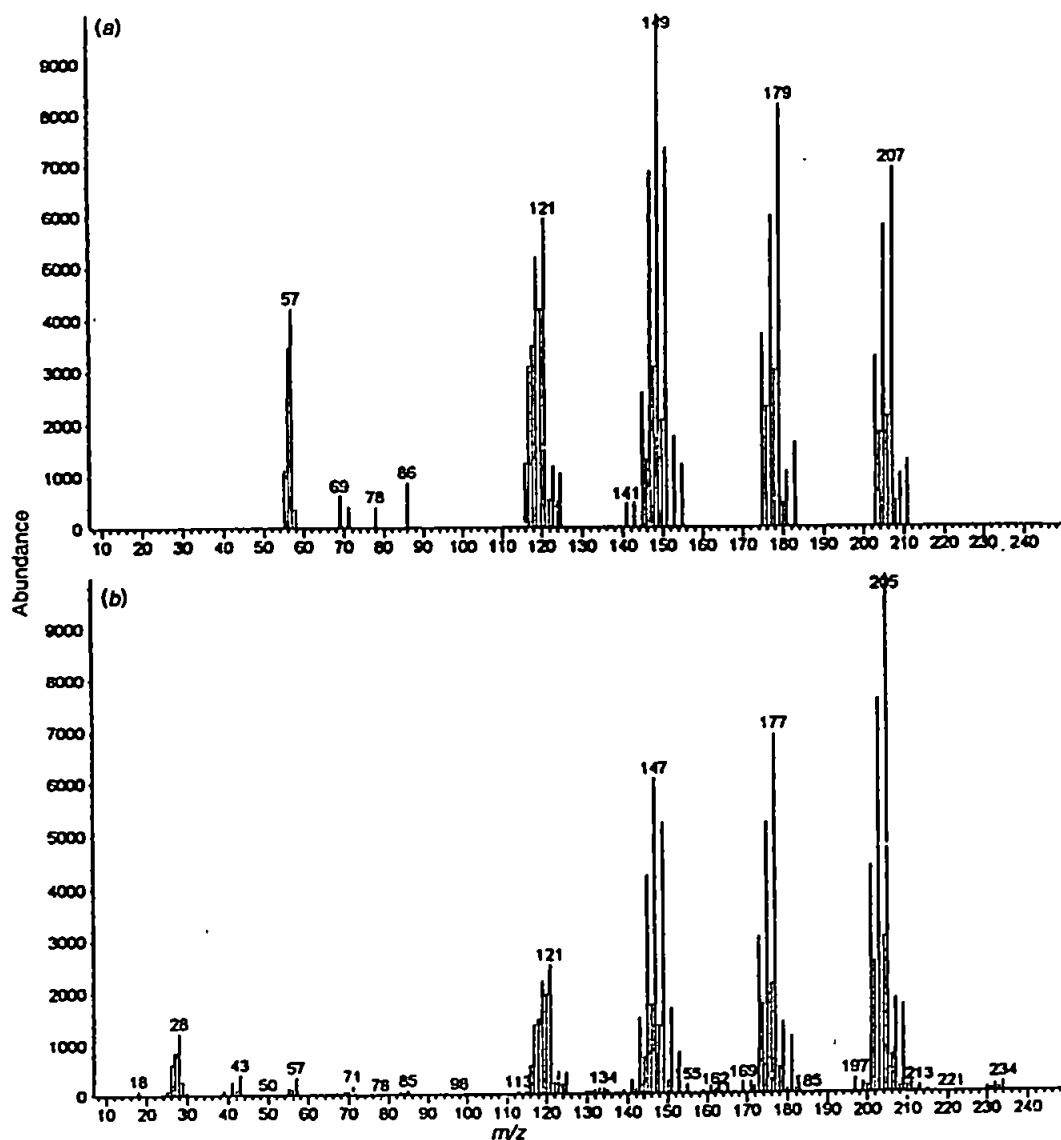where γ is the ratio of heat capacities at constant pressure and

Fig. 13   EI spectra of TEtSn obtained: (a) experimentally by GC–MS; and (b) from a computer library

volume. However, studies by Gray[15] and Luan et al.[16] indicated that subsidiary barrel shocks and Mach discs form downstream of the primary Mach disc when $P_0/P_1 < 100$ for an argon ICP. Because the pressure in the torch and the expansion region can change fairly considerably when different plasma gases are used (e.g., in the present study a plasma formed with helium at a flow rate of 3 cm³ min⁻¹ was investigated) the skimmer, which was a conventional nickel skimmer for a VG PlasmaQuad II with a 0.7 mm orifice, was mounted on a copper plate that could be moved back and forth by adding or removing copper spacing washers. Hence, the sampler–skimmer spacing could be optimized empirically.

The vacuum in the expansion stage was maintained using two rotary pumps (Leybold D16B). The downstream end of the expansion stage was machined with a 40 mm KF flange which was connected to a gate valve using a viton O-ring and a customized brace. The gate valve was then connected to the quadrupole vacuum housing, which had a 40 mm KF flange brazed onto it, using conventional vacuum fittings.

Ion optical array

Once the gas and ions have entered the skimmer it is necessary to collect and focus the ions into the quadrupole mass analyser.

The ion-focusing lenses are crucial for the overall sensitivity of the instrument, because incorrect focusing can lead to the ion beam being scattered or accelerated to such an extent that the residence time in the quadrupole mass analyser is insufficient for effective mass analysis.

The design of the ion optical lens system was aided by the use of a computer simulation program (SimIon, version 4.0, Argonne National Laboratory, IL, USA). However, this model does not account for field fringing effects and the effects of space charge in the ion beam. In order to compensate for such effects on the ion beam the entrance angle of the ions into the electrostatic array was varied and the model tested for a series of ions of different mass, with differing ion kinetic energies. The ion trajectories for ions entering the optimized ion optics at ± 20° off-axis are shown in Fig. 15. Hence, it was possible to design an ion optical array which consisted of two extraction lenses behind the skimmer and three ion focusing lenses just prior to the quadrupole. This lens system had no photon stop because the detector in the HP5970a MSD is offset and so was shaded from any photon noise. Also, the low-pressure plasma studied in the present work gave rise to very little photon noise.

To accommodate these ion-focusing lenses, some electrical and mechanical modifications were made to the MSD. First,
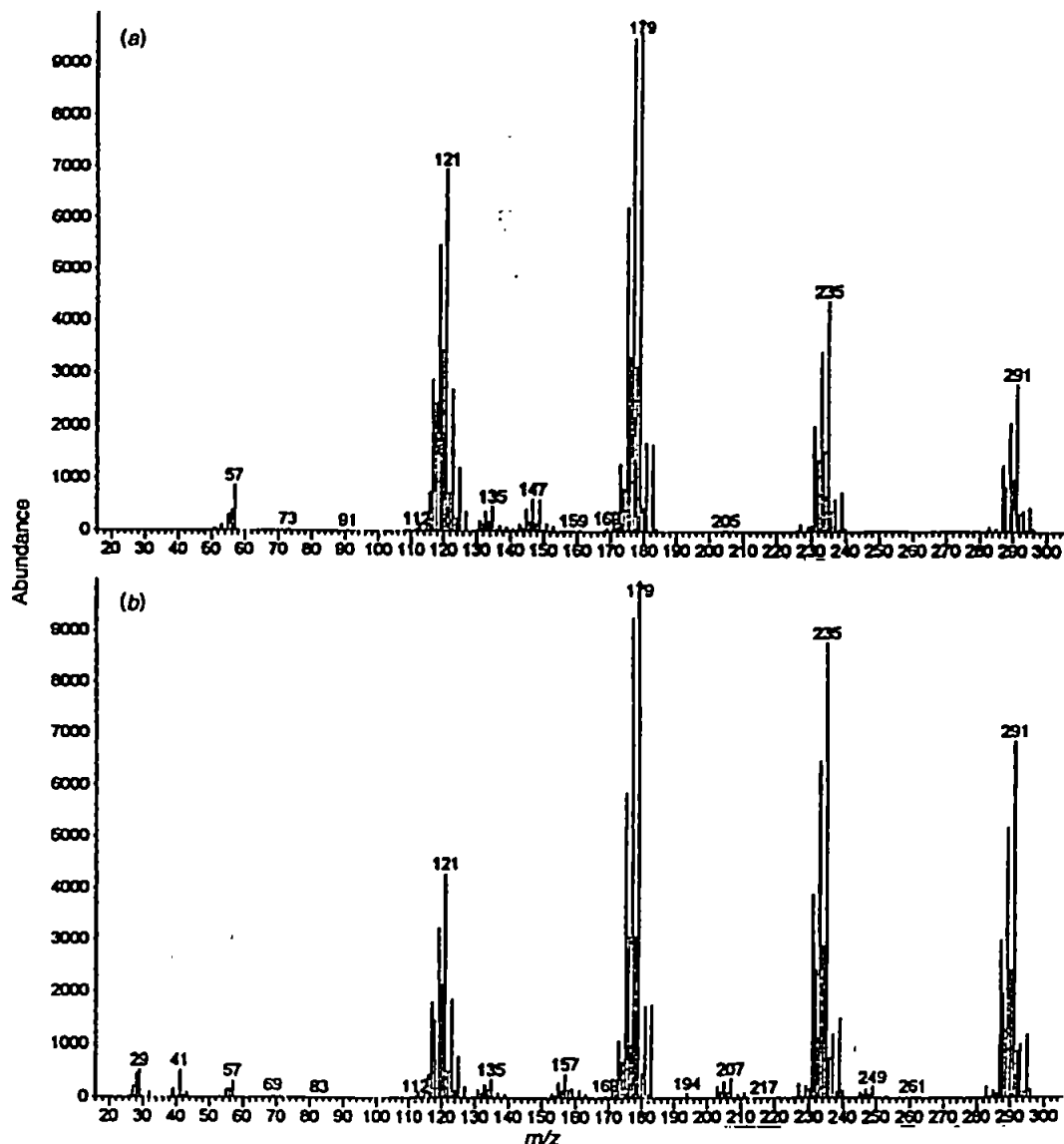
Fig. 14   EI spectra of TBuSn obtained: (a) experimentally by GC–MS; (b) from a computer library
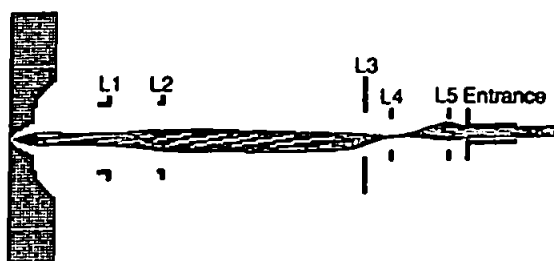
Fig. 15   SimIon plot of ion trajectories for ions, with an average ion kinetic energy of 10 eV, through the ion optical array designed for use in the customized LP-ICP-MS instrument with optimum voltage settings: L1, −75; L2, −10; L3, +1; L4, −64; L5, 0; entrance, −45 V ramped with quadrupole voltage

the existing interface was removed and the entrance to the quadrupole vacuum chamber was widened and welded with a 40 mm KF type vacuum flange. Inside the vacuum chamber, the existing ion-lenses and EI source were removed and replaced with the new set of ion lenses, which were connected to the existing stabilized voltage supplies of the MSD under computer control. Details of the lenses and voltage ranges are given in Table 3.

Table 3   Details of ion-lenses and voltage ranges for the LP-ICP-MS ion optical array

Lens	Voltage range/V	Computer control
L1	0 to −200	No
L2	+5 to −20	No
L3	0 to +10	Yes
L4	0 to −255	Yes
L5	0	Yes
Entrance	0 to −255	Yes

Once the individual components of the new instrument had been designed they were coupled together and evacuated for an initial trial. The configuration of the final instrument is shown in Fig. 16.

Optimization and Evaluation

Optimization study

In order to generate a useful analytical signal, a solution of perfluorotributylamine (PFTBA, Fluka Chemicals, Gillingham, Dorset, UK) was contained in a vial attached to the side-arm of the low pressure plasma torch, and introduced

Fig. 16 Diagram of the customized LP–ICP-MS instrument

to the low pressure plasma *via* a molecular leak (Fig. 16). PFTBA was chosen because the software on the MSD computer is typically configured to use the three fragment ion peaks from PFTBA, at 69, 219 and 502 m/z, to tune the quadrupole and ion optics. This enabled the mass calibration and resolution settings of the quadrupole, and the ion-lens voltage settings, to be optimized daily by the computer.

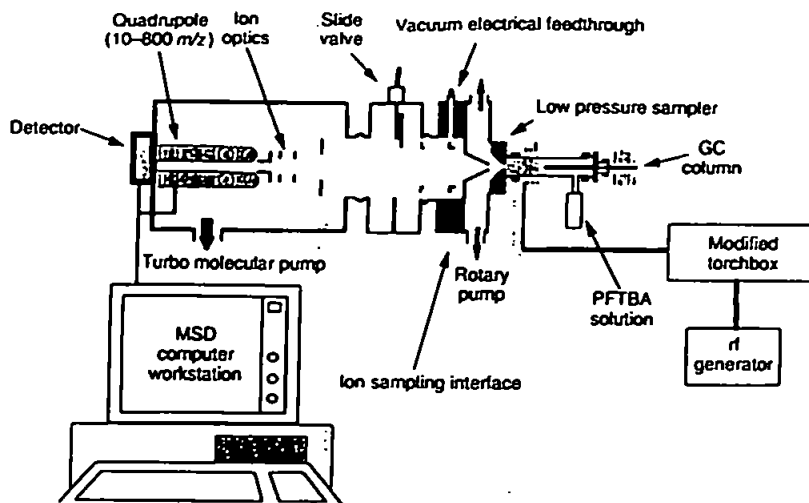The initial operating conditions for the low-pressure plasma are given in Table 4 and Fig. 17(a) shows the three mass peaks selected for tuning the quadrupole. It can be seen from the peak shape and width that good resolution and calibration were achieved using the modified instrument. A total mass spectrum for the PFTBA is shown in Fig. 17(b), and data pertaining to the major peaks are given in Table 5. Prior to conversion into an LP–ICP source, the EI mass spectrum for PFTBA was acquired using the instrument, and the abundances of the major peaks are also given in Table 5. The major difference between the data for the two sources was the higher abundance of ions at m/z 219 and 502 obtained using the EI source, although the abundances can be varied fairly considerably using either ionization source. Once the optimization procedure for the quadrupole and ion-lenses for the MSD had been completed, lenses L1 and L2 were adjusted manually to yield maximum signal for the three chosen m/z values.

When the instrument had been set up in this way an optimization of the skimmer-sampler spacing and the plasma forward power was performed. Surface plots of signal intensity

Fig. 17 Mass spectra of (PFTBA): (a) selected mass fragments at 69, 219 and 502 m/z used for quadrupole and ion-lens tuning; and (b) mass spectrum in the range 45–800 m/z

versus skimmer–sampler spacing and forward power, for the three fragment ions of PFTBA at 69, 219 and 502 m/z are shown in Fig. 18(a), (b) and (c), respectively. The contour plots have been represented in only two dimensions in order to reveal the pertinent features. The points labelled 'A' and 'B' correspond to maxima in the signal, hence the contour plots would look like twin peaks in three dimensions. The experiment was repeated and the observations were found to be reproducible.

Maxima in signal intensity occurred at two skimming distances, namely 6 and 8 mm downstream of the sampler orifice, with comparable signal intensities observed at each of the maxima. Gray[15] has shown that as the expansion stage pressure increases, the barrel shock downstream of the sampler shortens, and the Mach disc gets closer to the sampling orifice. The same worker also found that, for $P_0/P_1 = 76$, several shock regions and Mach discs could be observed downstream of the primary shock region. These observations have recently been confirmed by Luan *et al.*[16] In the present study $P_0 = 0.2$ Torr and $P_1 = 0.03$ Torr (1 Torr = 133.322 Pa), and $D_0 = 2.0$ mm.

Table 4 Operating conditions used for the initial studies with the LP–ICP-MS system

Mass spectrometer	Modified Hewlett-Packard MSD
Plasma–	
Forward power/W	6
Reflected power/W	0
Pressure/Torr*–	
Torch	0.2
Interface	0.03
Analyser	2×10^{-5}
Ion lens/V	
L1	−75
L2	−10
L3	+1
L4	−64
L5	0
Entrance	−45

* 1 Torr = 133.322 Pa.

	Abundance		Relative abundance	
m/z	LP-ICP-MS	EI	LP-ICP-MS	EI
69	1 547 264	1 825 280	100	100
219	383 680	1 100 288	24.80	60.28
502	141 184	223 808	9.12	12.26

Fig. 18 Surface contour plots showing the effect of plasma power and skimming distance on the signal intensity for: (a) 69; (b) 219; and (c) 502 m/z. The points labelled 'A' and 'B' indicate intensity maxima
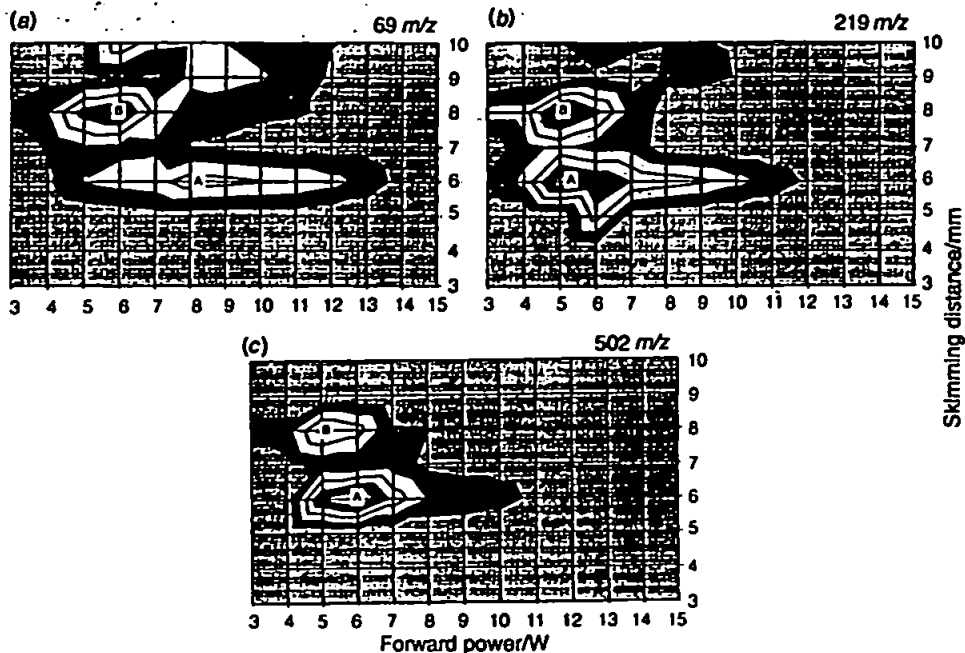
hence using eqn. (1), the position of the Mach disc is calculated to be $X_M = 3.5$ mm. The presence of two maxima in the signal intensity downstream of the Mach disc, observed in the present work, suggests that the fragment ions were formed not in the plasma itself but in the expansion stage, possibly in regions associated with one or two Mach discs downstream of the sampler orifice. At 3.5 mm, the theoretical position of the Mach disc, a maximum in signal intensity was not observed; however, the observations of Gray[15] suggested that the Mach disc becomes progressively larger in relation to the barrel shock as the P_0/P_1 ratio is reduced, so it could possibly extend out to 6 mm downstream of the sampler orifice. Visual observation of the expansion stage used in this work is underway to investigate this phenomenon further.

The power which yielded maximum signal was between 6 and 8 W, although this depended somewhat on which fragment ion and skimming distance were chosen (Fig. 19). At a skimming distance of 6 mm the signal intensity for the fragment ions at 219 and 502 m/z dropped rapidly above 6 W [Fig. 19(a)]. The signal intensity for the fragment ion at 69 m/z also decreased as the power increased, but not as sharply, suggesting that the high mass fragments were further fragmented, adding to the signal observed at 69 m/z. At a skimming distance of 8 mm the power which yielded maximum signal intensity was very similar for the three fragment ions [Fig. 19(b)].

Ion kinetic energies

In order for the helium LP-ICP to be used as a universal source it is necessary to obtain information on the range of
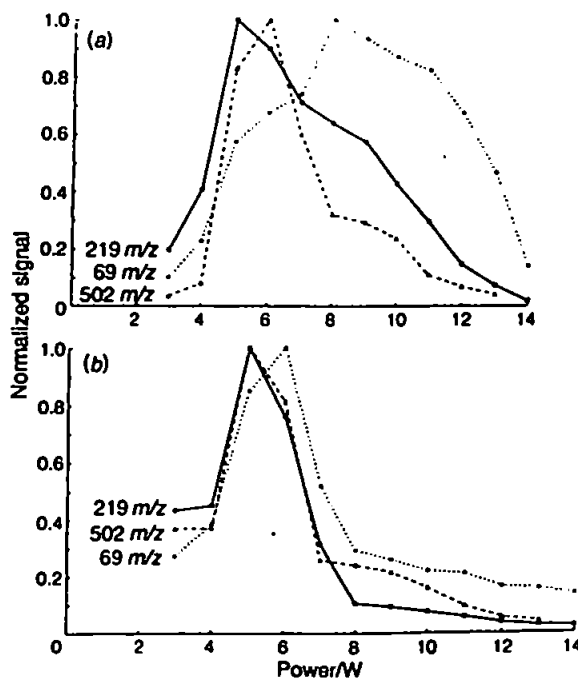

Fig. 19 Plots of normalized signal intensity against plasma power for fragment ions at 69, 219 and 502 m/z for two skimming distances: (a) 6 mm; and (b) 8 mm
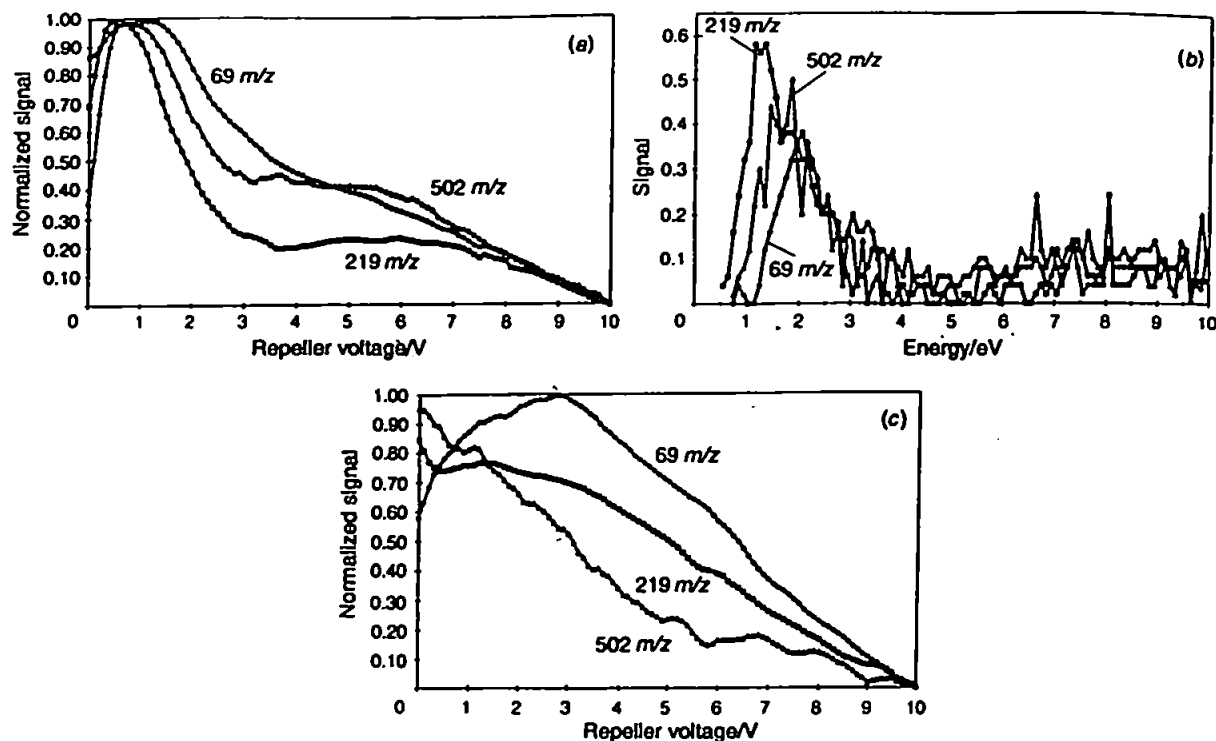
Fig. 20 Ion kinetic energies for ions of 69, 219 and 502 m/z obtained with a helium LP–ICP-MS. (a) Ion stopping curve at 6 W forward power; (b) derivative plot of ion stopping curve at 6 W forward power; and (c) ion stopping curve at 8 W forward power

ion kinetic energies produced by the plasma and extracted into the mass spectrometer. If ions have a wide range of ion kinetic energies it is difficult to arrive at compromise conditions for the quadrupole mass range calibration and ion-lens conditions. Also, if the spread in ion kinetic energy at an individual value of m/z is large it is difficult to maintain good peak resolution. Ion stopping curves for the three fragment ions of PFTBA at 69, 219 and 502 m/z, were generated by removing the L1 and L2 ion-lenses, and varying the potential on L3 from 0 to +10 V. From these, the mean ion kinetic energies and the ion energy spread could be calculated.

The ion stopping curves for ions extracted from the 6 W low-pressure helium ICP are shown in Fig. 20(a) and derivative plots of these curves are shown in Fig. 20(b). This shows that the mean ion kinetic energies for the three mass fragments were 1.2, 1.7 and 2.1 eV, for 69, 219 and 502 m/z respectively, at 6 W forward power, but increased when the power was increased. The spread in kinetic energies was less then 1.5 eV, which should result in well-resolved peaks for all three mass fragments. For ions extracted using a molecular beam type interface, one would expect ion kinetic energy to increase with mass, owing to the translational energy imparted by the gas sampling process; however, it can be seen from Fig. 20(b) that the mass fragment at 69 m/z had the highest ion kinetic energy. This suggests that this ion was formed in a different region of the plasma, an explanation which seems unlikely given the results shown in Fig. 18. A more plausible explanation is that the ions underwent different collisional ionization/fragmentation processes which influenced their ion energies.

Ion stopping curves for a plasma power of 8 W are shown in Fig. 20(c). The derivative plots are not shown because the variability is too great to yield a useful plot. However, it is evident that the spread in the ion kinetic energies increased greatly when the power was increased to 8 W. The only immediate explanation for this is that a secondary discharge existed in the expansion stage, which became more intense as power was increased, thereby accelerating the ions towards the skimmer.

In summary, the evidence seems to indicate the following. (a) Fragment ions are formed in the expansion region rather than the plasma torch. (b) Fragment ions are formed in, or downstream of, one or two separate Mach discs in the expansion region. (c) Ion energies may be influenced, in the first instance, by the nature of the ionization process. (d) A secondary discharge may exist in the expansion region which imparts a degree of acceleration to the ions.

Analytical utility

Previous studies have demonstrated that low-pressure plasmas have their place as atomic ionization sources. In the present work the analytical utility of the instrument pertaining to the formation of molecular fragment mass spectra was investigated, as this could be considered the more challenging application. In order to introduce analytically useful masses of analyte, a gas chromatograph was interfaced with the rear of the LP–ICP torch, via a heated transfer line, as shown in Fig. 16, with operating conditions given in Table 4.

Using this set-up, 1.0 μl of a 50 μg ml^{-1} solution of halobenzenes in pentane was injected on-column, and the gas chromatograph ramped from 40 to 200 °C at 20 °C min^{-1}. A total ion chromatogram (TIC) for this injection is shown in Fig. 21, and the mass spectra of the respective analyte compounds are shown in Fig. 22(a)–(c). The mass spectra obtained are similar to mass spectra obtained for the same analytes using an EI
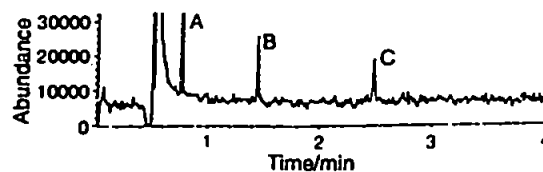

Fig. 21 TIC for 50 ng on-column injection of: A, chlorobenzene; B, iodobenzene; and C, dibromobenzene
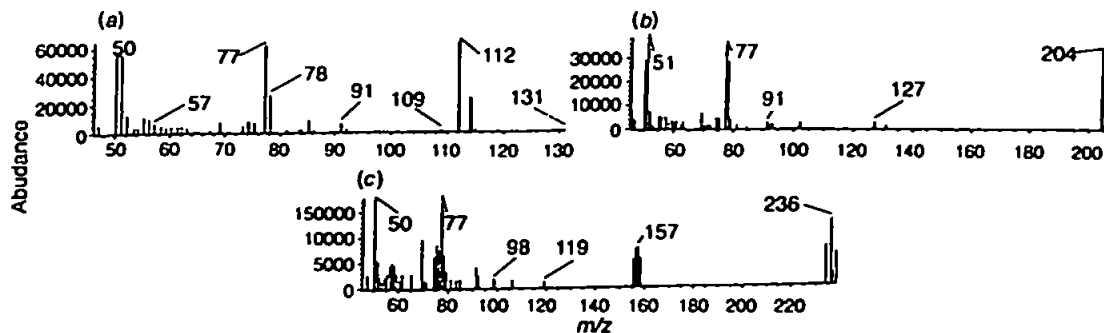
Fig. 22 Mass spectra for: (a) chlorobenzene; (b) iodobenzene; and (c) dibromobenzene
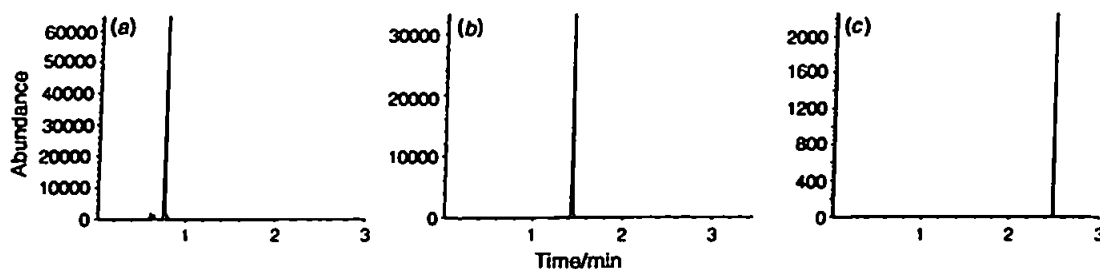

Fig. 23 Selected ion chromatograms for the molecular ions of: (a) chlorobenzene, m/z 112; (b) iodobenzene, m/z 204; and (c) dibromobenzene, m/z 236

ionization source on the same instrument before conversion, with the same parent ion peaks. However, as shown in the power and skimming distance studies (Figs. 18), the abundance of each fragment can be altered by the plasma power. The results of selective ion monitoring (SIM) for the molecular ion peak of each analyte can be seen in Fig. 23. The S/N of such an analysis suggests that the technique could easily be used for trace analysis, though the use of this instrument for such an application may be limited because the detector is configured in analogue mode whereas a pulse counting detector would be preferable.

Conclusions

The customized instrument has gone some way towards alleviating the problems associated with the use of commercial ICP-MS systems for low-pressure plasma work. Now that a dedicated instrument has been constructed it shows great promise for further development. Such an instrument is more economical to operate compared with conventional ICP-MS and helium MIP systems, and can potentially be operated in both atomic and molecular modes. This will also reduce capital costs because a single instrument with a single source could provide a wide range of mass spectral information.

FUTURE WORK

The possibility of developing the low-pressure, low-power ICP into a multi-purpose source for fragmentation and quantification is highly promising. One of the disadvantages of low-pressure techniques is that the relatively un-robust plasmas cannot sustain liquid sample introduction, thus limiting their applications. Further development of low-flow liquid sample introduction techniques (such as microbore LC and capillary electrophoresis), along with good desolvation techniques (i.e.,

the particle beam interface), will expand the analytical applications of low-pressure, low-power plasmas.

The fundamental properties of the LP-ICPs used in this application need to be addressed. Knowledge of temperature and electron number density of the plasma should improve understanding of plasma behaviour at different powers and pressures so that controlled fragmentation can be achieved.

REFERENCES

1 Evans, E. H., Giglio, J. J.,' Castillano, T. M., and Caruso, J. A., Inductively Coupled and Microwave Induced Plasma Sources for Mass Spectrometry, The Royal Society of Chemistry, Cambridge, 1995.
2 Heppner, R. A., Anal. Chem., 1983, 55, 2170.
3 Poussel, E., Mermet, J. M., Deruaz, D., and Beaugrand, C., Anal. Chem., 1988, 60, 923.
4 Olson, L. K., Story, W. C., Creed, J. T., Shen, W., and Caruso, J. A., J. Anal. At. Spectrom., 1990, 5, 471.
5 Shen, W., and Satzger, R. D., Anal. Chem., 1991, 63, 1960.
6 Chien, B. M., Michael, S. M., and Lubman, D. M., Anal. Chem., 1993, 65, 1916.
7 Evans, E. H., and Caruso, J. A., J. Anal. At. Spectrom., 1993, 8, 427.
8 Castillano, T. M., Giglio, J. J., Evans, E. H., and Caruso, J. A., J. Anal. At. Spectrom., 1994, 9, 1335.
9 Evans, E. H., Pretorius, W., Ebdon, L., and Rowland, S., Anal. Chem., 1994, 66, 3400.
10 Kantrowitz, A., and Grey, J., Rev. Sci. Instrum., 1951, 22, 328.
11 Campargue, R., J. Phys. Chem., 1984, 88, 4466.
12 Douglas, D. J., and French, J. B., J. Anal. At. Spectrom., 1988, 3, 743.
13 Hoglund, A., and Rosengren, L. G., Int. J. Mass. Spectrom. Ion. Processes, 1984, 60, 173.
14 Olivares, J. A., and Houk, R. S., Anal. Chem., 1985, 57, 2674.
15 Gray, A. L., J. Anal. At. Spectrom., 1989, 4, 371.
16 Luan, S., Pang, H. -M., and Houk, R. S., J. Anal. At. Spectrom., 1996, 11, 247.

Low Pressure Inductively Coupled Plasma Ion Source for Molecular and Atomic Mass Spectrometry: The Effect of Reagent Gases

GAVIN O'CONNOR, LES EBDON AND E. HYWEL EVANS*

Department of Environmental Sciences, University of Plymouth, Drake Circus, Plymouth, UK PL4 8AA

A low pressure inductively coupled plasma (LP-ICP) source, sustained at only 6 W and utilising 6 ml min^{-1} helium, has been investigated as an ionisation source for molecular and atomic mass spectrometry. Iodobenzene and dibromobenzene were introduced to the LP-ICP *via* gas chromatography and yielded purely atomic ion signals for the iodine and bromine present, with detection limits of 4 and 76 pg for iodobenzene and dibromobenzene, respectively. The addition of nitrogen to a LP helium ICP increased the molecular ion signal for chlorobenzene, with a detection limit of 2 pg. However, the addition of nitrogen did not aid the production of molecular ions of iodobenzene and dibromobenzene. A study of the effect of skimmer spacing and forward power revealed considerable spatial separation of ionisation processes within the expansion chamber of the molecular beam interface. On the addition of 0.07 ml min^{-1} isobutane the LP-ICP yielded mass spectra similar to those obtained by an electron impact source. However on the addition of more isobutane only the molecular ions (M$^+$) for chlorobenzene, iodobenzene and dibromobenzene were observed. The detection limits for the instrument operating in the molecular mode were 100, 140 and 229 pg for chlorobenzene, iodobenzene and dibromobenzene, respectively.

Keywords: *Low pressure inductively coupled plasma: helium plasma: mass spectrometry: reagent gas: element selective detection: molecular ion*

Mass spectrometry (MS) is a continuously growing area of analytical chemistry. Proof of this is the ever increasing number of analytes being qualitatively and quantitatively determined, in a wide selection of matrices. However, the increased use of MS can be partly attributed to the proliferation of sources now available. The use of soft ionisation techniques, such as chemical ionisation (CI), fast atom bombardment (FAB), matrix-assisted laser desorption/ionisation (MALDI) and electrospray ionisation (ESI), have allowed ionisation of fragile, long chain, high molecular weight hydrocarbons without the total destruction of the analyte molecular ion, hence allowing molecular weight determination. At the other end of the ionisation source spectrum are the harsh ionisation sources. These include inductively coupled plasmas (ICP), microwave induced plasmas (MIP) and glow discharge (GD) sources. These sources are generally used to totally atomise analyte compounds, in the case of ICP, MIP and GD sources, allowing ultratrace elemental analysis. Electron impact (EI) sources are intermediate sources, used to fragment organic compounds, providing structural information on the analyte. This dependence on ion source has led to many laboratories purchasing a selection of sources and employing the relevant experts to operate them. These extra capital and employment costs on top of instrumental running costs have made MS a costly field and hence unattractive to many potential users.

The search for a universal ionisation source, capable of operating as both a harsh and soft ionisation source and covering the range in-between, has been equated to that for the holy grail. However, a more realistic approach of using one ionisation source to provide alternately molecular and atomic information, but not covering the whole range, has been achieved by a number of research groups.[1]

Plasma sources for MS have generally been used for elemental analysis. This association can be mainly attributed to the success of the atmospheric argon ICP, which combines a high thermal temperature source with almost complete atomisation and ionisation. One disadvantage of the atmospheric ICP is that it is difficult to sustain plasmas using gases other than argon. An MIP can be formed using a variety of gases, including helium,[1,2] which has a higher ionisation potential than that of argon and so leads to a more ionising plasma. However, plasma sources have also been used to provide both molecular and atomic mass spectra. Shen and Satzger[3] have shown that it is possible to form molecular ions, indicative of the analyte compound, using an atmospheric pressure helium MIP. In this work the analyte was introduced into the after plume of the plasma so did not experience the full force of the source. Reduced pressure MIPs have also been investigated for providing both atomic and molecular mass spectra.[4-6] However, in these studies a pure compound or vapour was generally introduced into the source, which provides little information on how such a source would behave if used for trace level determinations.

ICPs, operated at reduced pressure and sustained with argon, have been used for the production of atomic mass spectra, using gaseous and vapour sample introduction.[7-9] Evans et al.[10] have investigated the use of a low pressure (LP) helium ICP, at powers between 4 and 40 W and 1 mbar pressure, for the production of mass spectra similar to those obtained with an EI source, for a series of organometallic and halogenated species introduced by gas chromatography (GC). On increasing the power and pressure of this source it was possible to increase the degree of fragmentation until at 150 W and 10 mbar pressure total fragmentation occurred. Kohler and Schlunegger[11] used a Penning ionisation source to provide a tuneable degree of fragmentation for a series of gaseous organic compounds. This source was investigated for both positive and negative ion formation and was said to give spectra similar to those obtained with EI, GD and ICP sources. Olson et al.[12] have used an rf GD source, with GC sample introduction, for the speciation of a series of organotin and organolead compounds, and observed molecular fragment peaks from the analyte compounds. From these studies it has become obvious that an LP plasma source is capable of being operated in a tuneable mode. Recently a specially designed instrument has been assembled to further investigate the use of an LP-ICP as a tuneable source.[13]

To date, the analytical figures of merit for the LP plasma sources have been determined using the source in its atomic mode. In order to obtain molecular spectra, large quantities

of the analyte have been introduced into the source. Thus, the source has been used for trace elemental analysis but has not been used for providing molecular fragment ion information on trace level analytes. It has been suggested that the partial pressure of the analyte in the LP-ICP is a contributing factor in molecular fragment ion formation.[13] This would explain the non-linear relationship between concentration and molecular ion signals in the LP-ICP.

In the present study some of the problems associated with the non-linear nature of calibration, for molecular fragment ions, in an LP-ICP have been addressed. Initial studies on the use of reagent gases in the LP-ICP suggest that by altering the composition of the plasma gas alone, it is possible to utilise the LP-ICP as a soft ionisation source, yielding spectra similar to that of a CI source, or as a harsh ionisation source which provides only elemental information, such as an atmospheric ICP. Furthermore the source can be operated in a tuneable mode between hard and soft ionisation regimes.

EXPERIMENTAL

Low Pressure Plasma Mass Spectrometer

A detailed description of the design and optimisation of the GC-LP-ICP-MS system used in this study has been given previously.[13] In brief, a Hewlett-Packard (Stockport, Cheshire, UK) mass selective detector (MSD) was modified to enable it to analyse and detect ions from the LP-ICP. This was achieved by using a custom made ion sampling interface. The LP plasma was sustained using a modified rf generator and matching network, in a 140 mm long quartz tube of 1/2″ od, with a 1/4″ od side arm to which a calibration vial containing perfluorotributylamine (PFTBA) was attached. The quartz plasma torch was connected to the ion sampling interface via an LP sampling cone (Machine shop, University of Plymouth), which was machined from aluminium, had a 2 mm orifice and an Ultra-torr fitting for a 1/2″ pipe. This enabled a vacuum seal to be formed between the LP torch and the ion sampling interface. The reagent gases were added to the plasma gas via the side arm tube of the quartz torch. The amount of gas added was controlled using a scaled needle valve (Edwards High Vacuum, Crawley, West Sussex, UK). Typical operating conditions are shown in Table 1.

Gas Chromatography

A gas chromatograph (PU 4550, Pye Unicam, Cambridge, UK) fitted with an on-column injector, was interfaced to the LP-ICP-MS instrument by way of a heated transfer line maintained at a constant temperature of 250 °C. The GC capillary column used was a DB5 0.32 mm × 30 m with a 0.1 μm film thickness (J & W, Fisons, Loughborough, UK). The capillary column was passed through the heated transfer line and into the LP torch, the vacuum seal being made using a combination of Ultra-torr and Swagelock fittings. This configuration has previously been described in more detail.[10] One microlitre of a mixed standard was injected on-column and the GC programme was typically 40–110 °C at

20 °C min⁻¹ with a helium carrier gas flow rate of 3 ml min⁻¹. A diagram of the instrumental set-up is shown in Fig. 1.

Data Acquisition Parameters

Data were acquired on a Hewlett-Packard MS workstation, with HPS9970A (Version 3.1) software, which was interfaced to the MSD. The ions were detected using two different MS operating modes. For structural information on the analytes the instrument was operated in scanning mode, where the mass range 60–800 m/z was monitored. For quantitative determination of the analytes the instrument was operated in selective ion monitoring (SIM) mode. In this mode of operation the molecular ions, halogen ions and phenyl ions of the analytes were monitored.

Reagents and Standards

Standards were diluted in pentane (HPLC grade, Rathburn Chemicals, Walkerburn, UK) to the required concentration. Chlorobenzene, iodobenzene and dibromobenzene were obtained from Aldrich (Gillingham, UK). Nitrogen (99.9%) and isobutane (99%) were obtained from Air Products (Crewe, Cheshire, UK).

RESULTS AND DISCUSSION

To date LP-ICPs have been sustained with mainly argon or helium gas. The 1 l min⁻¹ argon LP-plasma has been utilised for the production of atomic mass spectra, totally atomising analytes introduced to the source via a GC instrument. The helium LP-ICP has been used as a dual mode ionisation source producing both atomic and molecular ion mass spectra, depending on the gas flow, plasma power and torch pressure used. However, in the fragmentation studies relatively large amounts of analyte (> 50 ng on-column) have been required to facilitate the fragment ion formation. Also, the response obtained from the fragments produced by the LP-ICP was not linearly related to the analyte concentration. These two phenomena together are suggestive of the analyte playing a major role in the fragmentation and ionisation process, i.e., the analytes were self ionising above a certain concentration. In order to suppress this phenomenon in LP-ICP-MS it was decided to investigate the effect of reagent gases on analyte signal and molecular fragment formation.

Nitrogen Addition

Nitrogen was added to a 3 ml min⁻¹ helium plasma via the side arm tube of the quartz torch. The amount of nitrogen added was controlled using a scaled metering valve. The flow rate of the nitrogen gas through the valve was measured at atmospheric pressure, for a series of needle valve settings, and

Table 1 LP-ICP-MS operating conditions

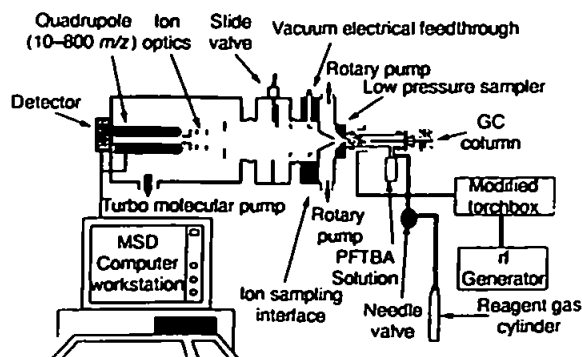| Mass spectrometer	Modified Hewlett-Packard MSD
Low pressure plasma—	
Forward power/W	6
Reflected power/W	0
Pressure/torr —	
Torch	0.2
Interface	0.03
Analyser	< 10⁻⁶

Fig. 1 Schematic diagram of the GC-LP-ICP-MS system.

the flow of gas through the orifice of the needle valve, while operating under LP conditions, was then calculated using Poiseuille's relationship.[14]

It would be expected that the helium–nitrogen plasma would differ in temperature from a helium only LP-ICP, due to the differing thermal conductivity of nitrogen compared with helium, but also because of the differing ionisation potentials of the gases. If a change in the plasma gas kinetic temperature occurred then the ion flux through the sampler and skimmer would also change. The physical processes that describe this phenomenon have been described in detail elsewhere.[1,10,15,16] It has been our experience that for an LP-helium ICP the experimental optimum pressure and flow conditions were different to those calculated using theory,[13] hence it was decided to experimentally optimise the ion sampling conditions. For the optimisation study PFTBA was introduced into a helium–nitrogen LP-ICP. Three fragment ions of PFTBA, at 69, 219 and 502 m/z, respectively, were continuously monitored while the plasma forward power and the sampler-skimmer spacing were optimised. Fig. 2 (a)–(c) shows the resulting plots of the signal intensity versus skimmer–sampler spacing and forward power for these fragment ions. The points labelled 'A' correspond to maxima on each plot. The plots are shown in two dimensions only to help reveal the pertinent features. If the plots were to be shown in three dimensions they would reveal three-peak plots with the central peaks being the most intense for the 69 and 219 m/z fragment ions. This phenomenon has been described previously for helium only LP-ICP-MS[13] and suggests the formation of several 'shock' regions behind the sampler. For the helium–nitrogen plasma the fragment ions at 69 and 219 m/z [Fig. 2 (a) and (b)] gave rise to maximum signal intensity at a skimming distance of 7 mm, with less intense peaks at 4 and 10 mm. However, the fragment ion at 502 m/z [Fig. 2 (c)] yielded no maxima between 5–9 mm and instead yielded maxima at 3 and 10 mm. This may be because the higher mass fragment at 502 m/z underwent a different ionisation process compared to the lower mass fragments or was ionised in a different part of the plasma or interface. Alternatively, the helium–nitrogen plasma may simply cause the molecular ion at 502 m/z to further fragment into smaller molecular species.

It is also evident that the optimum plasma operating power

differed greatly depending on the skimming distance and fragment ion studied. Fig. 3 shows the effect of power on the signal intensity for fragment ions for PFTBA with a sampler-skimmer distance of 7 mm. This shows that at this skimming distance the optimum power for the 69 and 219 m/z ions was between 6 and 8 W. The 69 m/z fragment ion optimises at the highest power, between 7 and 8 W, whilst the 502 m/z ion showed a rapid decrease in signal as the power was increased. As the power was increased the 502 m/z fragment of PFTBA was quickly broken down. The increase in the 219 and 69 m/z signals for the PFTBA suggests that the 502 m/z ion was further fragmented, hence increasing the signals of the lighter fragments. However, above 8 W forward power even the smaller molecular fragments began to disintegrate, which should add to the atomic ion signals, though these could not be monitored because of the high background signals between 12 and 32 m/z.

Optimisation of the helium carrier gas flow and the nitrogen reagent gas flow for the production of stable molecular ions was then performed by introducing 10 ng of chlorobenzene into the plasma via the GC instrument. The molecular ion for chlorobenzene (112 m/z) and the phenyl ion (77 m/z) were continuously monitored for three repeat injections of the 10 ng µl⁻¹ standard. The helium carrier gas flow had little effect
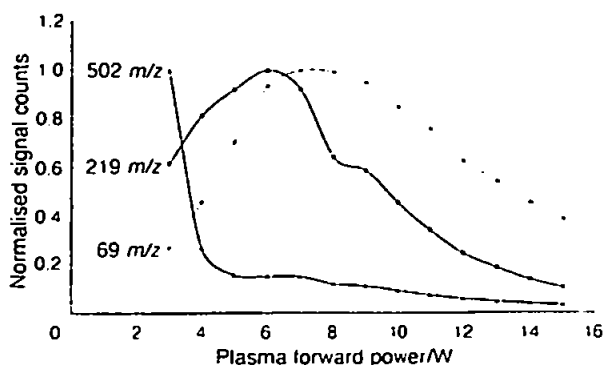

Fig. 3 Plot of normalised signal intensity versus plasma power for the fragment ions of PFTBA at 69, 219 and 502 m/z, at 7 mm skimming distance.
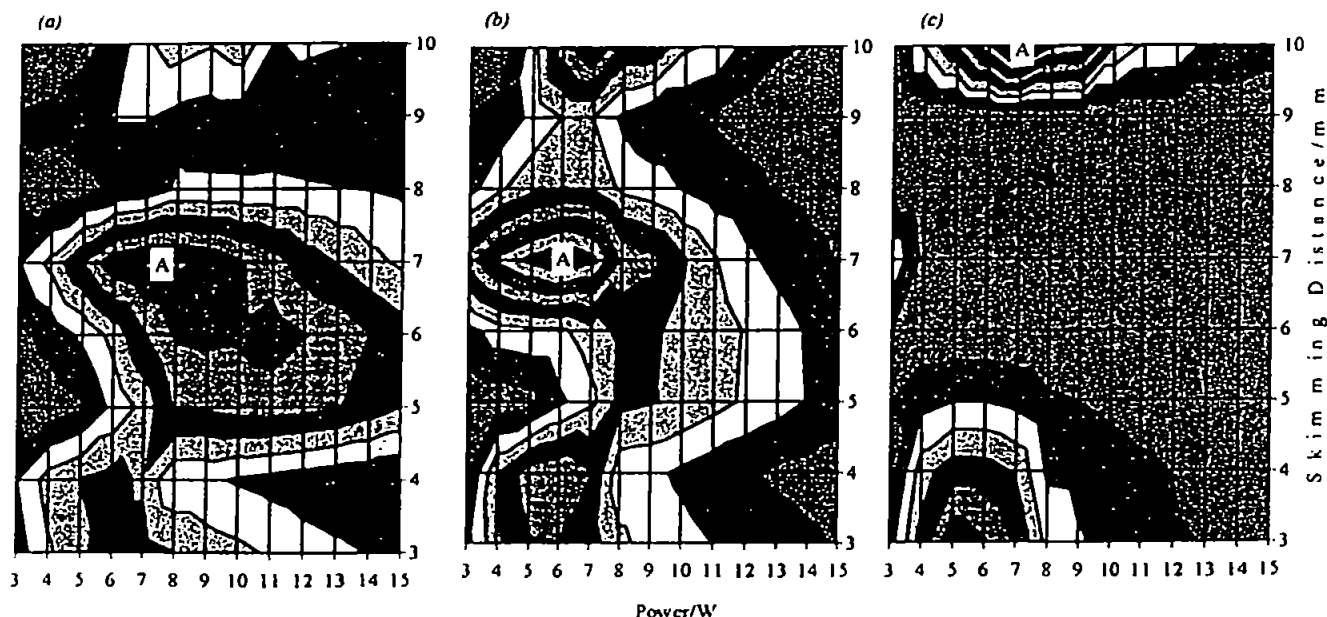

Fig. 2 Surface contour plots showing the effect of plasma power and skimming distance on the signal intensity of PFTBA at: (a) 69 m/z; (b) 219 m/z; (c) 502 m/z. The points labelled 'A' indicate intensity maxima.

on the chlorobenzene signal (Fig. 4), with both the phenyl and molecular ion remaining fairly constant in intensity between 2 and 5 ml min^{-1}. However, as the carrier gas flow was increased the signals became increasingly unstable, indicated by the increased standard deviations of the chlorobenzene signals, shown in Fig. 4. The optimum carrier flow rate was found to be 3 ml min^{-1}. The signal for the molecular ion decreased above 6 ml min^{-1} helium. This could be due to the extra gas increasing the electron and ion number density and thermalising the plasma. This would lead to a greater amount of collisions between the analyte and electrons, which in turn would lead to increased fragmentation of the analyte causing a reduction in the molecular signals. This theory would seem to be confirmed by the addition of more helium gas. On the addition of 7 ml min^{-1} of helium the molecular ion decreased whilst the phenyl ion signal increased. This may be indicative of the molecular ion fragmenting and adding to the phenyl ion signal, however, the precision was poor so it was not possible to draw a firm conclusion. Above 7 ml min^{-1} helium the phenyl and molecular signals disappeared, which could be because the ions became totally atomised, yielding only atomic information. Alternatively, these effects could be due to changing the chromatographic conditions.

The effect of the nitrogen gas added to a 3 ml min^{-1} helium plasma on the chlorobenzene signal is shown in Fig. 5. The signal for the molecular ion peak at 112 m/z for chlorobenzene was relatively unaffected by the nitrogen as the signal remained fairly constant up to 2.1 ml min^{-1}. With nitrogen flows above 2.1 ml min^{-1} the signals for both the molecular ion and the phenyl ion were reduced by over 50%. Again this may be due to the increased electron and ion density in the plasma further fragmenting the analyte. A point of interest is the stability of the analyte signals, even above a combined gas flow of 7 ml min^{-1}. This suggests that the unstable signals obtained on adding helium carrier gas were due to chromatographic
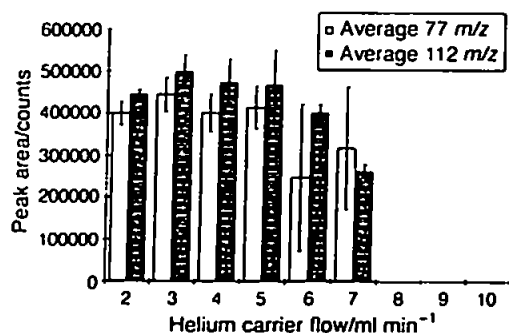

Fig. 4 Effect of helium carrier gas flow rate on the signal intensity of a 10 ng on-column injection of chlorobenzene, in a nitrogen–helium LP-ICP.
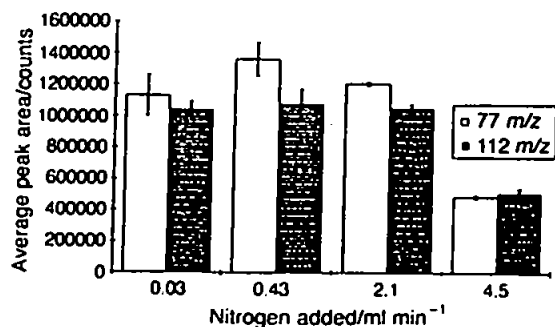

Fig. 5 Effect of nitrogen reagent gas flow rate on the signal intensity of a 10 ng on-column injection of chlorobenzene, in a 3 ml min^{-1} helium LP-ICP.

effects, or that the decreased thermal conductivity of the nitrogen may have stabilised the LP-ICP.

Once the optimisations were completed, an investigation of the analytical figures of merit (given in Table 2) was performed. The figures of merit were obtained by SIM for the molecular ion of chlorobenzene (112 m/z). The detection limit of 2 pg suggests that the LP helium–nitrogen plasma is capable of providing structural information on the analyte even at ultra trace levels. Also the nitrogen addition improved the linear range of calibration, with calibration over three orders of magnitude possible. This is a vast improvement compared to helium only LP-ICP-MS for which calibration was not possible. Fig. 6 shows a SIM chromatogram at 112 m/z for a 100 pg on-column injection of chlorobenzene illustrating the excellent signal to noise obtained.

These results suggest that addition of nitrogen to the LP-ICP-MS instrument would cure the problems observed previously.[10,13] However, on the addition of analytes with retention times greater than 2 min, only the atomic signals were observed. This was thought to be due to the influence of the tail of the solvent peak on chlorobenzene due to the short retention time of the latter. In order to minimise this effect it was decided to investigate the use of isobutane as the reagent gas.

Isobutane Addition

Isobutane was added to the LP helium plasma in a similar manner to nitrogen and its effect on the molecular, phenyl and atomic ion signals for a series of halobenzenes was investigated. The analytes were injected, approximately 10 ng each on-column, as a mixed standard. Fig. 7 (a) shows the effect of the isobutane on the signals for 10 ng on-column injection of chlorobenzene. The atomic signal for chlorine has not been shown because fragment ions from the reagent gas interfered with ion signals below 58 m/z. With a 3 ml min^{-1} helium only plasma, the molecular ion of chorobenzene was the parent ion. On the addition of the reagent gas both molecular ion and phenyl ion signals were greatly increased. However, as the reagent gas partial pressure was further increased the phenyl ion peak disappeared, leaving only the molecular ion. This is

Table 2 Analytical figures of merit for chlorobenzene using a 0.43 ml min^{-1} nitrogen, 3 ml min^{-1} helium LP-ICP

Single ion monitoring, mass monitored	112 m/z
Linear range studied/decades	3
Slope/counts pg^{-1}	99
r^2 (regression coefficient)	0.985
Slope of log–log plot	1.012
Detection limit*/pg	2
RSD† (%)	8.5

* LOD = 3σ/slope.
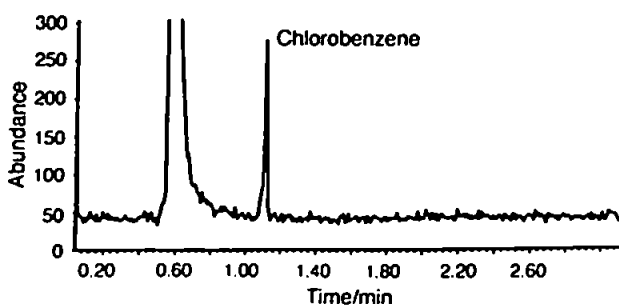† RSD (%) for five replicate 10 pg injections.

Fig. 6 Chromatogram of a 100 pg on-column injection of chlorobenzene for a helium–nitrogen (3.0 and 0.43 ml min^{-1}) LP-ICP using selected ion monitoring at 112 m/z.
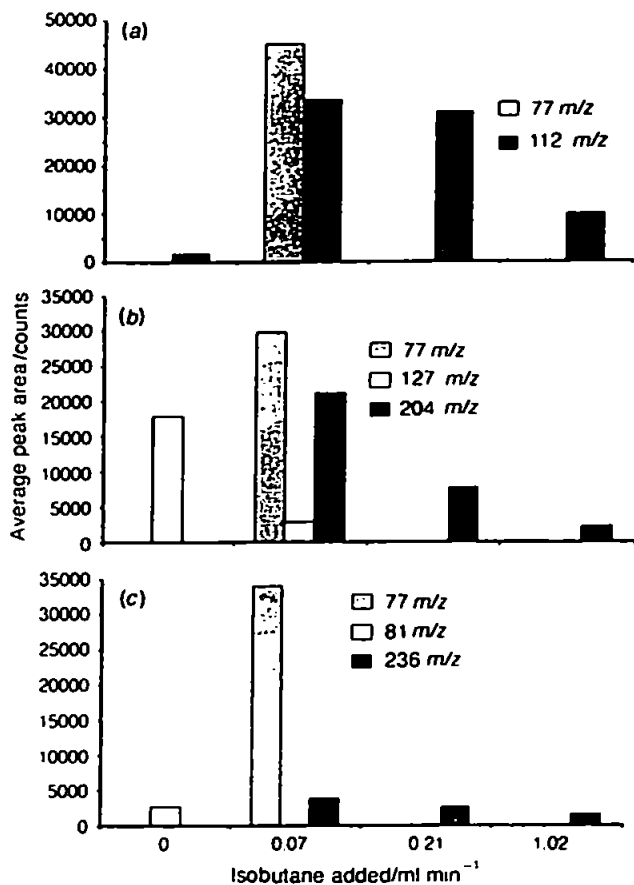
Fig. 7 Effect of isobutane reagent gas flow rate on the signal intensity of the molecular and fragment ions of (a) chlorobenzene, (b) iodobenzene and (c) dibromobenzene in a 3 ml min⁻¹ helium LP-ICP.
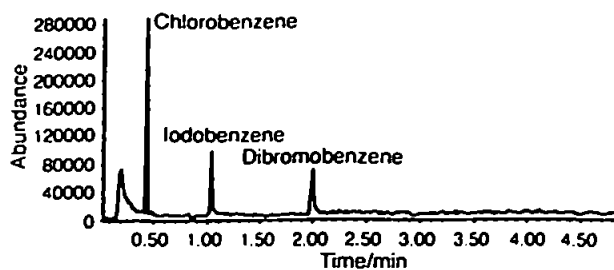

Fig. 8 Total ion chromatogram for 10 ng on-column injection of chlorobenzene, iodobenzene and dibromobenzene for a helium-isobutane (3.0 and 0.07 ml min⁻¹) LP-ICP.
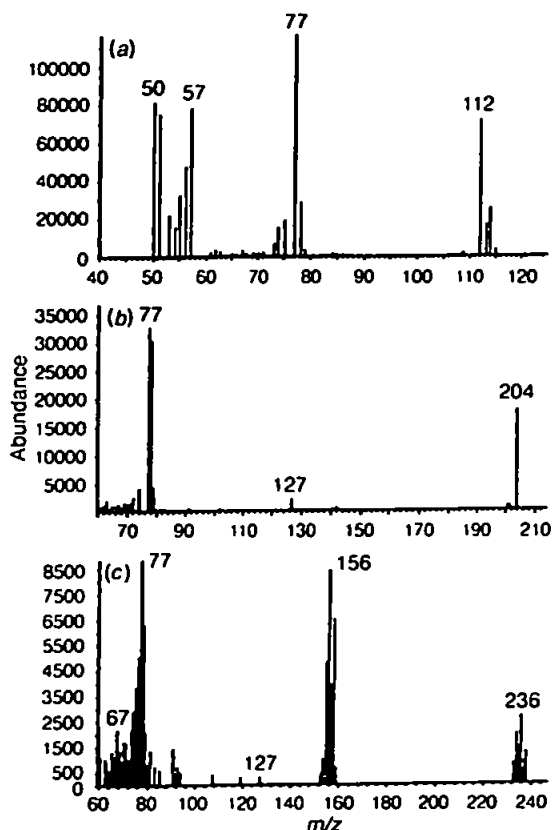

Fig. 9 Mass spectra scans obtained from an isobutane-helium (0.07 and 3.0 ml min⁻¹) LP-ICP for 10 ng on-column injection of (a) chlorobenzene, (b) iodobenzene and (c) dibromobenzene.

consistent with the isobutane–helium plasma acting as a conventional CI source where the partial pressure of the reagent gas often determines the analyte spectra obtained. Unlike the nitrogen reagent gas, the effects of the isobutane were consistent throughout the chromatographic run. Fig. 7 (b) and (c) show the effect of the isobutane on iodobenzene and dibromobenzene which had retention times of 1.1 and 2.0 min. respectively. For the 3 ml min⁻¹ helium plasma, with a 10 ng on-column injection, the only ions that were observed were the atomic signals for the halogens. When 0.07 ml min⁻¹ of isobutane reagent gas was added the phenyl and molecular ions were observed. This yielded spectra very similar to those obtainable by EI source MS. On the addition of more isobutane the phenyl and atomic halogen signals were no longer observed and only the compound molecular ion remained, yielding spectra similar to those expected from CI source MS. However. on the addition of greater than 1 ml min⁻¹ isobutane the molecular ion signals started to reduce in intensity. The halogen and phenyl ions for the analytes did not increase on the reduction of the molecular ions. This suggests a reduction in the ionisation power of the source, because if the ionisation power increased one would expect to see a corresponding increase in the signal of the lower mass fragment ions as the molecular ion decomposed.

Fig. 8 shows a total ion chromatogram for a 10 ng on-column injection of chlorobenzene, iodobenzene and dibromobenzene, obtained using a 0.07 ml min⁻¹ isobutane–3 ml min⁻¹ helium LP-ICP. The resulting mass spectra for each compound are shown in Fig. 9 (a)–(c). The predominant ionisation mechanism for isobutane in CI is proton transfer. However, the mass spectra of the halobenzenes studied [Fig. 9 (a)–(c)] show little sign of protonation with the MH⁺ peak being less than one third the intensity of the M⁺.

and in the case of iodobenzene no MH⁺ peak was visible. This, along with the reduction in molecular and fragment ion signals on increasing the isobutane partial pressure, suggests that the isobutane was not behaving as a proton transfer reagent gas. Also, no quasimolecular ions were observed. On the addition of 0.07 ml min⁻¹ of isobutane the major reagent ion was 57 m/z. This is consistent with the loss of a proton from the isobutane, however, it has already been shown that protonation of the analytes was not the dominant ionisation process. As the reagent gas concentration was increased the most abundant reagent ion changed from 57 to 43 m/z, which is consistent with the loss of a methyl group from isobutane. This suggests that as more isobutane was added the plasma ionisation processes were getting harsher, because greater fragmentation was observed, however, analyte fragmentation exhibited the opposite trend. An alternative explanation may be that the ionisation process of the helium plasma was suppressed by the presence of the isobutane, and that as more isobutane was added a greater amount of energy was required to form the reagent ions, thereby leaving less energy to ionise

Analyte	Chlorobenzene	Iodobenzene	Dibromobenzene
Selected ion monitoring, mass monitored	112 m/z	204 m/z	236 m/z
Linear range studied/decades	3	3	3
Slope/counts ng⁻¹	84 645	28 405	4905
r² (regression coefficient)	0.9925	0.9848	0.9925
Log–log slope	0.85	0.74	0.70
Detection limit*/pg	100	140	229
RSD† (%)	12	6	5

* LOD = 3σ/slope.

† RSD (%) for five replicate 380 pg injections.

the analyte and resulting in molecular ion production of the analyte.

This suggests that the source was not acting as a conventional CI source and that a number of ionisation mechanisms may be taking place. This is consistent with other plasma sources where a number of non-equilibrium properties are used to describe the plasma ionisation characteristics. This is a well known phenomenon because most plasmas do not exhibit thermal equilibrium even at atmospheric pressure, let alone at reduced pressure. Charge transfer is a well known ionisation mechanism in helium plasmas, and if ionisation was occurring *via* charge transfer in a helium–isobutane plasma one would expect a small degree of fragmentation and ionisation due to the low ionisation potential of isobutane (10.57 eV).[17] The figures of merit for the helium–isobutane plasma operating in the molecular mode are shown in Table 3.

Helium Addition

In the initial studies performed using an LP helium ICP the dependence of molecular ion formation on the analyte concentration was suggestive of chemical ionisation processes predominating in the plasma. If the helium was acting as a reagent gas for conventional CI the expected predominant ionisation process would be charge transfer. The rate of charge transfer is dependent on the partial pressure of reagent gas and analyte in the source. The survival of molecular ions in a charge transfer source is also dependent on the internal energy of the ion. If the internal energy is large (>5 eV) a great deal of fragmentation would be expected. The internal energy of a molecular ion can be calculated using eqn. (1):[18]

$$E_{int} = RE(X^+) - IP(M) \qquad (1)$$

where $RE(X^+)$ is the recombination energy of the reagent ion (24.6 eV for helium) and $IP(M)$ is the ionisation potential of the analyte molecule. This would lead to an internal energy of over 13 eV for the molecular ions of the halobenzene series studied, with ionisation potentials between 9–11 eV. Hence, extensive fragmentation of the analyte molecules would be predicted using a dense helium plasma. However, in conventional CI MS it is not unusual to observe molecular ions for organic molecules, with ionisation potentials less than 10 eV, when using helium as the reagent gas. Therefore, the presence of the rf magnetic field may induce collisional energy exchange between excited electrons and the analyte, increasing the ionisation power of the plasma. Hence, by increasing the helium partial pressure in the LP-ICP, the rate of charge exchange would increase. This should lead to greater fragmentation, and eventually atomisation, of the analyte molecules, leaving only the atomic ions to be detected. This suggests the possibility of utilising a low flow helium LP-ICP-MS for atomic MS.

To test this hypothesis a helium make up gas was added to the plasma gas, *via* the side arm of the LP torch. The helium was introduced using a mass flow controller (Unit Instruments,
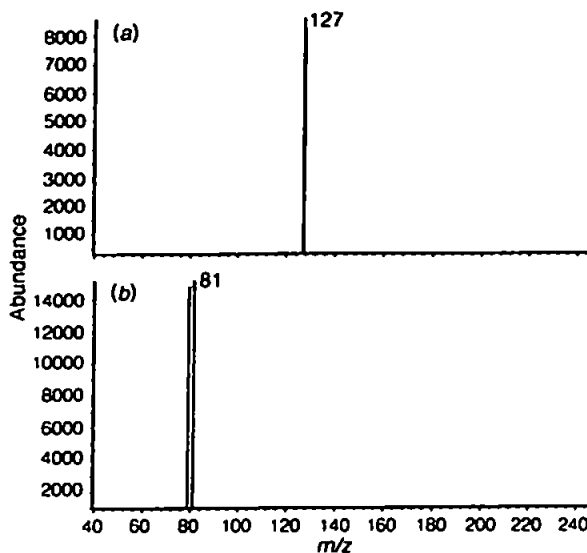

Fig. 10 Mass spectra scans obtained from a 6 ml min⁻¹ helium LP-ICP for a 50 ng on-column injection of (a) iodobenzene and (b) dibromobenzene.

Dublin, Ireland) in place of the needle valve. A 6 ml min⁻¹ helium LP-ICP was then studied for the production of elemental mass spectra for iodobenzene and dibromobenzene. Fig. 10 (a) and (b) show the resulting mass spectra scans (60–240 m/z) of a 50 ng on-column injection of the standards and shows the existence of only the atomic signals for the iodine (127 m/z) and bromine (79 and 81 m/z) even at this relatively high concentration. This shows that the 6 ml min⁻¹ helium plasma
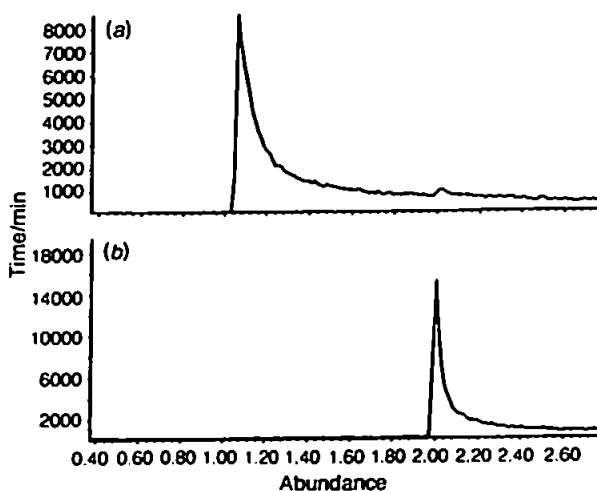

Fig. 11 Extracted ion chromatograms for a 50 ng on-column injection of (a) iodobenzene at 127 m/z and (b) dibromobenzene at 81 m/z, using a 6 ml min⁻¹ 6 W helium LP-ICP-MS instrument.

Table 4 Analytical figures of merit for iodobenzene and dibromobenzene, using a 6 ml min⁻¹ helium LP-ICP

Analyte	Iodobenzene	Dibromobenzene
Selected ion monitoring, mass monitored	127 m/z	81 m/z
Linear range studied/decades	3	3
Slope/counts pg⁻¹	235	129
r^2 (regression coefficient)	0.999	0.999
Log–log slope	0.890	0.881
Detection limit*/pg	4	76
RSD† (%)	8	12

* LOD = 3σ/slope.

† RSD (%) for five replicate 100 pg injections.

operating at only 6 W forward power can atomise and ionise the halobenzenes. Fig. 11 (a) and (b) show extracted ion chromatograms for 50 ng on-column of iodobenzene and dibromobenzene at 127 and 81 m/z, respectively. The chromatograms show extensive peak tailing which is thought to be due to the analyte atomic ion interacting with the wall of the plasma torch, whereas this does not occur for the molecular ion signals using the same chromatographic conditions.

The figures of merit for the 6 ml min⁻¹ helium only LP-ICP-MS are shown in Table 4. The detection limits for the instrument operating in the atomic mode, reported in this study, are comparable to those obtained by GC–LP–MIP-MS, namely 22, 0.1 and 3.5 pg for chlorotoluene, iodobenzene and bromononane, respectively.[1] Studies of a GC–LP–ICP-MS system sustained with 0.5 l min⁻¹ of helium have yielded element selective detection limits of 2.9 and 3.8 pg for chlorobenzene and bromobenzene.[1] In comparison, detection limits given for the Hewlett-Packard MS instrument operating with an EI source are typically 10 pg, for SIM of the molecular ion of methyl stearate at 298 m/z. It is interesting to note that in the previous study[10] no peak tailing for the atomic species was observed. With a 1 l min⁻¹ argon LP-ICP there is a distinct central channel evident, much like a conventional atmospheric pressure ICP. However, unlike an atmospheric pressure ICP this is thought to be formed by the pressure drop at the 2 mm diameter sampler orifice pulling the central portion out of the plasma. This effectively pulls the analyte ions into the centre of the plasma and away from the torch walls. At very low gas flows and pressures this effect is not observed so it is likely that the analyte interacts more with the walls of the torch.

CONCLUSIONS

The GC–LP–ICP-MS system has been shown to be capable of providing a tuneable degree of fragmentation for a series of halobenzene compounds. The problems associated with poor linear calibration range and high detection limits for the molecular ions have been addressed and alleviated by the use of reagent gases.

The addition of small amounts of nitrogen to the LP-ICP increased the stability of the plasma and the detection limits for the molecular fragments of chlorobenzene were greatly improved. However, this effect did not extend to the other halobenzenes studied.

The addition of isobutane enhanced all the analyte molecular and fragment ion signals. The isobutane did not seem to be acting as it would in a conventional CI source as proton transfer reactions were minimal. However, the isobutane seemed to reduce the ionisation energy of the plasma, yielding only molecular ions of the analytes, as it would in CI source MS, at low level concentrations.

An LP plasma sustained at 6 W and utilising only 6 ml min⁻¹ of helium has been used to totally atomise both iodobenzene and dibromobenzene, producing atomic mass spectra. This proves that a GC–LP–ICP-MS system is capable of providing different degrees of fragmentation for a series of halobenzenes.

REFERENCES

1 Evans, E. H., Giglio, J. J., Castillano, T. M., and Caruso, J. A., *Inductively Coupled and Microwave Induced Plasma Sources for Mass Spectrometry*, ed. Barnett, N. W., Royal Society of Chemistry, Cambridge, 1995.
2 Chambers, D. M., Carnahan, J. W., Jin, Q., and Hieftje, G., *Spectrochim. Acta, Part B*, 1991, 46, 1745.
3 Shen, W., and Satzger, R. D., *Anal. Chem.*, 1991, 63, 1960.
4 Heppner, R. A., *Anal. Chem.*, 1983, 55, 2170.
5 Poussel, E., Mermet, J. M., Deruaz, D., and Beaugrand, C., *Anal. Chem.*, 1988, 60, 923.
6 Olson, L. K., Story, W. C., Creed, J. T., Shen, W., and Caruso, J. A., *J. Anal. At. Spectrom.*, 1990, 5, 471.
7 Evans, E. H., and Caruso, J. A., *J. Anal. At. Spectrom.*, 1993, 8, 427.
8 Castillano, T. M., Giglio, J. J., Evans, E. H., and Caruso, J. A., *J. Anal. At. Spectrom.*, 1994, 9, 1335.
9 Yan, X., Tanaka, T., and Kawaguchi, H., *Appl. Spectrosc.*, 1996, 50, 2, 182.
10 Evans, E. H., Pretotius, W., Ebdon, L., and Rowland, S., *Anal. Chem.*, 1994, 66, 3400.
11 Kohler, M., and Schlunegger, U. P., *J. Mass Spectrom.*, 1995, 30, 134.
12 Olson, L. K., Belkin, M., and Caruso, J. A., *J. Anal. At. Spectrom.*, 1996, 11, 491.
13 O'Connor, G., Ebdon, L., Evans, E. H., Ding, H., Olson, L. K., and Caruso, J. A., *J. Anal. At. Spectrom.*, 1996, 11, 1151.
14 *Physical Chemistry*, Oxford University Press, Oxford, 4th edn., 1990.
15 Niu, H., and Houk, R. S., *Spectrochim. Acta, Part B*, 1996, 51, 779.
16 Douglas, D. J., and French, J. B., *J. Anal. At. Spectrom.*, 1988, 3, 743.
17 *Handbook of Chemistry and Physics*, CRC Press, Boca Raton, FL, 65th edn., 1984–1985.
18 Chapman, J. R., *Practical Organic Mass Spectrometry*, Wiley, Chichester, 2nd edn., 1993.